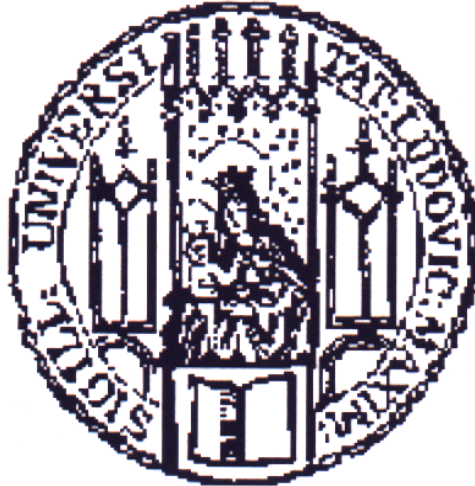


Modular Submicroliter Lab-on-a-chip in Forensic Sciences



Dissertation

an der Fakultät für Geowissenschaften
der Ludwig-Maximilians-Universität
München

Daniela Rita Woide

Dipl. Biol. (Univ.)

München, den 3. März 2010

Dekan:

Prof. Dr. Wolfram Mauser

1. Berichterstatter:

Prof. Dr. Wolfgang M. Heckl

2. Berichterstatter:

PD Dr. Stefan Thalhammer

Tag der Einreichung der Dissertation:

3. März 2010

Tag der Disputation:

12. Juli 2010

**„Science is a game we play with God
to find out what his rules are.“**

(Krasel, Cornelius)

Summary

Against the background of an ongoing demand on faster, more cost-effective and more sensitive analysis methods particularly in the area of DNA analytics, innovative analytic developments are necessary. Miniaturized laboratories on electrically driven chip devices present an example of such sophisticated technologies. Their application gains increasing importance in medical diagnostics as well as in the forensics field of research, most notably as often only a small amount of sample material is available which in addition requires to be analyzed free of contamination. In this work a multifunctional lab-on-a-chip system is presented, that is generally applicable to a wide variety of small-scale sample material. The lab-on-a-chip is characterized by a modular design. The single working units used for sample retrieval, processing and detection were optimized concerning their capacity. The applicability of the lab-on-a-chip in forensic DNA analytics was exemplified on several actual scientific problems. After contamination-free microdissection retrieved sample material was analyzed on a chip-based DNA amplification unit. On a chemically structured planar chip surface virtual reaction tubes were built in form of small droplets, that were stabilized by the liquid's surface tension. The facilitated miniaturization of the reaction volume to just 1 μl in total enabled analyses of smallest amounts of sample material free of contamination. In that manner, a higher sensitivity than in voluminous plastic tube-based reactions could be achieved. The miniaturized reaction volume permitted a decrease of analysis time to 15 seconds per PCR cycle. The required amount of starting material for a significant genetic analysis could be reduced to a minimum of 25 pg.

Based on reliable, reproducible and highly sensitive analyses using purified standard DNA the applicability of the lab-on-a-chip was tested on various samples of forensic relevant materials, liquid ones as well as solid ones. (1) Using just 1% (v/v) of unpurified whole blood in PCR-based analysis, full allelic DNA profiles for the generation of genetic fingerprints could be determined. (2) Dried blood spots were analyzed over a specific period of time ranging from several minutes up to three months of age. In dependence on the status of the drying and coagulation process, up to 92% full detectable DNA profiles could be attained. (3) Microdissected tissue particles of pathological relevant tissues could directly be subjected to PCR-based gender determining analysis and related to male and female individuals, while no additional DNA extraction steps were needed prior to analysis. (4) The self-posted demand on performing highly sensitive and contamination-free analyses was demonstrated using ancient bone tissue material derived from Egyptian mummy material. After laser microdissection

DNA fragments of up to 297 bp in length could be amplified in PCR-based analyses using just 60 pg of ancient DNA starting material. The authenticity of amplified fragments could be verified when compared to sequences recalled from current genome databases, showing identities of up to 98% concerning the DNA sequence. (5) This innovative laser microdissection-based nanotechnological approach for ancient DNA analysis of bone material could after all be highlighted versus a conventionally performed pathological technique for sample retrieval. The traditional method was based on pulverization of bone material. In using the novel technology considerably more authentic ancient DNA molecules could be isolated while simultaneously impacts of destructive factors could be eliminated.

Zusammenfassung

Vor dem Hintergrund eines ständig wachsenden Bedarfs an schnelleren, kostengünstigeren und sensitiveren Nachweisverfahren, insbesondere im Bereich der DNA Analytik, sind innovative Entwicklungen unerlässlich. Miniaturisierte Labore auf elektrischen Chips sind ein Beispiel solcher hochentwickelten Technologien. Ihr Einsatz gewinnt sowohl in der medizinischen Diagnostik als auch in der Forensik zunehmend an Bedeutung, vor allem deshalb, weil häufig nur sehr geringe Probenmengen zur Verfügung stehen und diese zudem kontaminationsfrei analysiert werden müssen. In dieser Arbeit wird ein multifunktionales Chiplabor vorgestellt, das zur Analyse kleinster Mengen sehr unterschiedlicher Probenmaterialien eingesetzt werden kann. Das Chiplabor zeichnet sich durch einen modularen Charakter aus. Die einzelnen Einheiten zur Probengewinnung, Prozessierung und Detektion wurden hinsichtlich ihrer Leistungsfähigkeit optimiert. Die Anwendbarkeit des Chiplabors in der forensischen DNA-Analytik wurde am Beispiel mehrerer aktueller wissenschaftlicher Fragestellungen demonstriert. Nach kontaminationsfreier Lasermikrodissektion wurden die gewonnenen Proben auf einer chip-basierten DNA-Vervielfältigungseinheit verarbeitet. Auf einer chemisch strukturierten planaren Chipoberfläche wurden virtuelle, durch Oberflächenspannung stabilisierte Reaktionsgefäße in Form kleiner Flüssigkeitströpfchen gebildet. Die dadurch ermöglichte Miniaturisierung des Reaktionsvolumens auf nur 1 µl ermöglichte kontaminationsfreie Analysen geringster Mengen von Probenmaterial. Auf diese Weise konnte eine höhere Sensitivität als in großvolumigen Plastikgefäß-basierten Reaktionen erzielt werden. Das miniaturisierte Reaktionsvolumen erlaubte eine Reduktion der PCR-Zykluszeiten auf 15 Sekunden pro Zyklus. Die für aussagekräftige genetische Analysen benötigte Menge an Ausgangsmaterial ließ sich auf eine minimale Menge von 25 pg DNA reduzieren.

Ausgehend von verlässlichen, reproduzierbaren und hoch sensitiven Analysen mit gereinigter Standard DNA, wurde die Anwendbarkeit des Chiplabors auf verschiedenartige, flüssige sowie feste Proben von forensisch relevantem Material getestet. (1) Bei Einsatz von nur 1% (v/v) ungereinigtem Vollblut konnten in PCR-basierter Analyse vollständige DNA-Profile zur Generierung genetischer Fingerabdrucke ermittelt werden. (2) Getrocknete Blutstropfen wurden über einen Zeitraum von mehreren Minuten bis zu drei Monaten untersucht. In Abhängigkeit vom Status des Trocknungs- und Koagulationsprozesses ließen sich bis zu 92% vollständig nachweisbare DNA-Profile gewinnen. (3) Mikrodissektierte Gewebepartikel aus pathologisch relevanten Geweben konnten direkt in PCR-basierter

Geschlechtsbestimmungsanalyse ohne vorherige DNA Extraktion männlichen und weiblichen Individuen zugeordnet werden. (4) Der selbst gestellte Anspruch, hochsensitive, kontaminationsfreie Analysen durchführen zu können, wurde an sehr altem Knochengewebe aus ägyptischem Mumienmaterial demonstriert. Nach Lasermikrodissektion konnten aus einer Startmenge von nur 60 pg historischen DNA Materials in PCR-basierten Analysen DNA-Fragmente von bis zu einer Länge von 297 bp vervielfältigt werden. Die Authentizität der vervielfältigten Fragmente konnte in Vergleichen mit gängigen Genom-Datenbanken bewiesen werden, mit einer Übereinstimmung hinsichtlich der DNA-Sequenzen bis zu 98%. (5) Die Vorzüge dieses innovativen, auf Lasermikrodissektion basierenden, nanotechnologischen Ansatzes zur DNA-Analyse aus Knochenmaterial wurden schließlich durch Vergleich mit Untersuchungen belegt, bei denen eine herkömmliche pathologische Technik zur Probengewinnung eingesetzt wurde. Die konventionelle Technik basierte auf einer Pulverisierung des Knochenmaterials. Mit der neuen Technologie konnten deutlich mehr authentische alte DNA Moleküle isoliert und gleichzeitig Einflüsse von schädlichen Faktoren vermieden werden.

Table of Contents

Acknowledgements	1
Publications	3
List of abbreviations	4
1. Introduction	6
1.1 DNA analysis	6
1.2 Micro total analysis systems	9
1.2.1 Miniaturization of PCR technology	11
1.2.2 Modes of microchip-based PCR	12
1.3 Scope of this work.....	16
2. Materials and Methods	17
2.1 Sample materials and preparation	17
2.1.1 Male and female human genomic reference DNA.....	17
2.1.2 Paraffin-embedded human intestine, mamma and bladder tissue.....	17
2.1.3 Anticoagulant treated whole blood	18
2.1.4 Time dependant setup of degrading dried blood spots.....	18
2.1.5 Ancient bone tissue material	19
2.1.6 Genomic sample material of individuals.....	20
2.2 Experimental techniques	20
2.2.1 Temperature measurement	21
2.2.2 Laser-based microdissection	22
2.2.3 Polyacrylamide gelelectrophoresis and DNA silver staining.....	24
2.2.4 Capillary electrophoresis and STR fragment length analysis	25
2.3 Molecular biological methods.....	26
2.3.1 Polymerase chain reaction.....	26
2.3.2 Real-time PCR.....	34
2.3.3 Microarray hybridization.....	37
2.3.4 Solid phase amplification	40
2.3.5 Sequencing of amplified ancient sample material.....	43
2.3.6 Precautions to prevent contamination in ancient sample material analysis	44
3. Description of the Lab-on-a-chip System	45
3.1 Laser microdissection module.....	46
3.2 SPATS particle transfer module.....	48
3.3 CytoCycler PCR module	50
3.4 BioSpot [®] fluid-dispensing module.....	55
3.5 Fluorescence Reader module	58
4. Technical Evaluation of the Lab-on-a-chip System	62
4.1 Reliability of heat transfer.....	62
4.2 Evaluating the minimum amount of target material.....	64
4.3 Ultimate speed of cycling.....	69
4.4 Sensitivity of the Fluorescence Reader	72
4.5 Viability of microarray hybridization	81
4.6 Operability of solid phase amplification	86
5. Applications of the Lab-on-a-chip System in Forensic Sciences	92
5.1 Gender determination of human intestine, mamma and bladder tissue	92
5.2 DNA profiling of whole blood	97
5.3 Nanotechnological analysis of ancient bone tissue material.....	107
5.4 Critical assessment of the analytical power of the lab-on-a-chip.....	124

6. Conclusion and Outlook	128
7. References	129
8. Curriculum Vitae	142
9. Appendix	143
9.1 Laboratory-internal operating procedures	143
9.1.1 LOP of building adsorbing heads for the SPATS	144
9.1.2 LOP of LMD (laser microdissection) & SPATS transfer	147
9.1.3 LOP of LOC chips.....	151
9.1.4 LOP of LV-PCR (low-volume PCR)	159
9.1.5 LOP of BioSpot [®] (PipeJet [™])	164
9.1.6 LOP of Fluorescence Reader.....	174
9.2 Table of oligonucleotides	181
9.3 Material list including source of supplier.....	183

Acknowledgements

I wish to express my gratitude to Prof. Dr. Wolfgang M. Heckl for being my first supervisor, and supporting this interdisciplinary project by means of facilities at the German Museum Munich.

Very special thanks I want to attribute to PD Dr. Stefan Thalhammer for giving me the exciting opportunity to perform this thesis at his lab and to work on this interesting topic, for supervising this work in every step from the beginning and for guiding this project streamlined with support on the biological and technical site. Big thanks also for the chance to attend international conferences and to give talks and present the work there – it was a really great experience for me. Furthermore and most of all thanks for advising me in paper writing skills, support with ideas, for reading the manuscript and teaching soft skills in operating a Mac PC and understanding the secrets behind.

Many thanks to PD Dr. Albert Zink for the great support during the mummy project, for providing the sample material as well as knowledge on ancient DNA analysis.

Thanks to staff from the AG5 Nanoanalytics for inspiring and motivating discussions about research and personal stuff, and especially for a friendship-like working atmosphere. Special thanks to Veronika Mayer, Teresa Neumaier and Anna-Lena Idzko for being more than just colleagues, for easy-going discussions, for enjoyable lunch sessions and most importantly for THE “pizza&cocktail”-evening sessions spent at the L’Osteria and the Sausalitos restaurants... for cheers on “motivation” and cheers on “frustration”! ☺ Thanks also to Veronika Mayer for most helping discussions about biological questions, connections to the MGZ and to sum up the minority of biologists in a group dominated by physicists. ☺ Thanks also to Anna-Lena Idzko for serving and supporting me with the best stress-balancing Cappuccino ever.

I would like to thank Dr. Klaus Wittmaack for reading the manuscript and giving me a lot of helpful suggestions, improvements and corrections. Thanks to Norbert Menzel for help concerning the Fluorescence Reader, support in software related questions and for reading the manuscript. Thanks to Gerolf Lieckfeld for providing perfectly arranged CAD program images and most efficient filming sessions. Thanks to Andreas Schmidt for his support in 3-D stereomicroscopy imaging as well as to Denis Adigüzel for his excellent technical skills in

Acknowledgements

AFM technology and provided images. Thanks to Helmut Niedermaier for technical support concerning the lab-on-a-chip system.

Special thanks go to the Medical Genetic Center (MGZ) for help in STR data analysis, provided equipment and fruitful discussion. I really want to thank the staff from the MGZ for providing always a warm welcome to external students like me, make them feel comfortable in their lab and for trying to help in any possible way they ever could. Thanks to Dr. Ulrike Schön for providing useful information about LV-PCR, AmpliGrids and microarray related support. And most importantly from the technical site I am grateful to Dr. Andreas Laner for a great support and assistance concerning STR analysis as well as being flexible with his working schedules.

Being a collaborative partner during the project I want to thank also Dr. Zeno von Guttenberg from Advalytix AG/Beckman Coulter Biomedical GmbH for all technical support concerning the CytoCycler device, for being always available for questions and problems which occurred especially during the first test phases of the CytoCycler in the beginning of the thesis, as well as for providing LOC chips and supporting probe spotting operations.

Thanks to all the collaborative project partners from the Deutsches Museum Munich, the University Augsburg, Norbert Höhn from XYZ High Precision, Advalytix AG/Beckman Coulter Biomedical GmbH, BioFluidix GmbH and from the Medical Genetic Center (MGZ) for effective efforts to push this interdisciplinary project forward. Thanks also to the Deutsche Forschungsgemeinschaft (DFG, SFB 486), the Bayrische Forschungsförderung (BayFo), the “Nanosystems Initiative Munich (NIM)” and the Center for NanoScience Munich (CeNS) for the great financial support.

And most importantly the biggest and most grateful thanks are dedicated to my family! To my parents, Reinhard and Elvira, and my grandma Lisbeth for always supporting and encouraging me throughout my personal and professional life, for all the understanding in times of trouble and for helpful advices all over! Thanks are addressed to my brother Markus and all my friends as well, for providing enjoyable time outs besides research & lab life.

Publications

Due to reasons of actuality parts of the presented work have been published in international journals and were presented on international conferences.

Peer-reviewed articles

Woide D, Mayer V, Wachtmeister T, Höhn N, Zink A, Köhler U and Thalhammer S. 2009. Single particle adsorbing transfer system. *Biomedical Microdevices* 11(3), 609-614.

Woide D, Zink A and Thalhammer S. 2010. PCR analyses of minimum target amount of ancient DNA. *Am. J. of Physical. Anthropol.* 142(2), 321-327.

Woide D and Thalhammer S. 2010. One step whole blood typing without DNA purification using low-volume PCR. *Biomedical Microdevices*, *submitted*.

Conference articles

Woide D, Mayer V, Neumaier T, Wachtmeister T, Paretzke HG, Guttenberg Z, Wixforth A and Thalhammer S. 2008. Programmable cytogenetic submicrolitre lab-on-a-chip for molecular diagnostic applications. *Biodevices 2008 Proceedings of the first international conference on biomedical electronics and devices Vol 2*, ISBN: 978-989-8111-17-3: 265-271.

Woide D, Mayer V and Thalhammer S. 2008. Non-contact manipulation of single cells. *11th Proc Actuator*, Hanseatische Veranstaltungs-GmbH, Bremen, ISBN-3-933339-11-1, 79-85.

Woide D, Strasser S, Janko M and Thalhammer S. 2008. Nanotechnology - Applications in forensic sciences. *Proceedings FH Linz Science Day*, Linz, Austria, 95-104.

Conference talks

“Programmable cytogenetic submicrolitre lab-on-a-chip for molecular diagnostic applications“, *Biostec 2008, International Joint Conference on Biomedical Engineering Systems and Technologies*, 28-31 January 2008, Funchal, Madeira

“Programmable Lab-on-a-Chip System in Nanomedicine“, *46th Annual Great Lakes Chromosomes Conference*, 15-16 May 2008, Toronto, Ontario, Canada

“Programmable submicrolitre lab-on-a-chip for molecular diagnostic applications“, *Microarrays in Medicine*, 19-20 May 2008, Boston, MA, USA

Conference contributing posters

“Programmable submicroliter lab-on-a-chip for single particle analysis“, *Manipulation von Materie auf der Nanometerskala - Nanoman in a Nutshell (DFG SFB 486)*, 16-19 September 2009, Venice, Italy

List of abbreviations

• λ	Wavelength
• A	Adenine
• aDNA	Ancient DNA
• AFM	Atomic force microscopy
• BLAST	Basic Local Alignment Search Tool
• bp	Base pairs
• C	Cytosine
• CAD	Computer aided design
• CCD	Continuous collision detection
• CE	Capillary electrophoresis
• CMOS	Complementary metal oxide semiconductor
• Ct	Threshold cycle
• d	Day
• DBS	Dried blood spots
• DMEM	Dulbecco's minimal essential medium
• DNA	Deoxyribonucleic acid
• dNTP	Deoxynucleotide triphosphate
• dsDNA	Double-stranded DNA
• EDTA	Ethylendiaminetetraacetic acid
• EDTA K	Potassic EDTA (<i>ger.:</i> <i>Kalium-EDTA</i>)
• EtOH	Ethanol
• G	Guanine
• H ₂ O	Dihydrogen monoxide (water)
• H ₂ O ^{dd}	Double-distilled water
• HF	High frequency
• HGP	Human Genome Project
• IDT	Interdigital transducer
• IgG	Immunoglobulin G
• IR	Infrared
• KOD	<i>Thermococcus kodakaraensis</i>
• kPa	Kilo pascal
• LASER (laser)	Light amplification by stimulated emission of radiation
• LCN	Low copy number
• LED	Light emitting diode
• LiNbO ₃	Lithium niobate
• LOC	Lab-on-a-Chip
• LOP	Laboratory-internal operating procedure
• LV-PCR	Low-volume PCR
• MEMS	Microelectro mechanical system
• μ M	Micromolar
• μ TAS	Micro total analysis system
• mM	Millimolar
• NCBI	National Center for Biotechnology Information
• PAAGE	Polyacrylamide gelelectrophoresis
• PCR	Polymerase chain reaction

List of abbreviations

- PEN Polyethylene naphthalate
- pg Picogram
- PJ PipeJet™
- rfu Relative fluorescence unit
- RT-PCR Real-time PCR
- SAW Surface acoustic wave
- SPA Solid phase amplification
- SPATS Single particle adsorbing transfer system
- ssDNA Single-stranded DNA
- STR Short tandem repeat
- *Taq* *Thermus aquaticus*
- T Thymine
- T_m Melting temperature
- U Unit (enzyme activity)
- VRC Virtual reaction chamber
- v/v Volume per volume

1. Introduction

During the past decade, molecular biologic genetic analysis tended to be performed at a high-resolution level, where only microscopically small amounts of sample material were needed for analysis. In this way, the handling of such small samples needs sophisticated miniaturized tools. The field of developing miniaturized and specified sample processing platforms has a highly interdisciplinary character. A convergence of several disciplines at the nanoscale must be achieved, namely engineering, electronics, informatics, biology, chemistry and physics. In order to find a way for adapting all necessary operations for sample handling onto a small device, one needs to combine technical skills with biological know-how. While a variety of sample materials need to be considered for application, they all need to be tracked down to the basic material used for analysis, which is the DNA molecule. The following paragraphs outline some fundamental knowledge of genetics and DNA analysis. Afterwards an overview is given over the present status of the efforts undertaken to integrate sample-processing steps, in particular the polymerase chain reaction, in microfluidic structures.

1.1 DNA analysis

Over the past years DNA analysis became one of the most fascinating fields of research and gained enormous importance in all areas of life: in ancestry research, prenatal diagnosis and criminalistics, diagnosis of diseases as well as in determination of paternity or natural abilities. Due to the great efforts, which had been made during 1990 and 2003 by the international Human Genome Project (HGP), the information kept in the DNA molecule became especially accessible and usable for well-directed analysis. The primary goal of the HGP was to determine the sequence of the three billion chemical base pairs, which make up human DNA and to identify approximately 30,000-35,000 genes in human DNA (http://ornl.gov/sci/techresources/Human_Genome/home.shtml).

The DNA, which stands for deoxyribonucleic acid (DNA), represents the unique molecule housing the total construction plan of living organisms. Together with structural proteins DNA is organized in complex structures called chromosomes, which are stored in the nucleus, the biggest cellular organelle in eukaryotic cells. Each human cell contains exactly 46 chromosomal DNA molecules differing in size and in their informational content. From the molecular side the DNA molecule is composed of two complementary strands described as double-helix (**figure 1 A**), each consisting of a sugar-phosphate backbone (blue strands in

1. Introduction

figure 1 A) carrying a definite sequence of four nucleotide bases adenine (A), guanine (G), thymine (T) and cytosine (C) (green and violet pairs in **figure 1 A**). These nucleotides, and thus both DNA strands, are connected via hydrogen bonds, while A and T form a dual bond and C and G a triple bond. Solely via the defined sequence of these four nucleotide bases, having a fixed order within three billion base pairs in total, the biologic information of approximately 30,000-35,000 genes is encoded. Genes are defined as domains of the genome that encode specific structural information for building polypeptide chains for the assembly of proteins. Among humans, the nucleotide sequence of each gene is fixed. However, areas encompassing genes coding for proteins comprise just 2% of the whole DNA genome. The information stored in the remaining non-coding 98% of the DNA, also called “junk DNA” (Venter JC *et al.*, 2001), provides no genetic information, does not code for proteins, but contains useful marker loci for DNA profiling, linkage information and recognition sequences for the DNA polymerase enzyme to start replication. The four nucleotides A, T, G and C in these non-coding parts of the DNA are organized in sequences of repeated tandem array modules. Several non-coding elements are known to be located there, for instance pseudogenes, transposons like *Alu* repeats, as well as microsatellite and minisatellite modules, which are simple sequence repeats also known as short tandem repeats (STRs). The number of these repeating units is highly variable among individuals as they inherited differing numbers of these allelic repeat units from their parents.

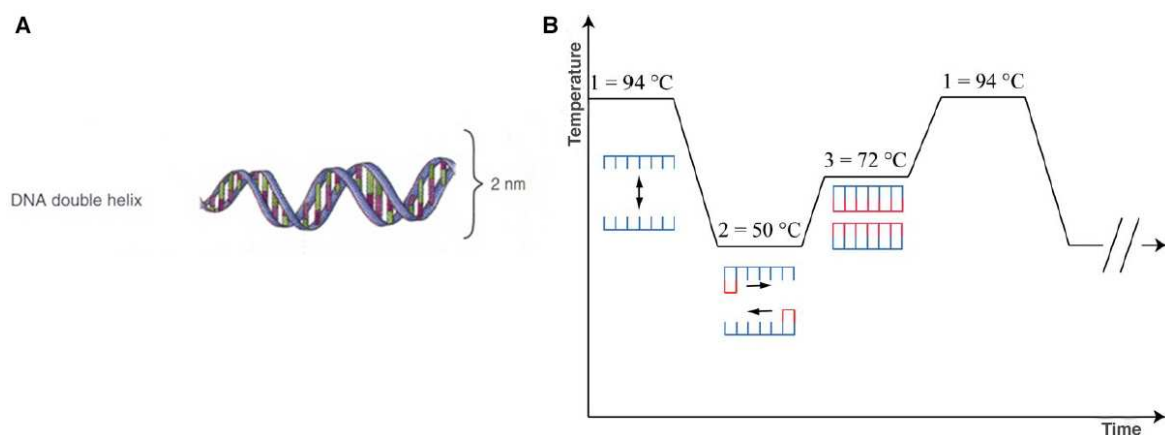


Figure 1. The structure of DNA and the principle of PCR analysis. A) The DNA is a macromolecule shaped in form of a twisted step-ladder named double-helix, which is 2 nm in width. Four nucleotide bases A, T, G, C are arrayed along two complementary strands (blue), bound via hydrogen bonds (two between A and T, three between C and G) and house genomic information. The DNA double helix is further coiled around nucleosomes and then twisted several times in a helical way to pack the amount of information into a single compact molecule (from Mange EJ and Mange AP, 1999). B) Schematic principle of the polymerase chain reaction. One PCR cycle is shown characterized via three particular temperatures effecting amplification. The three important steps are 1) DNA denaturation at 94°C to convert a double- into a single-stranded molecule, 2) primer annealing at 50°C and 3) primer extension to a complementary strand at 72°C by the action of a thermostable DNA polymerase. Repeated cycling for 30-45 times results in an exponential increase in the amount of DNA material that is supposed to be amplified.

1. Introduction

Thus, nowadays, these STR fragments provide the standard method for DNA profiling via a PCR-based method called STR fragment length analysis. DNA profiling kits generally test for 10-16 STR markers and a sex marker. The probability of a stochastic match between unrelated individuals is on average less than one in a billion, which makes DNA profiling very reliable.

There is a wide spectrum of procedures that have been established up to now to analyze genomic DNA, and all these procedures basically follow the same elementary steps. As DNA is stored in the cells of biological sample material, DNA molecules need to be made accessible and must be extracted, purified from cell debris and often concentrated prior to genetic analysis. As usually the amount of isolated DNA is not sufficient for direct detection, an amplification step is mandatory, like e.g. via the polymerase chain reaction.

The technique of polymerase chain reaction (PCR) was one of the greatest scientific discoveries in the last century. It is nowadays one of the most commonly used standard methods applied in modern biomolecular analytics to amplify segments of double-stranded DNA when only a small amount is available. Since its development in 1983 by Kary Mullis, who was honored with a Nobel prize in chemistry in 1993 for that, the PCR has revolutionized molecular biology (Saiki RK *et al.*, 1985; Mullis KB *et al.*, 1994). The PCR is an enzyme-catalyzed process, which makes use of the DNA polymerase, an enzyme catalyzing DNA replication within cells for purposes of DNA duplication and cell division. For performing PCR, besides enzymatic activity also a pair of primers is needed, that flank the DNA fragment that is to be amplified. Primers are short oligonucleotides that are designed to comprise a sequence complementary to the end parts of the DNA segment going to be amplified (Saiki RK *et al.*, 1988). The PCR is a temperature-dependent process, where three steps are mandatory to amplify a template DNA sample, namely denaturation, annealing and extension (**figure 1 B**). As the DNA polymerase can only work on single-stranded molecules, in the denaturation step both DNA strands are separated by overcoming binding forces and breaking the hydrogen bonds between base pairs at 94°C. After denaturation, temperatures between 50-65°C facilitate primer binding for bordering the target sequence. The specific annealing temperature is dependent on the primer length and its composition. This generated short double-stranded sequence provides the fundament for the DNA polymerase to start primer extension at a temperature of about 72°C, synthesizing a complementary DNA segment. Due to the high temperatures especially during the denaturation step, heat-stable variants of the DNA polymerase are utilized, originating from thermophile bacteria, like e.g. the *Taq* DNA polymerase from *Thermus aquaticus* (Saiki RK *et al.*, 1988). Repeated cycling

through these three temperatures, each doubling the amount of DNA theoretically, results in an exponential increase in the number of copies of a specific DNA sequence, relative to the original number of DNA template copies. Due to this exponential duplication, PCR is highly sensitive as theoretically one single DNA strand is sufficient to produce up to 10^{12} identical molecules. Sometimes the annealing and extension steps are combined into one step and performed at the annealing temperature comprising a 2-step PCR procedure in contrast to the generally performed 3-step protocols. During PCR, transition times between temperatures should be kept as short as possible to avoid formation of non-specific byproducts and to reduce the thermal stress on the DNA polymerase. Thus, fast cooling and heating times are mandatory. Since its conception, the PCR has become one of the main laboratory tools in the life sciences, and has revolutionized many applications including molecular biological-, clinical diagnostic-, medical-, biomedical-, forensic-, or agricultural-related analysis (Auroux PA *et al.*, 2002; Auroux PA *et al.*, 2004; Vilknær T *et al.*, 2004; Chen L *et al.*, 2007).

1.2 Micro total analysis systems

During the last decade, the miniaturization of bioanalytical processes has become a broad field of research due to the related enormous advantages. For instance, scaling down analyte volumes saves costs. Improving sample throughput through parallelization and automation is a further major advantage.

Miniaturization became possible by the development of microfabrication technology for generating micro-electro-mechanical-systems (MEMS), which was acquired from the rapidly evolving electronics industry in the early 1990s. This technology allowed the production of microfluidic devices that are capable of handling, manipulating and processing small amounts of liquid. An envisioned integration of all sample-processing steps to one single microdevice established growing interest in this field of research. In the 1990s the term “micro total analysis system (μ TAS)” was introduced describing the idea to operate whole processes on microfluidic platforms serving as a “lab-on-a-chip” (Manz A *et al.*, 1990; Auroux PA *et al.*, 2002; Reyes DR *et al.*, 2002; Vilknær T *et al.*, 2004; Dittrich PS *et al.*, 2006). A μ TAS device was projected being capable of incorporating many macroscale techniques like sample handling, analysis, and detection altogether onto just one single miniature microfluidic instrument. These μ TAS-related features were envisioned to enhance selectivity and sensitivity of analytical performances as well as enabling a more economical consumption of sample material, reagents, chemicals and reaction volumes. Within the last decade, the area of

microfluidic technology associated with μ TAS has been a rapidly developing field (Craighead H, 2006; deMello AJ, 2006; El-Ali J *et al.*, 2006; Janasek D *et al.*, 2006, Whitesides GM, 2006; Yager P *et al.*, 2006). A huge variety of excellent publications concerning μ TAS can be found in literature (for a broad overview see reviews of Reyes DR *et al.*, 2002; Auroux PA *et al.*, 2002; Roper MG *et al.*, 2005; Dittrich PS *et al.*, 2006; Zhang CS *et al.*, 2006; Horsman KM *et al.*, 2007; Zhang C and Xing D, 2007; Chen L *et al.*, 2007; Zhang Y and Ozdemir P, 2009). Almost day after day novel articles concerning miniaturized analysis systems are published online and the area of micro total analysis systems is still growing rapidly.

The rapid development of microdevices over the past decade has pioneered the interest for their application in forensic genetic analysis (Jin LJ *et al.*, 2001; Huang Y *et al.*, 2002; for a broad overview see Horsman KM *et al.*, 2007). In improving the particular macroscale sample processing steps, like e.g. sample preparation, yielding, cell sorting, DNA extraction, DNA quantitation, PCR amplification and DNA separation, microdevices are envisioned to become “the” technology in future forensic DNA laboratories. In this way, microdevices have the potential to revolutionize even forensic DNA testing with state-of-the-art analytical technology. In particular, great effort has been put into the miniaturization of genetic tests (Auroux PA *et al.*, 2004; Kricka LJ and Wilding P, 2003; Zhang C and Xing D, 2007), especially with regard to the miniaturization of the polymerase chain reaction. As the original cellular material available for genetic analysis is often extremely limited, miniaturized PCR gives the advantage of low reagent and sample consumption. Besides microchip PCR, miniaturizing labor-intensive preparative steps of biological material has brought some advancement as well, but still remains a delicate task due to complexity of methods and variety of target sample materials. Comparable efforts have been made in miniaturizing post-PCR product detection methods, like the size-dependent separation of DNA fragments in restriction fragment length polymorphism (RFLP) or STR analysis for purposes like DNA fingerprinting or DNA profiling.

Modular, single-process devices as well as totally integrated microfluidic systems are in development to fill both high-throughput batched and complete single-sample analysis niches. However, the standardization, commercialization and final manifestation of microdevices in forensics will surely take another decade.

1.2.1 Miniaturization of PCR technology

Enormous efforts have been undertaken to integrate the polymerase chain reaction in fluidic microdevices due to its universal importance for fast gene-based analytics and the advantages of miniaturization.

Conventionally, PCR is performed in thin-walled plastic tubes comprising reaction volumes in the range of 2-50 μl , which are inserted into a chambered temperature-controlled metal block for performing material amplification. This setup bears a number of issues being disadvantageous for a fast analysis performance. As not only the PCR mixture needs to be heated up and cooled down, but also the whole chambers, traditional PCR systems are characterized by a large thermal mass, leading to slow heating and cooling rates and lengthy PCR reactions. The key to faster thermocycling was either increasing the heat transfer rate or decreasing the thermal mass, or both. The long transition times and the high power consumption of these conventional bulky systems eliminate the possibility of making a battery-operated and portable PCR system. In addition, the reaction tubes are large and the required amount of PCR reagents makes the whole process expensive. As the detection of PCR products has generally to be done off-line, i.e. in another instrument, additional costs can be listed.

In comparison, the miniaturization of PCR devices offers numerous remarkable advantages over current conventional macroscopic technologies. First, the volume of PCR mixture thermocycled is reduced by several orders of magnitude, having PCR chambers with reaction volumes on the order of microliters to nanoliters. For microchip PCR this means a low reagent as well as sample consumption, decreasing the costs for genetic analysis dramatically. Second, due to the small dimension of microfluidic technology much faster analysis times can be achieved. As just the microchip substrate or the reaction solution undergoes heating and cooling procedures, the thermal mass is reduced massively providing a rapid heat transfer. As cycling rates depend on rapid heating and cooling rates of the device, microdevice PCR benefits with increased speed of thermocycling. Microchip PCR not only affords much shorter assay times, but also favors less power consumption and a great potential of integrating multiple processing modules for high-throughput purposes. High-throughput is one of the most important issues in fabricating PCR microdevices. As most conventional thermocyclers hold 24 to 96 polypropylene tubes, multiple PCR chambers for simultaneous reactions (most importantly positive and negative controls) and multiplex amplifications must also be integrated into microchip PCR devices.

Besides these quantitative advantages, analytical microchips offer further significant benefits over existing methods concerning quality of analysis. Due to the dramatic decrease in reaction volumes, these include enhanced analysis sensitivity and efficiency as well as increased quality of assays with respect to sample tracking and reproducibility due to the potential of automation (Auroux PA *et al.*, 2002; Reyes DR *et al.*, 2002; Vilkner T *et al.*, 2004; Dittrich PS *et al.*, 2006). Decreased sample handling due to automation of nearly all necessary processes, from sample preparation to outcome of analysis results, is also a remarkable attribute. This is a key feature particularly for the forensics community, providing less facility for sample contamination during processing steps. In order to eliminate cross-contamination between samples, the safest way is by using a disposable system (as reported and realized by Neuzil P *et al.*, 2006 (a+b)), while at the very least the part of the device, which comes into contact with the sample, should be disposable. A further attractive feature of miniaturized PCR is its portability, making it useful for in-the-field analysis.

Despite an enormous number of published and patented PCR microchips and miniaturization methods for integrating PCR into microdevices, only a few of them have been commercialized (Kricka LJ and Wilding P, 2003). One example is the miniature analytical thermal cycling instrument (MATCHI) (Ibrahim MS *et al.*, 1998; Northrup MA *et al.*, 1998). However, the market for PCR-on-chip systems is still triggered by the increasing demand for such systems in molecular diagnostics, for applications such as blood screening for infectious diseases, but also for forensics, paternity, food-safety, agri-diagnostics and veterinary applications.

1.2.2 Modes of microchip-based PCR

Numerous designs of PCR microdevices became popular varying in basic chip substrates (Reyes DR *et al.*, 2002), surface treatments to prevent sticking of biomolecules, chip architectures and purposes of being modular systems or integrated ones. The architecture of a microdevice is certainly the most important feature as it defines its function, reaction speed, reaction volume and the sequence of actions taking place on the device. Some devices were just concentrating on on-chip preparative steps, while PCR analysis of sample material was performed off-chip. Others just focused on on-chip PCR followed by on-chip detection methods like e.g. capillary electrophoresis or microarray, while applying pre-purified DNA sample material. The technically most challenging lab-on-a-chip devices integrated all sample processing steps. A review about these features was provided by Zhang C and Xing D (2007). Concerning the architecture, three modes of microchip PCR technologies have been

1. Introduction

established for fitting to a small chip. 3-dimensional approaches were realized as a) stationary cavity-based or b) continuous flow-through devices, while a 2-dimensional solution was provided in c) virtual reaction chamber-based ones. All three methods comprise special developed chip architectures, including various designs of PCR chambers and heating technologies (**figure 2**). The three modes of microchip-based PCR technology are described in brief in the following paragraphs.

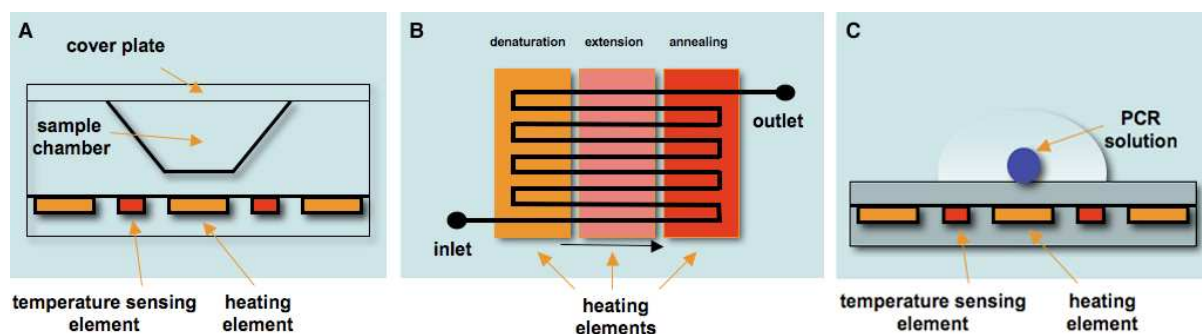


Figure 2. Modes of performing microchip PCR. A) Stationary chamber-based PCR. The PCR sample is thermocycled via heating the whole chamber. B) Continuous-flow or flow-through PCR. The PCR sample is thermocycled via being pumped along an unidirectional channel system through different temperature zones. C) Virtual reaction chamber PCR. The PCR sample is thermocycled via heating the chip surface locally. Figures were adapted from Thalhammer S (2009).

a) Stationary cavity- or chamber-based PCR microdevices. Stationary cavity-based PCR is performed in single or multiple miniaturized PCR chambers. The PCR solution is kept stationary within the cavity, while the temperature of the reaction chamber is cycled between PCR relevant temperatures. The first chamber-based PCR microdevice was presented by Northrup MA *et al.* (1993), followed by several similar approaches (Wilding PJ *et al.*, 1994; Waters LC *et al.*, 1998; Lagally ET *et al.*, 2001). In the following years, simple functions on microfabricated devices have been reported that can perform analysis of nucleic acids (Yang J *et al.*, 2002; Sethu P and Mastrangelo CH, 2004; Chung YC *et al.*, 2004) as well as detection of pathogenic bacteria and genotyping (Liu RH and Grodzinski P, 2003; Liu RH *et al.*, 2004; Liu Y *et al.*, 2003; Lagally ET *et al.*, 2004; Lagally ET *et al.*, 2001). The most straightforward stationary cavity-based PCR approaches fabricated integrate an array of reaction chambers of micro-, nano- or even picoliter volumes for parallel PCR reactions (Burns MA *et al.*, 1998; Krishnan M *et al.*, 2004; Lee DS *et al.*, 2004; Liu J *et al.*, 2003; Northrup MA *et al.*, 1998; Woolley AT *et al.*, 1996). Recently, a channel-based three-dimensional arrayed micro droplet-in-oil microfluidic easy-to-handle PCR platform was introduced by Zhang Y *et al.* (2009). It was used as efficient tool for DNA analysis, performing 108 reactions in parallel. A distinct advantage of stationary systems is the fact that only the temperature of the chamber needs to be cycled in order to modify the temperature of the PCR solution, while an external

pumping system or other means to move the PCR sample around are not required. However, due to complex architectures, very complicated microfluidic control modules were usually incorporated. These require experienced operational skills and thus are difficult to handle as well as difficult to fit into routine biological laboratories and clinical settings. Additionally, heating the whole chamber is quite disadvantageous, as that attributes a large total thermal mass to these PCR chips and heat transfer from the heater to the sample is a limiting factor for fast systems.

b) *Continuous flow-through PCR microdevices.* This mode of microchip PCR features a dynamic process, where the solution is continuously pumped through a microfluidic channel system into differently heated temperature zones. The first flow-through PCR device was introduced in 1994 (Nakano H *et al.*, 1994) and has been refined in subsequent approaches (Kopp MU *et al.*, 1998; Köhler JM *et al.*, 1998; Chiou J *et al.*, 2001; Liu J *et al.*, 2002; Chen ZY *et al.*, 2004; Hashimoto M *et al.*, 2004; Wang H *et al.*, 2006; Mohr S *et al.*, 2007). The latest developments of continuous-flow microfluidic PCR are summarized in a review of Zhang Y and Ozdemir P (2009).

The prominent advantage of flow-through systems is that they typically comprise zones at three constant temperatures, so that only the sample needs to change temperature by moving between zones. In this way the thermal mass is reduced to a minimum and cycling can be performed at high speeds. Based on this principle, an elegant solution was provided by infrared radiation (IR) as heat source (Oda RP *et al.*, 1998; Hühmer AFR and Landers JP, 2000; Giordano BC *et al.*, 2001 (a)). The IR light source was used to selectively heat the water in solution rather than the microdevice substrate, resulting in extremely rapid cycling times. The type of flow-through PCR is faster than the first one, but it requires an implementation of a mechanism to move the sample around. In both cases, the heaters are integrated with the PCR system, so it is not economical to dispose the device to avoid cross-contamination after performing only a single test. Another prominent disadvantage is the requirement of an external bulky syringe pump for moving the fluid, which negatively affects the development of compact, portable and integrated continuous-flow PCR chips. Additionally, high fabrication cost and difficulties controlling the continuous liquid flow have been reported, and parallelization cannot easily be realized as it complicates chip architecture.

c) *Virtual reaction chamber PCR microdevices.* In virtual reaction chamber (VRC) PCR devices, miniaturization is realized by performing PCR in free micro droplets on chemically modified surfaces. Using a hydrophobic and oleophobic structured planar surface providing

1. Introduction

fluid confinement, small-scale droplets themselves function as virtual test tubes held together by surface tension of the liquid and surface chemistry of the substrate. To prevent evaporation and cross-contamination, droplets are covered by mineral oil in an old-fashioned way. The first virtual reaction chamber PCR device was introduced in 2005 (Guttenberg Z *et al.*, 2005), which has been advanced in several ways (Neuzil P *et al.*, 2006 (a); Neuzil P *et al.*, 2006 (b); Pippner J *et al.*, 2007; Pippner J *et al.*, 2008). Actuating droplets on the planar surface rely on electrowetting (Srinivasan V *et al.*, 2004), dielectrophoresis (Gascoyne PRC *et al.*, 2004), (electro-)magnetic forces in combination with superparamagnetic particles (Lehmann U *et al.*, 2006), or surface acoustic waves (Guttenberg Z *et al.*, 2005).

An open and planar PCR microdevice excels a lot of advantages over conventional 3-dimensionally fabricated devices, following practicability issues. 1) While stationary chamber and flow-through PCR devices have complex three-dimensional architectures and are based on complicated MEMS processes, a planar VRC PCR device can be fabricated much simpler. 2) Especially the manipulation of individual droplets on a planar surface offers an attractive option for μ TAS devices with regard to flexibility purposes. The open chamber design provides easy access to surface modification and post-PCR sample retrieval for downstream analysis. 3) As the majority of micro PCR chips comprise closed chamber systems, requiring filling up the entire reaction chamber with reaction mixture, the reaction volume is indispensable defined by the chamber size once the device is fabricated. In open, planar, virtual reaction chamber devices, the reaction volume can be further reduced using the same device (Guttenberg Z *et al.*, 2005). 4) As reaction droplets are completely isolated from contaminating environmental influences due to hydrophobic coverage, the chance of contamination is minimized. 5) The temperature control box can be physically separated from the PCR reaction chip and reused, so that just the microchip needs to be replaced for each new reaction (Neuzil P *et al.*, 2006). Such kinds of disposable PCR chips are the most straightforward approach in order to eliminate sample-to-sample cross-contaminations in PCR microdevices. Since 2005, this slide-based virtual reaction chamber microPCR technology has been optimized for parallel processing, and became also known as low-volume PCR. Via chemical surface treatment 48-60 hydrophilic PCR reaction spots were generated on one single glass slide and arranged in an array-like manner. Several applications of this low-volume PCR based devices were reported, mostly employed in the forensics field of research (Proff C *et al.*, 2006; Schmidt U *et al.*, 2006; Lutz-Bonengel S *et al.*, 2007; Schmidt U *et al.*, 2008).

1.3 Scope of this work

When starting this work the presented lab-on-a-chip comprised two stand-alone units, a laser microdissection module for sample retrieval and a planar chip-based DNA amplification unit operating the virtual reaction chamber PCR technology. In course of this thesis, the two basic modules were combined to a whole modular lab-on-a-chip system by adding three more units (in collaboration with cooperative project partners). The implemented modules include a transfer system for loading the analysis chips of the DNA amplification unit with microdissected sample material, a PCR product detection unit and an automatic fluid dispensing device serving the planar analysis chip.

After integration, the aim of the presented work was to test the developed modular lab-on-a-chip system for its use in forensic genetic DNA analysis. The focus was to identify the smallest amount of sample material allowing for a fast, reliable and sensitive analysis. Furthermore, the analytical procedures for operating at the minimum level of contamination had to be explored. These features are especially important in forensic genetic DNA analysis, in which case the amount of available sample material is often very small. The approach described here also serves to minimize the time and cost of analyses.

2. Materials and Methods

2.1 Sample materials and preparation

In the following short paragraphs all kinds of sample materials utilized for genetic analyses are summarized. The particular procedures of sample preparation prior to analysis are described as well.

2.1.1 Male and female human genomic reference DNA

Male and female control DNA was extracted using the peqGOLD Tissue DNA Mini Kit (PeqLab Biotechnologie GmbH, Erlangen, Germany) to provide purified DNA material serving as reference samples. Female DNA was extracted from HeLa cells (cultivated in DMEM medium and kindly provided by a collaborative laboratory of the Ludwig-Maximilians-University, Munich, Germany), while male DNA was extracted from a fresh heparin-treated male blood sample originating from a laboratory member. DNA extraction was performed according to the respective protocols for blood or cultured cells, recommended by the manufacturer. Concentration of purified eluates was measured via UV spectrophotometry (NanoDrop[®] ND-1000, PeqLab Biotechnologie GmbH, Erlangen, Germany) and reached values from 291.1 ng/μl to 459.5 ng/μl concerning the female reference sample and values from 5 ng/μl to 10 ng/μl concerning the male reference sample. Using sterile water for dilution (Ampuwa[®], Fresenius, Bad Homburg, Germany), small aliquots of male and female reference DNA were prepared to known concentrations of 100 ng/μl, 10 ng/μl, 5 ng/μl and 1 ng/μl and stored in sterile 0.5 ml PCR-tubes (Eppendorf AG, Hamburg, Germany).

2.1.2 Paraffin-embedded human intestine, mamma and bladder tissue

Eight tissue samples of three human tissues were examined and were derived from male and female individuals. Tissues originated in one case from bladder tissue (named tissue3), in one case from mamma tissue (named tissue6) and in 6 cases from intestine tissue of individuals (named tissue1, tissue2, tissue4, tissue5, tissue7 and tissue8). Tissue pieces of about 2x2 cm in diameter were embedded into square paraffin blocks. Microtome-cut tissue sections of 2-4 μm were placed on an ultra thin 2 μm polyethylene-naphthalate laser supporting carrier

2. Materials and Methods

membrane (PEN), mounted on 1.00 mm thick standard microscope object slides (MicroDissect GmbH, Herborn, Germany). These paraffin-embedded tissue sample slides were kindly provided by the Institute of Pathology (Klinikum Bogenhausen, Munich, Germany). Deparaffinization was achieved by xylene incubation (Merck KGaA, Darmstadt, Germany) for 30 min and subsequent decreasing alcohol series (100% EtOH for 5 min, 90% EtOH for 2 min and 70% EtOH for 2 min; Merck KGaA, Darmstadt, Germany) at room temperature. After drying, tissue material, fixed on 2 µm PEN carrier membrane coated slides, was used for laser microdissection.

2.1.3 Anticoagulant treated whole blood

Whole blood samples from four individuals were examined, two male (named 1 and 2) and two female ones (named 3 and 4). Blood specimens were collected into EDTA K treated blood collection tubes (Monovettes, SARSTEDT AG & Co., Nümbrecht, Germany), to inhibit blood clotting and coagulation. Small 100 µl aliquots of 100% whole blood and 10% blood (v/v), diluted with sterile water (Ampuwa[®], Fresenius, Bad Homburg, Germany), were stored in sterile 0.5 ml PCR-tubes (Eppendorf AG, Hamburg, Germany). Consistently 0.1 µl of 100% and diluted 10% whole unpurified blood samples was used per 1 µl LV-PCR reaction volume, resulting in final dilutions of 10% and 1% blood (v/v) per reaction.

2.1.4 Time dependant setup of degrading dried blood spots

Whole blood specimens from a female individual were collected into conventional plastic syringes (Becton Dickinson GmbH, Heidelberg, Germany), without adding anticoagulants. Immediately after extraction, several blood spots of 1 µl of volume were spread onto pre-cleaned and decontaminated object slides (Carl Roth GmbH, Karlsruhe, Germany) and dried at room temperature. Before use, object slides were cleaned with 70% EtOH (Merck KGaA, Darmstadt, Germany) and decontaminated using a UVC light source (PCR Workstation, PeqLab Biotechnologie GmbH, Erlangen, Germany) for at least 60 min. For analysis, samples of dried blood spots were taken after 0 min, 30 min, 60 min, 120 min, 6 h, 24 h, 2 days, 4 days, 7 days, 2 weeks, 3 weeks, 4 weeks and 3 months. For sample take-up, single dried blood spots of 1 µl were resolved in 10 µl of sterile water (Ampuwa[®], Fresenius, Bad Homburg, Germany) on the surface of the object slide. Final dilutions of 10% blood (v/v) were transferred into sterile 0.2 ml PCR-tubes for storage (Eppendorf AG, Hamburg, Germany).

2. Materials and Methods

Using consistently 0.1 µl of this diluted 10% blood samples for analysis resulted in a final dilution of 1% blood (v/v) per 1 µl LV-PCR reaction volume.

2.1.5 Ancient bone tissue material

Bone tissue samples from four ancient Egyptian mummies of the ‘Mummy Collection of Munich’ were examined and derived from an independent laboratory after anthropological and archaeological study. The mummies originally originated from the so-called ‘Tombs of the Nobles’, the huge necropolis of Thebes-West that had been mainly built during the New Kingdom (NK) (c. 1550 – 1070 BC) and which had been used during the Third Intermediate Period (TIP) until the Late Period (LP) (ca. 500 BC). According to the collection records, the long bones originated from mummies found in four different tombs of the necropolis of Thebes-West. The four specimens were all long bone samples and comprised of a fibula (named mummy1), a distal part of a tibia (named mummy2), a distal part of a humerus (named mummy3) and a tibia diaphysis (named mummy4).

Paraffin-embedded ancient bone tissue material. Bones were first cleaned with sodium hypochlorite (0.5% solution) and subsequently the outer surface was removed mechanically with appropriate sterile tools. To avoid external contamination, several tissue samples were taken exclusively from the inner parts of the bones in a nested way using sterile blades. A tissue block from each of the four bone samples was removed and subsequently rehydrated (Parsche F and Nerlich A, 1997). For paraffin-embedding procedures, decalcification of bone particles was achieved by 0.1 M EDTA-solution, pH 7.4, followed by post-fixation with 4% buffered formaldehyde. After paraffin-embedding of nested isolated tissue blocks, sections of 3-5 µm in size were cut via microtome and placed on a 2 µm ultra thin polyethylenephthalate (PEN) laser supporting carrier membrane, mounted on 0.17 mm thin microscope cover glass slides (MicroDissect GmbH, Herborn, Germany). Prepared paraffin-embedded bone tissue sample slides were kindly provided by the Institute of Pathology (Klinikum Bogenhausen, Munich, Germany). Deparaffinization was achieved by xylene (Merck KGaA, Darmstadt, Germany) incubation for 30 min and subsequent decreasing alcohol series (100% for 5 min, 90% EtOH for 2 min and 70% EtOH for 2 min; Merck KGaA, Darmstadt, Germany) at room temperature. After drying, sample material, fixed on 2 µm PEN carrier membrane coated slides, was used for laser microdissection.

DNA extracts from pulverized ancient bone tissue material. Bones were first cleaned with sodium hypochlorite (0.5% solution) and subsequently the outer surface was removed mechanically with appropriate sterile tools. Bone particles of the four bone samples were pulverized using a mixer mill (MM200, Retsch, Haan, Germany). Pulverized bone specimens were subjected to conventional pathological DNA extraction (Zink A *et al.*, 2003). DNA extraction was tested by UV spectrophotometry (NanoDrop[®] ND-1000, PeqLab Biotechnologie GmbH, Erlangen, Germany), measuring the DNA concentration of extracted mummy DNA material. DNA amounts of 2.1 to 10.0 ng/ μ l were measured from 1 g of pulverized bone tissue. Amounts of 50 pg respectively 100 pg of this conventionally extracted mummy DNA material were used for LV-PCR analysis.

2.1.6 Genomic sample material of individuals

Genomic sample material was extracted from scientific staff for DNA profiling purposes in anticipation of introduced external contaminating events, in particular in regard to ancient sample materials. Saliva samples were taken from archaeologist/excavator of Egyptian mummy material, technical assistance staff, laboratory members and involved scientists, simply all people who have been knowingly in contact with laboratory equipment and consumables and any kind of mummy material used. In the following these individuals are termed ‘scientific staff’. Sample material of scientific staff as potential contaminants was extracted from saliva via sterile cotton buds (Nuova Aptaca, Canelli (AT), Italy) and dried for 20 min at 37°C. To isolate DNA out of dried saliva samples the First-DNA All-tissue DNA kit (Gen-ial, Troisdorf, Germany) was used according to the manufacturer’s protocol. To release saliva cell material from cotton buds, tips of cotton buds were transferred into 450 μ l of lysis solution. Finally, pellets were diluted with sterile water (Ampuwa[®], Fresenius, Bad Homburg, Germany) to a final volume of 20 μ l. For DNA typing reactions of scientific staff, 1 μ l of these DNA extracts was used in LV-PCR analysis.

2.2 Experimental techniques

The following sections summarize all techniques that were used for processing sample materials. Pre-PCR and post-PCR applications are described as well as all kinds of hardware devices utilized.

2.2.1 Temperature measurement

Temperature measurements were performed on the CytoCycler PCR module of the lab-on-a-chip system to test for heat transfer capabilities. The CytoCycler and its components were fabricated by the company Advalytix AG/Beckman Coulter Biomedical GmbH (Munich, Germany). It was a module of the lab-on-a-chip (LOC) system and provided the basis for performing PCR analysis. It comprised a chip-holder including a cavity for installing LOC chips, a temperature control device, a high frequency (HF) generator (FC 1201 HF) serving as SAW control device as well as particular software for programming PCR protocols.

Temperatures for thermal cycling were provided by a Peltier element, controlled via the appropriate software “CytoCycler” (Advalytix AG/Beckman Coulter Biomedical GmbH, Munich, Germany). To validate the temperature transfer from the Peltier element to LOC chip surface, temperature measurements were carried out using an adapted measurement LOC chip. The measurement LOC chip comprised a Pt100 temperature sensor fixed on the LOC chip surface, exactly positioned on reaction center B, centered to the middle of the Peltier element when implemented into the chip-holder. Connected to a temperature measurement device (Präzisionsthermometer GMH 3710, Greisinger electronic GmbH, Regenstauf, Germany), the heat transfer from the Peltier element through the glass substrate to the surface of the measurement LOC chip was analyzed. On the one hand, increasing temperatures steps comprising a temperature increment of +5°C per step were measured, starting from 25°C to 105°C. Each temperature was kept for a hold time of 30 sec, before raised to the next temperature level. On the other hand, temperature steps and hold time of each temperature were measured in a way relevant for PCR analysis, simulating repeated PCR temperature cycling. Starting at 95°C for 10 min, the measurements were continued by 3 to 5 cycles of the representative temperatures 94°C, 60°C and 72°C, each kept for a hold time of 30 sec. The duration of temperature steps was controlled using an alarm timer in parallel. Comparing input temperature of the software and output temperature of the temperature measurement device, differing temperatures were adapted in the software to fit the output. Data was evaluated by using graphically software (OriginPro 7.5 SR0, OriginLab Corporation, Northhampton, MA, USA). The latter measurements simulating thermal PCR cycling were performed on the AmpliSpeed slide cycler as well (Advalytix AG/Beckman Coulter Biomedical GmbH, Munich, Germany). In all applications of the lab-on-a-chip system, the AmpliSpeed slide cycler was used as reference LV-PCR device, validating the results of the LOC CytoCycler as providing reference, negative and positive controls. Measurements were repeated several times for validation.

2.2.2 Laser-based microdissection

Recovery and isolation of sample material out of paraffin-embedded fixed biological material was achieved by laser-based microdissection using a modified UVA-laser system (CryLaS GmbH, Berlin, Germany) integrated into an inverted optical microscope (Axio Observer.Z1, Carl Zeiss GmbH, Jena, Germany), based on the basic principle reported by Thalhammer S *et al.* (2003) and Thalhammer S *et al.* (2004).

Specimens and biological material destined for laser microdissection were applied directly onto a 2 µm ultra thin polyethylene-naphthalate (PEN) laser supporting carrier membrane. The PEN membrane was mounted on 0.17 mm thin microscope cover glass slides or on 1.00 mm thick standard microscope object slides (MicroDissect GmbH, Herborn, Germany) serving as supporting backbone for cutting and isolation of material while lowering adhesion forces. Before utilization, PEN membrane coated slides were decontaminated in a sterile environment by treatment with ultraviolet light using a UVC light source (PCR Workstation, PeqLab Biotechnologie GmbH, Erlangen, Germany) for at least 30 min, in order to exclude DNA contamination. Microdissection operations were optically controlled by either a color firewire camera (PixeLINK, BFI Optilas, Munich, Germany) or a black & white CCD camera (Rolera-XR, QImaging, Surrey BC, Canada) and appropriated software (QCapture Pro 6.0, QImaging, Surrey BC, Canada). The laser energy as well as the laser focus was regulated exactly to the focal plane of the PEN carrier membrane, providing a thin and sharp cutting line without scattering. When 0.17 mm thin microscope cover glass slides were used, the numerical aperture of the objective was adjusted to 1.5 for tuning the laser focus to the focused object plane. The numerical aperture was set to 1.0 when 1.00 mm thick standard microscope object slides were used. Biological material of interest was visualized using 5x, 10x, 40x or 63x magnifying objectives. For microdissection, the pulsed laser beam was directed from below through the objective lens and the microscope glass slide to the PEN membrane, on which the sample resided. Using 0.5-0.6 µJ/pulse laser energy, sample material of interest was separated from its surrounding by moving the microscope XY-stage and ablating unwanted material. Extraction blanks, microdissecting PEN carrier membrane devoid of sample material, were always included in every procedure.

After laser microdissection isolated material was extracted and transferred via a low-pressure operated transfer device named SPATS (single particle adsorbing transfer system) (XYZ High Precision, Darmstadt, Germany), integrated at the microscope. The SPATS provided a totally new approach for controlled horizontal material transfer after laser microdissection directly onto any planar microdevice (Woide D *et al.*, 2009; EU patent 08150662.8). The SPATS

2. Materials and Methods

device consisted of a copper collection grid, having a diameter of 500 μm . The grid was attached to a transparent glass capillary tube, comprising the adsorbing head. The glass capillary tube was fixed to a carrier device, providing both a connection to a micrometer step motor for XY-directed movements and a connection to a pressure-supplying pneumatic picopump (PLI-100 pressure control unit, Harvard Apparatus, Holliston, US). For contamination reasons, adsorbing heads were exchanged for every single isolation procedure, when sample material was diverse. Otherwise, grids were cleaned by 70% EtOH (Merck KGaA, Darmstadt, Germany) treatment and decontaminated using a UVC light source (PCR Workstation, PeqLab Biotechnologie GmbH, Erlangen, Germany) for at least 30 min when a new procedure on the same sample material was started. Via the micrometer step motor the low-pressure transfer device SPATS was fixed to the inverted optical microscope used for microdissection purposes (Axio Observer.Z1, Carl Zeiss GmbH, Jena, Germany).

Biological material destined for SPATS transfer was mounted on 2 μm ultra thin PEN carrier membrane mounted glass slides (MicroDissect GmbH, Herborn, Germany), as already described for laser microdissection. The PEN carrier membrane served as carrier substrate, favoring SPATS-mediated particle transfer out of surrounding material while keeping adhesion forces of the subjacent glass slide at a minimum. For sample uptake, the adsorbing head was approached to the sample surface keeping a distance of about 100 μm or less. The collection grid was centered to the sample shape for optimal sample uptake. Applying low-pressure (0–0.75 kPa) adsorbed single particles to the collection grid, while grid-directed low-pressure suction needed to surpass adhesion forces of the glass slide surface. Dissected particles in the range of 5–500 nm were selectively be adsorbed under optical control. Smaller particles fell below the diameter of the grid meshes, and larger ones exceeded the visible adsorption zone. For transfer, the adsorbing head was raised up again and moved vertically and horizontally to a desired, predefined unloading position. During material transfer low-pressure was maintained to avoid losing the sample. Release of sample material was controlled with μm -precision either onto the surface of any planar analysis microdevice or into a tube. Release was managed by approaching the grid to about 100 μm to the surface predefined for sample release and simply switching from low-pressure operation to a short high-pressure impulse (413 kPa, 2 milliseconds). After release, sample material was available for further biochemical processing. Optimally, sample unloading was performed into a small volume of fluid, prepared on the surface supposed for sample release. Droplet volumes on planar chip surfaces for sample uptake ranged between 0.2–1.0 μl , while sterile water as well as directly PCR reaction mix was used. By this means sample material was adsorbed,

2. Materials and Methods

transferred and released in a highly precise, safe, reliable and gentle way at a predefined, designated position on a planar surface.

Laser microdissection and transfer of human intestine, mamma and bladder tissue material. Small tissue particles of about 500 μm in diameter were microdissected and then isolated out of tissue sections and transferred via the SPATS device. Sample material was transferred onto a planar multi LV-PCR microdevice comprising 48 hydrophilic reaction sites for performing virtual reaction chamber PCR (AmpliGrid™ AG480F, Advalytix AG/Beckman Coulter Biomedical GmbH, Munich, Germany). Sample material was released directly into 0.5 μl of sterile water (Ampuwa®, Fresenius, Bad Homburg, Germany) prepared on hydrophilic reaction sites and dried at room temperature for subsequent LV-PCR analysis. In an analogous manner, sample material was applied to the hydrophilic reaction center B of LOC chips and directly released into 1.0 μl of LV-PCR master mix.

Laser microdissection, particle transfer and DNA extraction from ancient Egyptian mummy bone tissue material. Single osteon areas in the range of 350 μm in diameter were microdissected, and then isolated out of bone tissue material and transferred via the SPATS device. Osteon bone particles were released directly into a sterile 0.5 ml PCR-tube (Eppendorf AG, Hamburg, Germany) containing 112.5 μl of lysis solution for subsequent DNA extraction using the First-DNA All-tissue DNA kit (Gen-ial, Troisdorf, Germany) according to the manufacturer's protocol. In a final step, extracted DNA was pelleted and resolved in 10 μl of sterile water (Ampuwa®, Fresenius, Bad Homburg, Germany) serving as total extraction solution. Concentration of extracted ancient DNA was about 60 $\text{pg}/\mu\text{l}$ as measured using real-time PCR (**chapter 2.3.2**). Amounts of 60 pg of the extracted mummy DNA material were used for LV-PCR analysis.

2.2.3 Polyacrylamide gelelectrophoresis and DNA silver staining

Horizontal polyacrylamide gelelectrophoresis (PAAGE) followed by DNA silver staining was used for standard detection of PCR products. Via polyacrylamide gelelectrophoresis, charged molecules were separated according to their size. Due to their charge these molecules were forced to migrate through the polyacrylamide gel, serving as support medium, in an electric field under controlled conditions of temperature, pH, voltage, and time. As PCR products were negatively charged due to the sugar-phosphate backbone of DNA, migration happened towards the anode and PCR fragments were separated according to their size-dependant

2. Materials and Methods

charge. For PAAGE precast 10% polyacrylamide DNA gels (CleanGel 10% or CleanGel HyRes, ETC GmbH, Kirchentellinsfurt, Germany) were utilized. Before use, gels were rehydrated in appropriate buffers: 10% CleanGels for 1.5 h in Delect Gel Buffer and HyRes CleanGels for 2.0 h in DNA HyRes Buffer (ETC GmbH, Kirchentellinsfurt, Germany). PAAGE was performed using a horizontal gel electrophoresis device (GenePhor electrophoresis unit, Amersham Biosciences Europe GmbH, Freiburg, Germany), a power supply (Electrophoresis Power Supply EPS 601, Amersham Biosciences Europe GmbH, Freiburg, Germany) and appropriated anode and kathode buffers, provided with the CleanGels by the manufacturer: (-) Delect Cathode Buffer and (+) Delect Anode Buffer for 10% CleanGels and (+/-) DNA HyRes Buffer for HyRes CleanGels. Using 10% CleanGels electrophoretic separation was performed using 580 V for about 60 min. Settings for HyRes CleanGels were 180 V for 40 min followed by 360 V for about 60 min.

For DNA staining via silver nitrate a prepared silver staining system was used (DNA silver staining kit, GE Healthcare, Uppsala, Sweden). According to the manufacturer's protocol, CleanGels were first incubated in 1x Fixing Solution (35 min for 10% CleanGels, 45 min for HyRes CleanGels), washed 3x for 10 min in H₂O^{dd}, incubated in 1x Staining Solution (35 min for 10% CleanGels, 45 min for HyRes CleanGels), washed 2x for 1 min in H₂O^{dd}, followed by applying 1x Developing Solution (time depended on the staining grade) and final incubation for 30 min in 1x Stopping & Preserving Solution. Stained CleanGels were scanned for documentation and sealed in plastic bags for long time storage.

2.2.4 Capillary electrophoresis and STR fragment length analysis

Fully automated capillary electrophoresis (CE) was used for fast and sensitive separation of PCR amplified STR fragments for genetic profiling purposes. Short tandem repeats (STRs), located in non-coding DNA domains, are short sequences of DNA which are repeated in tandem several times, while the number of repeats varies between complementary DNA strands and between individuals. In CE, small-diameter capillaries, a little larger than the width of a human hair and about 20 centimeters in length, are used to separate the various STR fragments due to electroosmotic flow. The surface of the capillary contains negatively charged functional groups, while positively charged ions migrate towards the negative electrode and carry solvent molecules in the same direction. Positively charged ions move faster and negatively-charged ones slower, thus separation of PCR products happens via their size-dependant charge. Due to fluorescently labeled STR primers amplified DNA fragments are fluorescently tagged and excited by a laser beam. As data analysis is performed by a

2. Materials and Methods

computer with appropriate software, capillary electrophoresis allows a higher resolution than gel electrophoresis, a greater sensitivity and on-line detection of PCR products, displayed as electropherograms.

PCR reactions of amplified STR fragments were diluted 1:5 with sterile water (Ampuwa[®], Fresenius, Bad Homburg, Germany). An aliquot of 1 μ l of this dilution was mixed with 12.7 μ l of Hi-Di[™] Formamide (Applied Biosystems GmbH, Darmstadt, Germany) and 0.3 μ l of GeneScan[™]-500LIZ[™] size standard (Applied Biosystems GmbH, Darmstadt, Germany) in a 96-well plate (ABgene[®] PCR Plates, Thermo Scientific, Epsom, Surrey, UK). In experimental setups using the AmpF/STR[®] SEfiler[™] PCR amplification kit, 1 μ l of the AmpF/STR[®] SEfiler[™] Allelic Ladder (Applied Biosystems GmbH, Darmstadt, Germany) was run in parallel. Amplified STR fragments were analyzed via a 3130xL Genetic Analyzer (Applied Biosystems GmbH, Darmstadt, Germany). Data was either interpreted using GeneScan[™] 3.7 software in combination with Genotyper[™] 3.7 software for EDTA K treated blood samples, Egyptian mummy and scientific staff samples, or using GeneMapper[®] ID v.3.2 software for dried blood spot analysis (Applied Biosystems GmbH, Darmstadt, Germany). The signals of the fluorescent dyes incorporated into each amplicon through a 5'-end labeled oligonucleotide primer, was a measure of quantity of the amplified target. Sample peak heights, in relative fluorescent units (rfu), of all true alleles were used for quantitative analysis and heterozygous peak ratio calculations. The minimum peak height threshold was set at 50 rfu to allow for detection of all peaks clearly above background. This mode of data analysis, that signals below 50 rfu were not evaluated, is accepted as general accreditation-threshold, validating authentic marker peaks.

2.3 Molecular biological methods

In the following sections utilized molecular biological reactions are summarized. All kinds of PCR analyses performed, especially the application of low-volume PCR, are described as well as real-time PCR, array-based approaches and general precautions, which were taken to eliminate risks of contamination.

2.3.1 Polymerase chain reaction

Conventional polymerase chain reaction (PCR) was performed as well as low-volume PCR. The technique of low-volume PCR (LV-PCR, also “virtual reaction chamber PCR (VRC

2. Materials and Methods

PCR)", Guttenberg Z *et al.*, 2005), performed on microdevices, is based on a chemically structured surface providing hydrophilic reaction sites surrounded by hydrophobic background. LV-PCR was performed on two microfabricated devices, in fact a multi LV-PCR microdevice (AmpliGrid™ AG480F, Advalytix AG/Beckman Coulter Biomedical GmbH, Munich, Germany) and LOC chips designed for the lab-on-a-chip system (Advalytix AG/Beckman Coulter Biomedical GmbH, Munich, Germany). The AmpliGrid™ AG480F is a commercially available multi LV-PCR microdevice, offering 48 hydrophilic reaction sites with 1.6 mm in diameter, each surrounded by a hydrophobic circle to hold 1 µl of aqueous PCR master mixes in place. A short-distanced hydrophilic ring comprising 3 mm in diameter and surrounding the hydrophilic reaction site, centers 5 µl of mineral oil cover solution (Sealing Solution, Advalytix AG/Beckman Coulter Biomedical GmbH, Munich, Germany) to the aqueous droplet. For performing thermal reactions, the AmpliGrid™ AG480F slide was placed on a corresponding thermal cycler (AmpliSpeed slide cycler, Advalytix AG/Beckman Coulter Biomedical GmbH, Munich, Germany). LOC chips present a single LV-PCR microdevice. For PCR performance, these chips offer one hydrophilic reaction site with 500 µm in diameter, surrounded by a hydrophobic circle to keep 1 µl aqueous PCR master mixes in place (named reaction center B). A short-distanced intermitted hydrophilic ring comprising 3 mm in diameter and surrounding the hydrophilic reaction site, centers 5 µl of mineral oil cover solution (Sealing Solution, Advalytix AG/Beckman Coulter Biomedical GmbH, Munich, Germany) to the aqueous droplet. For performing thermal cycling reactions, LOC chips were installed into the LOC CytoCycler. For all experiments, LOC chips of the Cyto3 design were used.

Setup of LV-PCR reactions. LOC chips and multi LV-PCR microdevices were decontaminated for 15-20 min using a UVC light source prior to use (PCR Workstation, PeqLab Biotechnologie GmbH, Erlangen, Germany). Additionally, LOC chips were preheated for 15 min at 95°C prior to PCR for adapting the material to heat and to eliminate material stress when starting the initial denaturation step of a PCR. LV-PCR reactions were setup in the following way: after master mixes were mixed thoroughly, 1 µl of prepared master mix was placed on reaction center B of LOC chips or on reaction sites of the multi LV-PCR microdevice and was immediately covered with 5 µl of Sealing Solution to prevent evaporation and external cross-contamination. Evaporation might inhibit LV-PCR due to loss of reactants, loss of volume and increase of salt concentrations present in the reaction mix. As LOC chips offer only one reaction site for performing VRC PCR, reactions were run on the multi LV-PCR microdevices in parallel for validation and as a reference system. In addition,

2. Materials and Methods

positive and negative controls were included. When using fluorescently tagged primers like D7S1824, D9S302, D10S2325, AmpF/STR[®] SEfiler[™] Primer Set, Amel1-f-Cy3 or SYBR Green I-based LV-PCR setups, reactions were performed in darkness by capping PCR cyclers with light impermeable stuff to exclude ambient light and to inhibit bleaching effects.

Amelogenin and β -actin LV-PCR on reference DNA for evaluating the minimum amount of target material needed for cycling on the lab-on-a-chip integrated CytoCycler. To test the sensitivity and to analyze the product detection limit of the LOC CytoCycler PCR amplification device, LV-PCR was performed on purified human genomic male and female reference DNA. PCR reactions were performed using the QuantiFast[™] SYBR[®] Green I PCR kit for 2-step PCR (QIAGEN GmbH, Hilden, Germany) according to the protocol recommended by the manufacturer, but reaction volumes were adapted to low-volume PCR applications. 1 μ l total PCR reaction mix contained 0.5 μ l of 2x QuantiFast[™] SYBR[®] Green I PCR Master Mix (final 1x), 0.1 μ l of 10 μ M primer solutions β -Actin up and β -Actin down or Amel1 and Amel2 respectively (final 1 μ M per primer), 0.2 μ l of sterile water (Ampuwa[®], Fresenius, Bad Homburg, Germany) as well as 0.1 μ l of 10x concentrated input DNA (final 1x). Primer sequences were listed in the appendix, **chapter 9.2**. For input target DNA concentrations of 10 ng/ μ l, 5 ng/ μ l, 1 ng/ μ l, 500 pg/ μ l, 250 pg/ μ l, 125 pg/ μ l and 100 pg/ μ l were used, resulting in final concentrations of 1 ng, 500 pg, 100 pg, 50 pg, 25 pg, 12.5 pg and 10 pg present in 1 μ l total reaction mix. 1 μ l of prepared master mix was placed on reaction center B of LOC chips or on reaction sites of a multi LV-PCR microdevice and was immediately covered with 5 μ l of Sealing Solution to prevent evaporation and external cross-contamination. 2-step PCR cycling conditions recommended by the manufacturer's protocol were slightly changed concerning temperature hold times: 5 min initial denaturation at 95°C, followed by 40 cycles of 95°C for 30 sec and 60°C for 60 sec (instead of 95°C for 10 sec and 60°C for 30 sec). PCR products were analyzed on polyacrylamide gels (CleanGel 10% or CleanGel HyRes, ETC GmbH, Kirchentellinsfurt, Germany) and subsequent DNA silver staining (DNA silver staining kit, GE Healthcare, Uppsala, Sweden) (**chapter 2.2.3**). Blank and negative controls (containing no DNA) were included in every reaction batch and all experiments were performed in triplicates.

Amelogenin and β -actin LV-PCR on reference DNA for cycling efficiency tests of the lab-on-a-chip integrated CytoCycler. To test the cycling efficiency of the LOC CytoCycler PCR amplification device, LV-PCR was performed on purified human genomic male reference DNA. PCR reactions were performed using the QuantiFast[™] SYBR[®] Green I PCR kit for 2-

2. Materials and Methods

step PCR (QIAGEN GmbH, Hilden, Germany) as well as the QIAGEN[®] Fast Cycling PCR kit for 3-step PCR (QIAGEN GmbH, Hilden, Germany). Kits were used according to the protocol recommended by the manufacturer, but reaction volumes were adapted to low-volume PCR applications. Furthermore, temperature hold-times were scaled down, speeding up cycling times to amplification limits.

Using the QuantiFast[™] SYBR[®] Green I PCR kit, 1 μ l of total PCR reaction mix contained 0.5 μ l of 2x QuantiFast[™] SYBR[®] Green I PCR Master Mix (final 1x), 0.1 μ l of 10 μ M primer solutions β -Actin up and β -Actin down or Amel1 and Amel2 respectively (final 1 μ M per primer), 0.2 μ l of sterile water (Ampuwa[®], Fresenius, Bad Homburg, Germany) and 0.1 μ l of 10x concentrated input DNA (final 1x). Primer sequences were listed in the appendix, **chapter 9.2**. For input target DNA 5 ng/ μ l male reference DNA was used, resulting in a final concentration of 500 pg present in 1 μ l total reaction mix. 1 μ l of prepared master mix was placed on reaction center B of LOC chips or on reaction sites of a multi LV-PCR microdevice and was immediately covered with 5 μ l of Sealing Solution to prevent evaporation and external cross-contamination. The 2-step PCR protocol was adapted to shorter cycling times, starting with 95°C for 5 min, 40 cycles of 95°C for 30 sec and 60°C for 60 sec to 95°C for 5 min, 40 cycles of 95°C for 10 sec and 60°C for 30 sec.

Using the QIAGEN[®] Fast Cycling PCR kit, 1 μ l of total PCR reaction mix contained 0.5 μ l of 2x QIAGEN[®] Fast Cycling PCR Master Mix (final 1x), 0.06 μ l of 5x Q-Solution (final 0.3x), 0.1 μ l of 10 μ M primer solutions β -Actin up and β -Actin down or Amel1 and Amel2 respectively (final 1 μ M per primer), 0.14 μ l of sterile water (Ampuwa[®], Fresenius, Bad Homburg, Germany) and 0.1 μ l of 10x concentrated input DNA. Primer sequences were listed in the appendix, **chapter 9.2**. For input target DNA 5 ng/ μ l, 1 ng/ μ l, 500 pg/ μ l and 250 pg/ μ l male reference DNA was used, resulting in final concentrations of 500 pg, 100 pg, 50 pg and 25 pg present in 1 μ l total reaction mix. 1 μ l of prepared master mix was placed on reaction center B of LOC chips or on reaction sites of a multi LV-PCR microdevice and was immediately covered with 5 μ l of Sealing Solution to prevent evaporation and external cross-contamination. The 3-step PCR protocol was adapted to shorter cycling times, starting with a) 95°C for 5 min, 30 cycles of 94°C for 30 sec, 60°C for 30 sec, 72°C for 30 sec, and 1 min final extension at 72°C, to b) 95°C for 5 min, 30 cycles of 94°C for 10 sec, 60°C for 10 sec, 72°C for 10 sec, and final extension for 1 min at 72°C and finally c) 95°C for 5 min, 30 cycles of 94°C for 5 sec, 60°C for 5 sec, 72°C for 5 sec, and final extension for 30 sec at 72°C.

PCR products were analyzed on polyacrylamide gels (CleanGel 10%, ETC GmbH, Kirchentellinsfurt, Germany) and subsequent DNA silver staining (DNA silver staining kit,

2. Materials and Methods

GE Healthcare, Uppsala, Sweden) (**chapter 2.2.3**). Blank and negative controls (containing no DNA) were included in every reaction batch and all experiments were performed in triplicates.

Amelogenin LV-PCR on human intestine, mamma and bladder tissue material. For LV-PCR analysis of tissue material, performed on a multi LV-PCR microdevice, the QIAGEN[®] Fast Cycling PCR kit was used for 3-step PCR (QIAGEN GmbH, Hilden, Germany) according to the protocol recommended by the manufacturer, but reaction volumes were adapted to low-volume PCR applications. Dried tissue fragments, fixed on reaction sites of a multi LV-PCR microdevice, were covered with 1 µl of PCR reaction mix. 1 µl of total PCR reaction mix contained 0.5 µl of 2x QIAGEN[®] Fast Cycling PCR Master Mix (final 1x), 0.2 µl of 5x QIAGEN[®] Q-Solution (final 1x), 0.1 µl of 10 µM primer solutions Amel1 and Amel2 (final 1 µM per primer) and 0.1 µl of sterile water (Ampuwa[®], Fresenius, Bad Homburg, Germany). Primer sequences were listed in the appendix, **chapter 9.2**. 1 µl of positioned master mix was immediately covered with 5 µl of Sealing Solution to prevent evaporation and external cross-contamination. 3-step PCR cycling conditions recommended by the manufacturer's protocol were slightly changed concerning temperature hold times: 20 min initial denaturation and cell lysis at 97°C, followed by 40 cycles of 94°C for 30 sec, 60°C for 30 sec and 72°C for 30 sec, and final product extension at 72°C for 1 min. PCR products were analyzed on polyacrylamide gels (CleanGel HyRes, ETC GmbH, Kirchentellinsfurt, Germany) and subsequent DNA silver staining (DNA silver staining kit, GE Healthcare, Uppsala, Sweden) (**chapter 2.2.3**). Blank and negative controls (containing no DNA) were included in every reaction batch and all experiments were performed in triplicates. Positive controls comprising male and female reference DNA were included as well.

For LV-PCR analysis of tissue⁵, performed on a LOC chip, the QIAGEN[®] Fast Cycling PCR kit was used for 3-step PCR (QIAGEN GmbH, Hilden, Germany) according to the protocol recommended by the manufacturer, but reaction volumes were adapted to low-volume PCR applications. Fragments of tissue⁵ were released directly into 1 µl of LV-PCR master mix on reaction center B of LOC chips after microdissection. 1 µl of total PCR reaction mix contained 0.5 µl of 2x QIAGEN[®] Fast Cycling PCR Master Mix (final 1x), 0.06 µl of 5x Q-Solution (final 0.3x), 0.1 µl of 10 µM primer solutions Amel1 and Amel2 (final 1 µM per primer) and 0.24 µl of sterile water (Ampuwa[®], Fresenius, Bad Homburg, Germany). Primer sequences were listed in the appendix, **chapter 9.2**. 1 µl of sample-loaded master mix was immediately covered with 5 µl of Sealing Solution to prevent evaporation and external cross-

2. Materials and Methods

contamination. Adding volumes of 1 μl of master mix and 5 μl of Sealing Solution was performed using the automatic dispensing device BioSpot[®] and appropriate software “BioSpot[®]” (BioFluidix GmbH, Freiburg, Germany). PipeJetTM1 was used for applying the master mix, while PipeJetTM3 provided the oil coverage just by dispensing the liquid onto the chip surface. 3-step PCR cycling conditions recommended by the manufacturer’s protocol were slightly changed concerning temperature hold times: 20 min initial denaturation and cell lysis at 97°C, followed by 40 cycles of 94°C for 30 sec, 60°C for 30 sec and 72°C for 30 sec, and final product extension at 72°C for 1 min. PCR products were analyzed on polyacrylamide gels (CleanGel 10%, ETC GmbH, Kirchentellinsfurt, Germany) and subsequent DNA silver staining (DNA silver staining kit, GE Healthcare, Uppsala, Sweden) (**chapter 2.2.3**). Blank and negative controls (containing no DNA) were included in every reaction batch and experiment was performed in triplicate.

Amelogenin and β -actin LV-PCR on ancient Egyptian mummy bone tissue material. For LV-PCR analysis of extracted mummy DNA samples, microdissected as well as conventionally extracted ones, the QIAGEN[®] Fast Cycling PCR kit (QIAGEN GmbH, Hilden, Germany) was used for 3-step PCR according to the protocol recommended by the manufacturer, but reaction volumes were adapted to low-volume PCR applications. 1 μl of extracted mummy DNA sample solution was dried up either on reaction center B of LOC chips or on reaction sites of a multi LV-PCR microdevice at 30°C for 10 min. Dried input DNA sample material, comprising 60 pg of microdissected mummy DNA or 50-100 pg of pulverized mummy DNA, was covered with 1 μl of PCR reaction mix. 1 μl of total PCR reaction mix contained 0.5 μl of 2x QIAGEN[®] Fast Cycling PCR Master Mix (final 1x), 0.2 μl of 5x QIAGEN[®] Q-Solution (final 1x), 0.1 μl of 10 μM primer solutions β -Actin up and β -Actin down, or Amel1 and Amel2 respectively (final 1 μM per primer) and 0.1 μl of sterile water (Ampuwa[®], Fresenius, Bad Homburg, Germany). Primer sequences were listed in the appendix, **chapter 9.2**. 1 μl of positioned master mix was immediately covered with 5 μl of Sealing Solution to prevent evaporation and external cross-contamination. 3-step PCR cycling was performed as recommended by the manufacturer’s protocol: 5 min initial denaturation at 95°C, followed by 40 cycles of 94°C for 30 sec, 60°C for 30 sec and 72°C for 30 sec, and final product extension at 72°C for 1 min. PCR products were analyzed on polyacrylamide gels (CleanGel 10% and CleanGel HyRes, ETC GmbH, Kirchentellinsfurt, Germany) and subsequent DNA silver staining (DNA silver staining kit, GE Healthcare, Uppsala, Sweden) (**chapter 2.2.3**). Blank and negative controls (containing no DNA) were

2. Materials and Methods

included in every reaction batch and all experiments were performed in triplicates. Positive controls comprising male and female reference DNA were included as well.

Multiplex STR PCR on ancient Egyptian mummy bone tissue material and DNA of scientific staff. For DNA profiling analysis on extracted mummy material as well as on extracted genomic material of scientific staff, PCR typing reactions were performed using two PCR setups amplifying distinct STR marker combinations. The QIAGEN[®] Multiplex PCR kit (QIAGEN GmbH, Hilden, Germany) was used for 3-step PCR amplifying STR markers D7S1824, D9S302 and D10S2325. The AmpF/STR[®] SEfiler[™] PCR amplification kit (Applied Biosystems GmbH, Darmstadt, Germany) is a STR multiplex assay that simultaneously co-amplifies 11 STR loci and the amelogenin locus. Kits were used according to the protocol recommended by the manufacturer, but concerning the QIAGEN[®] Multiplex PCR kit reaction volumes were adapted to low-volume PCR applications, while AmpF/STR[®] SEfiler[™] reaction volumes were just scaled down to 16.5 µl for conventional PCR performances.

Using the QIAGEN[®] Multiplex PCR kit, 1 µl of total PCR reaction mix contained 0.5 µl of 2x QIAGEN Multiplex PCR Master Mix (final 1x), 0.2 µl of 5x QIAGEN Q-Solution (final 0.33x), 0.12 µl of AdvaGold (Advalytix AG/Beckman Coulter Biomedical GmbH, Munich, Germany), 0.2 µl of sterile water (Ampuwa[®], Fresenius, Bad Homburg, Germany) and 0.04 µl of 50 pmol STR primer-pair solutions D7S1824-F/R and D9S302-F/R and D10S2325-F/R (final 2 pmol = 2 µM per primer-pair solution). Primer sequences were listed in the appendix, **chapter 9.2**. 1 µl of extracted DNA sample solution from mummy and scientific staff was dried up on reaction sites of a multi LV-PCR microdevice at 30°C for 10 min. Dried input DNA sample material, comprising 60 pg of microdissected mummy DNA or several ng of scientific staff DNA, was covered with 1 µl of PCR reaction mix. 1 µl of positioned master mix was immediately covered with 5 µl of Sealing Solution to prevent evaporation and external cross-contamination. For PCR cycling a „touch-down“ protocol was used comprising the following conditions: 15 min initial denaturation at 95°C, 14 cycles of 94°C for 30 sec, 64°C to 50°C for 60 sec (temperature increment -1°C per cycle), 72°C for 30 sec, continued by 25 cycles of 94°C for 30 sec, 50°C for 30 sec, 72°C for 30 sec, and a final product extension at 72°C for 7 min. Blank and negative controls (containing no DNA) were included in every reaction batch and all experiments were performed in triplicates. Data acquisition was performed via STR fragment length analysis (**chapter 2.2.4**).

2. Materials and Methods

Using the AmpF/STR[®] SEfiler[™] PCR amplification kit, DNA typing reactions were performed according to the manufacturer's recommendations, but reaction volumes were scaled down to 16.5 µl for conventional PCR performances. 16.5 µl of total PCR reaction volume, prepared in sterile 0.2 ml PCR-tubes (Eppendorf AG, Hamburg, Germany), contained 10 µl AmpF/STR[®] PCR Reaction Mix, 5 µl of AmpF/STR[®] SEfiler[™] Primer Set, 0.5 µl of AmpliTaq Gold[®] DNA Polymerase 5U/µl (final 2.5 U) and 1 µl of DNA sample solution from mummy and scientific staff. 3-step PCR cycling was performed as recommended by the manufacturer's protocol of the AmpF/STR[®] SEfiler[™] PCR amplification kit: 11 min initial denaturation at 95°C, 28 cycles of 94°C for 60 sec, 59°C for 60 sec, 72°C for 60 sec, followed by a final product extension at 60°C for 45 min. Data acquisition was performed using STR fragment length analysis (**chapter 2.2.4**).

Multiplex STR PCR on anticoagulant treated whole blood and degrading dried blood spots.

For LV-PCR analysis of whole blood a combined setup of the AmpF/STR[®] SEfiler[™] PCR amplification kit (Applied Biosystems GmbH, Darmstadt, Germany) and the KOD Xtreme[™] Hot Start DNA Polymerase PCR system (Novagen[®], Merck, Darmstadt, Germany) was used for 3-step PCR and reaction volumes were adapted to low-volume PCR applications. The AmpF/STR[®] SEfiler[™] PCR amplification kit is a STR multiplex assay that simultaneously co-amplifies 11 STR loci and the amelogenin locus. 1.12 µl of total PCR reaction mix contained 0.5 µl of 2x Xtreme[™] Buffer (final 1x), 0.2 µl of Xtreme[™] dNTPs (2 mM each), 0.02 µl of KOD Xtreme[™] Hot Start DNA Polymerase 1U/µl (final 0.02U), 0.3 µl of AmpF/STR[®] SEfiler[™] Primer Set and 0.1 µl of 10x concentrated blood sample (either EDTA K treated blood or resolved blood spots). For input blood samples concentrations of 100% whole blood or 10% whole blood were used, resulting in final concentrations of 10% or 1% whole blood present in 1 µl total reaction mix. According to Ganong WF (2003), 1 µl of whole blood target material contains 4000 to 11000 leukocytes. That means 400 to 1100 leukocytes present in 10% blood typing reactions and equivalently 40 to 110 leukocytes present in 1% blood typing reactions, representing a target DNA amount of 2.8 to 7.0 ng or 280 to 700 pg respectively. 1 µl of prepared master mix was placed on reaction center B of LOC chips or on reaction sites of a multi LV-PCR microdevice and was immediately covered with 5 µl of Sealing Solution to prevent evaporation and external cross-contamination. 3-step PCR cycling was performed as recommended by the manufacturer's protocol of the AmpF/STR[®] SEfiler Plus[™] PCR amplification kit: 11 min initial denaturation and cell lysis

2. Materials and Methods

at 95°C, 28 cycles of 94°C for 60 sec, 59°C for 60 sec and 72°C for 60 sec, followed by a final product extension at 60°C for 45 min.

Blank, negative (containing no DNA) and positive controls (AmpF/STR[®] SEfiler Plus[™] Control DNA 9947A, Applied Biosystems GmbH, Darmstadt, Germany) were included in every reaction batch and all experiments were performed in triplicates. 100 pg of the AmpF/STR[®] SEfiler[™] Control DNA 9947A was amplified simultaneously via LV-PCR as positive control (named “PK-1”). Additionally, Control DNA 9947A was amplified in a conventional in-tube PCR reaction using a standard thermocycler (Cyclone25, PeqLab Biotechnologie GmbH, Erlangen, Germany) and the recommended PCR protocol of the AmpF/STR[®] SEfiler[™] kit as a pure positive control (named “SE-PK-2”). Reaction volumes, prepared in sterile 0.2 ml PCR-tubes (Eppendorf AG, Hamburg, Germany), were scaled down to about 5.5 µl of total PCR reaction volume, containing 2.7 µl of AmpF/STR[®] PCR Reaction Mix (final 1x), 1.35 µl of AmpF/STR[®] SEfiler[™] Primer Set, 0.45 µl of AmpliTaq Gold[®] DNA Polymerase 5U/µl (final 2.25U) and 1 µl of AmpF/STR[®] SEfiler[™] Control DNA 9947A 100 pg/µl (final 100 pg). Blank and negative controls (containing no DNA) were included in every reaction batch and experiments were performed in triplicates. Total data acquisition was performed via STR fragment length analysis (**chapter 2.2.4**).

2.3.2 Real-time PCR

Real-time PCR (RT-PCR) is a special form of PCR, quantifying the amount of amplified DNA present after each round of PCR cycling via measuring fluorescence signals (Wilhelm J and Pingoud A, 2003). As the fluorescence increases proportional with the amount of DNA, after each cycle the amount of DNA can be detected in the exponential phase. Signals are either indicated by fluorescently tagged PCR primers or a DNA-intercalating fluorescent dye is added to the PCR mixture, of which the most popular is SYBR Green I binding to double-stranded DNA. A big drawback of the SYBR Green I method is the low specificity as no differentiation between PCR products can be achieved. Only when performing an additional melting point analysis after PCR, the fragment lengths and thus the specificity of the PCR products can be detected and authentic PCR products can be distinguished from occurring unspecific primer dimers. During a melting point analysis DNA is melted via raising the temperature continuously from 50°C to 95°C. At fragment-specific melting temperatures the double-stranded DNA molecules denature, whereas the fluorescence dye is released and a

2. Materials and Methods

decrease in fluorescence intensity is detected. As specific PCR products have a higher melting point as unspecific primer dimers, a differentiation is possible.

Real-time PCR using the Stratagene Mx 3000P thermocycler. Real-time PCR was applied on microdissected ancient bone samples of Egyptian mummy material. RT-PCR was performed to quantify the amount of extracted DNA originating from microdissected ancient bone samples of Egyptian mummy material. Real-time PCR was applied to sample mummy4, exemplary for all of four mummy samples, in a Stratagene RT-PCR cycler (Stratagene Mx 3000P, Stratagene, La Jolla, CA, USA) using the QuantiFast™ SYBR® Green I PCR kit (QIAGEN GmbH, Hilden, Germany) for 2-step PCR according to the protocol recommended by the manufacturer. RT-PCR DNA amplification rates of sample mummy4, were compared to RT-PCR amplification rates of 1 ng/μl, 500 pg/μl, 100 pg/μl, 50 pg/μl and 20 pg/μl male and female starting DNA target material concentrations serving as reference probes and internal target amount standards. 1 μl of these standard concentrations was used for analysis, while just 0.5 μl of extracted mummy DNA was used due to the scarcity of mummy material. The mummy sample was filled up to 1 μl with sterile water (Ampuwa®, Fresenius, Bad Homburg, Germany). In a 96-well plate (ABgene® PCR Plates, Thermo Scientific, Epsom, Surrey, UK) 1 μl of DNA sample solution was mixed with 24 μl of RT-PCR master mix, containing 12.5 μl of 2x QuantiFast™ SYBR® Green I PCR Master Mix (final 1x), 2.5 μl of 10 μM primer solutions Amel1 and Amel2 (final 1 μM per primer) and 6.5 μl of RNase-Free water. Primer sequences were listed in the appendix, **chapter 9.2**. 2-step PCR conditions were used according to the manufacturer's protocol recommending 5 min initial denaturation at 95°C, followed by 40 cycles of 95°C for 10 sec and 60°C for 30 sec and subsequent melting curve analysis. Conditions for generating these dissociation curves were 95°C for 1 min, 55°C for 30 sec, slowly ramping the temperature from 55°C to 95°C, and final denaturation time of 95°C for 30 sec. Data was obtained during ramping, while continuously fluorescence data was collected. Data analysis was performed via appropriate software for the Stratagene Mx 3000P "MxPro™ – Mx3000P v3.00" (Stratagene, La Jolla, CA, USA).

Real-time PCR using the lab-on-a-chip integrated Fluorescence Reader. The Fluorescence Reader module of the lab-on-a-chip system comprised a blue LED ($\lambda_{\text{max}} = 470 \pm 2$ nm) for excitation light (LUXEON Rebel LXML-PB01-0023, 3.4 V forward bias, 0.7 A operating current), filter sets, a self-made LED power control box, a trigger signal break-out box (NI SCB-68 with the PCI ADC/DAC, Quick Reference Label, S-Series Devices, National Instruments Germany GmbH, Munich, Germany) and a CCD camera as detection device for

2. Materials and Methods

capturing emitted light (Rolera-XR, QImaging, Surrey BC, Canada). Filter sets included an excitation filter with $\lambda_{\max} = 482$ nm (spread 36 nm = 464-500 nm excitation spectrum) and an emission filter with $\lambda_{\max} = 536$ nm (spread 40 nm = 516-556 nm emission spectrum) (Interferenzfilter of BrightLine series, AHF Analysentechnik AG, Tübingen, Germany). For automatic picture taking, a self-programmed LabVIEW-based software was used “Grand_NIVision_Intensity_Consec_Subtract_Loopback_NewCamera.VI” (LabVIEW 8.6, National Instruments Germany GmbH, Munich, Germany). The software was adapted for taking pictures manually (named “Norbert.VI”). For real-time PCR operations, excitation and emission devices of the Fluorescence Reader were directed to reaction center B on the LOC chip surface.

Calibration of fluorescence intensities. The fluorescence signal was calibrated using the QuantiFast™ SYBR® Green I PCR kit (QIAGEN GmbH, Hilden, Germany). Decreasing amounts of DNA were used to synthesize dilution series, whereas 0.1 μ l of 10x concentrated DNA was mixed with 0.9 μ l of 2x QuantiFast™ SYBR® Green I PCR Master Mix. DNA concentrations of 100 ng/ μ l, 50 ng/ μ l, 10 ng/ μ l, 5 ng/ μ l and 1 ng/ μ l of male and female reference DNA were used, resulting in final concentrations of 10 ng, 5 ng, 1 ng, 500 pg and 100 pg present in prepared dilutions. 1 μ l of each dilution was placed on reaction center B of a LOC chip, covered with 5 μ l of Sealing Solution (Advalytix AG/Beckman Coulter Biomedical GmbH, Munich, Germany) and centered to the detection path of the CCD camera. This whole setup was darkened by capping it totally with a black cloth in order to exclude interfering ambient light. Pictures were taken manually via LabVIEW-based software “Norbert.VI”. Increasing exposure times were chosen starting with 200 ms, to 400 ms, 600 ms, 1000 ms, 2000 ms and 4000 ms. Measurements were performed at room temperature as well as at 55°C and 72°C. Measurements were repeated several times and pictures concerning fluorescence intensity were analyzed visually.

Experimental setups of performing real-time PCR. Real-time PCR was performed using the QuantiFast™ SYBR® Green I PCR kit for 2-step PCR (QIAGEN GmbH, Hilden, Germany) according to the protocol recommended by the manufacturer, but reaction volumes were adapted to low-volume PCR applications. 1 μ l total LV-PCR reaction mix contained 0.5 μ l of 2x QuantiFast™ SYBR® Green I PCR Master Mix (final 1x), 0.1 μ l of 10 μ M primer solutions β -Actin up and β -Actin down or Amel1 and Amel2 respectively (final 1 μ M per primer), 0.2 μ l of sterile water (Ampuwa®, Fresenius, Bad Homburg, Germany) and 0.1 μ l of 10x concentrated input DNA (final 1x). Primer sequences were listed in the appendix, **chapter 9.2**. For input male and female reference target DNA concentrations of 10 ng/ μ l,

2. Materials and Methods

5 ng/μl and 1 ng/μl were used, resulting in final concentrations of 1 ng, 500 pg and 100 pg present in 1 μl total reaction mix. 1 μl of prepared master mix was placed on reaction center B of a LOC chip, covered with 5 μl of Sealing Solution (Advalytix AG/Beckman Coulter Biomedical GmbH, Munich, Germany) and centered to the detection path of the CCD camera. This whole setup was darkened by capping it totally with a black cloth in order to exclude interfering ambient light. 2-step PCR cycling conditions recommended by the manufacturer's protocol were slightly changed concerning temperature hold times: 5 min initial denaturation at 95°C, 40 cycles of 95°C for 30 sec and 60°C or 55°C respectively for 60 sec. Increasing fluorescence intensities were recorded by taking pictures at the end of each annealing and extension step at 55°C or 60°C during 35-45 cycles in total. Pictures were either taken manually via LabVIEW-based software "Norbert.VI" or automatically via LabVIEW-based software "Grand_NIVision_Intensity_Consec_Subtract_Loopback_NewCamera.VI". Chosen exposure times chosen ranged from 200 ms, to 400 ms and 600 ms. PCR reactions were repeated several times and pictures concerning fluorescence intensity were analyzed visually. Real-time PCR was also performed using the QuantiTect™ SYBR® Green I PCR kit for 3-step PCR (QIAGEN GmbH, Hilden, Germany) according to the protocol recommended by the manufacturer, but reaction volumes were adapted to low-volume PCR applications. 1 μl total LV-PCR reaction mix contained 0.5 μl of 2x QuantiTect™ SYBR® Green I PCR Master Mix (final 1x), 0.1 μl of 10 μM primer solutions β-Actin up and β-Actin down or Amel1 and Amel2 respectively (final 1 μM per primer), 0.2 μl of sterile water (Ampuwa®, Fresenius, Bad Homburg, Germany) and 0.1 μl of 10x concentrated input DNA (final 1x). 3-step PCR cycling conditions recommended by the manufacturer's protocol were slightly changed concerning temperature hold times: 15 min initial denaturation at 95°C, 35-45 cycles of 95°C for 30 sec, 55°C for 60 sec, 72°C for 30 sec, and final product extension at 72°C for 7 min. Conditions for picture taking and real-time PCR performances were according to the 2-step PCR performance just described.

2.3.3 Microarray hybridization

In microarray applications biological probes are arrayed onto planar surfaces and slides through the use of a robotic array spotter, while biological probes comprise short single stranded DNA oligonucleotides. PCR-amplified DNA fragments in solution are subjected to hybridization with these surface coupled complementary strands, providing information on the corresponding nucleotide sequence (Schna M, 1999). Hybridization happens specifically

2. Materials and Methods

via the building of hydrogen bonds between complementary sequences of probes and amplified DNA fragments. Due to the small size, a huge amount of probes detecting for thousands of gene fragments can be arrayed, just dependent on the size of the supporting surface. As fluorescently tagged primers were utilized, e.g. tagged with chromogenic dyes “Cy3” or “Cy5”, PCR products are fluorescently labeled as well. Detection of hybridization events between surface-bound probes and primer-labeled fluorescent PCR products is performed via on-line detection methods.

Spot array design. A 2x2 spot array was designed for the determination of PCR-amplified male and female sample material, according to gender determining approaches used in forensic research. Probes of the microarray were designed in a way, to detect a 6 bp insertion sequence AAAGTG between male and female PCR-amplified amelogenin fragments. So either probes matched the 106 bp X-chromosomal sequence or were complementary to the 112 bp Y-chromosomal sequence. Three different probes were designed for hybridization providing distinct sites for specific PCR product hybridization. Probes Amelo1(Y) and Amelo3(Y) were designed for binding male amelogenin PCR products having the 6 bp insert, while probe Amelo2(X) was destined for hybridizing to female PCR products lacking the 6 bp insert (probe sequences were listed in the appendix, **chapter 9.2**). Successful hybridization events of fluorescently labeled PCR products were detected via the intensity of fluorescence signals.

For microarray applications, probes were spotted on reaction sites (\varnothing 1.6 mm) of a multi LV-PCR microdevice (AmpliGrid™ AG480F, Advalytix AG/Beckman Coulter Biomedical GmbH, Munich, Germany; **chapter 2.3.1**) and on reaction center B (\varnothing 500 μ m) of LOC chips (**chapter 2.3.1**). Probes were spotted in a 2x2 array structure using a *Nadelspotter* (spotting operations were performed by Advalytix AG/Beckman Coulter Biomedical GmbH, Munich, Germany). There were 6 different array designs spotted. Each array consisted of 4 spots, while full arrays were spotted with 4 spots having the same probe content (array designs 1-3), and split arrays where only 2 spots had the same probe content (array designs 4-6). Array designs were as follows: (1) 4 spots of Amelo1(Y), (2) 4 spots of Amelo2(X), (3) 4 spots of Amelo3(Y), (4) 2 spots of Amelo1(Y) + 2 spots of Amelo2(X), (5) 2 spots of Amelo2(X) + 2 spots of Amelo3(Y), (6) 2 spots of Amelo1(Y) + 2 spots of Amelo3(Y). Spot size was about 120 μ m (100-160 μ m) with a spot distance of about 160 μ m, comprising an array diameter of about 400 μ m. Spotting solution contained 50 μ M oligonucleotide probe solution dissolved in 1x Advalytix spotting buffer AT100. Spotting, washing and passivation steps after spotting were done by Advalytix AG/Beckman Coulter Biomedical GmbH, Munich, Germany as well.

2. Materials and Methods

PCR and hybridization of male and female human genomic reference DNA. For PCR amplification prior to hybridization and for detection of hybridized PCR products, a Cy3 fluorescently labeled primer Amel1-f-Cy3 was used in combination with an unlabeled primer Amel2. Primer sequences were listed in the appendix, **chapter 9.2**. For amplification and hybridization, the QIAGEN[®] Fast Cycling PCR kit (QIAGEN GmbH, Hilden, Germany) was used for 3-step PCR. 1 µl total reaction volume contained 0.5 µl of 2x QIAGEN[®] Fast Cycling PCR Master Mix (final 1x), 0.2 µl of 5x QIAGEN[®]Q-Solution (final 1x), 0.1 µl of 10 µM primer solutions Amel1-f-Cy3 and Amel2 (final 1 µM per primer) and 0.1 µl of sterile water (Ampuwa[®], Fresenius, Bad Homburg, Germany) for negative controls or 0.1 µl of 10x concentrated input DNA. For input DNA concentrations of 1 ng male or female reference DNA was used, resulting in a final concentration of 100 pg present in 1 µl total reaction mix. 1 µl of prepared master mix was placed on spotted reaction center B of LOC chips or on spotted reaction sites of a multi LV-PCR microdevice and was immediately covered with 5 µl of Sealing Solution to prevent evaporation and external cross-contamination. 3-step PCR cycling was performed according to the manufacturer's protocol: 5 min initial denaturation at 95°C, 40 cycles of 94°C for 30 sec, 60°C for 30 sec, 72°C for 30 sec, and final product extension at 72°C for 1 min. PCR performance was subsequently followed by a hybridization protocol comprising 3 min denaturation at 95°C and 40°C hybridization for 30-60 min.

Washing protocol. After hybridization, Sealing Solution was washed away from reaction sites using sterile water and array chips were subjected to the following washing protocol (originally provided by Alopex (Kulmbach, Germany) for using the "Chromo Chip System") comprising washing solutions Wash 1 and Wash 2 (**table 1**) (washing solutions were taken from the Medical Genetic Center, Munich). Washing procedures removed the Sealing Solution efficiently as well as unbound PCR products.

Table 1. Washing protocol and compositions of washing buffers Wash 1 and Wash 2 after PCR and array hybridization. Buffers Wash 1A and Wash 2 needed to be autoclaved at 120 °C for 20 min prior to use. Washing procedures were performed at room temperature.

Washing solutions	Composition	Concentrated Buffer Solutions
1.01 Wash 1 (working solution)	100 ml Wash 1A (10x) 20 ml Wash 1B (5x) 880 ml H ₂ O ^{dest.}	Wash 1A (10x) = 3 M NaCl 0.3 M Na ₃ Citrate 2H ₂ O pH 7.0 Wash 1B (5x) = 10% (w/v) Natriumdodecylsulfate (SDS)
1.01 Wash 2 (working solution)	100 ml Wash 2 (10x) 900 ml H ₂ O ^{dest.}	Wash 2 (10x) = 0.3 M NaCl 30 mM Na ₃ Citrate 2H ₂ O pH 7.0
Washing protocol	5x 1 min Wash 1 2x 1 min Wash 2 1x 3 min Wash 2	

2. Materials and Methods

For washing the multi LV-PCR microdevice an automated washing station appropriate for these slides was utilized (AdvaWash, Advalytix AG/Beckman Coulter Biomedical GmbH, Munich, Germany). LOC chips were washed manually by applying a 10 μ l overlay of buffers onto the hybridization reaction center B of the chips. After washing, array chips were dried for 5 min at 37°C until slide surfaces were totally dry and stored in darkness for the scanning process (max. 3 h).

Detection. The multi LV-PCR microdevice was scanned for hybridized PCR products using an automated PMT laser-based microarray scanner system (ProScanArray Microarray Analysis System, PerkinElmer Life and Analytical Sciences, Shelton, CT, USA) and appropriate software (ProScanArray Scanner Software, PerkinElmer Life and Analytical Sciences, Shelton, CT, USA). LOC chips were scanned using an inverted optical microscope (Axio Observer.Z1, Carl Zeiss GmbH, Jena, Germany) with integrated fluorescence unit for excitation and appropriate filters for excitation, emission and detection. Excitation was done using a HBO 100 high-pressure mercury lamp (HBO 100, Leistungselektronik JENA GmbH, Jena, Germany). Due to the Stokes-transition between the absorption and emission spectrum, it is possible to separate the bright excitation light from the weak fluorescence light in the light path of the microscope via using appropriate filter sets. Pictures of fluorescence intensities were taken using a CCD camera (Rolera-XR, QImaging, Surrey BC, Canada) and QCapture Pro 6.0 imaging software (QImaging, Surrey BC, Canada).

2.3.4 Solid phase amplification

Solid phase amplification (SPA) was performed as a special form of arrayed on-chip amplification using directly surface-bound primers forming a very dense carpet like probes in microarray applications (Bing DH *et al.*, 1996; Adessi C *et al.*, 2000; Nickisch-Roseneck M *et al.*, 2005; Fedurco M *et al.*, 2006). Amplification can occur via two processes. First “interfacial amplification”, where freely diffusing DNA target molecules attach to surface-bound primers, primers are elongated to complementary DNA copies and these ssDNA molecules stay attached to the surface, while the initial DNA molecule returns to the solution after the annealing step. Second “surface amplification”, where the free end of the attached ssDNA copy hybridizes to a sequence-complementary surface-attached primer in immediate proximity. This time primer elongation leads to building bridges between primers, as both elongated DNA molecules stay attached to the surface. SPA thus leads to the generation of a colony of molecules attached to the surface and located in the same region. Synthesized PCR

2. Materials and Methods

products can be visualized either by confocal microscopy or fluorescence microscopy using Cy5-dye fluorescence of modified primers, or the fluorescence of intercalating dyes.

Spot array design. For solid phase amplification applications, 3 different surface-bound primer-pairs were spotted on reaction center B (\varnothing 500 μm) of LOC chips (**chapter 2.3.1**). Primer-pairs were spotted in a 2x2 spot array structure using a *Nadelspotter* (spotting operations were performed by Advantix AG/Beckman Coulter Biomedical GmbH, Munich, Germany). The following array design was spotted: the array consisted of 4 spots, while each spot comprised a different primer-pair content. On one spot primer-pairs DY-fw and DY-rv for amplifying male locus DYS392 were spotted, on a second spot primer-pairs DX-fw and DX-rv for amplifying female locus DXS10134, on a third spot primer-pairs AM-fw and AM-rv for amplifying human amelogenin as a positive control and on the fourth spot primers DY-fw and DX-fw as negative control, providing no complementary sequences after amplification. Primer sequences were listed in the appendix, **chapter 9.2**. Spot size was about 120 μm (100-160 μm) with a spot distance of about 160 μm , comprising an array diameter of about 400 μm . Spotting solution contained 50 μM oligonucleotide probe solution dissolved in 1x Advantix spotting buffer AT100. Spotting, washing and passivation steps after spotting were done by Advantix AG/Beckman Coulter Biomedical GmbH, Munich, Germany as well.

Solid phase amplification PCR reactions. For performing solid phase amplification on LOC chips the QuantiFast™ SYBR® Green I PCR kit was used for 2-step PCR (QIAGEN GmbH, Hilden, Germany). Several PCR protocols were tested as described in the following, first only “SPA PCR” using genomic DNA and second a “combined PCR setup” using preamplified PCR products. Before PCR, array-spotted LOC chips were preheated for 15 min at 95°C for adapting the material to hot temperatures (**chapter 2.3.1**).

Using “SPA PCR”, 1 μl of total reaction mix contained 0.5 μl of 2x QuantiFast™ SYBR® Green I PCR Master Mix (final 1x), 0.3 μl of sterile water (Ampuwa®, Fresenius, Bad Homburg, Germany) and 0.2 μl of 10x concentrated input DNA. For input DNA 5 ng/ μl of male or female reference DNA was used, resulting in a final concentration of 1 ng reference DNA present in 1 μl total reaction volume. 1 μl of prepared master mix was placed on primer-array spotted reaction center B of LOC chips and was immediately covered with 5 μl of Sealing Solution to prevent evaporation and external cross-contamination. 2-step SPA PCR cycling conditions were 5 min initial denaturation at 95°C, followed by 35 cycles of 95°C for 30 sec and 60°C for 60 sec.

2. Materials and Methods

Using the “combined PCR setup”, preamplified PCR products were used as input DNA. For preamplification the QuantiTect™ SYBR® Green I PCR kit was used for 3-step PCR (QIAGEN GmbH, Hilden, Germany), while 10 µl of total PCR reaction mix contained 5 µl of 2x QuantiTect™ SYBR® Green I PCR Master Mix (final 1x), 1 µl of 10 µM primer solutions (DYS392-fw and DHS392-rv or DXS10134-fw and DXS10134-rv or Amel1 and Amel2; final 1 µM per primer), 2 µl of sterile water (Ampuwa®, Fresenius, Bad Homburg, Germany) and 1 µl of 10x concentrated input DNA. For input DNA 5 ng/µl of male and female reference DNA was used, resulting in a final concentration of 500 pg reference DNA present in 10 µl total reaction volume. Primer sequences were listed in the appendix, **chapter 9.2**. Reactions were performed in sterile 0.2 ml PCR-tubes (Eppendorf AG, Hamburg, Germany) using a conventional in-tube PCR thermocycler (advanced Primus 96, PeqLab Biotechnologie GmbH, Erlangen, Germany). 3-step PCR cycling conditions were 15 min initial denaturation at 95°C, followed by 35 cycles of 94°C for 30 sec, 55°C for 60 sec, 72°C for 30 sec, and final product extension at 72°C for 7 min. PCR products were analyzed on polyacrylamide gels (CleanGel 10%, ETC GmbH, Kirchentellinsfurt, Germany) and subsequent DNA silver staining (DNA silver staining kit, GE Healthcare, Uppsala, Sweden) (**chapter 2.2.3**). Blank and negative controls were included in every reaction batch. For 0.1 µl input DNA in the following “combined PCR setup”, 0.033 µl of each preamplified PCR product tube DHS392, DXS10134, Amel for male or female DNA was utilized. The “combined PCR setup” comprised three reaction steps performed consecutively on LOC chips, which were summarized in **table 2**, while the QuantiFast™ SYBR® Green I PCR kit was used for 2-step PCR (QIAGEN GmbH, Hilden, Germany).

Table 2. Combined PCR setup. Interfacial amplification, surface amplification and a hybridization step were performed consecutively on the LOC chip’s surface for optimizing solid phase amplification output.

Order of performance	Composition of reaction mix	Thermal cycling conditions
1. Interfacial amplification	1 µl total reaction mix contained 0.5 µl of 2x QuantiFast™ SYBR® Green I PCR Master Mix (final 1x), 0.4 µl of sterile water (Ampuwa®, Fresenius, Bad Homburg, Germany) and 0.1 µl of preamplified PCR products.	2-step PCR protocol: 5 min initial denaturation at 95°C, followed by 30 cycles of 95°C for 30 sec and 55°C for 60 sec.
2. Surface amplification	1 µl total reaction mix contained 0.5 µl of 2x QuantiFast™ SYBR® Green I PCR Master Mix (final 1x) and 0.5 µl of sterile water (Ampuwa®, Fresenius, Bad Homburg, Germany).	2-step PCR protocol: 5 min initial denaturation at 95°C, followed by 30 cycles of 95°C for 30 sec and 55°C for 60 sec.
3. Hybridization	1 µl total reaction mix contained 0.5 µl of 2x QuantiFast™ SYBR® Green I PCR Master Mix (final 1x) and 0.5 µl of preamplified PCR products.	Hybridization protocol: 3 min denaturation at 95°C, followed by 40°C hybridization temperature for 30-60 min.

Washing protocol and detection. After finishing “SPA PCR” or “combined PCR setup”, Sealing Solution was washed away from reaction center B using sterile water and array chips were subjected to the washing protocol described in **table 1**. Washing procedures removed the Sealing Solution efficiently as well as unbound PCR remainings. LOC chips were washed manually by applying a 10 μ l overlay of buffers onto the SPA reaction center B of the chips. After washing, array chips were dried for 5 min at 37°C until slide surfaces were totally dry and stored in darkness for the scanning process (max. 3 h). LOC chips were scanned using an inverted optical microscope (Axio Observe.Z1, Carl Zeiss GmbH, Jena, Germany) with integrated fluorescence unit for excitation and appropriate filters for emission and detection. Excitation was done using a HBO 100 high-pressure mercury lamp (HBO 100, Leistungselektronik JENA GmbH, Jena, Germany). Due to the Stokes-transition between the absorption and emission spectrum, it is possible to separate the bright excitation light from the weak fluorescence light in the light path of the microscope via using appropriate filter sets. Pictures of fluorescence intensities were taken using a CCD camera (Rolera-XR, QImaging, Surrey BC, Canada) and QCapture Pro 6.0 imaging software (QImaging, Surrey BC, Canada). Additionally, fluorescence signal were detected using the lab-on-a-chip integrated Fluorescence Reader and appropriate software “Norbert.VI” for manual picture taking (LabVIEW 8.6, National Instruments Germany GmbH, Munich, Germany). Pictures were taken with exposure times of 1000 ms, 2000 ms and 4000 ms at room temperature as well as at 40°C and 60°C. Furthermore, to check for detached primers and PCR products in the SPA reaction solution, reaction mixes were analyzed on polyacrylamide gels (CleanGel 10%, ETC GmbH, Kirchentellinsfurt, Germany) and subsequent DNA silver staining (DNA silver staining kit, GE Healthcare, Uppsala, Sweden) (**chapter 2.2.3**).

2.3.5 Sequencing of amplified ancient sample material

Sequencing was performed on PCR products of microdissected ancient bone tissue sample mummy4, exemplary for all of four microdissected mummy samples. For subsequent sequencing, PCR was performed using the QIAGEN[®] Fast Cycling PCR kit (QIAGEN GmbH, Hilden, Germany) for 3-step PCR according to manufacturer’s recommendations. Reaction volumes were scaled down to 20 μ l, prepared in sterile 0.2 ml PCR-tubes (Eppendorf AG, Hamburg, Germany). Cycling was performed in a conventional PCR thermocycler (Cyclone 25, PeqLab Biotechnologie GmbH, Erlangen, Germany). 20 μ l total PCR reaction mix contained 10 μ l of 2x QIAGEN Fast Cycling PCR Master Mix (final 1x), 4 μ l of 5x QIAGEN Q-Solution (final 1x), 2 μ l of 10 μ M primer solutions Amel1 and Amel2,

or primer solutions β -Actin up and β -Actin down respectively (final 1 μ M per primer), 1 μ l of sterile water (Ampuwa[®], Fresenius, Bad Homburg, Germany) and 1 μ l extracted mummy DNA (corresponds to 60 pg). Primer sequences were listed in the appendix, **chapter 9.2**. 3-step PCR cycling was performed as recommended by the manufacturer's protocol: 5 min initial denaturation at 95°C, followed by 40 cycles of 94°C for 30 sec, 60°C for 30 sec and 72°C for 30 sec, and final product extension at 72°C for 1 min. For product purification and sequencing analysis, PCR products were sent to GENEART AG sequencing service (Regensburg, Germany).

2.3.6 Precautions to prevent contamination in ancient sample material analysis

During experiments, numerous precautions were taken to minimize the risk of contamination, which were summarized by Pääbo S *et al.* (2004). Furthermore, to exclude possible cross-contaminations between ancient sample material and scientific staff, DNA typing reactions were performed using selected STR markers D7S1824, D9S302, D10S2325 and also the AmpF/STR[®] SEfiler[™] PCR amplification kit (**chapter 2.3.1**). DNA profiling of extracted mummy material as well as genomic material of involved scientists, archaeologist/excavator, technical assistance staff, laboratory personnel and all people who had been knowingly in contact with any kind of mummy material (including bone particles, paraffin-embedded tissue blocks, tissue slides and mummy DNA extracts) and also with laboratory equipment (e.g. laboratory working places and laboratory working tools like laser microdissection microscope, DNA extraction accessory and the PCR thermocyclers) was accomplished.

3. Description of the Lab-on-a-chip System

The existing lab-on-a-chip (LOC) system was designed as a modular composition comprising five independent working modules (**figure 3**). There were two modules for sample preparation prior to PCR analysis, in fact a laser-based microdissection unit (**chapter 3.1**) for retrieval of sample material as well as a particle transfer module (SPATS, **chapter 3.2**) providing an interface to the PCR unit after microdissection. The PCR module CytoCycler (**chapter 3.3**) represented the core of the LOC system encompassing a progressive microchip design, flexible and open for a huge amount of sample types and analytical applications including sample processing, amplification and detection. For informational output, a Fluorescence Reader was integrated for post-PCR product detection methods like real-time PCR and array applications (**chapter 3.5**). Following the envisioned automation of all sample-processing steps, additionally an automatic fluid-dispensing device was integrated compensating manual pipetting operations (BioSpot[®], **chapter 3.4**). While each unit was handling important sample processing functions individually and totally software controlled, altogether these modules combined comprehensively to a universal and programmable micro total analysis system. Due to an intelligent slide rail-based integration of all modules sterical interferences of modules, while serving the small LOC chip surface, could successfully be circumvented.

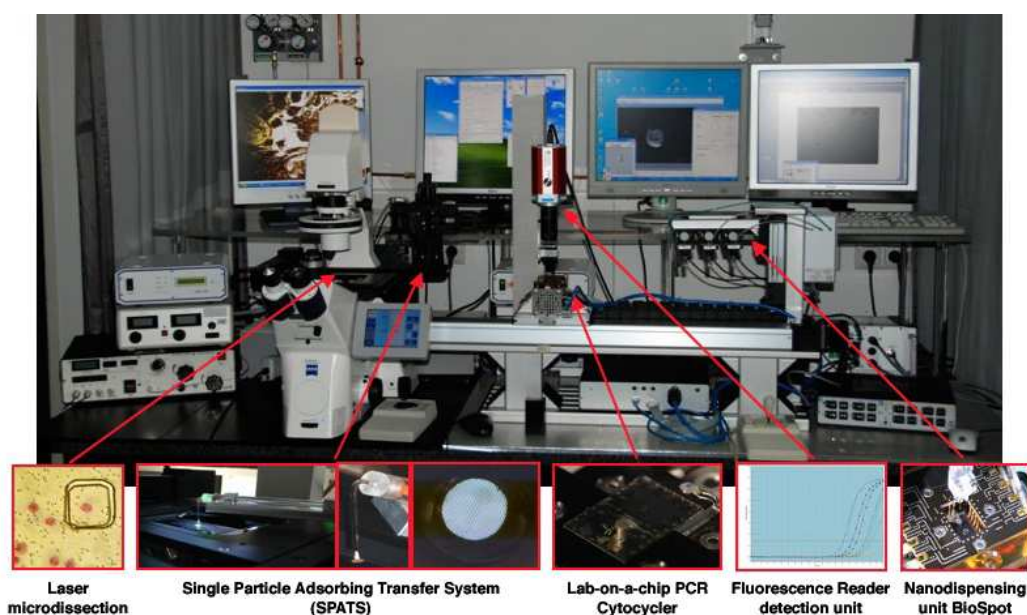


Figure 3. Overview of the complete lab-on-a-chip system. The modular design includes a laser-based microdissection unit for sample retrieval and a transfer unit SPATS for loading the PCR-CytoCycler with sample material. While being served by an automatic liquid dispensing unit BioSpot[®], the CytoCycler PCR amplification unit and the fluorescence detection unit provide all necessary equipment for genetic analysis of sample material.

3. Description of the Lab-on-a-chip System

During the last years, this lab-on-a-chip system was referred in a couple of scientific articles (Thalhammer S *et al.*, 2007; Woide D *et al.*, 2008; Thalhammer S *et al.*, 2008; Thalhammer S, 2009; Thalhammer S *et al.*, 2009), conference sessions (Woide D *et al.*, 2008, Actuator 2008, Bremen; Woide D *et al.*, 2008, Science Day 2008, Linz) as well as most notably in a professorial dissertation (Thalhammer S, 2009). In the following sections an overview over the total LOC system as well as technical features and functional operations of each particular modular unit is illustrated. Detailed descriptions of laboratory internal operating procedures of each individual LOC module were summarized in the appendix (**chapter 9.1**) and are available on an external media.

3.1 Laser microdissection module

During the last decade, laser-based systems have become state-of-the-art technologies for precise and non-contact micromanipulation of biological material in biology and medicine. However, the initiation of using focused light for micromanipulation goes back to 1912, when Tschachotin focused the light of a bulb lamp through the microscope objective onto an object plane (“Strahlenstich” method, Tschachotin S, 1912). After the invention of lasers in 1960, the first laser was coupled into a microscope to achieve much smaller laser focal spots for manipulation purposes (Bessis M *et al.*, 1962). Since then, laser technologies were developed further for a broad area of medical applications, while in 1987 optical tweezers as well as pulsed UV-lasers integrated in optical instruments began to revolutionize micromanipulation of cells and particles without any mechanical contact (Ashkin A *et al.*, 1987; Ashkin A and Dziedzic JM, 1987; Srinivasan R, 1986; for a general overview refer to Thalhammer S *et al.* (2003) and Thalhammer S *et al.* (2004)). Today, modern molecular research and diagnosis rely increasingly on the capability to isolate pure single sample particles and their precise positioning for further biochemical analysis. Non-contact manipulation techniques based on laser microdissection provide not only highly selective isolation and extraction but also the precise manipulation of smallest fractions of genetic material due to laser ablation with microbeams and with minimum risk of contamination.

The available laser microdissection unit at hand comprised a modified UVA-laser system integrated into an inverted optical microscope. For material isolation the principle of material ablation was utilized based on a pulsed nitrogen UVA laser beam ($\lambda = 337 \text{ nm}$) having a maximal pulse frequency of 30 Hz and a pulse-duration of 3 ns (pulse energy $>270 \text{ }\mu\text{J}$). For laser ablation the laser was coupled via the epifluorescence path into the light path and was

3. Description of the Lab-on-a-chip System

focused through the microscope objective to less than one micrometer in diameter. Diameters of the laser focus were set via the numerical aperture of the objective. The force of the focused, near diffraction limited pulsed UVA laser light was utilized for microdissection of biological material with high spatial resolution. As only UVC light ($\lambda = 200\text{-}290\text{ nm}$) was identified to cause DNA damage, as the main absorption peaks of DNA and proteins are located at 260 nm for DNA and 280 nm for proteins, the 337 nm wavelength was well outside of the DNA damaging region. Biological material within the focal spot of the laser was ablated due to photofragmentation, a photochemical process without heat transformation into the surroundings (“cold-ablation”), also called “ablative photodecomposition” (APD) (details in Thalhammer S *et al.*, 2003). Within the focal spot of the laser an extreme photon density was achieved (intensity of more than 1 Megawatt/cm²), photofragmenting unwanted cut material into small molecules and atoms, which were blown away at supersonic velocities. As the ablative force was restricted to the minute laser focal spot only, directly aside of the laser focus spot the photon density was not sufficient to cause ablation, leaving the adjacent specimen entirely intact (Srinivasan R, 1986).

The total system for laser-based microdissection included the inverted optical microscope with laser interface, motorized and joystick-controlled microscope XY-scanning stage as well as particular software “Nanosauger”. The laser interface was a one-box device, which housed the laser and all necessary optics to guide the laser into the microscope and to bring the laser focus coincide with the optical focus of the microscope at the object plane. The well-directed positioning of object slides with nano- and micrometer precision was possible via stepping-motor-controlled XY-scanning stage while joystick movements were translated into two dimensional stage displacements. The stage speed could be adapted software-controlled. Via an external control board the laser focus as well as cut energy could be set at the object plane. Thus, the laser focus could be changed into z-direction independently from the microscope focus. For adjusting the focus plane to the object plane, a telescopic device was applied in the light path, while the focus point could also be leveled above/beneath the object via a lens, which was especially necessary when working with different objectives or varying sample thickness. The beam focus was dependent on the beam quality of the laser, the numerical aperture of the focusing objective and the absorption behavior of the specimen (Thalhammer S *et al.*, 1997). The nitrogen laser emitted fixed laser energy; for energy settings a grey wedge filter was fixed behind the laser coupling out, absorbing the remaining energy. This allowed adjusting the laser energy continuously without beam displacement. For documentation there were two cameras available, a black & white CCD camera and a color firewire camera.

3.2 SPATS particle transfer module

Based on PEN-membrane supported laser ablation using a pulsed UVA laser, a special approach for material extraction was developed for being integrated into the lab-on-a-chip system. The device was called “SPATS” meaning single particle adsorbing transfer system and facilitated horizontal single particle transfer to any planar devices after UVA laser-based microdissection like e.g. on the LOC system, gently controlled via low-pressure technology. The device was reported as a novel approach for horizontal transfer of single particles after laser microdissection and EU patented (EU patent 08150662.8), published (Woide D *et al.*, 2009) and tested for various scientific relevant applications (Mayer V *et al.*, 2009; Woide D *et al.*, 2010).

The SPATS was fabricated by the company XYZ High Precision (Darmstadt, Germany) and consisted of several components combining mechanical, optical, pneumatical and electronic components. Due to its modular character, the SPATS was fixed to the inverted optical microscope via a micrometer stepping motor, which provided movements in XY-direction for horizontal as well as vertical particle transfer with μm -precision. The SPATS sample take-up device comprised a copper collection grid with meshes, attached to a bended transparent glass capillary tube, both comprising the adsorbing head, which is connected to the moving part of the device, the collection arm (**figure 4**). For transfer of various samples, adsorbing heads could be exchanged by an “easy-to-fit” click system. The glass capillary tube had an external diameter of 1.7-2.0 mm, an internal diameter of 500 μm and a length of 60 mm. The collection grid was biologically inert, antistatic and UV-C resistant, comprised a diameter of 500 μm with meshes of 5 μm in diameter. Fixed at the micrometer stepping motor, the collection arm was connected to a pneumatic picopump. Low- and high-pressure adaptors allowed fine-tuning of both low-pressure and high-pressure for sample take-up and release. All functions and parameters of hardware components like scanning microscope XY-scanning stage (for positioning sample uptake), camera (for optical control), SPATS device movement and pressure-supply box were controlled by particular software “Nanosauger”.

The new approach was based on the laser pressure catapulting method using a PEN supporting membrane for material extraction, but progressive low-pressure technology was utilized for sample take-up and release instead of laser shot and formation of a microplasma (Thalhammer S *et al.*, 2003). The SPATS device was qualified for extraction and transfer of hard material, like e.g. bone tissue particles (Woide D *et al.*, 2010), as well as soft material, like tissue sections, single cells (Mayer V *et al.*, 2009) or chromosomes (**figure 4 B**).

3. Description of the Lab-on-a-chip System

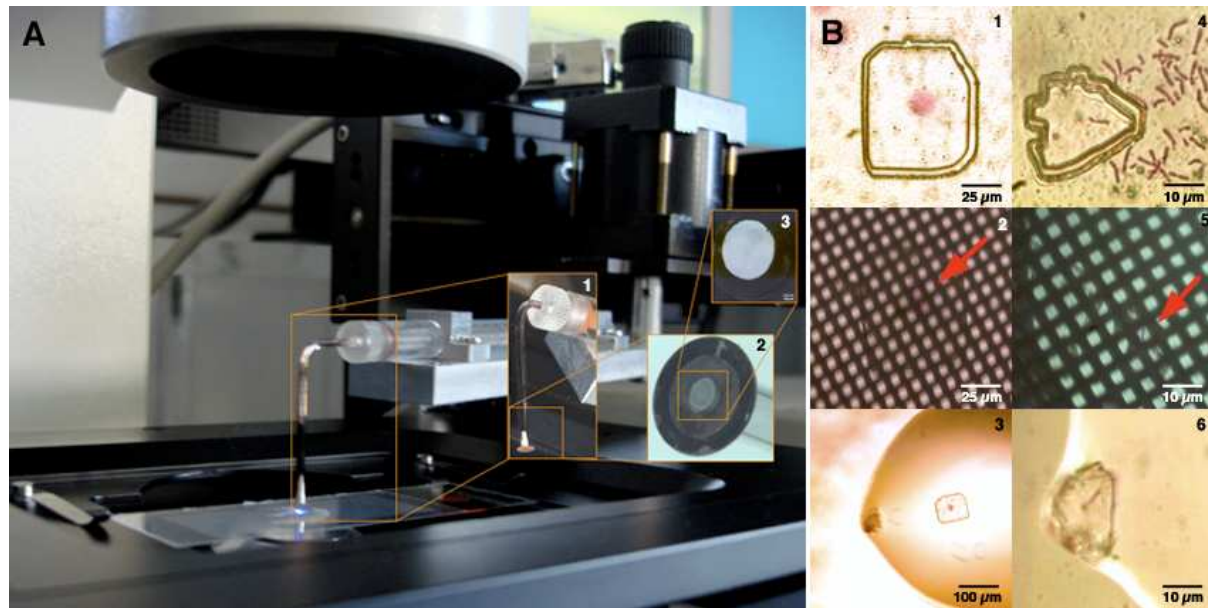


Figure 4. SPATS device. **A)** Closeup of the sample take-up device “single particle adsorbing transfer system” SPATS. The adsorbing head comprised a bended glass capillary tube (insert 1, 500 μm internal diameter) and a copper collection grid (insert 2 and 3, 500 μm in diameter with meshes of 5 μm in diameter). Insert 2 shows a view on the whole adsorption area, while insert 3 provides a view through the microscope onto the sample collecting area. **B)** Workflow of sample transfer. Via applied low-pressure technology the SPATS was capable of transferring soft material like e.g. single cells (20 μm in diameter, picture 1-3), or cellular components like nuclei and chromosomes (1-10 μm in size, pictures 4-6) as well as hard material like e.g. bone tissue particles (about 350x250 μm in size). A typical workflow consisted of material isolation via laser microdissection (pictures 1 and 4), adsorption to the collection grid (pictures 2 and 5) and followed by release into a small amount of fluid (pictures 3 and 6).

Microdissected particles in the range from 5-500 μm in diameter could be transferred, whereas the adsorption limit of 5 μm however applied only to the size of microdissected PEN-membrane carrier fragments. Smaller particles fell below the diameter of the grid meshes, and larger ones exceeded the visible adsorption zone. The size of the biological sample isolated could be smaller (e.g. a single metaphase chromosome). Particle shape should be planar and particle weight depended on the applied pressure and the suction volume according to the grid diameter. Due to the chemical composition of the supporting membrane, the PEN membrane was stable up to 155°C and did not interfere with subsequent PCR analysis. Low-pressure was used to attach isolated material to the collection grid, allowing precisely controlled positioning for sample release to any desired predefined target position into test tubes as well as onto any planar microchip device. During the transfer process, the sample was neither changed morphologically, chemically nor biologically. The SPATS was the first device enabling gentle horizontal and highly precise transfer of microdissected material, thus emerging a high potential for sample handling in regard to lab-on-a-chip technologies. Using virtual reaction chamber microdevices like the lab-on-a-chip system described here, small amounts of microdissected material could be directly transmitted and immediately used for analysis.

3.3 CytoCycler PCR module

The CytoCycler represented the microfluidic component of the total lab-on-a-chip system, driven by surface acoustic wave (SAW) actuation and controlled via interdigital transducers (IDT). The CytoCycler PCR device could be considered the core of the whole lab-on-a-chip system, providing all necessary equipment for performing virtual reaction chamber PCR amplification of genetic sample material. It included LOC chips providing the platform for sample analysis, a chip-holder, a temperature control device, a high frequency (HF) generator for SAW control via joystick, and particular software “CytoCycler”. The whole CytoCycler equipment was fabricated and provided by the company Advantix AG/Beckman Coulter Biomedical GmbH (Munich, Germany). The software “CytoCycler” controlled PCR performances via the temperature control device and a temperature sensor at the chip-holder, and also transmitted trigger signals to the trigger signal break-out box of the Fluorescence Reader (**chapter 3.5**). The temperature control device was software-controlled, while the HF generator and thus droplet actuation via SAW was controlled via joystick operations.

LOC chip design. LOC chips were designed as virtual reaction chamber (VRC) low-volume LV-PCR chips, according to the basic principle of a virtual reaction chamber PCR chip as introduced in 2005 (Guttenberg Z *et al.*, 2005). The device was fabricated from piezoelectric LiNbO₃ as basic material followed by a metal gold layer for the SAW interdigital transducers (IDTs), contact wires and gold contacts. Epoxy groups were used to make the surface hydrophilic at distinct reaction areas and to form virtual hydrophilic tracks. This surface was chemically treated via hydrophobic/oleophobic fluorsilane coating to present an epoxysilane hydrophilic tracksystem surrounded by hydrophobic/oleophobic background (**figure 5 A**). The chemically heterogeneous structured fluorsilane/epoxysilane surface of the LiNbO₃ chip was produced in a structuring process by coating with silanes (Brzoska JB *et al.*, 1994) followed by applying photolithography on the resulting organic film (Xia Y and Whitesides GM, 1998). The track system included hydrophilic reaction centers, providing high contact areas for fluids for fixation and optimal heat transfer. The complete chip was protected with sputtered silicon dioxide, which was removed above the gold contact pads. All these hydrophilic/hydrophobic structures were patterned by photolithography (**figure 5 B**). An aqueous droplet, e.g. containing sample material and reaction solution, formed a virtual reaction chamber when placed on the structured surface. This virtual confinement, forming an own wall- and tube-free virtual test tube, was achieved due to surface tension of the liquid and surface chemistry of the substrate (**figure 7**). Depending on the kind of chemical surface

3. Description of the Lab-on-a-chip System

modification, droplets with high contact angle could slide on the surface (hydrophilic droplet on hydrophobic surface) or the liquid could wet the surface due to low contact angles (hydrophilic droplet on hydrophilic surface). Each chip had three reaction centers comprising low contact angles and 10 track lanes served by 10 separately addressable SAW transducers on crossover directions for aligning the droplets on the heater structures and for fusing droplets in reaction centers (**figure 5 B**). Opposing transducers had different spatial periods to avoid crosstalk.

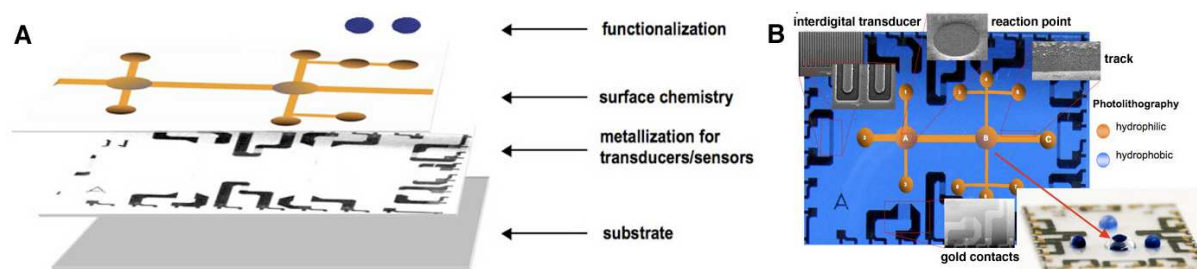


Figure 5. LOC chip design and structuring lithography. **A)** The chip architecture comprised a layer-by-layer design based on LiNbO_3 as basic substrate. After a metallization layer including IDTs and gold contacts surface chemistry provided the basis for functional compartments. **B)** Hydrophilic areas (hydrophilic reaction centers A+B+C and guiding tracks for the oil droplet movement, orange pattern) were patterned on the chip with positive photoresist, while an organic layer of a hydrophobic perfluoroalkylsilane was bound to the whole surface (blue pattern). After removing the photoresist, epoxysilane was grafted from an organic solution. Small inlets show electron microscopy images of the various functional structures on the chip surface like interdigital transducers, reaction points, tracks and gold contacts. Hydrophilic tracks were about $15\ \mu\text{m}$ in width for side tracks and $200\ \mu\text{m}$ for the main track from A to C. Reaction centers A and B comprised a diameter of $500\ \mu\text{m}$, while center C was designed as a square with $1 \times 1\ \text{mm}^2$ in size. Small anchor spots at sidetracks comprised about $40\ \mu\text{m}$ in diameter.

Chip-holder. The chip-holder itself provided a cavity for installing a LOC chip in contact with a Peltier element and with a load resistor heating, a temperature sensor, and a contacting lid for the high frequency support of the IDTs (**figure 6 A**). The contacting lid housed gold contact pins for contacting the gold contact pads on the chip surface, thus transferring the high frequency signal from the HF generator to the designated transducers on the chip surface. At the transducers, electrical high frequency signals were converted into mechanical vibrations, propagating as surface acoustic waves on the surface (**figure 6 B**). Heat transfer from the Peltier element to the LOC chips was achieved by close contacting of the Peltier element's surface with the chip's undersurface, thus providing direct heat transfer.

Heating structures and reaction centers. There were 3 hydrophilic reaction centers (A, B, C) chemically generated on the chip surface being heated by two heating devices located within the cavity of the chip-holder to contact the chip's undersurface (**figure 6 B**). Heating devices were a load resistor heating ($2 \times 2\ \text{mm}^2$ in size) for isothermal cycling and a Peltier element ($1 \times 1\ \text{cm}^2$ in size) with an integrated temperature sensor for thermal PCR cycling. Hydrophilic

3. Description of the Lab-on-a-chip System

reaction center A comprised 500 μm in diameter and was thermally served by the load resistor heating for isothermal reactions. Hydrophilic reaction center B comprised 500 μm in diameter and was thermally served by the Peltier element for PCR and microarray applications (**figure 6** and **figure 7 C**). Hydrophilic reaction center C comprised a square of 1 x 1 mm^2 and was designed for array applications, while being thermally served by the Peltier element as well. In the area around the heaters, the temperature dropped fast. Heating rates for the load resistor heating could be adjusted to 0.01 – 10 K s^{-1} , while heating rates for the Peltier were fixed to 3 K s^{-1} and cooling rates to 4 K s^{-1} . To avoid disturbing air streams and dust on the chip surface, the reaction area cavity was covered with a glass slide during PCR performances.

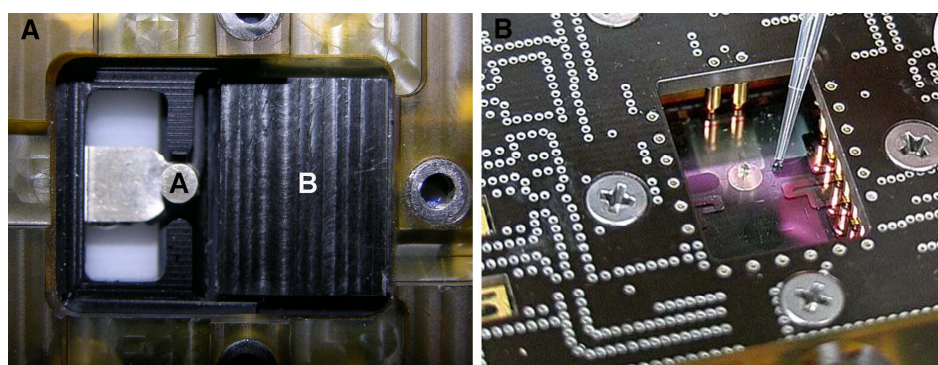


Figure 6. Chip-holder and heating elements of the CytoCycler. A) Basis of the chip-holder: the cavity for installing a LOC chip is shown (2.5 x 2.0 cm^2), as well as the two heating devices, a load resistor heating (2x2 mm^2 , marked with an “A”) and a Peltier element (1x1 cm^2 , marked with a “B”). **B)** Assembled chip-holder with a transparent LOC chip installed. The contacting lid held gold pins, which were in contact with gold contact pads on the chip surface. Via this contacting, HF signals were transmitted to the interdigital transducers and transformed into surface acoustic waves propagating on the chip surface.

SAW droplet actuation. Actuation for moving droplets on the surface of the piezoelectric substrate was done by surface acoustic waves (SAW) (Shiokawa S *et al.*, 1989; Uchida T *et al.*, 1995) for to bring reagents into contact and to reaction centers. Surface acoustic waves were generated by interdigital transducers, which were patterned on the planar LiNbO_3 substrate (**figure 5 B** and **figure 7 C**). Electrical signals, sent by the HF generator, were conducted via the gold contact pins of the lid to the gold contact pads on the chip surface. Gold contacts on the chip served IDTs, where electrical signals were transferred into mechanical vibrations propagating on the surface substrate as acoustic sound waves (also called acoustic streaming (Moroney RM *et al.*, 1991; Wixforth A, 2003)). When a SAW coupled into a droplet, this led to a pressure gradient in the liquid. Depending 1) on the size of the gradient, namely the applied HF power, as well as depending on 2) the wetting angle of the liquid (namely its contact angle on hydrophilic/-phobic substrate) and on 3) the angle with which the wave coupled into the fluid, the droplet either started an internal streaming (small gradient) or was pushed to move forward (large gradient) in the same direction as the sound

3. Description of the Lab-on-a-chip System

wave (Guttenberg Z *et al.*, 2004; Nyborg WL, 1998). Internal streaming could e.g. be used for mixing and a large gradient e.g. for moving droplets as well as for dispensing small droplets out of a larger volume (Strobl CJ *et al.*, 2004).

The LOC chips comprised 10 IDTs located around the chip to serve each lane of the tracksystem (**figure 5 B** and **figure 7 C**). The high frequency generator was operated via a joystick, controlling the actuation of each particular SAW transducer on the chip. Using this joystick, droplets could be actuated in a very precise manner in either direction following the virtual track system on the chemically structured chip surface. Thus, an exact alignment on reaction centers could be achieved. On the chip, SAW provided the connection of subsequent sample processing steps, like e.g. moving sample-loaded droplets to various reaction areas on the chip surface. SAW were used for providing the oil coverage by simply fusing an aqueous sample-containing droplet with a larger-volume mineral oil droplet as well.

Performing virtual reaction chamber LV-PCR. Reactions were performed on the open 2-dimensional planar chemically structured surface of the microfluidic chip device. To prevent external cross-contamination and evaporation of PCR reagents and sample material at high temperatures, the aqueous droplet (including e.g. reaction solution and sample material) was encapsulated within a droplet of mineral oil (**figure 7**).

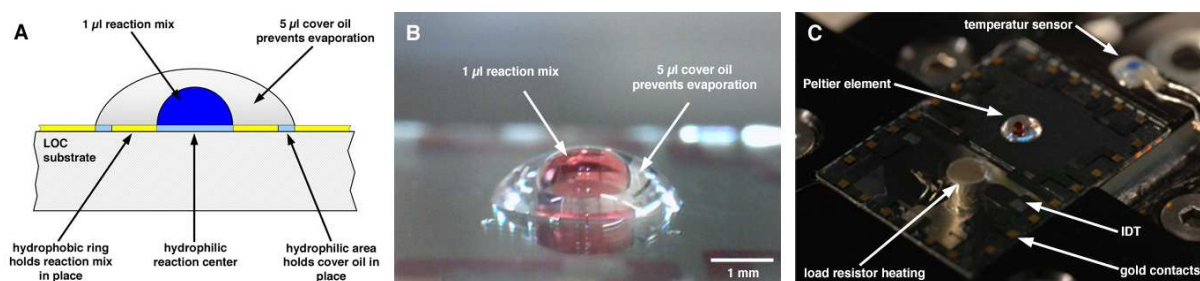


Figure 7. Principle of virtual reaction chamber PCR. A) Schematic drawing of virtual reaction chamber PCR. An aqueous droplet of reaction mix is placed on a chemically modified surface and covered by mineral oil to prevent evaporation. A proper arrangement of both droplets was achieved by chemical surface treatment via photolithography. A hydrophilic reaction center (500 µm in diameter) is enclosed by a hydrophobic ring, holding the reaction mix in place; a surrounding hydrophobic area keeps the cover oil (3 mm in diameter) in place. B) Surface chemistry provided virtual confinement on LOC chip surfaces. The different surface tensions of both liquids kept the spherical phase separation. For visualizing phase separation, a small droplet of 1 µl of dyed aqueous solution was covered with 5 µl of mineral oil. C) Gold contact pads were located around the chip, serving the IDTs to generate SAWs in any desired direction on the tracksystem. Via surface acoustic waves VRC droplets could be moved between reaction centers and both heater devices, the load resistor heating and the Peltier element. The whole chip comprises a size of 2.5 x 1.8 cm².

The different surface tensions of the two liquids provided the spatial separation, while still retaining the ability to be moved by SAW actuation (**figure 7 B**). This kind of fluid arrangement was transported in single oil covered droplets on a chemically modified surface using surface acoustic waves (SAW) on the piezoelectric LiNbO₃ substrate (**figure 7 C**).

3. Description of the Lab-on-a-chip System

Benefits of the planar virtual reaction chamber microdevice. The main purpose of a lab-on-a-chip system is to simplify and automate labor intensive, time consuming and costly laboratory procedures. However, conventional 3-dimensionally constructed microfluidic systems are using channel networks, in which the liquid is controlled with external or integrated miniaturized pumps and valves or via electrocapillary forces bearing some major problems (as already described in the introductory part). As the pressure required for moving the liquid scales inversely with the channel dimension (Brody JP *et al.*, 1996), the power of the pumps therefore has to be increased in the same way the size is reduced, which complicates integration into a complete system. According to the channel diameter only laminar flow is possible due to low Reynolds numbers. The Reynolds number characterizes the tendency of a fluid to develop turbulence. Low Reynolds numbers involve high viscosity and laminar flow, while high Reynolds numbers involve low viscosity and turbular streaming. But laminar flow is useless for biochemical reactions as this leads to insufficient mixing and diffusion takes too much time. For generating turbular flow in channel systems, actuators, mixers, sensors and all that stuff are needed. With hydrophilic channels that are filled by capillary forces no pumps are needed, but the fluid control is delicate. Furthermore, when a biological solution is pumped through a narrow tube, the risk of reagent loss by adhesion to the wall is large due to unfavorable surface to volume ratio. Other problems are that small channels get easily clogged and that surface modification and functionalization is difficult to control. Furthermore, channels are hard to clean so one has to deal with contamination. Otherwise these complex structures were too expensive in fabrication to be disposables. To overcome all these problems, using a virtual reaction chamber device beared a lot of benefits. The fluid actuation was done on a planar surface via SAW generated by IDTs via HF signals, so no external pumps and no large pressure were needed. Furthermore, no channels were needed, as fluids were confined in virtual test tubes in form of free droplets due to surface tension and surface chemistry. Small amounts of liquid did not need to be confined in tubes or trenches, they formed their own test tubes held together by surface tension, but dependent on the wettability of the surface substrate. There was no large pressure needed, as the droplet-in-oil arrangement was easily moved via SAW power. Tracks and reaction chambers were defined by a chemically modified surface. As chips could be made cheap and served as disposables, even contamination or channel clogging did not play a role.

3.4 BioSpot[®] fluid-dispensing module

The BioSpot[®] device was a nano pipetting system for non-contact liquid handling and was fabricated and provided with appropriate software by the company BioFluidix GmbH (Freiburg, Germany). It comprised several parts featuring a) a PipeJet[™] dispenser moving in Z-directions for liquid uptake and delivery, b) a sample slay fixed on a slide rail moving in X-directions and c) a power control box also housing a syringe pump supporting aspiration and dispensation of liquid. Onto the sample slay the chip-holder device of the CytoCycler device was installed, carrying a flask-filled reservoir device (**figure 10 A**). The slide rail was about 70 cm in length and guided the chip-holder with an accuracy of $\pm 50 \mu\text{m}$, thus enabling a seamless motion of LOC chips to a sample take-up position close to the microscope, to the dispensing PipeJet[™] module and to the Fluorescence Reader (**figure 8**).

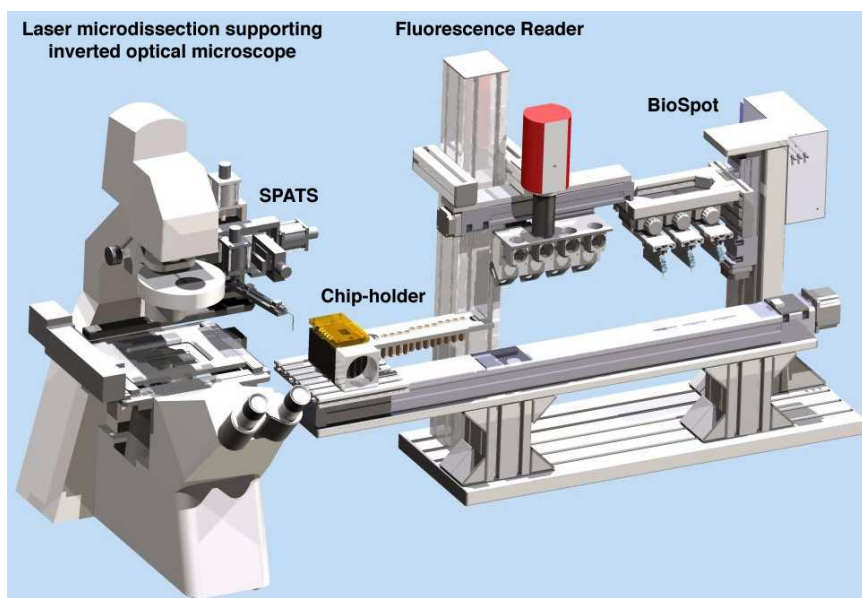


Figure 8. Overview of the particular units of the whole LOC system. The five modules of the lab-on-a-chip are shown namely the microscope combining laser microdissection and SPATS transfer, the chip-holder of the CytoCycler fixed on a moving slay, the BioSpot[®] dispensing device and components of the Fluorescence Reader. The slide rail enabled X-directed motion of the chip-holder, thus providing an elegant connection between individual LOC modules. The housing for all the optical components of the Fluorescence Reader as well as this graphical overview picture was designed in a computer aided design (CAD) program (SolidWorks 2006, Solid Works Corp.) and was kindly provided by G. Lieckfeld.

The BioSpot[®] operating unit consisted of three PipeJets[™] named PipeJet[™]1 (PJ1), PipeJet[™]2 (PJ) and PipeJet[™]3 (PJ3) executing all aspiration, dispensation and shooting operations. The PipeJets[™] were equipped with a tube reservoir, which was connected to a syringe pump for handling the aspiration and dispensation of liquids. PJ1 and PJ2 could handle aqueous liquids up to 50 μl , while PJ3 could handle up to 1 ml of mineral oil for droplet coverage when performing virtual reaction chamber PCR. Each PipeJet[™] housed an elastic polymer tube,

3. Description of the Lab-on-a-chip System

which was actuated by a piezostack driven piston supporting shooting operations. Polymer tubes were of low cost and could be used as disposables. “Shooting” meant a sequential dispensation of liquids at tiniest amounts of a few nl. Squeezing the tube via the piston resulted in a fast displacement of the filled liquid to both, the open end of the tube and the end connected to the reservoir (**figure 9**). Thereby a small droplet of about 22.5 nl of liquid was dispensed to the designated surface or reservoir, forming droplets of a few μl when repeated several times. Dosage volumes could be controlled by the amplitude of the piezo actuator, while other parameters involved in the dispensing process could be defined via the freely programmable software “BioSpot[®]”.

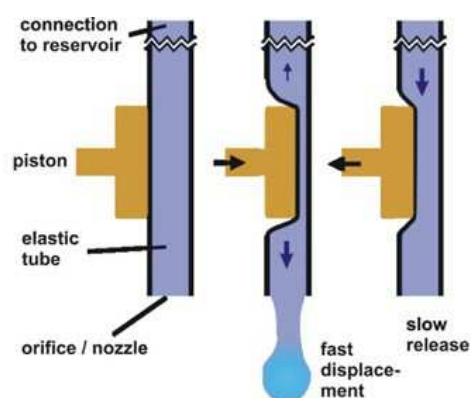


Figure 9. Dosage principle of the BioSpot[®]'s PipeJet[™] modules. The figure shows the piston driven actuation of a polymer tube as housed in PipeJets[™] PJ1, PJ2 and PJ3, resulting in the bidirectional dispensation of nanoliter droplets. Via a principle of fast displacement and slow release, smallest droplet sizes of 22.5 nl could be loaded precisely on the chip surface (BioFluidix GmbH, Freiburg, Germany; Lindemann T *et al.*, 2004).

The BioSpot[®] provided the easiest way to combine all LOC modules due to the 70 cm long slide apparatus, included with the BioSpot[®], and furthermore it will provide the important interface for enabling automation of the total LOC system. As a modular unit of the lab-on-a-chip system, the BioSpot[®] was used as a dispenser for various liquids needed for the molecular biological analysis executed on the LOC chip surface. The BioSpot[®], as a computer-controlled dispensing platform, was capable of unloading reagents at any destined domain on the LOC chip surface. The z-axis, where the PipeJets[™] were attached to, allowed movements of up to 40 cm, while y-positions of the PipeJets[™] needed to be adjusted manually. The distance between the three PipeJets[™] provided enough space that each PipeJet[™] could reach the chip surface.

The software gave access to four single active control windows for operating the whole BioSpot[®] device, namely (1) Axis Control and Axis Movement, (2) PipeJet[™] Control, (3) Valve Control and Pump Control and (4) Batch Mode. A total operating procedure of the BioSpot[®] started with dispensing e.g. 1 μl of master mix to reaction center B on the LOC chip

3. Description of the Lab-on-a-chip System

surface for sample uptake. For that, the designated PipeJet™ was approached to a reservoir flask (**figure 10 A and B**), was driven to aspirate a distinct amount of fluid and was moved to the chip surface for unloading (**figure 10 C**). Subsequently, the chip-holder was moved to the microscope, waiting for sample uptake after microdissection and SPATS transfer. Sample material, released into predispensed fluid, was immediately covered by mineral oil. For that, the chip-holder was moved back to the designated PJ3 for applying Sealing Solution either directly by dropping onto the liquid droplet or by dispensing onto the LOC chip surface (**figure 10 D**), while droplet fusion was achieved by surface acoustic wave actuation.

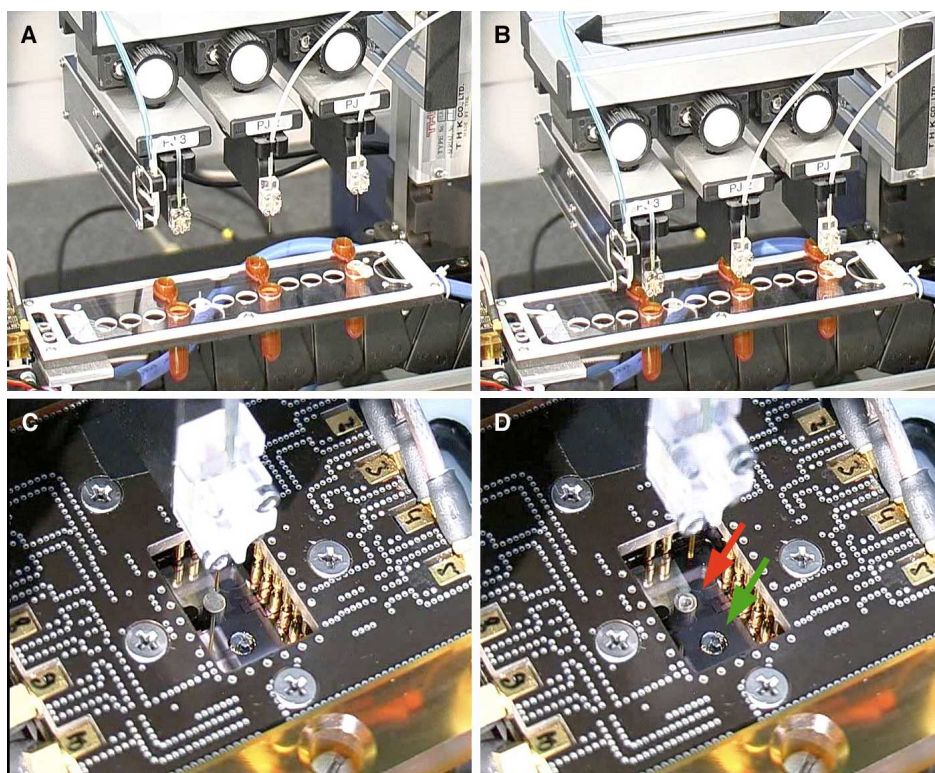


Figure 10. Workflow of the BioSpot® applied on the lab-on-a-chip system. A) Via the slide rail the flasks-holding reservoir device was centered to the PipeJets™. B) A distinct amount of fluid was aspirated by one of the PipeJets™. C) The designated PipeJet™ was approached to the LOC chip surface and centered to reaction center A for liquid dispensation. D) Via the piston actuation a small volume of 1 μ l of liquid was dispensed onto the chip surface (red arrow), which was going to be covered with 5 μ l of pre-dispensed mineral oil (green arrow) for forming a virtual reaction chamber PCR droplet arrangement.

Pipetting workflows like this could either be performed manually by operating the various active control windows of the software or automatically by executing pre-programmed operations using the “Batch mode” setting of the software.

3.5 Fluorescence Reader module

For PCR-based systems, detection of amplified products is surely the most important thing to fulfill requirements of an entire modular “sample-in-answer-out” μ TAS device, while optical detection methods still dominate over others due to sensitivity purposes. However, for complexity reasons in most μ TAS the optical detection is commonly accomplished using a microscope located off-chip. Due to the modular and “open” character of the LOC comprising a perfect accessibility to chips installed in the CytoCycler PCR device, a fluorescence detection unit “Fluorescence Reader” could be integrated easily as not being part of any fabrication process. The Fluorescence Reader consisted of a commercially available CCD camera and control equipment. A similar simple, portable and modular fluorescence detection system for lab-on-a-chip applications was developed by Novak L *et al.* (2007).

The Fluorescence Reader module of the lab-on-a-chip system typically consisted of a) a light source for emitting light at a suitable wavelength range (blue LED $\lambda_{\max} = 470 \pm 2$ nm with collimating optics (inhibiting power losses over the length of the optical path), b) an ET482/35 excitation and ET536/40 emission filter set ($\lambda_{\max \text{ ex}} = 482$ nm, $\lambda_{\max \text{ em}} = 536$ nm), c) a CCD camera as detector for signal processing (capturing emitted light), d) external electronics like a LED power supply control box and a trigger signal break-out box and e) software for image data analysis. The optical path of excitation light and emission light was designed in a 45° arrangement for the optical separation of excitation and emission channels (**figure 12**). A LED was chosen as light source as fluorescence systems based on light emitting diodes (LEDs) became popular in the last few years for their low cost, due to their long lifetime and that LED’s light output can be modulated (Dasgupta PK *et al.*, 2003). Additionally, traditionally used light sources like mercury lamps and lasers, were too bulky and expensive for combination with the LOC devices. Due to collimation, the stray light of the LED was minimized, in order to reduce the signal-background relation. The optical system including LED and filter set was adapted to the fluorescence requirements of SYBR Green I providing a typical standard fluorescence detection system. SYBR Green I is a fluorescence dye intercalating into double-stranded DNA molecules, absorbing blue light at an absorption maximum of 498 nm and emitting green light at an emission maximum of 521 nm (**figure 11**). Accordingly, integrated filter sets included an excitation filter with a transmission of $\lambda_{\max} = 482$ nm (spread 36 nm = 464-500 nm) and an emission filter with a transmission of $\lambda_{\max} = 536$ nm (spread 40 nm = 516-556 nm).

3. Description of the Lab-on-a-chip System

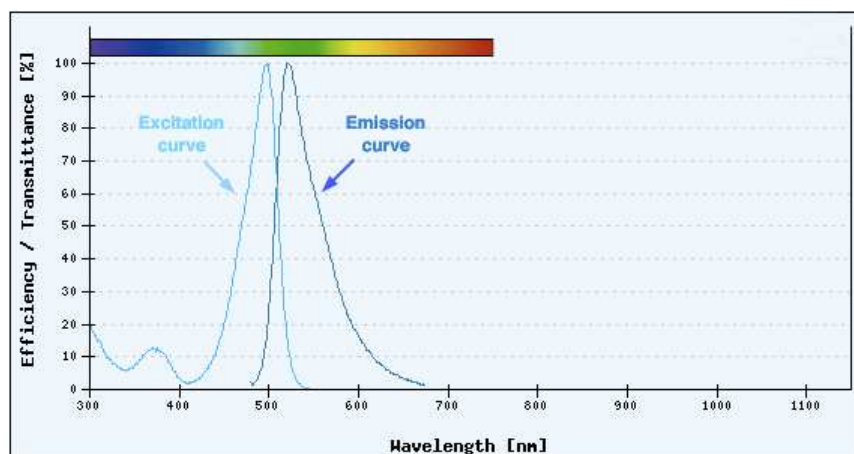


Figure 11. SYBR Green I spectra. Excitation and emission curves of the DNA intercalating fluorescence dye SYBR Green I are shown (from Fluorescence Dye and Filter Database at www.micro-shop.zeiss.com). The dye comprised an emission maximum of 521 nm when enlightened with excitation light at a maximum of 498 nm.

The Fluorescence Reader was positioned stationary in the middle of the LOC slide, between microscope and BioSpot[®] (**figure 12**). For excitation the LED as light source was placed at an angle of 45° shining to the sample positioned on reaction center B on the LOC chip surface. LED collimated light was filtered by an exciter ET482/35, exciting the SYBR Green I dye to produce fluorescing light. Fluorescent light was detected passing through an emission filter ET536/40, followed by the collection of light by a CCD camera (**figure 12**).

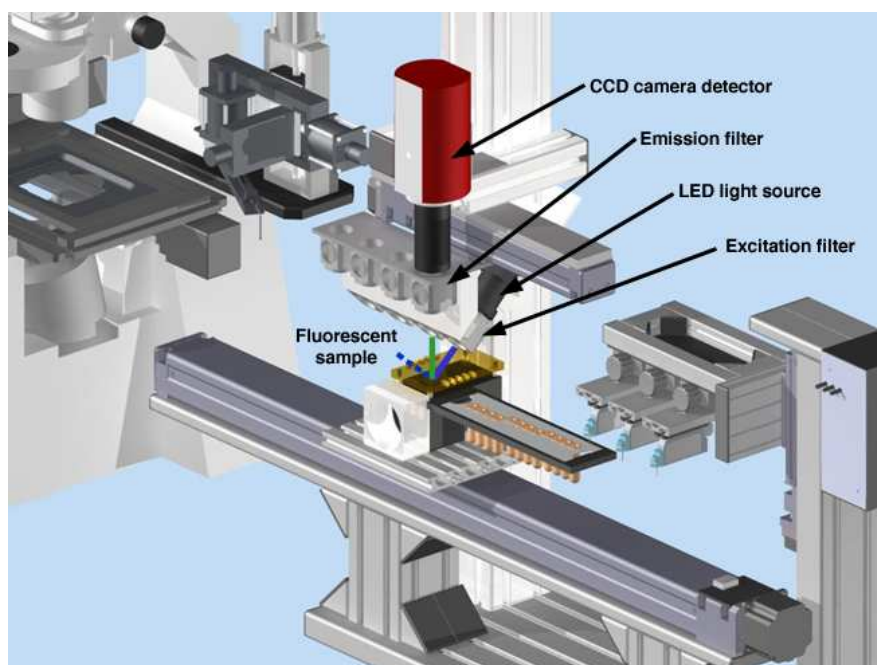


Figure 12. Design of the Fluorescence Reader including CCD camera detector, LED light source and filter sets. The Fluorescence Reader was integrated on the LOC slide, located between microscope and BioSpot[®]. A fluorescent sample was positioned to reaction center B of a LOC chip installed in the CytoCycler. For detection of fluorescent sample signals, an angled arrangement of excitation and emission devices including appropriate filters was chosen. Thus the optical part could be split into two paths: excitation light was directed in an angular way to a fluorescent sample (blue light path), while emitted fluorescing light was detected and captured direct vertically by the CCD camera positioned above (green light path). CAD (SolidWorks 2006, Solid Works Corp.) image was kindly provided by G. Lieckfeld.

3. Description of the Lab-on-a-chip System

The basic setup of the Fluorescence Reader, including LED light source, filter set, LED power control box, trigger signal break-out box and CMOS (Complementary Metal Oxide Semiconductor) sensor as fluorescence signal detector was developed in the context of a diploma thesis (“Fluoreszenzreader zur Detektion von Biomolekülen auf einem ‘Lab-on-a-chip’/Fluorescence reader for detecting biomolecules on a lab-on-a-chip device”, submitted by Taner Sari, April 2008). This work dealt with the coupling of an optical Fluorescence Reader to a “lab-on-a-chip”, whereas DNA molecules (enriched with fluorescent marker) were optically excited and quantitatively detected via a detection unit. The setup was optimized to the actual state in the context of an internship program (“RT-PCR automation for lab-on-a-chip using LabVIEW”, submitted by Muhammad Atyab Imtaar in January 2009), where an appropriate LabVIEW-based detection software was written (“Grand_NIVision_Intensity_Consec_Subtract_Loopback_NewCamera.VI”) for automatic picture taking and the CMOS chip detection unit was exchanged by a CCD camera for sensitivity and resolution purposes. Additionally, this software was adapted for manual picture taking purposes (“Norbert.VI”).

For performing fluorescence detection, the chip-holder of the hardware heating-device CytoCycler needed to be centered to the Fluorescence Reader (**figure 12**). The temperature control box of the CytoCycler provided the connecting to the software control, but also was programmed to give trigger signals to the trigger signal break-out box of the Fluorescence Reader. Trigger signals were produced for indicating the end of a PCR cycle. There were three trigger signal output-plugs at the backside of the temperature control device named 1, 2 and 3, representing the three periodically-repeated temperature steps of a PCR protocol. Outlet 1 gave a signal after the denaturation step, outlet 2 after the annealing step and outlet 3 after the extension step. Which of these outlets was connected to the Fluorescence Reader depended on the kind of PCR performed. In 2-step PCR, when annealing and extension were combined in one step, outlet 2 was the choice, in 3-step PCR outlet 3 needed be connected. The trigger signal break-out box captured the trigger signal from the temperature control box and activated the image capture and image processing process controlled by the particular LabVIEW-based software. The LED was turned on to illuminate the sample for fluorescence and a picture of the sample was captured by the CCD camera arrangement (**figure 13**).

3. Description of the Lab-on-a-chip System

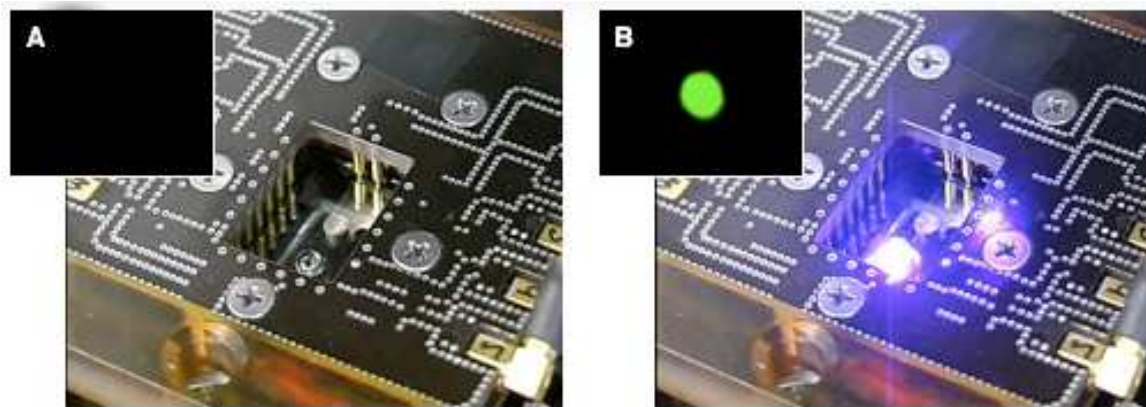


Figure 13. Illumination of a fluorescent sample during a PCR cycle. The inserts show the software captured images at the specific temperatures of a PCR cycle. The optical units for excitation of a fluorescent sample and detection of emitted fluorescence signal were placed above reaction center B of the LOC chip in a 45° design. For excitation of the fluorescing dye in the sample through a blue LED, the optical excitation path was focused through the oil into the aqueous reaction mix solution. **A)** When the sample droplet was enlightened at 94°C during the denaturation step, no fluorescence was emitted from the fluorescent dye inside the oil-covered sample droplet. This was due to the denatured DNA strands, being single-stranded and thus eliminating binding of the fluorescent dye SYBR Green I. Thus, software captured images showed no fluorescence signals. **B)** When the sample droplet was enlightened at 60°C during the annealing and extension step of a 2-step PCR performance, green fluorescence signals were emitted from the SYBR Green I dyed sample and captured by the optical detection unit. This was due to the double-stranded DNA molecules at the end of this temperature step, enabling the incorporation of the fluorescent dye.

Taken pictures were stored in a separate folder and fluorescence intensities produced at the end of each cycle were plotted graphically by the software. At the end, an excel file was generated summarizing all the collected and measured intensities. There were two kinds of pictures generated, “original” ones as well as “processed” ones. “Original” pictures represented the real image, while “processed” pictures represented subtracted fluorescence intensities. The previous image was subtracted from current image, so just the fluorescence increase was displayed.

4. Technical Evaluation of the Lab-on-a-chip System

In this section, the performance of the individual LOC elements as well as their interplay was characterized concerning operating efficiency. Especially the capability of the PCR amplification device CytoCycler was analyzed in several biochemical reactions concerning amplification efficiency and detection sensitivity of a small amount of sample material.

4.1 Reliability of heat transfer

Temperature measurements were performed by installing an adapted measurement LOC chip into the chip-holder of the CytoCycler. Input temperatures, controlled by the software and measured by the chip-holder's temperature sensor, were compared to output temperatures measured on reaction center B of the measurement LOC chip by a temperature sensor. Thus, the heat transfer from the software to the Peltier element and finally onto the chip surface was validated. Various temperatures in a PCR relevant temperature range from 25°C up to 100°C were tested. Additionally, the performance of an AmpliSpeed slide cycler was tested as a reference PCR system.

The first temperature profile comprised measurements with increasing temperatures, starting from 30°C, and followed by stepwise temperature increments of +5°C up to 100°C, while each temperature was held for about 30 sec. There were slight negative deviations detectable in the upper temperature range from 70-100°C at an average of -0.243°C, but rather randomly distributed than in an increasing linear manner. In the lower temperature range from 30°-65°C, however, decreasing positive deviations were measured at an average of +0.527°C. Results derived for the CytoCycler were summarized in **table 3**.

The second temperature profile comprised measurements with temperatures simulating 3-step thermal PCR cycling, starting from 95°C held for 10 min, followed by 3-5 cycles of 94°C for 30 sec, 60°C for 30 sec and 72°C for 30 sec. Two independent runs were performed. Temperature measurement results derived for the CytoCycler at each specific temperature were summarized in **table 3**. In both runs there were slight but tolerable positive temperature deviations detectable. At 95°C, simulating an initial denaturation step, the averaged positive deviation was about +0.90°C. At 94°C, simulating the denaturation steps at each PCR cycle, positive deviations were measured at an average of +0.98°C. At 60°C, simulating the annealing step at each PCR cycle, the positive deviations were at an average of +0.26°C. And

4. Technical Evaluation of the Lab-on-a-chip System

at 72°C, simulating the extension step of each PCR cycle as well as the final product extension step, averaged positive deviations were about +0.67°C.

Table 3. Temperature deviations between input and output temperature measured at the CytoCycler device. The particular deviations at each measured temperature are given in brackets and are marked with a delta sign (Δ).

Input temperature by software [°C]	Averaged output temperature on chip surface [°C]	Input temperature by software [°C]	Averaged output temperature on chip surface [°C]	Averaged output temperature on chip surface [°C]
Temperature increment +5°C		Simulating PCR cycling		
30	31.05 ($\Delta +1.05$)		Run 1	Run 2
35	35.92 ($\Delta +0.92$)	95	95.21 ($\Delta +0.21$)	96.60 ($\Delta +1.60$)
40	40.73 ($\Delta +0.73$)	94	94.47 ($\Delta +0.47$)	95.02 ($\Delta +1.02$)
45	45.59 ($\Delta +0.59$)	60	60.21 ($\Delta +0.21$)	60.32 ($\Delta +0.32$)
50	50.43 ($\Delta +0.43$)	72	72.51 ($\Delta +0.51$)	72.86 ($\Delta +0.86$)
55	55.26 ($\Delta +0.26$)	94	94.28 ($\Delta +0.28$)	95.37 ($\Delta +1.37$)
60	60.19 ($\Delta +0.19$)	60	60.37 ($\Delta +0.37$)	60.28 ($\Delta +0.28$)
65	65.05 ($\Delta +0.05$)	72	72.64 ($\Delta +0.64$)	72.68 ($\Delta +0.68$)
70	69.89 ($\Delta -0.11$)	94		95.23 ($\Delta +1.23$)
75	74.69 ($\Delta -0.31$)	60		60.22 ($\Delta +0.22$)
80	79.73 ($\Delta -0.27$)	72		72.67 ($\Delta +0.67$)
85	84.84 ($\Delta -0.16$)	94		95.26 ($\Delta +1.26$)
90	89.87 ($\Delta -0.13$)	60		60.22 ($\Delta +0.22$)
95	94.78 ($\Delta -0.22$)	72		72.70 ($\Delta +0.70$)
100	99.50 ($\Delta -0.50$)	94		95.23 ($\Delta +1.23$)
		60		60.18 ($\Delta +0.18$)
		72		72.63 ($\Delta +0.63$)

Values of input temperatures were plotted against output temperatures and illustrated in a graphical image (**figure 14 A**). The distinct deviation values were related to measured temperatures and were shown graphically in an additional plot (**figure 14 B**).

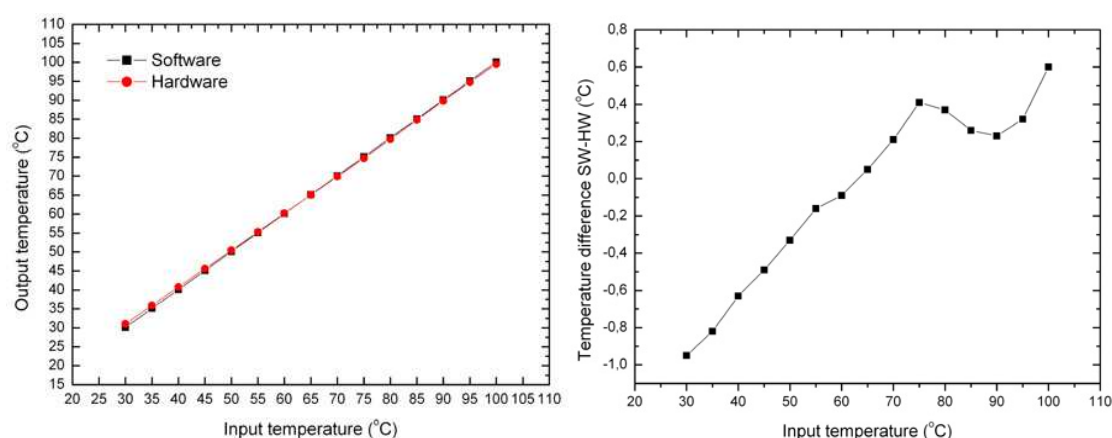


Figure 14. Temperature measurements of the LOC CytoCycler. A) Graphical display of measured input temperature (via software) versus output temperature (via hardware on the chip surface). Slight deviations could be detected at each measuring point. The drift of both graphs clearly showed positive deviations at lower temperatures and negative deviations at higher temperatures. B) Graphical illustration of the deviations of each particular temperature. Input temperatures were plotted against measured temperature deviations.

4. Technical Evaluation of the Lab-on-a-chip System

The PCR-simulated temperature profile of 94°C, 60°C and 72°C was applied to the AmpliSpeed slide cycler as well. Slight deviations of constantly about $\pm 0.5^\circ\text{C}$ were recorded for the slide cycler, featuring this cycler as an ideal reference system for the LOC system, especially for performing negative and positive control reactions during PCR performances.

According to an optimal setup based on contacting surfaces of the Peltier element and the chip underside, the CytoCycler provided a stable heat transfer onto the chip surface. Besides an efficient and optimal temperature transfer, a stable temperature support could be provided by this setup. Repeated temperature measurements were performed in two independent runs. Temperature output was quite constant at simulated PCR cycling any time tested, accounting for reproducible temperature measurements. In several independent measuring approaches, constantly slightly positive temperature deviations close to the desired input temperature were detected. These positive temperature deviations represented an optimal temperature transfer effectivity from the Peltier element to the LOC chip surface. This optimal temperature output on the chip surface validated the CytoCycler for reliable PCR performances on the LOC system. This setup of direct contact between the heating element and the microchip was comparable to the used multi LV-PCR microdevices, which were applied on conventional thermocycler devices using an appropriate *in situ* adapter, like e.g. reported in Schmidt U *et al.* (2006), Proff C *et al.* (2006), Lutz-Bonengel S *et al.* (2007) and Schmidt U *et al.* (2008). This contacting setup was also applied in the special thermocycler designed for slide-based PCR (AmpliSpeed slide cycler, Advalytix AG/Beckman Coulter Biomedical GmbH, Munich, Germany). This commercially available AmpliSpeed slide cycler device provided a comparable contact heating method for performing low-volume PCR amplification reactions using a multi LV-PCR microdevice. Thus, it was taken as reference system for all conducted measurements. As temperature measurement results were quite comparable between both devices, the AmpliSpeed slide cycler was taken as a permanent reference PCR system for validating the results obtained from the LOC CytoCycler PCR performances.

4.2 Evaluating the minimum amount of target material

The CytoCycler was characterized for product detection limits of amplification using decreasing amounts of input DNA for low-volume PCR (LV-PCR) analysis. The effectivity of the PCR was tested by reducing template concentrations until no successful amplification product could be detected after a large number of cycles. The minimum amount of target material was detected, thus validating the detection limit of PCR analysis performed on the

4. Technical Evaluation of the Lab-on-a-chip System

CytoCycler. Thermal cycling performances of LOC chips on the CytoCycler were validated against reference performances of a multi LV-PCR microdevice (AmpliGrid™ AG480F) on an AmpliSpeed slide cycler during parallel cycling including positive and negative controls. Concentrations for input DNA were 1 ng, 500 pg, 100 pg, 50 pg, 25 pg and 12.5 pg of purified human female genomic reference DNA material. Amplifications were performed on a 297 bp fragment of the human high copy gene β -actin as well as on 106/112 bp fragments of the human gender determining gene amelogenin. As a 106 bp fragment is amplified from the X-chromosome and a 112 bp fragment from the Y-chromosome, a determination of male and female samples was possible.

Concerning the upper range of input DNA, performances of LOC chips and the multi LV-PCR microdevice were quite comparable in β -actin amplification (**figure 15**). Both devices revealed positive and reliable product detection data starting from 1 ng down to 25 pg of human genomic female input DNA, whereas product bands produced by the multi LV-PCR microdevice were always slightly stronger. Amplification results of 1 ng and 500 pg were not shown due to most stable performances and thus lack of comparability. While the multi LV-PCR microdevice could successfully amplify even 12.5 pg of genomic input DNA (**figure 15 D**), the minimal amount of genomic starting material which gave still a reproducible result for LOC chip amplification was 25 pg (**figure 15 C**). Amplification of 10 pg of genomic input DNA failed in both devices (**figure 15 A**). For a better overview, results of sensitivity tests were summarized in a schedule (**table 4**).

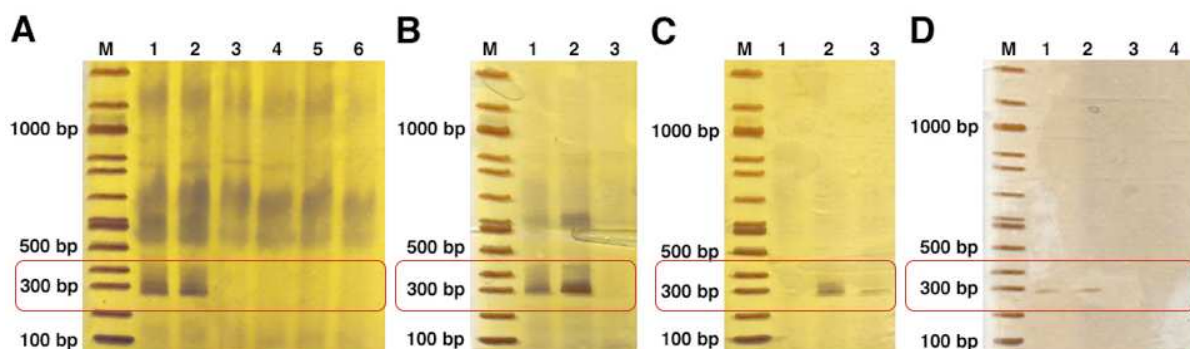


Figure 15. PAAGE data of detection limits for PCR amplification of a 297 bp β -actin fragment. Validation of the amplification efficiency of LOC chips compared to a multi LV-PCR microdevice is shown. Decreasing concentrations of genomic female reference DNA were used as input DNA. M = molecular length standard (100 bp DNA ladder, New England BioLabs, Beverly, MA, USA). NC = negative control. **A) Amplification of 100 pg and 10 pg target DNA material.** Lane 1: 100 pg on LOC chip; lane 2: 100 pg on multi LV-PCR microdevice; lane 3: NC on multi LV-PCR microdevice; lane 4: 10 pg on LOC chip; lane 5: 10 pg on multi LV-PCR microdevice; lane 6: NC on multi LV-PCR microdevice. **B) Amplification of 50 pg target DNA material.** Lane 1: 50 pg on LOC chip; lane 2: 50 pg on multi LV-PCR microdevice; lane 3: NC on multi LV-PCR microdevice. **C) Amplification of 25 pg target DNA material.** Lane 1: NC on multi LV-PCR microdevice; lane 2: 25 pg on multi LV-PCR microdevice; lane 3: 25 pg on LOC chip. **D) Amplification of 12.5 pg target DNA material.** Lanes 1+2: 12.5 pg on multi LV-PCR microdevice; lane 3: 12.5 pg on LOC chip; lane 4: NC on multi LV-PCR microdevice.

4. Technical Evaluation of the Lab-on-a-chip System

In amelogenin amplification, performances of LOC chips and the multi LV-PCR microdevice were comparable as well (**figure 16**). Both devices revealed positive and reliable product detection data starting from 1 ng down to 50 pg of genomic female input DNA, whereas again product bands produced by the multi LV-PCR microdevice were always slightly stronger. Amplification results of 1 ng and 500 pg were not shown due to most stable performances and thus lack of comparability. At lower DNA concentrations, the multi LV-PCR microdevice could successfully amplify 25 pg of genomic input DNA, but failed in amplifying 12.5 pg. For amelogenin, a reliable LOC chip performance was detected down to 50 pg. As LOC chips failed in amplifying 25 pg and 12.5 pg of genomic input DNA, the minimal amount of genomic starting material which gave still a reproducible result indicating a reliable LOC chip amplification performance was 50 pg. According to the previous results, the amplification of 10 pg was not even tried. For a better overview, results of sensitivity tests were summarized in a schedule (**table 4**).

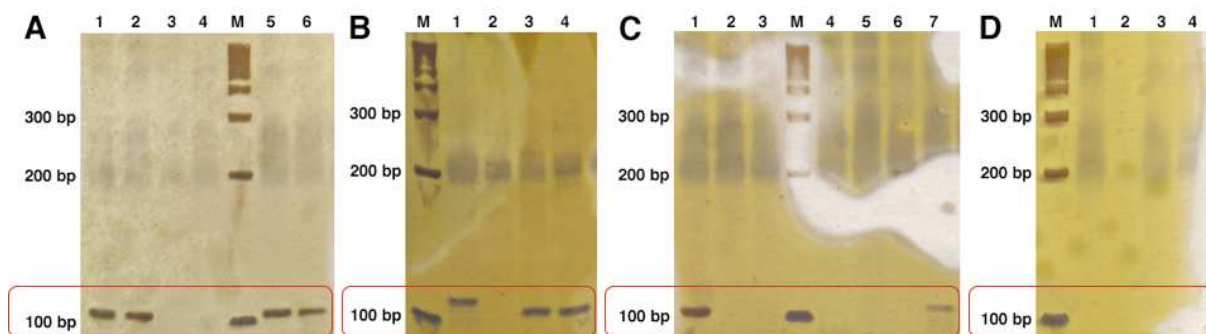


Figure 16. PAAGE data of detection limits for PCR amplification of 106 bp amelogenin fragments. Validation of the amplification efficiency of LOC chips in comparison to a multi LV-PCR microdevice is shown. Decreasing concentrations of genomic female reference DNA were used as input DNA. M = molecular length standard (Superladder-low 100 bp ladder with ReddyRun™, Thermo Scientific, ABgene, Epsom, Surrey, UK). NC = negative control. **A) Amplification of 100 pg and 50 pg target DNA material.** Lane 1: 100 pg on LOC chip; lane 2: 100 pg on multi LV-PCR microdevice; lanes 3+4: NC on multi LV-PCR microdevice; lane 5: 50 pg on LOC chip; lane 6: 50 pg on multi LV-PCR microdevice. **B) Amplification of 25 pg target DNA material.** Lane 1: 25 pg on LOC chip; lane 2: NC on multi LV-PCR microdevice; lanes 3+4: 25 pg on multi LV-PCR microdevice. **C) Amplification of 25 pg and 12.5 pg target DNA material.** Lane 1: 25 pg on multi LV-PCR microdevice; lanes 2+4: NC on multi LV-PCR microdevice; lane 3: 25 pg on LOC chip; lane 5: 12.5 pg on LOC chip; lanes 6+7: 25 pg on multi LV-PCR microdevice. **D) Amplification of 12.5 pg target DNA material.** Lane 1: 12.5 pg on LOC chip; lanes 2+3: 12.5 pg on multi LV-PCR microdevice; lane 4: NC on multi LV-PCR microdevice.

At higher concentrations from 1 ng to 50 pg, results of PCR performances were always constantly positive and quite comparable between both cyclers and both amplification performances, β -actin as well as amelogenin. There were just slight differences in the thickness of bands in the PAAGE gel data.

As summarized in **table 4**, for LOC chips 25 pg genomic input DNA was the detection limit for amplifying β -actin gene fragments and 50 pg for the amplification of amelogenin

4. Technical Evaluation of the Lab-on-a-chip System

fragments. Below these thresholds, no bands could be detected reliably any more. In comparison, the multi LV-PCR microdevice managed to amplify 12.5 pg of genomic DNA reliably in β -actin application and 25 pg in amelogenin PCR, thus having a slightly better detection limit than LOC chips.

Table 4. Summary of detection limits of LOC chips compared to a multi LV-PCR microdevice. Positive PCR products were marked with a “+”, while failed amplifications were marked with a “-”.

	1 ng	500 pg	100 pg	50 pg	25 pg	12.5 pg	10 pg
	β -actin PCR amplification detection limit						
LOC chip	+	+	+	+	+	-	-
Multi LV-PCR microdevice	+	+	+	+	+	+	-
	Amelogenin PCR amplification detection limit						
LOC chip	+	+	+	+	-	-	/
Multi LV-PCR microdevice	+	+	+	+	+	-	/

Differences in the various detection limits of LOC chips and the multi LV-PCR device when amplifying β -actin and amelogenin gene fragments could be attributed to the nature of these genes amplified. The β -actin gene is known as a gene having a high copy number distributed throughout the whole genome in pseudogenes (Ng SY *et al.*, 1985), thus presenting a much higher amount of target material, which is going to be amplified. Amelogenin, in contrast, is only located on gender chromosomes (Lau EC *et al.*, 1989) and thus presents a less amount of target sequences that potentially can be amplified during PCR.

General differences in detection limits between LOC chips and the multi LV-PCR microdevice could be related to the diverse architectures of reaction centers and the associated capability of heat transfer. The multi LV-PCR device comprised hydrophilic reaction centers of 1.6 mm in diameter, where attached liquids had a low contact angle and could wet the substrate in a way that they are forced to form a semicircular shape. Reaction center B of LOC chips offered just a hydrophilic area of 500 μ m in diameter, where attached liquids had a higher contact angle and could wet the substrate less efficiently forming an almost circular shaped droplet. This design might seem kind of suboptimal, but it was definitely needed for sustaining the capability of actuating and moving droplets by the power of surface acoustic waves. The multi LV-PCR microdevice could provide a better heat transfer into the oil-covered master mix droplet, as having a larger contact area to the heated surface of the microdevice. As LOC chips provided a smaller contact area of the almost roundly shaped master mix droplet to the heated chip surface, the heat transfer was less efficient and resulted in a less sensitive amplification threshold. Additionally, the design of the outer hydrophilic ring, which keeps the mineral oil centered to the aqueous droplet, was different and could also had an effect on cycling efficiency. While this ring completely surrounded the reaction

4. Technical Evaluation of the Lab-on-a-chip System

centers on the multi LV-PCR microdevice, on LOC chips these border was intermitted by the virtual tracks to all four sides providing access to the reaction center for SAW actuated droplets. However, these four gaps favored a movement of the oil in some cases, interfering with the shape of the covered PCR droplet and enabling evaporation effects. These possible evaporation events could also have shrunk the sensitivity limit of LOC chip PCR performances. However, despite these little handicaps, the PCR performance on LOC chips was quite promising, as a DNA amount of about 7 human genome copies (about 50 pg) was enough for a reliable amplification of amelogenin fragments. In β -actin PCR only a DNA amount of 3-4 human genome copies (about 25 pg) was sufficient due to the high-copy character of this gene.

Furthermore, amplification was done on human genomic DNA, which can be considered a “difficult” template as it has a high sequential and spatial complexity. In genomic DNA analysis a well-known problem of PCR is the lack of specificity for the desired product resulting in a number of longer or smaller fragments that can also be detected after the process. As can be seen in **figure 15** and **figure 16**, there were some unspecific products, some smear bands, detected besides the authentic product, especially when higher input DNA concentrations were used. Side products were reduced when less DNA was used, accounting again for a more specific analysis when using just a small amount of genomic target DNA, as favored in LV-PCR analysis. However, these stained smears were also detected in lanes of negative controls, where demonstrably no specific product was detected. As these smears were not stronger in these blank lanes, this accounts still for staining artifacts as well as a highly specific amplification, when real input DNA was available, as otherwise blank band strengths were expected to be stronger due to less competition for target DNA. Generally, these side products can be suppressed when analysis conditions get optimized concerning temperatures and cycling times. However, also reducing the amount of target material could reduce these side products, as was shown especially for the β -actin cycling results (**figure 15**). An enhanced sensitivity and efficiency of analysis when using low-volume PCR was reported several times in literature when departing from big voluminous standard reaction volumes (Guttenberg Z *et al.*, 2005; Schmidt U *et al.*, 2006; Proff C *et al.*, 2006; Lutz-Bonengel S *et al.*, 2007; Schmidt U *et al.*, 2008). In such a small reaction volume of just 1 μ l in total, sensitivity is believed to increase especially due to a higher impact probability between reactants present in the biochemical reaction mixture. As reactants are in closer contact and valuable target material gets less diluted in microfluidic devices (Gaines ML *et al.*, 2002; Kloosterman AD and Kersbergen P, 2003; Kricka LJ and Wilding P, 2003; Leclair B *et al.*,

2003; Proff C *et al.*, 2006; Schmidt U *et al.*, 2006) also the highest sensitivity within a PCR device could be reached. The successful amplification of a single DNA template was shown for a glass microchamber (Lagally ET *et al.*, 2000; Lagally ET *et al.*, 2001), however, just pre-purified DNA material was used. As the ultimate achievement of a micro total analysis system is to analyze crude unpurified samples of low-copy number down to a single cell, low-volume PCR applied on microdevices provides a good basis for that.

4.3 Ultimate speed of cycling

The effectivity of the CytoCycler PCR device was characterized for product detection limits of amplification using decreasing cycling times as well as decreasing DNA amounts of input DNA for low-volume PCR (LV-PCR) analysis. Thus, the ultimate speed of cycling performances was determined. Cycling times were reduced starting from 30 sec to 10 sec and down to a minimum of 5 sec temperature hold-time per PCR temperature step, while the number of cycle repetitions was constantly set to 30 cycles in total. Amplifications were performed on a 297 bp fragment of the human high copy gene β -actin as well as on 106/112 bp fragments of the human gender determining gene amelogenin. A 2-step PCR protocol as well as a 3-step protocol was tested, using DNA amounts of 500 pg, 100 pg, 50 pg and 25 pg of human genomic male reference input DNA. Thermal cycling performances of LOC chips on the CytoCycler were validated against reference performances of a multi LV-PCR microdevice (AmpliGrid™ AG480F) on an AmpliSpeed slide cycler during parallel cycling including positive and negative controls.

Concerning the 2-step PCR procedure, temperature hold-times could successfully be adapted to a fast PCR performance, speeding up total cycling times for the amplification of β -actin as well as amelogenin fragments. Denaturation time in each cycle was performed at 95°C for 10 sec instead of 30 sec, while combined annealing and extension times were shortened to 30 sec in total instead of 60 sec standard PCR protocol (**figure 17 A**). Despite a lot of side products, fragments could successfully be amplified from 500 pg human genomic male reference input DNA and the total PCR amplification time for LOC chips was reduced from 1 h 30 min to about 1h, and for the multi LV-PCR microdevice from 1 h 45 min to about 1h 15 min. Results of speeding up reactions were summarized in **table 5**.

4. Technical Evaluation of the Lab-on-a-chip System

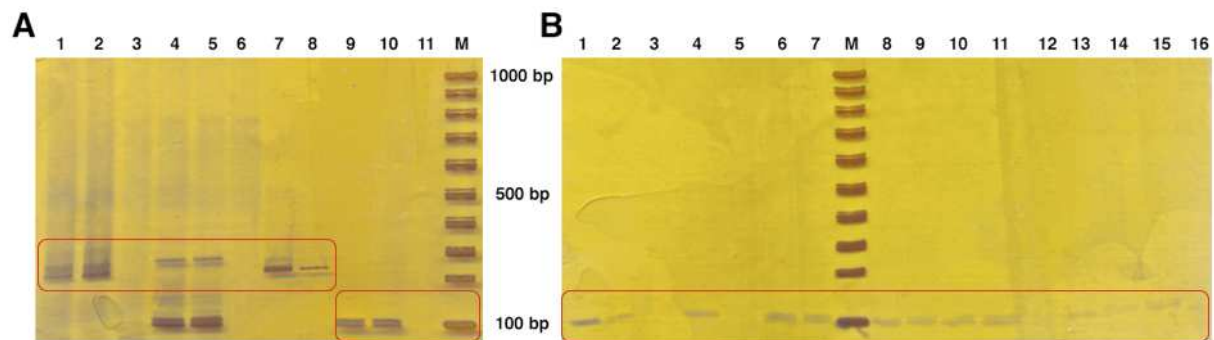


Figure 17. PAAGE data of cycling efficiency concerning temperature hold-times. Validation of the amplification efficiency of LOC chips in comparison to a multi LV-PCR microdevice is shown. Decreasing cycling times for LV-PCR amplification of 297 bp β -actin and 106/112 bp amelogenin gene fragments were tested, while male and female reference DNA was used, in concentrations ranging from 500 pg to 100 pg, 50 pg and 25 pg. M = molecular length standard (ReddyRun Superladder-low 100 bp ladder, Thermo Scientific, ABgene, Epsom, Surrey, UK). NC = negative control. **A) Lanes 1-6 = 2-step PCR, 500 pg input DNA.** Lane 1: 500 pg β -actin on LOC chip; lane 2: 500 pg β -actin on multi LV-PCR microdevice; lane 3: NC on multi LV-PCR microdevice; lane 4: 500 pg amelogenin on LOC chip; lane 5: 500 pg amelogenin on multi LV-PCR microdevice; lane 6: NC on multi LV-PCR microdevice. **Lanes 7-11 = 3-step PCR, 500 pg input DNA.** Lane 7: 500 pg β -actin on LOC chip (10 sec); lane 8: 500 pg β -actin on multi LV-PCR microdevice (10 sec); lane 9: 500 pg amelogenin on LOC chip (10 sec); lane 10: 500 pg amelogenin on multi LV-PCR microdevice (10 sec); lane 11: NC on multi LV-PCR microdevice. **B) Lanes 1-16 = 3-step PCR on amelogenin. Lanes 1-3 = 500 pg input DNA.** Lane 1: 500 pg on LOC chip (5 sec); lane 2: 500 pg on multi LV-PCR microdevice (5 sec); lane 3: NC on multi LV-PCR microdevice (5 sec). **Lanes 4-7 = 100 pg input DNA.** Lane 4: 100 pg on LOC chip (10 sec); lane 5: 100 pg on multi LV-PCR microdevice (10 sec); lane 6: 100 pg on LOC chip (5 sec); lane 7: 100 pg on multi LV-PCR microdevice (5 sec). **Lanes 8-11 = 50 pg input DNA.** Lane 8: 50 pg on LOC chip (10 sec); lane 9: 50 pg on multi LV-PCR microdevice (10 sec); lane 10: 50 pg on LOC chip (5 sec); lane 11: 50 pg on multi LV-PCR microdevice (5 sec); lane 12: NC on multi LV-PCR microdevice (5 sec). **Lanes 13-16 = 25 pg input DNA.** Lane 13: 25 pg on LOC chip (10 sec); lane 14: 25 pg on multi LV-PCR microdevice (10 sec); lane 15: 25 pg on LOC chip (5 sec); lane 16: 25 pg on multi LV-PCR microdevice (5 sec).

Concerning the 3-step PCR procedure, temperature hold-times could successfully be adapted to a fast PCR performance, speeding up total cycling times for the amplification of β -actin as well as amelogenin fragments. In each cycle, temperature hold-times for the denaturation, annealing and extension steps were reduced to a duration of 10 sec as well as 5 sec in total for each temperature instead of 30 sec standard PCR protocol (**figure 17 A and B**). Additionally, the final product extension time was shortened from 60 sec to 30 sec. In the 10 sec protocol, fragments could successfully be amplified for 500 pg down to 25 pg on both devices, while only amplification of 100 pg on the multi LV-PCR microdevice failed. In the 5 sec protocol, input DNA amounts from 500 pg down to 25 pg succeeded in amplification on both devices, LOC chips as well as the multi LV-PCR microdevice (**figure 17 B**). The “10 sec”-based total 3-step PCR amplification time for LOC chips could be reduced from 1 h 30 min to about 33 min, and for the multi LV-PCR microdevice from 1 h 45 min to about 54 min. The “5 sec”-based total PCR amplification time for LOC chips was successfully reduced from 1 h 30 min to about 26 min, and for the multi LV-PCR microdevice from 1 h 45 min to about 47 min. Results of speeding up reactions were summarized in **table 5**.

4. Technical Evaluation of the Lab-on-a-chip System

Table 5. Overview of PCR amplifications performed while shrinking down cycling times. Positive PCR products were marked with a “+”, while failed amplifications were marked with a “-“. Amelogenin amplifications were marked as “am”, and β -actin ones as “act”.

PCR kit	Original PCR protocol	Adapted PCR protocol	LOC chips		Multi LV-PCR microdevice	
QuantiFast™ SYBR® Green I PCR kit (2-step PCR)	<u>95°C 5 min</u> 40 x	<u>95°C 5 min</u> 40 x	500 pg - act	+	500 pg - act	+
	95°C 30 sec 60°C 60 sec	95°C 10 sec 60°C 30 sec	500 pg - am	+	500 pg - am	+
QIAGEN® Fast Cycling PCR kit (3-step PCR)	<u>95°C 5 min</u> 30 x	<u>95°C 5 min</u> 30 x	500 pg - act	+	500 pg - act	+
	94°C 30 sec 60°C 30 sec	94°C 10 sec 60°C 10 sec	500 pg - am	+	500 pg - am	+
	<u>72°C 30 sec</u> 72°C 60 sec	<u>72°C 10 sec</u> 72°C 30 sec	100 pg - am	+	100 pg - am	-
			50 pg - am	+	50 pg - am	+
QIAGEN® Fast Cycling PCR kit (3-step PCR)	<u>95°C 5 min</u> 30 x	<u>95°C 5 min</u> 30 x	25 pg - am	+	25 pg - am	+
	94°C 30 sec 60°C 30 sec	94°C 5 sec 60°C 5 sec	500 pg - am	+	500 pg - am	+
	<u>72°C 30 sec</u> 72°C 60 sec	<u>72°C 5 sec</u> 72°C 30 sec	100 pg - am	+	100 pg - am	+
			50 pg - am	+	50 pg - am	+
		25 pg - am	+	25 pg - am	+	

An optimal heat transfer to the sample as well as fast heating and cooling rates of the microdevice are main characteristics for rapid cycling times and fast reaction performances, as focused in microdevice application. Heating and cooling rates are mainly featured through the thermal mass of the device destined for thermal control. Compared to LOC chips, the heat transfer to the sample was ensured in a more optimal way in the multi LV-PCR device due to the architecture of reaction centers, as discussed in **chapter 4.2**. Thus, band strength was again stronger in multi LV-PCR microdevice applications for 2-step PCR cycling times up to 30 sec combining annealing and extension steps. However, for shorter cycling times in “10 sec”- and “5 sec”-based 3-step PCR performances, band intensity of LOC chip amplification products was slightly stronger. These benefits in effectivity could be attributed to faster heating and cooling rates of the LOC CytoCycler. As the AmpliSpeed slide cycler device applied on the multi LV-PCR microdevice comprised heating and cooling rates of 3 K s^{-1} , the LOC CytoCycler comprised a heating rate of 3 K s^{-1} as well but also a faster cooling rate of 4 K s^{-1} . The faster cooling rate is due to the lower thermal mass of the $1 \times 1 \text{ cm}^2$ sized heating area of the Peltier element of the LOC CytoCycler in comparison to the larger $7.6 \times 2.5 \text{ cm}^2$ sized heating area of the AmpliSpeed slide cycler. This lower thermal mass resulted in more efficient and specific amplification reactions when cycling times of PCR were speeded up and of course in a more rapid amplification performance as well. As both heating devices, the CytoCycler as well as the AmpliSpeed slide cycler had notably a lower

thermal mass and higher heating and cooling rates as conventional thermal cyclers, which are around $1\text{-}2\text{ K s}^{-1}$, times needed for amplification reactions could successfully be reduced to 5 sec per temperature step. Surely, the LOC CytoCycler system is inferior to other PCR microdevices using flow-through applications or IR-heating, designed for setting kind of world records in PCR cycling within 1.7 min (Hashimoto M *et al.*, 2004), 5 min (Oda RP *et al.*, 1998; Hühmer AFR and Landers JP, 2000; Giordano BC *et al.*, 2001 (a) + (b)) or 6 min total time (Obeid PJ *et al.*, 2003). However, mostly high concentrations of input DNA were used there and the LOC CytoCycler was not designed for ultra-fast reaction performances. Here, higher values were rather set on a) providing a modular solution capable of accepting various kinds of tiny sample materials, b) on a universal applicability for pre- and post-PCR sample processing based on a planar surface device and c) on disposability purposes, which are the reasons for having chosen the Peltier element-based design.

Additionally, there were other virtues favoring rapid operations in LV-PCR applications. Faster cycling times further provide a minimized risk of possible evaporation effects influencing the PCR results, which were reported to occur to 10% (v/v) in virtual reaction chamber LV-PCR amplifications (Guttenberg Z *et al.*, 2005). Short process times also have a positive effect on the effectivity of the polymerase in the PCR solution, as the lifetime of the enzyme is reduced during the high temperature states. And finally, fast cycling times hold the potential to prevent temperature gradients and thus to reduce the generation of unwanted and unspecific side products and smear bands during PCR amplification. Compared to amplification results shown in **chapter 4.2**, where a lot of smear could be detected, shorter cycling times as shown in this chapter were capable of eliminating these kinds of genomic side products almost totally due to less genomic target material used on the one side, and optimized analysis conditions on the other side.

4.4 Sensitivity of the Fluorescence Reader

Besides the evaluation of sensitivity and efficiency of reactions that can be performed on the LOC CytoCycler, the capacity (namely the operating efficiency) or respectively the sensitivity of the LOC integrated Fluorescence Reader was analyzed. SYBR Green I treated sample droplets of 1 μl total volume were positioned on reaction center B on LOC chips installed in the CytoCycler, were covered with mineral oil and illuminated via the Fluorescence Reader setup after eliminating ambient light. When enlightened with blue exciting light, green fluorescence signals were emitted from the sample by the dsDNA intercalating dye SYBR

4. Technical Evaluation of the Lab-on-a-chip System

Green I, present in sample droplets. The intensity of the emission depended on the amount of double-stranded DNA present in the solution, because its quantum yield increased by orders of magnitude when it intercalated. Interpretation of pictures, concerning fluorescence quantity and quality, was performed visually by image data analysis.

Calibration of fluorescence intensities was performed according to the DNA amount present in 1 μ l reaction volume. Decreasing standard concentrations of 10 ng, 5 ng, 1 ng, 500 pg and 100 pg of reference DNA were mixed with fluorescent SYBR Green I dye. Fluorescence intensities were recorded as image data using LabVIEW-based software at exposure times of 200 ms, 400 ms, 600 ms, 1000 ms, 2000 ms and 4000 ms at room temperature as well as at 55°C and 72°C. Latter temperatures were chosen as simulating relevant temperatures of picture taking during PCR performances. Image data of calibration tests performed at room temperature was summarized in **figure 18**. Strong fluorescence signals at nearly each exposure time were provided by samples containing concentrations of 10 ng, 5 ng and 1 ng DNA, and also the sample containing 500 pg DNA showed clear intensities down to an exposure time of 200 ms. The 100 pg loaded sample, however, gave just hardly detectable signals at exposure times of 200 ms and 400 ms, but stronger signals from 600 ms on. Thus, 600 ms was considered the best-suited exposure time used for validation of subsequent real-time PCR performances due to two reasons. First, at 600 ms a clear signal was achieved even when using a small amount of target DNA material like e.g. 100 pg input DNA. And second, exposure times were aimed to be kept as short as possible to avoid dye bleaching, thus longer exposure times could be neglected. Image data of calibration tests performed at simulated PCR cycling times 55°C and 72°C was summarized in **figure 19**. Only image data of using an exposure time of 600 ms is shown, as this setting was considered most relevant for real-time PCR performances. At 55°C and 72°C strong fluorescence signals could be detected using input DNA concentrations of 10 ng and 5 ng present in the sample droplet. Lower concentrations of 1 ng, 500 pg and 100 pg produced weaker but still reliably detectable signals at 55°C. However, at 72°C these lower concentrations were even harder to detect. As signal intensities dropped dramatically, 500 pg and 100 pg DNA concentrations could no more be detected reliably as a clear fluorescence signal.

4. Technical Evaluation of the Lab-on-a-chip System

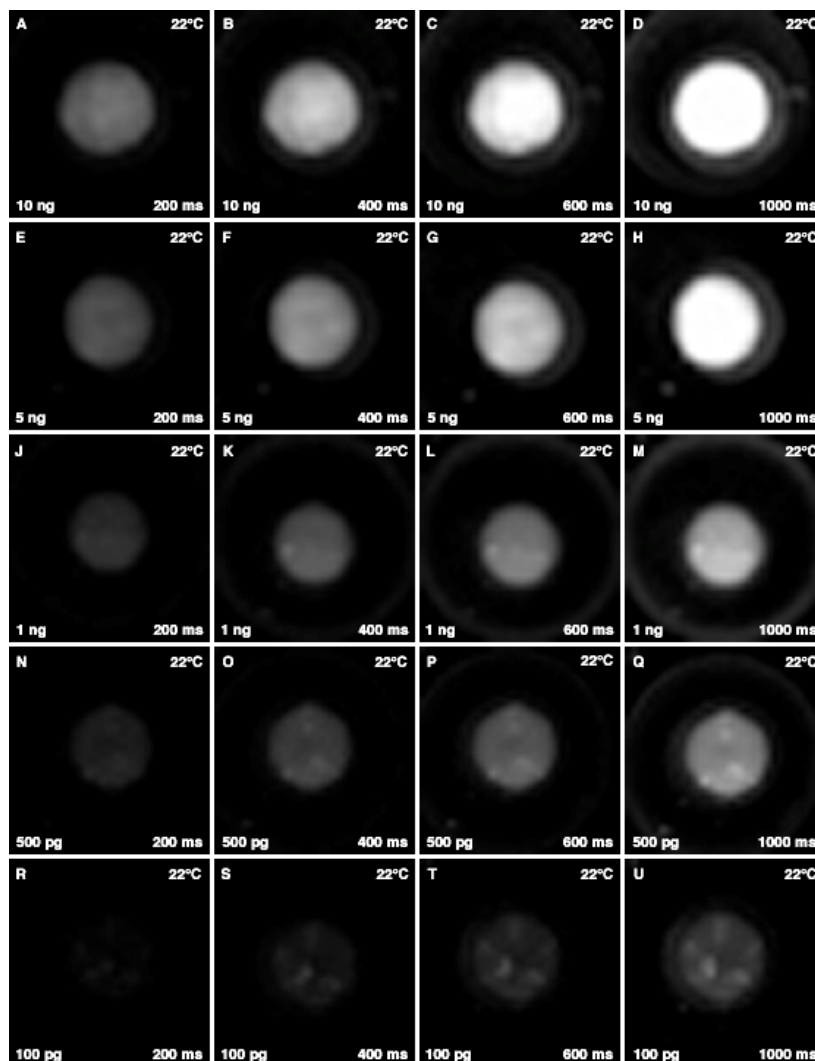


Figure 18. Calibration of fluorescence intensities measured at room temperature. Pictures of evaluated fluorescence intensities of various decreasing standard DNA concentrations from 10 ng down to 100 pg are shown at exposure times from 200 ms to 1000 ms. Longer exposure times like 2000 ms and 4000 ms just provided even stronger signals, but this data was not shown due to unrealistic applicability when regarding bleaching effects of fluorescing dyes over time.

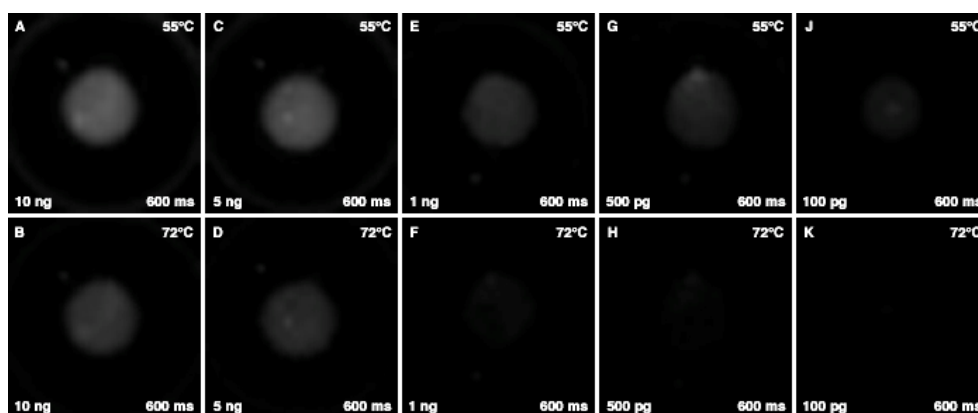


Figure 19. Calibration of fluorescence intensities measured at 55°C and 72°C. Pictures of evaluated fluorescence intensities of various decreasing standard DNA concentrations from 10 ng down to 100 pg are shown at an exposure time of 600 ms, as most relevant for PCR performances. Measurements were performed at PCR relevant temperatures of 55°C simulating an annealing/extension step at 2-step PCR performances and 72°C simulating the extension step when using 3-step PCR performances.

4. Technical Evaluation of the Lab-on-a-chip System

Experimentally, real-time PCR was carried out on the LOC CytoCycler using a SYBR Green I-based fluorescence detection system. In real-time PCR, the direct observation of the amount of DNA present in the reaction mix after each cycle is facilitated. Increasing fluorescence signals in dependence of increasing amounts of amplified DNA products are detected, indicating a successful amplification. As the amount of dsDNA is highest at the end of each extension phase during PCR, at this point the intensity was captured, pictures were taken and the ratio of cycle number to intensity signal was plotted to a graph in the software screen. The actual state of the PCR during the temperature cycles was continuously displayed by LabVIEW-based software. Different amounts of male and female human genomic reference input DNA comprising 1 ng, 500 pg and 100 pg were amplified via LV-PCR on the chip surface. Amplified products were detected both via conventional PAAGE and as image data using LabVIEW-based software. Both, 2-step and 3-step PCR performances were analyzed for validation, while exposure times were 200 ms, 400 ms and 600 ms. In 2-step PCR performances, pictures were taken at 55°C or 60°C, while in 3-step PCR pictures were taken at 55°C and 72°C for comparability reasons.

Exemplarily for a broad range of real-time PCR amplification reactions performed, 2-step ones as well as 3-step ones, which all showed quite comparable results, the image data of three amplification reactions were shown. In **figure 20** the amplification of β -actin fragments using 500 pg input DNA and a 2-step PCR procedure was illustrated. Pictures were taken at 60°C after the combined annealing/extension step. By trend, an increase in fluorescence intensity against increasing cycle numbers could be detected via software and a graph was plotted. About the same proportional rise in fluorescence intensities were detected when starting amounts of 1 ng or 100 pg were used. Additionally, amplified β -actin products could successfully be detected via PAAGE afterwards.

In **figure 21** the amplification of amelogenin fragments using 500 pg input DNA in a 2-step PCR procedure is demonstrated. Pictures were taken at 55°C after the combined annealing/extension step. Again, a considerable increase in fluorescence intensity could be detected continuously by software and a graph was plotted. Comparable results were obtained when 1 ng or 100 pg input DNA was used. Additionally, PAAGE was applied on amplified amelogenin products. In different approaches, some positive bands could be detected successfully, while in other approaches no positive amplification bands could be detected at all despite a software-recorded increasing fluorescence (**figure 21 J**).

4. Technical Evaluation of the Lab-on-a-chip System

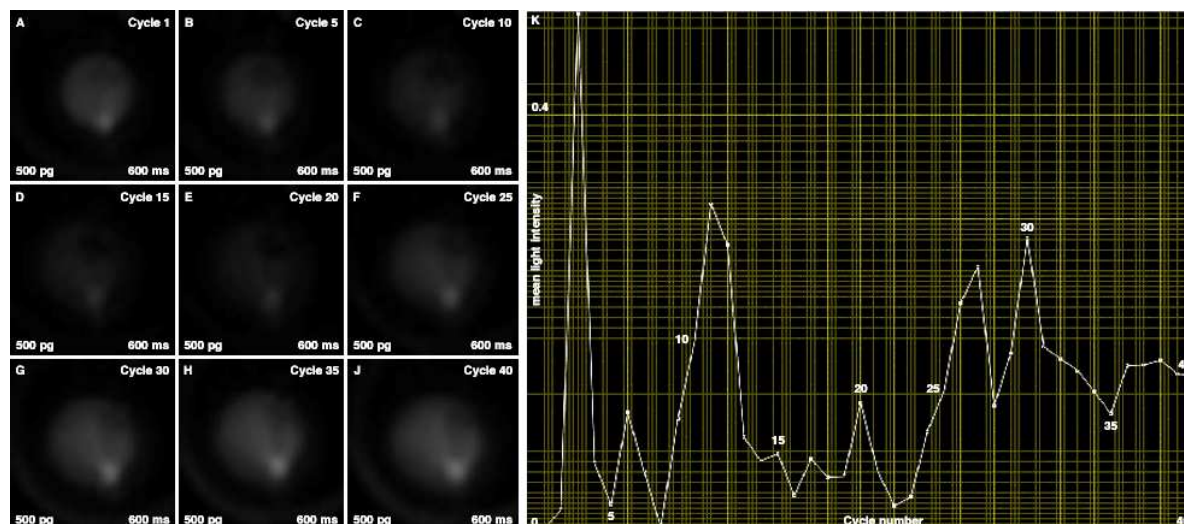


Figure 20. Image data of 2-step β -actin real-time PCR. The amplification of 500 pg input DNA starting material was used in a 2-step PCR protocol amplifying a 297 bp fragment of the human β -actin gene. Pictures were taken at the end of the combined annealing/extension steps at 60°C at an exposure time of 600 ms. **A-J)** The summarized picture alignment shows the increase in fluorescence intensity over cycling times, taken at the end of each PCR cycle. Pictures of every fifth cycle out of 40 cycles in total are shown. **K)** The graph of the RT-PCR reaction is shown, which was plotted by the LabVIEW-based software according to the measured values at each cycle. The graph displayed very fluctuating values up to 0.4 of mean light intensity, while only hardly an increase in fluorescence intensity values could be detected.

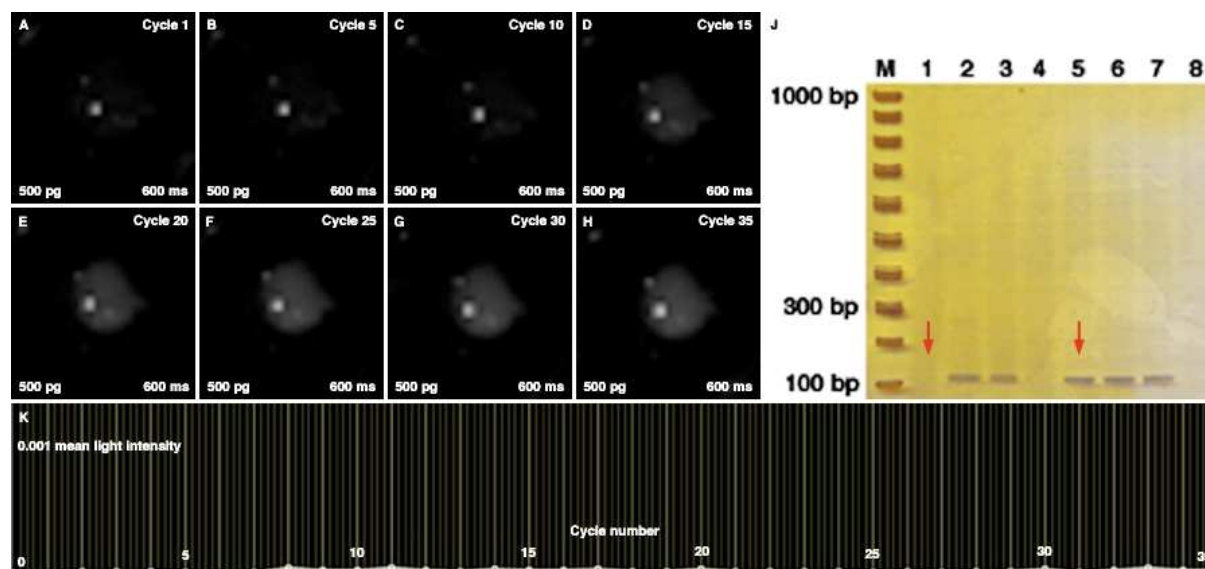


Figure 21. Image data of 2-step amelogenin real-time PCR. The amplification of 500 pg input DNA target material was used in a 2-step protocol amplifying 106/112 bp fragments of the human amelogenin gene. Pictures were taken at the end of the combined annealing/extension steps at 55°C at an exposure time of 600 ms. **A-H)** Aligned pictures show the increase in fluorescence intensity over cycling times, taken at the end of each PCR cycle. Pictures of every fifth cycle out of 35 cycles in total are shown. **J)** PAAGE image data of amplified amelogenin PCR products. Either there were positive bands detectable after real-time PCR performed on LOC chips (lanes 5-8), or there were no bands detectable on the gel for real-time PCR performed on LOC chips (lanes 1-4). M = Molecular length standard (ReddyRun Superladder-low 100 bp ladder, Thermo Scientific, ABgene, Epsom, Surrey, UK). Lane 1: 500 pg on LOC chip; lanes 2+3: 500 pg on multi LV-PCR microdevice (positive controls); lane 4: negative control on multi LV-PCR microdevice. Lane 5: 500 pg on LOC chip; lanes 6+7: 500 pg on multi LV-PCR microdevice (positive controls); lane 8: negative control on multi LV-PCR microdevice. **K)** The graph of the RT-PCR reaction is shown, which was plotted by the LabVIEW-based software according to the measured values at each cycle. The graph displayed a plane run, with relatively stable values around zero mean light intensity, while no increase in fluorescence intensity values could be detected.

4. Technical Evaluation of the Lab-on-a-chip System

In **figure 22** the amplification of amelogenin fragments using 1 ng input DNA in a 3-step PCR procedure is presented. Pictures were taken at 55°C after the annealing step as well as at 72°C after the extension step for validation of fluorescence intensities compared to 2-step procedures. Thereby, the duration of the annealing step was chosen that long as performed in 2-step PCR, where annealing and extension times were combined in one step. At 55°C, the rising of fluorescence intensity could be detected continuously by the software. At 72°C, there could no increase in fluorescence intensity be detected. A graph counting measured values for 55°C and 72°C directly afterwards was plotted by the software (**figure 22 V**). Comparable results were obtained when 500 pg or 100 pg input DNA was used. In subsequent PAAGE application, no amplified products could be detected on gel data at all.

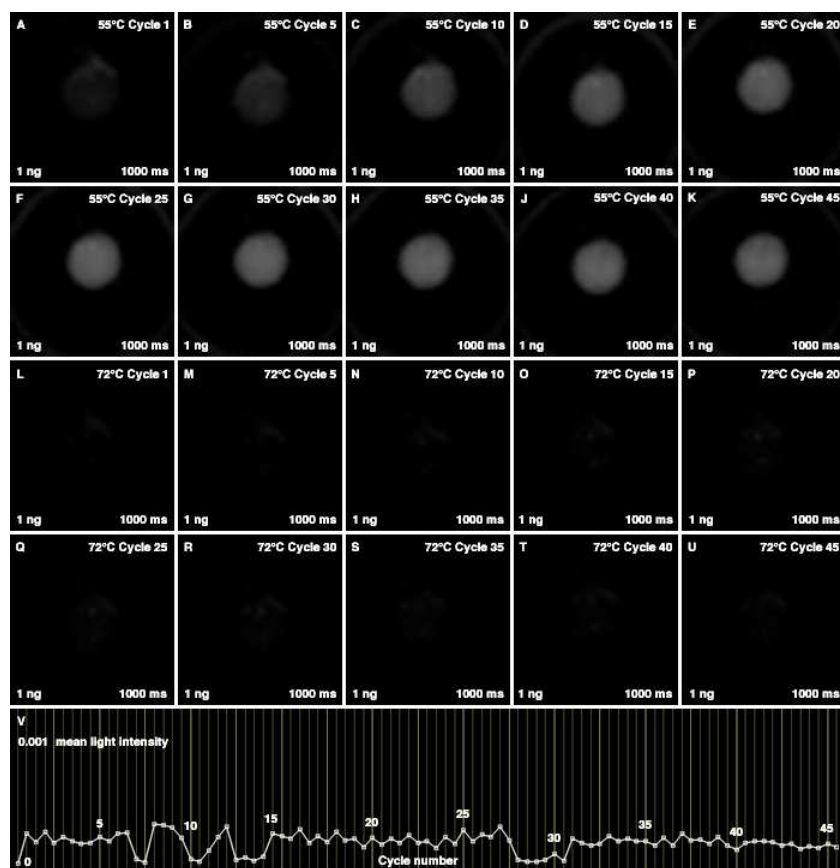


Figure 22. Image data of 3-step amelogenin real-time PCR. The amplification of 1 ng input DNA target material was used in a 3-step protocol amplifying 106/112 bp fragments of the human amelogenin gene. Pictures were taken at the end of annealing steps at 55°C as well as at the end of extension steps at 72°C, using an exposure time of 1000 ms. **A-K**) Aligned pictures show the increase in fluorescence intensity over cycling times, taken at the end of each annealing step at 55°C. Pictures of every fifth cycle out of 45 cycles in total are shown. **L-U**) The picture alignment shows the increase in fluorescence intensity over cycling times, taken at the end of each extension step at 72°C. Pictures of every fifth cycle out of 45 cycles in total are shown. **V**) Graphical illustration of measured fluorescence intensities during 3-step amelogenin real-time PCR. The graph of the RT-PCR reaction is shown, which was plotted by the LabVIEW-based software according to the measured values at 55°C and subsequently 72°C during each cycle of 45 cycles in total. The graph displayed a plane run, with relatively stable values around zero mean light intensity, while no increase in fluorescence intensity values could be detected. Even fluctuations between values measured at 55°C and those measured at 72°C were illustrated as tiniest differences in fluorescence intensity, absolutely not matching the pictured fluorescence intensities recorded at these temperatures.

4. Technical Evaluation of the Lab-on-a-chip System

Graphical images plotted by the LabVIEW-based software always showed unordinary characteristics. Graphs were never increasing, never reached a plateau phase. Graphs were very inconsistent as either some kind of “mountain range”-like run was displayed with values fluctuating up and down (**figure 20**) or a quite plane distribution of fluorescence intensity values (**figure 21** and **figure 22**). Thus, measured values plotted by the software were not reliable at all, and just showed some measurement inaccuracies instead of a real graph following the principle of real-time PCR. Definitely, there were some cumulative fluorescence signals pictured from the beginning to the end of real-time PCR cycling, but the values of those signals did not conform to the characteristics of a real-time PCR curve. Generally, during a successful experiment, the signal curves away from the plateau of the background at a certain cycle number and increases until saturation is reached. The start point of the signal change depends on the template concentration. Such a value distribution could never be reached for the real-time PCR experiments performed with the Fluorescence Reader. The recorded fluorescence intensities in the graph did definitely not fit to the amount of amplified products. As shown in **figure 21**, there was a strong band for amelogenin fragments detectable via PAAGE, and there must have been a strong increase detectable via the software-plotted graphical illustration. However, there was no increase detectable as the graph just showed a plane run without rising signals. Moreover, the expected really big increase in fluorescence especially at the end of the PCR for reaching saturation was totally missing even when a huge amount of 45 cycles of PCR was performed (**figure 20** and **figure 22**).

Additionally, pictures of increasing fluorescence intensities did not always match the results when detecting amplified PCR products via PAAGE application. Gel images showed quite inconsistent amplification products. For instance, in one approach there were clear positive amplification bands detectable on a polyacrylamide gel after real-time PCR, indicating a successful PCR performance, while in another approach no bands could be detected after real-time PCR. However, in fluorescence pictures of foregoing real-time PCR, both approaches showed quite the same increasing fluorescence intensities, which in the end accounted for an unreliable performance of the total Fluorescence Reader device (**figure 20** and **figure 21**). The same phenomenon was observed when 3-step PCR was performed and fluorescence signals were recorded by the software, but no amplification bands could be detected via PAAGE afterwards to verify the authenticity of fluorescence signals via detection of amplified products (**figure 22**). As the recorded fluorescence intensity was always quite the same in pictures taken at 55°C and almost invisible at pictures taken at 72°C, no matter if there was a band detectable on the PAAGE gel or not, was a clear evidence, that the whole

4. Technical Evaluation of the Lab-on-a-chip System

Fluorescence Reader setup needed really to be optimized. There were some discrepancies supposed to be in the total setup, which are described in the following.

First, the utilized filter set was supposed to be somehow suboptimal for SYBR Green I applications and needed to be optimized. The chosen filter set indeed covered the excitation and emission spectrum of SYBR Green I. For the excitation a range from 464 – 500 nm was provided by the filter ET482/36, while the excitation maximum of the filter lied at 482 nm. The excitation maximum of SYBR Green I, however, is around 498 nm, thus just within the range of the filter, but clearly too far away from its maximum. This could have led to losses in excitation power and thus could have shrunk the excitation signal from the beginning on. Comparably, the emission filter ET536/40 provided a range between 515 – 556 nm, having its maximum at 536 nm, while the emission maximum of SYBR Green I is around 521 nm, thus as well within the range but far aside the maximum. Thus, both filters were not optimally suited for the SYBR Green I dye. However, according to the manufacturer, these filters were capable of not losing fluorescence intensity within their range, so that at the marginal filter range still a signal with sufficient intensity is guaranteed to be generated. Ordered filters were considered having a wide bandwidth, serving almost their whole range. However, as tested several times, there might definitively had been a loss in fluorescence intensity, which was more important than expected and made the detection of fluorescence signals during PCR quite hard.

Second, the interaction of trigger signals, software and LED control was supposed to be somehow deranged and not perfectly coordinated in interacting timings. Maybe the cross-talk between the software, the trigger and the camera was affected.

Third, the values for fluorescence intensities recorded by the software during RT-PCR were subjected to a deficient calculation as those values did not really match the pictures. Similar values were e.g. given for fluorescence intensities when 10 ng standard DNA was measured and was compared to maybe 500 pg afterwards. Independent of utilized amounts of DNA, the values for fluorescence intensity were always quite the same and were fluctuating around zero. Thus, values were believed to count anything else, but no usable fluorescence intensities. Graphical illustrations plotted by the software according to those values were always far away from an authentic real-time PCR curve showing the characteristic curvature. The software also included a function of generating processed images that the actual picture is going to be subtracted from the previous one. Maybe the software did some strange calculation in behind and gave values counted from irreproducible calculations. This value data definitely needed to be optimized.

4. Technical Evaluation of the Lab-on-a-chip System

Forth, the area on the chip surface, where the picture was taken, was maybe chosen too large and too wide. Actual, just almost the whole chip surface was focused and recorded when pictures were taken, showing a large dark area having just a small fluorescent droplet in the middle. Maybe this large black background was the reason, that measured values arranged always around zero as small changes in fluorescence intensity could only hardly be detected. An additional refinement of the picture taking area would definitely improve measurements, even if this could not explain the strange values and the missing increase in fluorescence intensity.

Fifth, special software was utilized to validate the fluorescence intensities of taken pictures, integrating the fluorescence intensity over each pixel of the fluorescing droplet sphere. Integrated pixel intensities were combined to a total fluorescing droplet, and this was done for the fluorescence intensity picture of each PCR cycle. However, even this software did not generate an authentic real-time PCR curve according the calculations. The graph looked similar to the one generated by the LabVIEW-based software. Thus, something must be wrong in the total setup of picture taking. The problems could not be attributed to the PCR mix, as there were products detectable on the polyacrylamide gel. It was not a problem of the fluorescence dye, as reactions performed in a conventional real-time PCR cycler (Stratagene Mx 3000P) worked perfectly well. Problems were not due to the utilized CCD camera, as it worked always brilliant when used at the optical inverted microscope. Additionally, it was not a problem of the LED, as light was emitted at the correct time points at the end of a PCR cycle. Additionally, the camera, the software, the LED and the trigger were somehow working well when used individually, but together the whole setup did not match and was not sensitive enough to be used for valuable and most importantly reliable real-time PCR performances on the LOC.

Finally, as the software was just written for taking pictures of fluorescence, the analysis of fluorescence results was not reliable at all. Originally, the software was written for a prototype application of real-time PCR using the dsDNA intercalating dye SYBR Green I. Generally, when SYBR Green I is used for the online detection of the DNA amplification, no specific information about the kind of dsDNA in the solution is given. As this dye binds to specific PCR products as well as to unspecific ones, there was no possibility included in the software to differentiate between real positive product and false positive products or unspecific side products, as any amplified product's fluorescence was detected. Thus, the software needed an additional update implementing a subsequent melting curve analysis after real-time PCR performance to determine the specificity of PCR products using SYBR Green I

4. Technical Evaluation of the Lab-on-a-chip System

(Fixman M and Freire JJ, 1977; Rutledge RG, 2004), which is performed by conventional real-time PCR cyclers as well. It is the standard procedure and the method of choice to identify the desired product, capturing the transition temperature from ssDNA to dsDNA, which is dependent on the length and sequence of the product. As this step is completely missing in our system of RT-PCR performance the system could not really be validated.

However, with a few improvements the system could be made competitive to fluorescence readers like reported and shown by Guttenberg Z *et al.* (2005) and Novak L *et al.* (2007) for microdevice applications. Guttenberg Z *et al.* (2005) provided an elegant solution, indeed, but this device was fixed to just one part of the chip. It was a fluorescence detection device, which was integrated into the fabrication of the chip and thus was fixed in application, not separable from the PCR device and just one specific area of the chip surface could be analyzed. Our Fluorescence Reader, in comparison, is free of focusing a sample anywhere on the chip surface due to a very flexible modular design. Additionally, our device can easily be extended to an approach using several kinds of filter sets, analyzing various kinds of fluorescence signals and thus various kinds of differently labeled PCR products.

4.5 Viability of microarray hybridization

Besides the detection of PCR products directly on the chip surface via real-time PCR, on-chip LV-PCR was also combined with a kind of microarray for on-chip hybridization. Thus, the feasibility of microarray applications on the lab-on-a-chip was evaluated. Arrayed on-chip hybridization was performed by hybridization of fluorescently labeled primer specific PCR products to complementary probes predefined on the LOC chip surface. On-chip hybridization arrays were designed for gender determination of sample material via amplified gene amelogenin, as used in forensics research. Amelogenin is generally used as gender determining gene, as its genetic sequence is located on the X- as well as on the Y-chromosome, while having particular sequence dissimilarities, which can be detected due to varying length of PCR products. The most commonly used PCR primer set for amplifying amelogenin fragments spans a region encompassing a 6 bp difference AAAGTG between male and females, thus generating 106/112 bp fragments in male and 106 bp fragments in female individuals (**figure 23**).

4. Technical Evaluation of the Lab-on-a-chip System

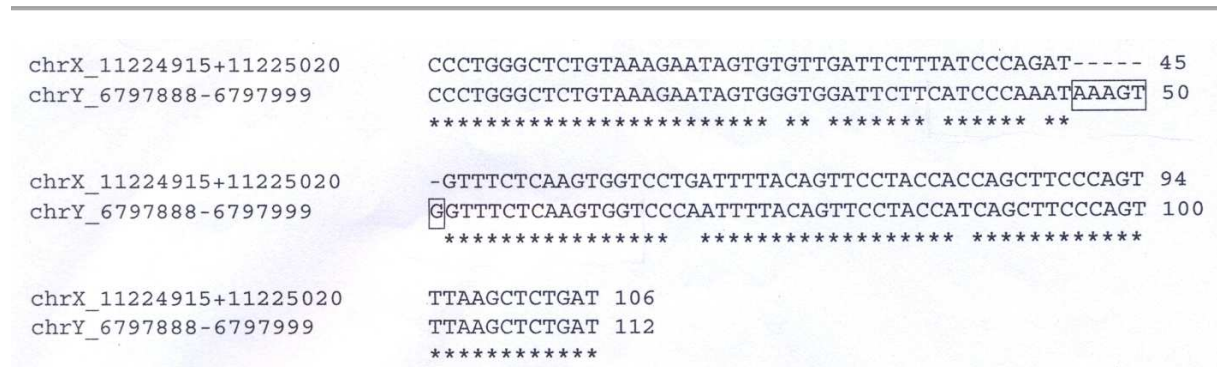


Figure 23. Sequence data and sequence BLAST (Basic Local Alignment Search Tool) of amelogenin fragments. Sequence alignment of amplified X- (106 bp) and Y-chromosome (112 bp) specific amelogenin fragments, showing a 6 bp difference at a particular genomic location within the amelogenin gene sequence. Sequences were taken from the UCSC Genome Browser (<http://genome.ucsc.edu>). Sequence alignment was performed at the webpage of the European Bioinformatics Institute (www.ebi.ac.uk).

Based on the well-established amelogenin system (Lau EC *et al.*, 1989; Shadrach B *et al.*, 2004), amplification of X- and Y-chromosomal fragments of the amelogenin gene was performed, which were hybridized to surface-bound probes Amelo1(Y) and Amelo3(Y) matching Y-chromosomal fragments and Amelo2(X) complementary to X-chromosomal products (**figure 24**). For amplification, purified male and female human genomic reference DNA was used.

5'-TGTAAGAATAGTGGGTGGATTCTTCATCCCAAATAAAGTGGTTTCTCAAGTGGTCCCAATTTTACAGTTCCTA-3'

Hybridization sequence 1 5'-CCCAAATAAAGTGGTTTCTC-3'
 Hybridization sequence 2 5'-CATCCCAAAT-----GTTTCTCAAG-3'
 Hybridization sequence 3 5'-AAAGTGGTTTCTCAAGTGGT-3'

Hybridization probe for sequence 1: Amelo1(Y) 5'-C6-Aminolink-(T)₁₃-GAGAAACCACTTTATTTGGG-3'
 Hybridization probe for sequence 2: Amelo2(X) 5'-C6-Aminolink-(T)₁₃-CTTGAGAAAC-----ATTTGGGATG-3'
 Hybridization probe for sequence 3: Amelo3(Y) 5'-C6-Aminolink-(T)₁₃-ACCACTTGAGAAACCACTTT-3'

Figure 24. Design of microarray probes Amelo1(Y), Amelo2(X) and Amelo3(Y). The area of interest, namely the 6 differing base pairs AAAGTG between X- and Y-chromosomal sequences, is marked explicitly in each scheme. Hybridization probe Amelo1(Y) was spanning a domain of 20 bp named “Hybridization sequence 1”, whereas the sequence of the 6 relevant bases CACTTT for hybridizing to AAAGTG was located directly in the middle, thus marking a male binding probe. Hybridization probe Amelo2(X) was spanning an area of 20 bp named “Hybridization sequence 2”, where the 6 relevant bases for hybridization were missing, marking a female binding probe. Hybridization probe Amelo3(Y) was spanning an area of 20 bp named “Hybridization sequence 3”, where the sequence of the 6 relevant bases CACTTT for hybridizing to AAAGTG was located at the 3'-end, marking a male binding probe.

On a multi LV-PCR microdevice 6 different array designs were spotted comprising not only single probes Amelo1(Y), Amelo2(X), or Amelo3(Y), but also combined setups of these probes in configurations like Amelo1(Y)/Amelo2(X), Amelo3(Y)/Amelo2(X) or Amelo1(Y)/Amelo3(Y) (**figure 25**).

4. Technical Evaluation of the Lab-on-a-chip System

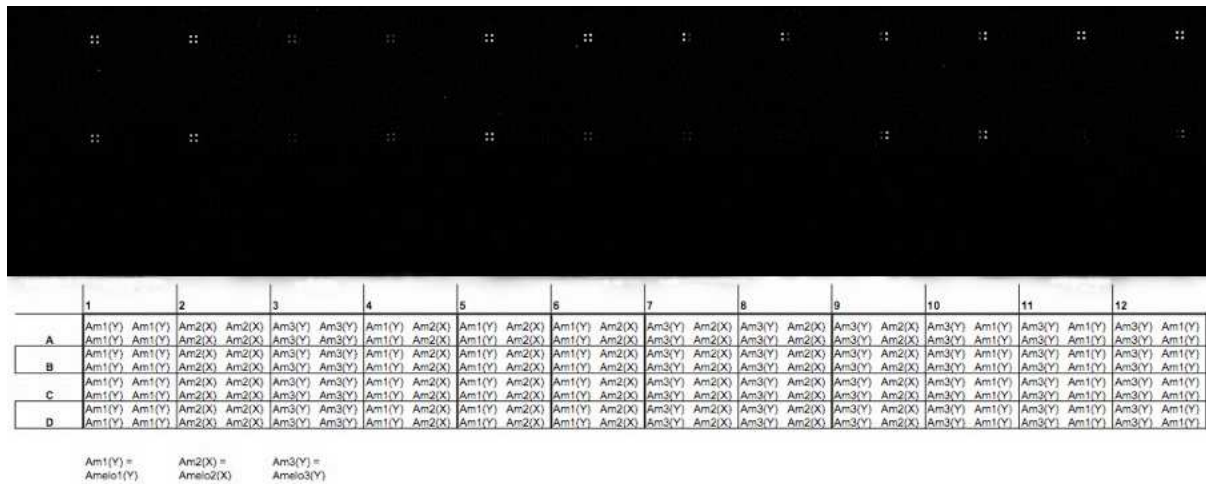


Figure 25. Amelogenin-based microarray data of the multi LV-PCR microdevice. Rows 1-12 were divided into 6 array fields, each comprising various combinations of hybridization probes. Probe names were shortened in the scheme for better overview, while “Am” was always short for “Amelo”, displaying Am1(Y) for probe Amelo1(Y), Am2(X) for probe Amelo2(X) and Am3(Y) for probe Amelo3(Y). Constantly, line A contained male input DNA in amplification reactions, while line B contained female input DNA and line C and D no DNA, serving as negative controls.

As can be seen in figure 25, on-chip hybridization after PCR worked quite well for the established amelogenin system. The various array designs showed quite interpretable results of the different array designs. Negative controls were negative at all times, thus contaminating effects could be excluded. Array Amelo1(Y) showed positive signals for male DNA in line A, as well as for female DNA in line B, but signals in line B were slightly weaker than those in line A. Normally, there was no direct binding expected for female PCR products to male probe Amelo1(Y). This indefinite and ambiguous signal for probe Amelo1(Y) was inapplicable for an analysis differentiating between male and female PCR products. Array Amelo2(X) showed positive signals for male DNA in line A as well as for female DNA in line B, with both signals having about the same intensity. As X-specific fragments were expected in male as well as in female PCR products, these positive hybridization signals were taken as an internal positive control, showing a successful working performance. Array Amelo3(Y) showed a stronger positive signal for male DNA in line A, and just a very weak signal for female DNA in line B. This could be taken as a more reliable probe for gender differentiation compared to probe Amelo1(Y), as here sequence differences between male and female PCR products revealed clear varying fluorescence signals.

The combined array with the Amelo1(Y)/Amelo2(X) design showed no real differences between male and female hybridization signals. All 4 spots of an array showed the same fluorescence intensity, while probe Amelo1(Y) should have given a stronger signal when male DNA was amplified and hybridized. Hybridization results were quite ambiguous, thus array design and hybridization conditions needed be optimized for a reliable gender

4. Technical Evaluation of the Lab-on-a-chip System

determining analysis. The combined array with the Amelo3(Y)/Amelo2(X) design showed a quite good differentiation between male DNA in line A and female DNA in line B. Male DNA in rows 7 and 8 showed strong signals for male probe Amelo3(Y), and weak signals for female probe Amelo2(X), while female DNA in these two rows showed just weak signals for both probes, Amelo3(Y) and Amelo2(X). These results were considered as a promising basis for a differentiating analysis between male and female DNA. However, these two rows showed just 60% positive results, as row 9 showed just completely different results. Here, male as well as female DNA showed strong signals for female probe Amelo2(X) and weak signals for male probe Amelo3(Y). Thus, 30% of the experiment showed completely different results. This might be due to the annealing temperature, and means, that temperature of hybridization needs to be optimized. However, these results were quite promising, despite those varying results, as at least 60% of the experiment gave good results with expected signals for male and female hybridization. The combined array with the Amelo3(Y)/Amelo1(Y) design showed a quite good differentiation between male DNA in line A and female DNA in line B. Male DNA in rows 11 and 12 showed strong signals for both male probes Amelo3(Y) as well as Amelo1(Y), while female DNA in these rows showed just very weak signals. These results could be considered as a real evidence for a differentiating analysis between male and female DNA. However, again, the results of these two rows showed just 60% positive results, as row 10 showed just completely different results. Here, male as well as female DNA showed strong signals for male probe Amelo1(Y) and weak signals for male probe Amelo3(Y). Thus, 30% of the experiment showed completely different results. This might again be due to the annealing temperature, and means, that temperature of hybridization needs to be optimized. However, these results were quite promising, despite those varying results, as at least 60% of the experiment gave good results with expected signals for male and female hybridization products. Finally, considering probe combinations, combined designs Amelo1(Y)/Amelo2(X) and Amelo3(Y)/Amelo2(X) were detected as the most reliable ones for application on the multi-LV-PCR microdevice.

According to results of the multi LV-PCR microdevice, on LOC chips 2 different array designs were spotted on reaction center B comprising combined configurations of probes Amelo1(Y)/Amelo2(X) and Amelo3(Y)/Amelo2(X) (**figure 26**). Results of hybridization events of amplified male and female PCR products are summarized in **figure 27**.

4. Technical Evaluation of the Lab-on-a-chip System

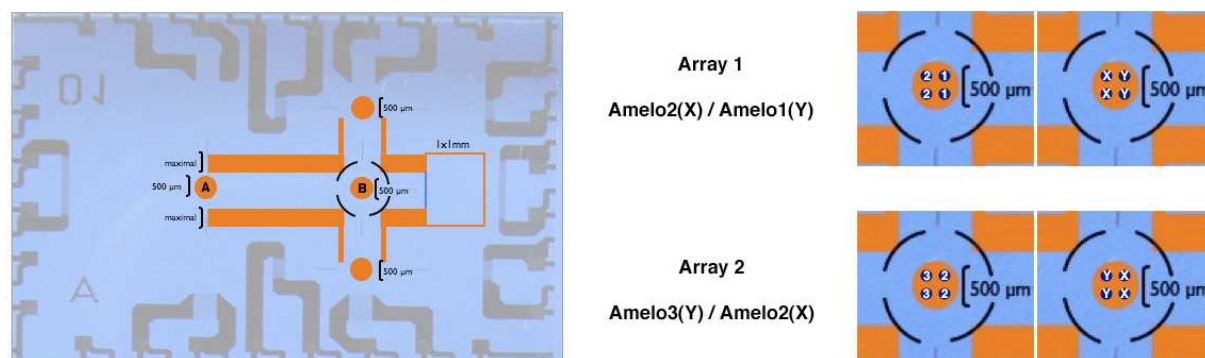


Figure 26. Array designs for microarray application on LOC chips. Array designs were spotted on reaction center B. Combined array designs are shown, comprising both probes for X-chromosomal as well as Y-chromosomal amelogenin PCR product hybridization. Probe names were shortened in the scheme for better overview, while “1, 2 and 3” were short for probes Amelo1(Y), Amelo2(X) and Amelo3(Y). Letters “X” and “Y” in the right scheme just simplify the particular hybridization pattern provided by the three probes.



Figure 27. Amelogenin-based microarray data of LOC chips. A) Original, unhybridized microscopy image of a probe array spotted on reaction center B on a LOC chip. B) Hybridization signals of 100 pg amplified male sample on array design Amelo2(X)/Amelo1(Y). C) Hybridization signals of 100 pg amplified female sample on array design Amelo2(X)/Amelo1(Y). D) Hybridization signals of 100 pg amplified male sample on array design Amelo3(Y)/Amelo2(X). E) Hybridization signals of 100 pg amplified female sample on array design Amelo3(Y)/Amelo2(X).

On-chip hybridization on LOC chips could successfully be performed and different hybridization pattern could clearly be detected according to the gender of amplified male or female sample material. Male samples showed strong fluorescence signals when amplified Y-chromosomal amelogenin products were hybridized to probes Amelo1(Y) and Amelo3(Y). Female samples never showed a strong fluorescence for male determining probes Amelo1(Y) and Amelo3(Y). Amplified X-chromosomal fragments of male and female samples showed consistently homogenous fluorescence signals with intensities below those of Y-chromosomal fragments. On LOC chips, for both array designs a clear differentiation between male and female sample products could successfully be detected.

On-chip hybridization was performed on a multi LV-PCR microdevice as well as on LOC chips, while applications on LOC chips generated more reliable results. On the multi LV-PCR microdevice, hybridization signals within a single probe were quite inconsistent despite an analogous performance. And in combined array designs, fluorescence signal intensities could not reliably be attributed to successful hybridization events, as e.g. female samples showed fluorescence signals for male probes Amelo1(Y) or Amelo3(Y). In contrast, on-chip hybridization performed on LOC chips revealed absolutely reliable signals, contributing to a

4. Technical Evaluation of the Lab-on-a-chip System

well-defined gender determination between male and female samples. Hybridization on the chip worked reproducibly with low background fluorescence and high specificity to clearly detect bp differences via varied fluorescence intensities between a male and a female sample. Solely, the Fluorescence Reader setup needed to be optimized, to get usable for microarray applications. However, successful on-chip hybridization validated the lab-on-a-chip for further array-based applications, like e.g. those performed by Guttenberg Z *et al.* (2005), where a single bp deletion was detected between wildtype and mutant DNA via a simple on-chip microarray application. Furthermore, a successful microarray performance further featured the lab-on-a-chip for combining PCR analysis with a highly sensitive downstream product detection application, representing a big step toward the envisioned automation of all steps from sample extraction to final product detection performed on just one single chip.

4.6 Operability of solid phase amplification

Besides conventional on-chip amplification in combination with on-chip hybridization, as just described in the previous microarray-related chapter, an extended and more sophisticated array application was performed on the surface of LOC chips. Solid phase amplification (SPA), also known as “bridge amplification” is based on the principle of performing a local PCR via surface-bound primers. Four amplification spots were spotted on the chip surface, locally defined and arranged in a 2x2 array-like structure, while each spot was loaded with a different kind of primer-pair (**figure 28**). Thus, the feasibility of locally performed PCR applications on the lab-on-a-chip was evaluated.

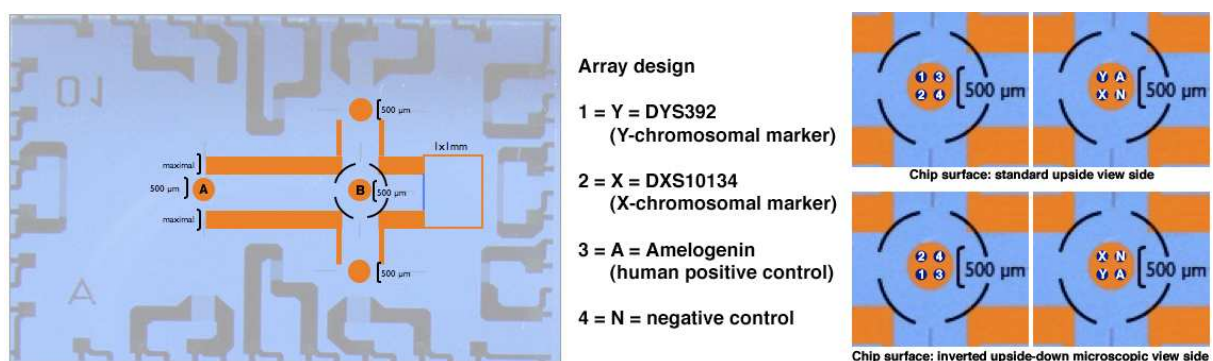


Figure 28. Design of the primer array for performing solid phase amplification. The scheme shows the four array spots, comprising each a different primer-pair for providing simultaneous local PCR amplification of four different PCR products. Primer-pairs were immobilized on a plane chip surface and covered by the same master mix in a 1 μ l total reaction volume droplet. Spot 1 was loaded with primers amplifying the Y-chromosomal STR marker DYS392, while spot 2 and 3 served as positive controls, amplifying the X-chromosomal STR marker DXS10134 as well as fragments of the amelogenin gene. The fourth spot served as negative control containing a pair of forward primers, thus eliminating a bridge-based amplification due to non-matching of amplified sequences.

4. Technical Evaluation of the Lab-on-a-chip System

Four primer pairs were spotted on distinct, separate array spots, while forward and reverse primers were spotted simultaneously and equally concentrated into single spots. Just 1 μl of PCR reaction mix was used to serve all 4 primer spots with reagents necessary for performing SYBR Green I-based real-time PCR, thus enabling 4 different amplification reactions at a time to take place in just 1 droplet. Again, the arrayed layout of on-chip SPA amplification was designed for forensic relevant determination and differentiation of male and female PCR products, when binding to and amplified by the appropriate XY-specific primer-pair. LOC chips with spotted SPA array were applied on male and female human genomic reference DNA. Results of solid phase amplification reactions were summarized in **figure 29**. Solid phase amplification as well as various amplification, annealing and hybridization procedures, including combined and separated “interfacial amplification” and “surface amplification” was tested on several LOC chips A_{12} , A_{03} , A_{21} and A_{01} .

Using spotted LOC chip A_{12} (**figure 29 A-C**), a 2-step SPA PCR with 1 ng of female reference input DNA was carried out. Due to the female nature of the DNA, two fluorescent signal spots were expected. As can be seen in **figure 29 C**, there were 4 fluorescent spots detectable, indicating a totally wrong array result. However, due to the geometry of the array (**figure 29 A**), at least 2 fluorescent signal spots out of these four fluorescent spots did not match the pattern. Spot arrangement was somehow out of alignment. The most possible authentic spots seemed to be the upper one and the outer right one. These were supposed to represent spots for the locus DXS10134 and Amelogenin, and thus the right and expected loci for a female sample. But there were a lot of non-specific fluorescent spots detectable outside the array area as well (**figure 29 B**), so the result of the array area still remained quite unreliable.

Using spotted LOC chip A_{03} (**figure 29 D-F**), the same SPA PCR procedure as applied on chip A_{12} was performed, using 1 ng of female reference input DNA, intended to repeat the previous experiment and to confirm the detected result. Again, due to the female input DNA, just two fluorescent spots were expected. As can be seen in **figure 29 F**, there were just two fluorescent spots detectable, one in the upper left area and one in the lower right area. Again, both spots seemed to present the expected result, but those spots did definitely not match to the quadratic geometry of the array and seemed somehow displaced (**figure 29 D**). Additionally, after washing steps there were a lot of precipitates detected present on the chip surface (**figure 29 E**), which could have influenced the amplification reaction and led to non-working reactions on the right array positions.

4. Technical Evaluation of the Lab-on-a-chip System

Using spotted LOC chip A₂₁ (**figure 29 G-J**), a 2-step SPA PCR with 1 ng of male reference input DNA was carried out. Due to the male nature of the DNA, three fluorescent signal spots were expected. As can be seen in **figure 29 J**, there were just 2 fluorescent spots detectable. However, due to the geometry of the array (**figure 29 G**), these 2 fluorescent signal spots did not match the pattern at all. Spots were detected close to the borders of the reaction center and were arranged in a non-square manner. The most possible authentic spot seemed to be either the upper one or the outer right one. These were supposed to represent spots for the locus DXS10134 or Amelogenin, and thus the right and expected loci for a male sample. But still, the third male spot for the DYS392 locus was missing which should be located in the lower left area, thus all three spots forming an “L”-like shape. However, no such pattern could be detected at all, and it was very questionable, if any of these two spots represented an authentic signal. There were a lot of precipitates present after the PCR (**figure 29 H**) and a lot of non-specific fluorescent spots detectable outside the array area as well (**figure 29 J**), so the result of the array area still remained quite unreliable and questionable.

As those normal solid phase amplification reactions did not turn out the expected results, or reliable results at all, another approach was tested. Instead of human genomic input DNA, preamplified PCR products were used to enhance the starting amount of input DNA, thus facilitating more interfacial amplification reactions to take place on the chip surface. For amplification, a combined 3-step PCR procedure was applied encompassing a) a SPA PCR with preamplified PCR products, followed by b) a reaction where just PCR master mix was applied, to enhance surface amplification, and finally c) a hybridization of preamplified PCR products, to cover single amplified strands bound to the surface but having failed to form bridges. The combined setup was tested on used chips A₀₃ and A₂₁, but did not bring an optimized result compared to conventional SPA PCR performed previously. No male or female specific fluorescence pattern could be detected on these chips. Combined PCR reactions with preamplified PCR products were repeated with chip A₀₁ (**figure 29 K-O**). As the master mix contained male and female specific PCR products, a male result was expected, showing an “L”-like pattern. After reactions, there were a lot of precipitates visible on the chip surface (**figure 29 L**), while fluorescence detection revealed four fluorescent signals (**figure 29 M**). The signals, however, showed no quadratical arrangement and did not match the square-like pattern of the spotted array at all (**figure 29 K**). Even after an additional washing procedure, there was still some precipitation visible on the surface (**figure 29 N**), which, however, did not improve fluorescence signal output (**figure 29 O**). Thus, even these combined PCR procedures did not reveal a successful performance.

4. Technical Evaluation of the Lab-on-a-chip System

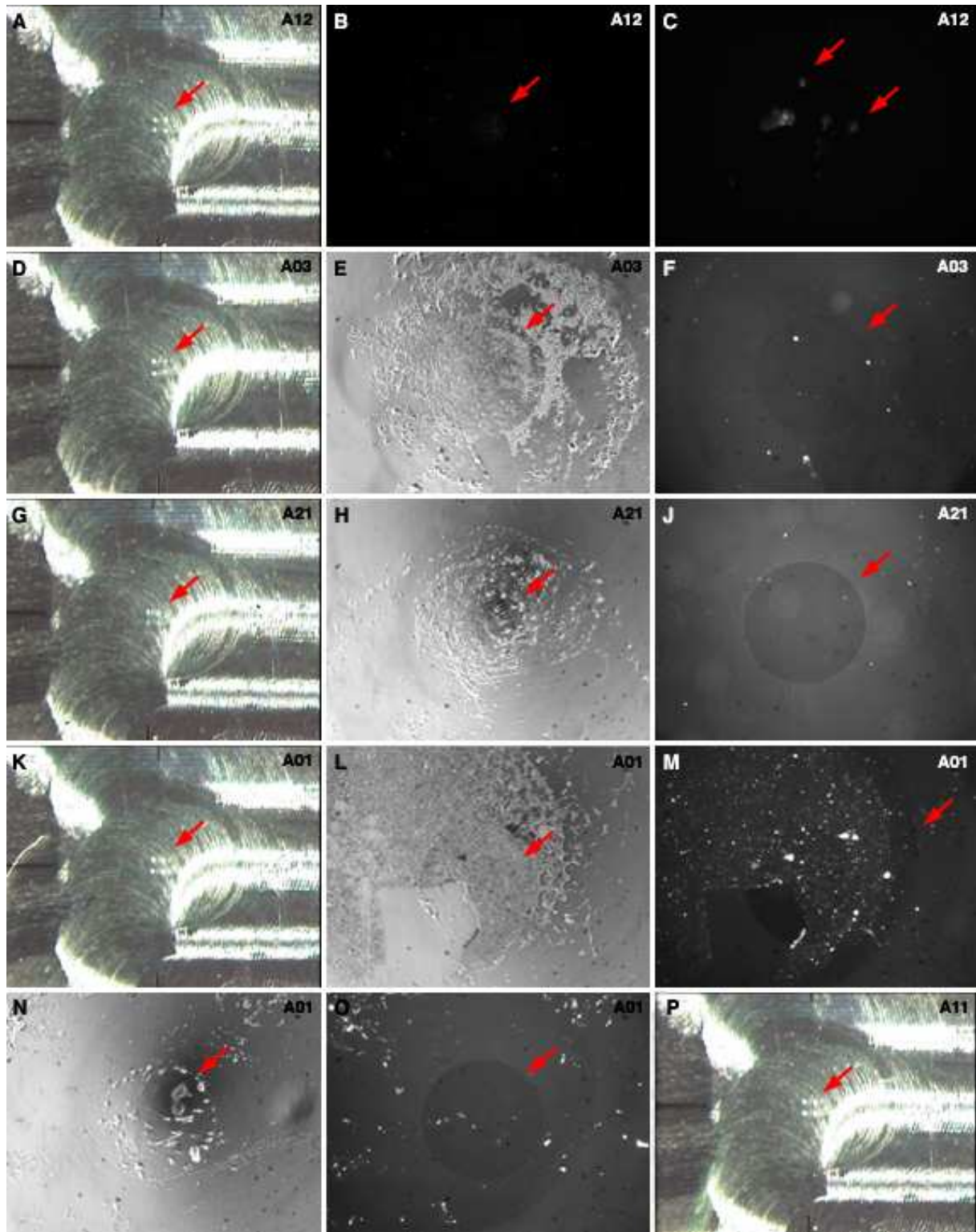


Figure 29. Image data of solid phase amplification. Amelogenin, X-chromosomal and Y-chromosomal fragments were amplified from male and female human genomic reference DNA in SYBR Green I-based SPA reactions. Array spots comprised each a diameter of about 100-150 μm and were spotted within the hydrophilic area of 500 μm of reaction spot B (marked by red arrows). Spotted 2x2 primer arrays were pictured before use via stereo microscope (A, D, G, K, P). **A-C) SPA array chip A₁₂.** Images of fluorescence signals taken after SPA PCR using the Fluorescence Reader (B) or the fluorescence microscope (C). **D-F) SPA array chip A₀₃.** Image of precipitates visible on the chip surface after SPA PCR (E). Image of fluorescence signals (F). **G-J) SPA array chip A₂₁.** Image of precipitates visible on the chip surface after SPA PCR (H). Image of fluorescence signals (J). **K-O) SPA array chip A₀₁.** Images of precipitates visible on the chip surface after SPA PCR (L) and hybridization (N). Images of fluorescence signals taken after SPA PCR (M) or hybridization (O). **P) SPA array chip A₁₁.** The array structure of this chip was analyzed via atomic force microscopy prior to use (figure 30).

4. Technical Evaluation of the Lab-on-a-chip System

After SPA, reaction mixes were also applied to PAAGE, to check for the presence of PCR products. Those could have been generated via detached primers in the reaction solution that could also have destroyed a working SPA performance. However, no PCR products were detected on polyacrylamide gels, accounting for a stable coupling of primers to surfaces.

To check for a proper structure of array spots, besides using a stereomicroscope for optical detection, atomic force microscopy was applied to a new and unused LOC chip A₁₁. Atomic force microscopy (AFM) is a technique for mapping the atomic-scale topography of a sample surface by means of the repulsive electronic forces between the surface and the tip of a microscopic probe moving above the surface. AFM imaging was done and supported by D. Adigüzel (research participate), and images were kindly provided. An AFM image of a possible spot of the 2x2 spot array, located in the supposed area of reaction center B, was generated (**figure 30**). It comprised a spot size of about 100 μm in diameter with a height of about 6.5 μm , but revealed a strange shape of the array spot. The spot height was not distributed equally throughout the spot size, but could only be measured in an area within the diameter, where the spotting solution was concentrated while the rest of the spot area was plane.

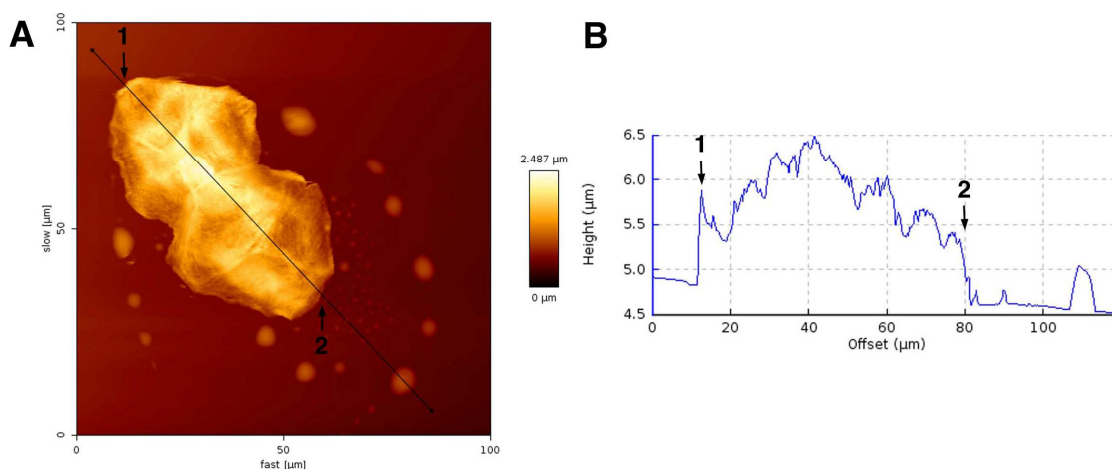


Figure 30. Image data of atomic force microscopy applied to a single array spot. A) The AFM image represented the shape, size and structure of a possible spot of the 2x2 spotted primer array, located in the supposed area of reaction center B on LOC chips. **B)** Cross section of the pictured spot revealed an elevation of about 6.5 μm , which is about 70 μm in length, while the whole spot was supposed to be 100 μm in diameter.

Despite the strange shape of the array spot detected via AFM, the measured spot diameter of about 100 μm fitted perfectly well with the supposed total size of this array. According to the spotting protocol of the company, which performed the spotting (Advalytix AG/Beckman Coulter Biomedical GmbH, Munich, Germany), spot size was supposed to be between 100-150 μm , while spot-spot distance was fixed to 160 μm in both dimensions. Thus, a total array diameter of about 400-500 μm was spotted, fitting perfectly well within the hydrophilic

4. Technical Evaluation of the Lab-on-a-chip System

reaction center on reaction spot B, comprising a diameter of about 500 μm . However, due to the strange shape of the spot, it seemed like as the spotting solution has somehow contracted after the spotting process, as it comprised just an area of 70 μm in length while a wide area of originally about 100 μm in diameter was indicated on the surface through the remainings of spotting solution. This shrinking could be an explanation why hybridization and solid phase amplification did not work well, as probably the reactive site, the primers on the surface, could not be contacted properly by the target DNA material, as they were somehow condensed. For further application, the spotting process as well as the interplay of spotting solution with LOC chip surface must be checked for optimization. Additionally, concerning the precipitations after PCR performance, the interaction between spotting solution as well as PCR reaction mix must be improved in a way that mostly saltless aqueous solutions were utilized to eliminate precipitations.

Besides the accumulated structure of the surface of the array spot, a general problem of performing SPA on LOC chip surface could have been the design of the array. Due to spotted primer-pairs, the amplification products for the male STR locus DYS392 were supposed to be 290-323 bp, for the STR locus DXS10134 240-291 bp and for amelogenin 106 bp and 112 bp. Product lengths of STR loci were amongst the longest used for DNA profiling applications on sex chromosomes (www.chrx-str.org; www.yhrd.org) and used as standard STR loci in forensic DNA profiling kits worldwide. However, possibly the PCR products generated by STR loci as well as amelogenin were chosen too short and thus no “bridge-building” via surface amplification was possible in solid phase amplification reactions, but only interfacial amplification to surface bound primers. Compared to the literature, in successful SPA only quite long PCR products of about 427 bp (Fedurco M *et al.*, 2006), 545 bp (Bing DH *et al.*, 1996), or 666 bp and 800 bp (Adessi C *et al.*, 2000) were reported to having been applied. Additionally, SPA reactions were performed in reaction volumes of 25-100 μl in total, while either plasmid DNA (Nickisch-Rosenegk M *et al.*, 2005) or preamplified DNA fragments were used (Bing DH *et al.*, 1996; Adessi C *et al.*, 2000). The products used for LOC chip SPA comprised just about 300 bp in maximum, and reactions were performed in just 1 μl total reaction volume using human genomic DNA, which has never been reported for SPA application before. Maybe a possible solution could also be the use of labeled primers, like used for microarrays, which are going to be spotted on the surface. To attribute difficulties to input DNA, primers, chip surface, reaction volume, master mix, failing interfacial or surface amplification, and to definitely judge on a successful working performance of SPA on LOC chips, applications according to cited articles remain to be tested on LOC chips.

5. Applications of the Lab-on-a-chip System in Forensic Sciences

The developed lab-on-a-chip system (LOC) incorporated several working units that were combined to one total system in a modular way. Due to the unique flexible character of the open, planar lab-on-a-chip system, it provided all qualifications being used as a stand-alone enabling technique for applications in various fields of molecular biological diagnostics. Based on the characterization and validation of the working performance and the efficiency in low-volume PCR amplification of purified human genomic DNA material, the capability of the lab-on-a-chip system for applicability on various forensically relevant sample materials was tested.

5.1 Gender determination of human intestine, mamma and bladder tissue

In forensic pathology, pieces of internal soft tissues are generally used to yield information about sex, age, and medical conditions of the inspected sample material. Thereby, the separation of various cell types and extraction of distinct cell clusters is most important in forensic analysis to guarantee for a detailed, sensitive and reliable analysis. The introduction of laser-based microdissection techniques in this field of research has greatly improved the capability to select distinct areas of interest out of surrounding tissue material, while reducing the risk of any cross-contamination. The use of microscopic instrumentation supported by a focused laser beam provides an elegant solution for direct visualization and dissection of defined cells and tissue sections out of microscope object slides (Schütze K and Lahr G, 1998). In the field of forensic medicine, laser microdissection has been reported e.g. for isolation of sperm cells and dissection of tissue sections (Elliott K *et al.*, 2003; Sanders CT *et al.*, 2006; Bauer M *et al.*, 2002; Di Martino D *et al.*, 2004 (a)) as well as on cells isolated from single hair follicles (Di Martino D *et al.*, 2004 (b)) which have successfully been typed by STR profiling. Thus, sensitive material amplification methods are necessary as well to generate reliable PCR products from that very few amount of individual cell material.

An enhancement of short tandem repeat (STR) analysis sensitivity could be achieved by downscaling reaction volumes, as was shown several times on chemically structured slides to have improved genotyping success (Proff C *et al.*, 2006; Schmidt U *et al.*, 2006; Lutz-Bonengel S *et al.*, 2007; Schmidt U *et al.*, 2008). For instance, complete STR profiles from as little as 32 pg of genomic DNA have been reported when performing virtual reaction chamber-based low-volume PCR on chemically structured chips (Schmidt U *et al.*, 2006).

5. Applications of the Lab-on-a-chip System in Forensic Sciences

Thus, linking laser microdissection and low-volume on-chip PCR together, as realized on the lab-on-a-chip, was supposed to be a valuable tool for most sensitive analysis. Fixed and paraffin-embedded tissue sample material was applied to LV-PCR after microdissection to validate the applicability of the LOC system to unpurified sample material, as often used in medical genetic analysis, like e.g. cytogenetics, cancer research and forensic pathology. As most lab-on-a-chip systems were designed for accepting just minor sample amounts of a specific type, preferably purified DNA material, here genetic analysis was performed directly on tiny tissue particles after laser microdissection without DNA extraction.

Laser microdissection was applied to paraffin-embedded tissue pieces, originating from three different human tissue types, that were intestine, bladder and mamma tissues (**figure 31**).

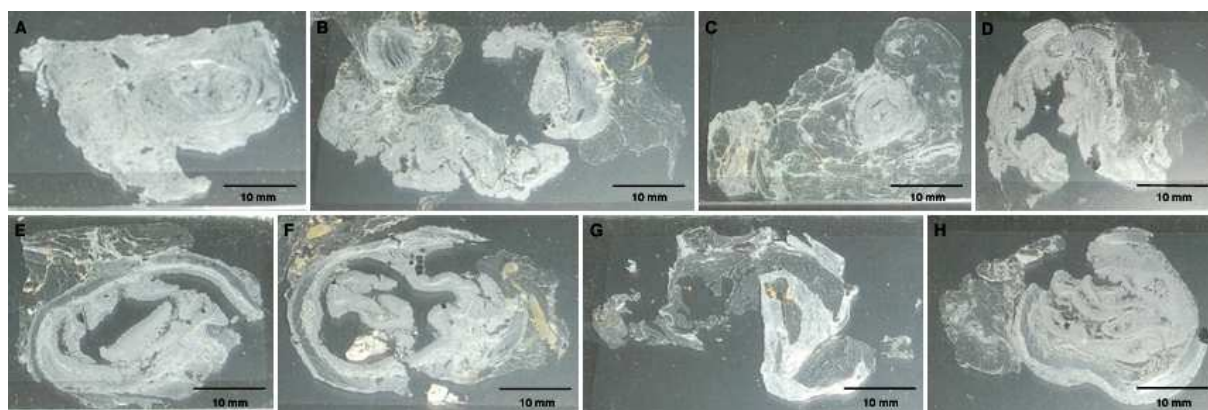


Figure 31. Paraffin-embedded tissue slides comprising various tissue types. Tissues were named tissue 1-8, while tissue 1 (A), 2 (B), 4 (E), 5 (F), 7 (H) and 8 (D) originated from intestine tissue, tissue 3 (C) from bladder tissue and tissue 6 (G) from mamma tissue.

After deparaffinization, small pieces of eight masked human soft tissue samples were successfully isolated via laser microdissection. Single tissue particles of about 500 μm in diameter were microdissected and were gently separated from histological tissue sections. Using the SPATS device, dissected tissue islets were extracted out of the surrounding tissue material via low-pressure supported adsorption to the SPATS-related collection grid (**figure 32 A-C**). Tissue particles were transferred horizontally and released exactly into a 0.5 μl droplet of H_2O , while controlled with μm -precision. Droplets for sample material take-up were placed directly on chemically defined reaction sites of a multi LV-PCR microdevice or on reaction center B of LOC chips (**figure 32 D**). A total of eight different tissue samples, released in a highly precise manner exactly onto reaction sites, was successfully tested for gender determination using directly LV-PCR analysis on primer-specific amelogenin fragments.

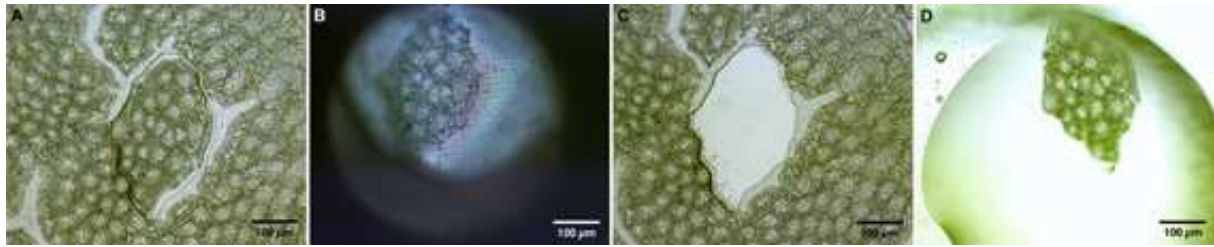


Figure 32. Workflow of the tissue transfer process via low-pressure single particle adsorbing transfer system. Scale bar in every illustration is about 100 μm . **A)** Laser microdissection of tissue material and isolation of a tissue fragment in the range of about 500 μm in diameter out of surrounding histological material. **B)** Low-pressure uptake and subsequent transfer of single microdissected tissue fragments were visually controlled via adsorption to the collection grid of the SPATS-related adsorbing head. **C)** The area of tissue fragment extraction out of surrounding tissue material is shown. **D)** Precisely controlled release of adsorbed sample material was performed into a small droplet of 0.5 μl of H_2O via operated high-pressure impulse. The fluid was placed directly onto a reaction site of a LV-PCR microdevice, defined via a chemically modified surface.

As access to DNA enclosed in the cellular material was achieved by incorporating an extended initial heat step in the PCR protocol for cell lysis, no additional precedent DNA purification was necessary. After PAAGE four out of eight masked tissue samples turned out to originate from a male, and the other 50% of the tissue samples turned out to originate from a female individual (**figure 33 A-C**). Intestine tissues 1, 2 and 5 as well as bladder tissue 3 showed 106/112 bp male-specific amelogenin amplification products, while intestine tissues 4, 7 and 8 as well as mamma tissue 6 showed 106 bp female-specific amelogenin products. Clear and sharp amplification bands could be detected on polyacrylamide gels, without any unspecific or contaminating bands and side products of larger or smaller size being present.

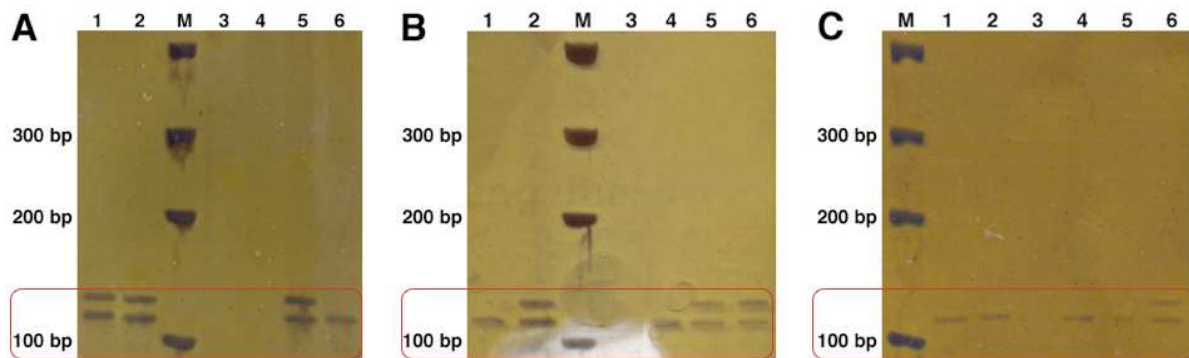


Figure 33. PAAGE data of LV-PCR amplification applied on eight microdissected human tissue samples. LV-PCR of amelogenin fragments for sex determination purposes were performed on a multi LV-PCR microdevice. M: molecular length standard (O'GeneRuler DNA Ladder, ultra low range, Fermentas, St. Leon-Rot, Germany). **A) Intestine tissue 1 and intestine tissue 2.** Lane 1: tissue 1, showing 106/112 bp male amelogenin fragments; lane 2: tissue 2, showing 106/112 bp male amelogenin fragments; lanes 3+4: negative controls (PCR master mix, H_2O control); lanes 5+6: positive controls (standard 106/112 bp male and 106 bp female human genomic reference DNA). **B) Bladder tissue 3, intestine tissue 4 and intestine tissue 5.** Lanes 1+2: positive controls (standard 106 bp female and 106/112 bp male human genomic reference DNA); lane 3: negative control (PCR master mix); lane 4: tissue 4, showing 106 bp female amelogenin fragments; lane 5: tissue 3, showing 106/112 bp male amelogenin fragments; lane 6: tissue 5, showing 106/112 bp male amelogenin fragments. **C) Mamma tissue 6, intestine tissue 7 and intestine tissue 8.** Lane 1: tissue 6, showing 106 bp female amelogenin fragments; lane 2: tissue 7, showing 106 bp female amelogenin fragments; lane 3: negative control (PCR master mix); lane 4: tissue 8, showing 106 bp female amelogenin fragments; lanes 5+6: positive controls (standard 106 bp female and 106/112 bp male human genomic reference DNA).

5. Applications of the Lab-on-a-chip System in Forensic Sciences

Tissue experiments for amplifying crude, unpurified fixed sample material were also performed on LOC chips. Sample extraction, transfer of dissected tissue particles as well as LV-PCR amplification was performed in a comparable performance. However, due to the integrated BioSpot[®] device, manual pipetting operations could successfully be neglected. 1 μ l of master mix for sample material uptake and performing LV-PCR on the chip surface as well as 5 μ l of mineral oil cover solution were provided by means of the automatic dispensing device BioSpot[®]. A whole workflow procedure of the lab-on-a-chip system could successfully be run, including microdissection-based sample isolation, SPATS transfer onto the LOC chip surface and finally LV-PCR (**figure 34**), while handling of fluids was completely done using the automatic pipetting functions of the BioSpot[®] device. Small particles of about 600 μ m in diameter were successfully microdissected out of male intestine tissue 5 and transferred directly into 1 μ l of master mix, which had afore been dispensed on reaction center B of the LOC chip by using PipeJet[™]1 of the BioSpot[®] (**figure 34 A-D**). After sample take-up, the master mix droplet could immediately successfully be covered by about 5 μ l of Sealing Solution (**figure 34 E and F**). A proper amount of Sealing Solution was dispensed by operating PipeJet[™]3 of the BioSpot[®], as this PipeJet[™] was designated for handling viscous fluids like the mineral oil. Successful amplification of male specific 106/112 bp fragments of the amelogenin gene could be detected for tissue 5 via PAAGE (**figure 34 K**).

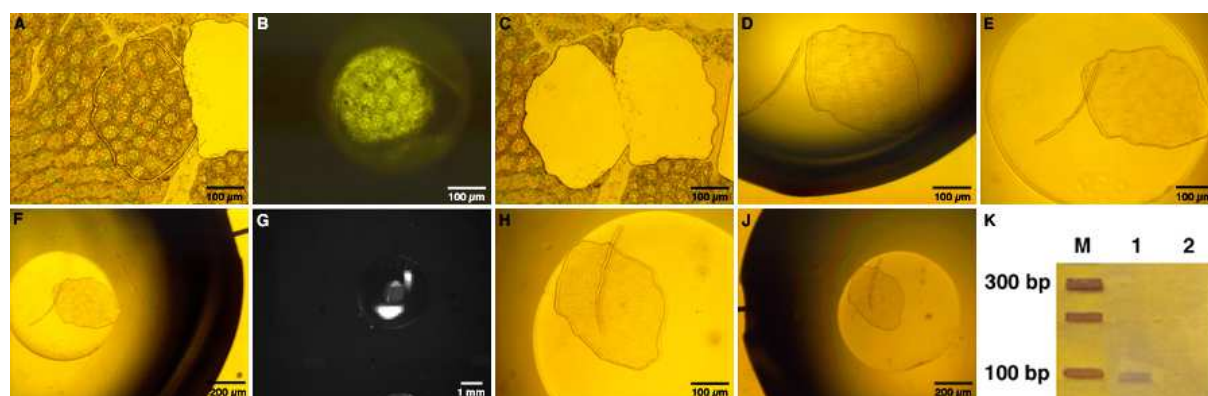


Figure 34. Workflow of laser microdissection, SPATS transfer and LV-PCR amplification performed on the lab-on-a-chip. Results were shown for male sample tissue 5, exemplarily for all of eight tissues. **A)** Isolation of a tissue particle with about 600 μ m in diameter via laser microdissection. **B)** Transfer of dissected particle via low-pressure operated SPATS. The particle was adsorbed to a sample collection grid. **C)** Control of successful particle extraction out of surrounding tissue. **D)** Release of tissue particle directly into 1 μ l of master mix, prepared on the chip surface via BioSpot[®]-operated fluid dispensation. **E-F)** 1 μ l of master mix containing tissue was covered with 5 μ l of mineral oil and was thus prepared for subsequent PCR analysis. The oil cover was provided via dispensing functions of the BioSpot[®]. **G)** Low-volume PCR performance: image was taken during the first cycles of PCR via the CCD camera associated with the Fluorescence Reader. **H+J)** Images taken directly after PCR, to control the proper arrangement of particle, master mix and covering oil. **K)** PAAGE image data of amplified PCR products. M = molecular length standard (Superladder-low 100 bp ladder with

5. Applications of the Lab-on-a-chip System in Forensic Sciences

ReddyRun™, Thermo Scientific, ABgene, Epsom, Surrey, UK). Lane 1: tissue 5, showing 106/112 bp male amelogenin fragments; lane 2: negative control on multi LV-PCR microdevice.

Performing genetic analysis directly from fixed, paraffin-embedded tissue material without preceding DNA purification could successfully be achieved by LV-PCR application. Genders of eight different masked human tissue samples were reliably determined via amplification of human amelogenin fragments. No matter if LV-PCR was applied on a multi LV-PCR microdevice or on LOC chips, clear bands of amplified PCR products could be detected on polyacrylamide gels. Amplification results of gender determination were validated with existing data sets about these samples, provided by the Institute of Pathology (Klinikum Bogenhausen, Munich, Germany). These data sets confirmed the results obtained in our laboratory. These successful amplification results accounted not only for the successful application of the LOC modules, but also for successful lysis of cellular material via an additionally performed heat step, thus making any external DNA purification and extraction procedures invalid. However, concerning the results of the LOC-based procedure, the band representing the larger 112 bp fragment originating from the Y-chromosome showed just a very weak signal compared to the 106 bp band of the smaller X-chromosomal fragment. This might more probably be due to inhomogeneous staining rather than to an imbalanced amplification performance, thus presented results for the LOC chip performance could nevertheless be attributed to a reliable, sensitive and unambiguous analysis.

However, there was a lot of bubbling observed in master mixes during the initial denaturation and cell lysis step of the LOC-based PCR performance. Generally, when performing VRC LV-PCR, causing air bubbles was avoided during the preparation of the master mix solution, as smallest air bubbles in the aqueous master mix were known to expand when treated with heat. In the master mix prepared on the chip surface, there were seemingly a lot of air bubbles present. The air bubbles leaking from the master mix ruined the proper arrangement of virtual reaction chamber PCR, causing the master mix to evaporate while the oil was bubbling. The dimension of destroyed reactions was about three ruined reactions out of five. This phenomenon of bubbling reaction mixes on the LOC chip surface might be due to the automatic dispensing process performed by the BioSpot®, where 5 nl droplets of master mix were shot onto the chip surface building a droplet of 1 µl after a certain amount of repeats. When a liquid droplet present on the chip surface was shot by several tiniest droplets at high speed, this meant an enormous mixture, stirring and agitation inside this droplet. This extensive actuation was supposed to have generated smallest invisible bubbles in dispensed master mix droplets, which might have spread during PCR performance, when the master mix was heated to hot temperatures. The same phenomenon was reported and happened, when

stirring the master mix extensively with a pipet, by pipetting up and down for mixing reagents. Thus, the automatic dispensation performance definitely needed further improvement to circumvent extensive agitation especially of aqueous master mix solutions.

Anyway, several LOC units like e.g. laser microdissection, SPATS transfer, CytoCycler-based material lysis and amplification as well as using the BioSpot[®] for loading reaction volumes onto the chip surface, could for a first time successfully be joined in a whole interplay. This performance showed a promising first application to perform a combined run of independently operating modules of the lab-on-a-chip system. Especially the coupling of a pipetting robot like the BioSpot[®] upgraded the whole performance, as manual sample handling between single analysis steps could be eliminated totally, thus reducing the risk of introducing external contaminations, which is quite important in every field of genetic analysis. And additionally, the successful material isolation via laser microdissection, particle extraction and transfer via SPATS, as well as successful LV-PCR DNA amplification, represented the applicability of the various LOC modules on forensic or forensic pathological relevant sample material, either working apart from each other as well as in a combined performance. No comparable system has been reported up to now, which can fulfill all of these processing steps on one microfluidic device, and definitely not with such kind of crude solid sample material. No comparable system exists, which combines laser microdissection with low-volume PCR, both highly predestined approaches, serving the needs of handling smallest amounts of sample material. Thus, this lab-on-a-chip system provides highest potential for becoming integrated and utilized in research areas, where genetic analyses are dependent on other sample materials than liquid ones.

5.2 DNA profiling of whole blood

Microdissected fixed tissue sample material was shown to perform well when directly applied to LV-PCR genetic analysis. No additional DNA purification or preprocessing steps were needed as cell lysis was achieved by a simple extended initial heat step, to get access to genetic material. However, there, relevant sample material had to be prepared for laser microdissection purposes and needed to be fixed and applied onto PEN carrier-membrane mounted object slides. Though, for a real fast, sensitive and reliable analysis, a lab-on-a-chip must be capable of accepting crude, untreated, authentic sample material, solid specimen as well as liquid ones, like e.g. whole blood.

Blood samples or traces are excellent evidences used for genetic analysis. PCR is a well described powerful tool for molecular genetic analysis of blood samples, currently applied for diagnostic purposes in medical analysis as well as ancestry surveys and human identification in forensics. However, one of the major limitations with PCR-based analysis is the sensitivity of *Taq* DNA polymerases to inhibitory substances present in crude specimens such as blood (Panaccio M and Lew A, 1991; Al-Soud WA *et al.*, 1998; Al-Soud WA and Radström P, 2000; Kermekchiev MB *et al.*, 2009). Generally, whole blood cannot be used for direct genetic testing, due to several characterized PCR inhibitors influencing the *Taq* DNA polymerase activity. Inhibitory effects were either attributed to natural components of blood like mainly the heme from hemoglobin, lactoferrin, immunoglobulin G (IgG), or to added anticoagulants such as EDTA and heparin. Therefore complex and extensive DNA purification procedures are mandatory prior to PCR to generate PCR-usable material. However, generally these additional pretreatment steps are time-consuming, labor-intensive, and may further lead to loss of target nucleic acids during processing and unlike may remove inhibitors subtotal. Indeed, there are several reports about thermal or chemical treatments of blood sample or PCR mixture prior to PCR to overcome purification procedures and the inhibitory effects of blood on *Taq* DNA polymerase (Schwartz EI *et al.*, 1990; Mercier B *et al.*, 1990; McCusker J *et al.*, 1992; Burckhardt J, 1994; Park SJ *et al.*, 2008). However, despite these remedies, the application of this enzyme in whole blood amplifications remains still quite controversial. AmpliTaq Gold[®] DNA polymerase, currently the standard enzyme in several multiplex short tandem repeat (STR) kits worldwide, was found to be among the most sensitive to inhibition (Al-Soud WA and Radström P, 1998). This underlines the importance of meticulous sample handling and DNA purification when using this polymerase in STR analysis. To overcome all these limitations associated with *Taq* DNA polymerases, the choice of using a non-*Taq* DNA polymerase was reported to have a huge impact on resistance to inhibition. These DNA polymerases were shown to have less sensitivity to inhibitors, could tolerate higher concentrations of whole blood (Panaccio M and Lew A, 1991; Katcher HL and Schwartz I, 1994; Wiedbrauk DL *et al.*, 1995; Al-Soud WA and Radström P, 1998) and outperformed AmpliTaq Gold[®] as recently reported (Hedman J *et al.*, 2009).

Besides a good interaction between DNA quality and used DNA polymerase, a high sensitivity of analysis is desirable. Enhancement of sensitivity can to some extent be achieved by simply reducing the reaction volume (Gaines ML *et al.*, 2002; Kloosterman AD and Kersbergen P, 2003; Leclair B *et al.*, 2003), as adding less crude target material to the amplification is proven to improve performances greatly. Low-volume PCR (LV-PCR),

performed in 1 μl total reaction volume, provided enhanced sensitivity when applied to commercial multiplex STR assays (Proff C *et al.*, 2006; Schmidt U *et al.*, 2006; Lutz-Bonengel S *et al.*, 2007; Schmidt U *et al.*, 2008). For instance, low copy number samples produced 27% complete allelic profiles in LV-PCR, while in-tube PCR just revealed incomplete allelic profiles (Schmidt U *et al.*, 2008). Unfortunately, there, purification procedures were used prior to typing analysis.

To overcome these *Taq*-related problems of inhibition and purification, a more appropriate, less-sensitive thermostable non-*Taq* DNA polymerase was used for LV-PCR based DNA profiling directly from whole unpurified blood. By using a KOD DNA polymerase-based PCR system, predestined for amplification of crude sample material, tube-less low-volume PCR was performed in extremely small reaction volumes of maximum 1 μl on chemically structured microdevices. EDTA K treated fresh and aged whole blood samples as well as time-dependently aged dried blood spots were taken as sample material and used for DNA typing via STR fragment length analysis. No previous pretreatment or preparation steps were applied besides dilution. Anticoagulant treated blood was directly used for LV-PCR in 10% or 1% dilutions and dried blood spots were directly resolved and used in 1% dilutions.

Whole blood DNA typing was performed on blood samples with added anticoagulant EDTA K. Direct DNA STR profiling could be performed repeatedly successful and reliably in 1 μl low-volume PCR reactions using as little as 0.1 μl of unpurified blood samples as target material. A small detail of typing profiles can be seen in **figure 35**. Typing of four individual blood samples gave reproducible results for 10% as well as 1% reaction batches, showing a clear effect of decreasing peak intensities with decreasing blood concentrations (**figure 35**, vertical black arrows). For instance, here peak intensities of 3000 rfu could be reached for 10% blood samples, while 1% blood samples showed just peak heights of 300 rfu. Peak heights reached from 2000 to 8000 rfu maximum and 300 to 1000 rfu minimum in 10% blood samples and from 80 to 400 rfu maximum and 50 to 400 rfu minimum for 1% blood samples. Fragment peaks were unsoiled, showing no contamination profiles and no stutter peaks and had sufficient heights, indicating values clearly above the general accepted detection threshold of 50 rfu. An overview of typing results is given in **table 6**, displaying averaged percentages of loci drop out, allelic drop out as well as complete allelic profiles obtained. Concerning the 10% blood samples, the rate of complete allelic profiles observed ranged from 83.4% to 89% on average. Regarding the 1% blood samples, this rate ranged at an average from 61.2% to 87.6%. Allelic drop out simulating homozygosity as well as drop out of

5. Applications of the Lab-on-a-chip System in Forensic Sciences

individual STR systems was found randomly distributed. Although the sensitivity was enhanced in those 1 µl low-volume PCR reactions, drop out of loci and single alleles were observed more often in 1% reactions, which probably occurred as a consequence of a higher dilution factor and thus could be interpreted as stochastic effects due to pipetting of very small volumes as already reported by Kloosterman AD and Kersbergen P (2003).

Table 6. Typing results of 4 individual EDTA K treated blood samples using LV-PCR. Data analysis of every single sample was performed in triplicates in two independent approaches leading to 6 peak profiles per sample. Only peak signals above 50 rfu were counted. The percentages represented the averaged rate of loci drop out, allelic drop out and of complete allelic profiles obtained in samples 1-4 as well as positive controls PK-1 and SE-PK-2.

		Age of blood sample	AmpF/STR® SEfiler™ kit (11 STR loci + amelogenin)		
Material	EDTA K treated blood samples; 2 male (1, 2) and 2 female (3, 4) samples	1 = 3 months 2, 3, 4 = 1-3 weeks	Loci drop out	Allelic drop out	Complete allelic profiles
PCR-Kits	- KOD Xtreme™ Hot Start DNA Polymerase kit - AmpF/STR® SEfiler™ PCR amplification kit	1-10% 2-10% 3-10% 4-10%	16.6 % 13.8 % 16.6 % 8.3 %	- - - 2.7 %	83.4 % 86.2 % 83.4 % 89 %
Preparation	Blood samples of 100% and 10% (diluted with sterile water)	1-1% 2-1% 3-1% 4-1%	11.1 % 8.3 % 36.1 % 11.1 %	1.3 % 8.3 % 2.7 % 5.5 %	87.6 % 83.4 % 61.2 % 83.4 %
Starting amount of blood for PCR	10% or 1% blood in 1 µl reaction mix (= 0.1µl of 100% or 10% blood sample)	PK-1 SE-PK-2	3.1 % -	- -	96.9 % 100 %

Negative controls were included in every reaction batch and were consistently negative (**figure 35**). Two kinds of positive controls were performed using control DNA. On the one hand, control DNA was amplified using LV-PCR, the KOD Xtreme™ PCR reaction mix and the AmpF/STR® SEfiler™ Primer Set, the same setup as used for whole blood sample analysis (named PK-1). On the other hand, control DNA was amplified using a standard thermocycler and the original AmpF/STR® SEfiler™ PCR Reaction Mix, as recommended by the manufacturer's kit manual (named SE-PK-2). This pure positive control validated results obtained in the mixed kits' setup, as using just the AmpF/STR® SEfiler™ Primer Set, without the recommended PCR system provided with the AmpF/STR® SEfiler™ kit, might have changed the optimized PCR setup of the kit. As can be seen in **figure 35**, the KOD Xtreme™ master mix matched well with the AmpF/STR® SEfiler™ Primer Set. Clear peaks were detectable and allelic profiles could be obtained from the LV-PCR-based positive controls PK-1 showing a rate of 96.9% compared to a rate of 100% of complete allelic profiles,

5. Applications of the Lab-on-a-chip System in Forensic Sciences

obtained with SE-PK-2 (**table 6**). Slight drop out of loci in PK-1 compared to SE-PK-2 could again be attributed to stochastic effects due to pipetting of very small volumes (Kloosterman AD and Kersbergen P, 2003).

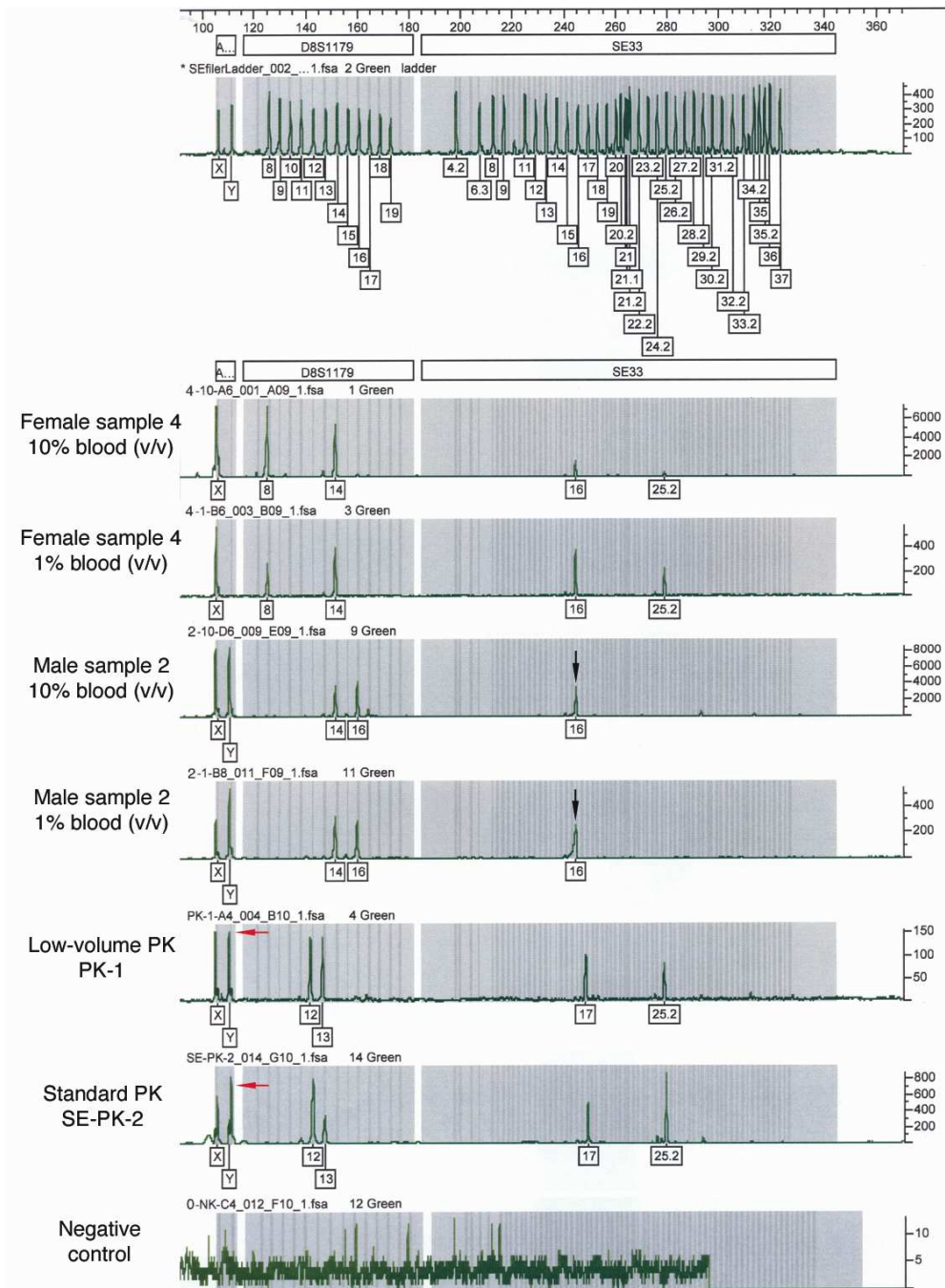


Figure 35. Blood typing allelic profiles of 10% and 1% (v/v) EDTA K-treated whole blood samples using LV-PCR. The figure represents just an excerpt, exemplarily for all four individual typing profiles and loci of samples 1-4. Allelic profiles for the amelogenin locus (A...), as well as for 2 STR loci (D8S1179, SE33) were shown, derived from two blood samples, a female (sample 4) and a male (sample 2) one, as well as negative control and two positive controls (PK-1, SE-PK-2). Samples yielded clear allelic profiles, comprising pure peaks without contamination or stutter peaks and displaying concentration dependant peak heights (vertical black arrows). PK-1, showing complete allelic profiles, validated that the KOD Xtreme™ PCR master mix in combination with the AmpF/STR® SEfiler™ Primer Set harmonized well. Fragment sizes of PK-1 compared to SE-PK-2 clearly showed the 1 bp-shifting caused by using the KOD DNA polymerase (horizontal red arrows).

5. Applications of the Lab-on-a-chip System in Forensic Sciences

The conventionally cycled positive control SE-PK-2, using the complete SEfiler™ PCR setup, produced peaks matching perfectly with the provided SEfiler™ Allelic ladder, as AmpliTaq Gold® DNA polymerase was used.

Besides the described positive profiling results, it has to be noted that the AmpF/STR® SEfiler™ Allelic ladder peaks were displaced exactly 1 bp to sample peaks of LV-PCR-based analysis (**figure 35**, horizontal red arrows). Allelic ladder peaks just matched perfectly well with the positive control SE-PK-2, cycled according to manufacturer's recommendations using AmpliTaq Gold® DNA polymerase (**figure 35**, horizontal red arrows). This fragment size shifting was due to the used polymerases. AmpliTaq Gold® DNA Polymerase, provided by the kit, catalyzed the addition of a single nucleotide (predominately adenosine) to the 3' ends of double-stranded PCR products (Clark JM, 1988; Magnuson VL *et al.*, 1996). This non-template adenylation was not performed by the KOD DNA polymerase therefore all fragment lengths of LV-PCR products, including PK-1, were 1 bp shorter. Generating an appropriate allelic ladder using the KOD DNA polymerase would solve this discrepancy.

Whole blood DNA typing was performed on dried blood specimens over time without added anticoagulants. Dried blood spots were resolved in sterile water after several time intervals and 1% blood (v/v) was used for DNA typing analysis in a total reaction volume of 1 μ l, to check for successful allelic profiling in dependence of sample age (**figure 36**). Allelic profiles were obtained for up to 3 months old blood spots.

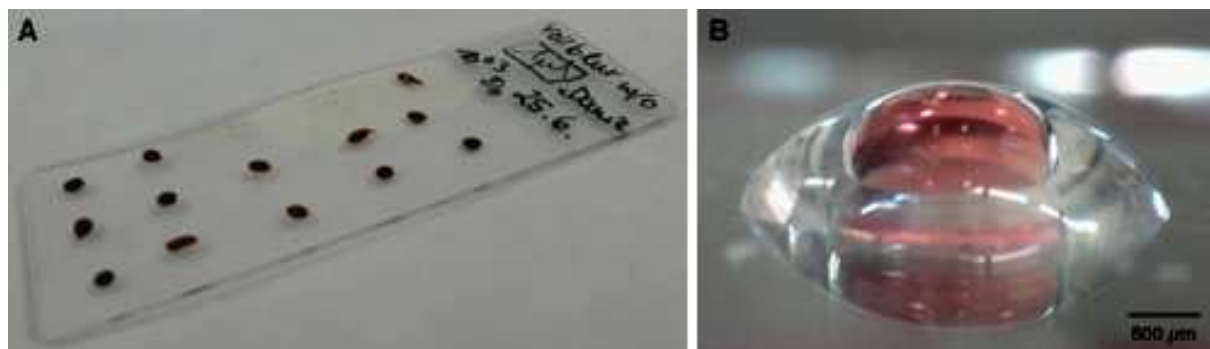


Figure 36. Sample preparation and low-volume amplification of dried blood spots (DBS). **A)** Preparation of dried blood spots. Fresh blood was spotted in 1 μ l drops on a pre-cleaned object slide (76 x 26 mm) and dried at room temperature. After distinct periods of time samples were taken: a 1 μ l dried blood spot was resolved in sterile water and 10% blood solutions were then used for LV-PCR typing analysis, comprising a final concentration of 1% blood (v/v) present in 1 μ l total reaction mix. **B)** Low-volume virtual reaction chamber PCR: 1 μ l total blood containing reaction mix (red enclosed solution, 500 μ m in width) was covered by 5 μ l of Sealing Solution (transparent covering oil, 3 mm in width) to prevent evaporation and external contamination as well as cross-contamination.

The obtained data of sample analysis are summarized in **table 7**, showing typing results in averaged percentages grouped into loci drop out, allelic drop out and complete allelic profiles obtained. In the “0 min” samples one single locus dropped out completely, resulting in 98% successful typing of untreated fresh blood samples. Sample analysis after a drying time from

5. Applications of the Lab-on-a-chip System in Forensic Sciences

30 to 360 min showed quite inconsistent allelic peaks. At these time intervals allelic profiles ranged between no allelic profiles at all as well as a huge amount of loci drop out and allelic drop out, either producing no signals or peaks going below the threshold. Here, rates of successful typing reached from 56.8% to 20.9% on average. In samples dried for 1 day, 2 days, 4 days and 1 week minor fluctuations concerning typing efficiency were detected, ranging at an average from 90% to 70%, which might be due to a terminated drying process, while blood components still have unchanged properties. Here, a few loci drop out were observed that were very randomly distributed over all of the loci. 2 weeks, 3 weeks and 4 weeks old samples showed consistent marker peaks, most stable in appearance and height. They ranged from 89% to 91.7%, whereas locus drop out occurred preferably in one particular locus. Concerning the 3 months old samples, the obtained complete allelic profile rate was about 85.9% on average. Drop out of single loci or alleles may be due to pipetting artifacts, as a volume of 0.1 µl blood sample is a random mixture of solid particles like e.g. lymphocytes out of the sample, so stochastic effects could be expected (Kloosterman AD and Kersbergen P, 2003). To obtain statistically reliable results, LV-PCR was performed in three- to sixfold series. In most instances 2-4 complete profiles could be obtained, while 1 or 2 samples showed enhanced drop out due to pipetting artifacts. Allelic drop out, as a consequence of a higher dilution factor, was randomly distributed and not correlated to size of missing alleles. Thereby, getting usable DNA typing profiles with clear marker peaks was successful even after 3 months of storage of dried blood spots and DNA remained very stable in dried blood.

Table 7. Typing results of dried blood spots using low-volume PCR. Data analysis of every single time interval was performed in multiplicates (double to threefold runs) in two independent approaches leading to 3 to 6 peak profiles per time point. Only peak signals above 50 rfu were counted. The percentages represented the averaged rate of loci drop out, allelic drop out and of complete allelic profiles obtained.

		Age of blood sample	AmpF/STR® SEfiler™ kit (11 STR loci + amelogenin)		
Material	Untreated blood (w/o anticoagulants)	Fresh blood, dried at room temperature	Loci drop out	Allelic drop out	Complete allelic profiles
PCR-Kits	- KOD Xtreme™ Hot Start DNA Polymerase kit - AmpF/STR® SEfiler™ PCR amplification kit	0 min	2 %	-	98 %
		30 min	41.6 %	1.6 %	56.8 %
		60 min	60 %	-	40 %
		120 min	61.6 %	1.6 %	36.8 %
		360 min	79.1 %	-	20.9 %
Preparation	Blood spots of 1 µl dried at RT on glass slide; samples taken after time intervals of 0, 30, 60, 120 min, 6 h, 24 h, 2 d, 4 d, 7 d, 2 we, 3 we, 4 we, 3 months	1 day	10 %	-	90 %
		2 days	15.2 %	1.3 %	83.5 %
		4 days	20 %	-	80 %
		7 days	30 %	-	70 %

5. Applications of the Lab-on-a-chip System in Forensic Sciences

Starting amount of blood for PCR	- 1µl blood spot dissolved in 10µl H ₂ O (10% blood solution)	2 weeks	8.3 %	-	91.7 %
	- final 1% blood in 1 µl reaction mix (0.1µl of 10% blood spot solution)	3 weeks	8.3 %	-	91.7 %
		4 weeks	8.3 %	2.7 %	89 %
		3 months	13.3 %	0.8 %	85.9 %

Blood DNA profiling analysis of dried blood spots could successfully be applied to a multi LV-PCR microdevice as well as on LOC chips. Results of loci drop out, allelic drop out and full allelic profiles obtained were quite comparable at each distinct time point during 3 months of aging. However, signal intensities of allelic profiles obtained were always stronger when using a multi LV-PCR device. Peak heights reached from 120 rfu up to 600 rfu, as illustrated in allelic profiles of dried blood spots obtained after 4 weeks of aging (**figure 37**).

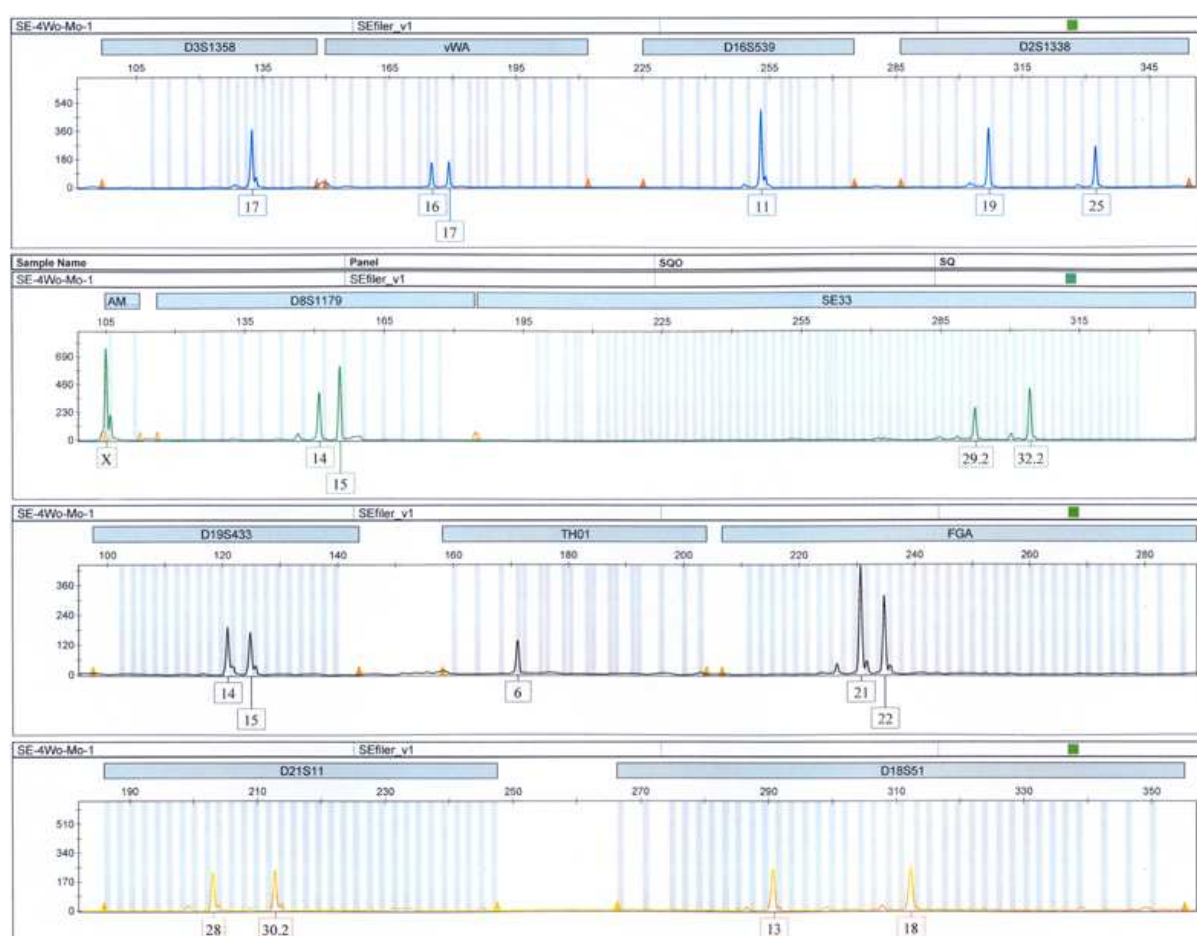


Figure 37. Fragment length analysis of dried blood spots after 4 weeks of drying using a multi LV-PCR microdevice. Peak heights reached values clearly above the generally accepted threshold of 50 rfu, signaling authentic marker peaks. Clear marker peaks without contaminating effects could be detected. Values of 120 rfu at minimum and 600 rfu at maximum were obtained for 4 weeks old dried blood spots, analyzed on a multi LV-PCR microdevice.

Concerning blood samples analyzed on LOC chips, peak heights were well below the ones obtained when a multi LV-PCR microdevice was used. Exemplarily, in **figure 38** profiling peaks from dried blood spots aged for 3 months were shown, reaching signal intensities from 20 rfu up to 350 rfu. Despite partly marker peaks below the accepted threshold of 50 rfu were

5. Applications of the Lab-on-a-chip System in Forensic Sciences

detected, these peaks could clearly be identified as authentic and reliable profiling peaks, as background signals were perfectly low. No interfering allelic peaks, no competing stutter peaks and no fluctuating background signal could influence a clear data analysis in distorting authentic signals. Thus, profiling peaks, even when detected below threshold level, could successfully be applied for an unambiguous validation.

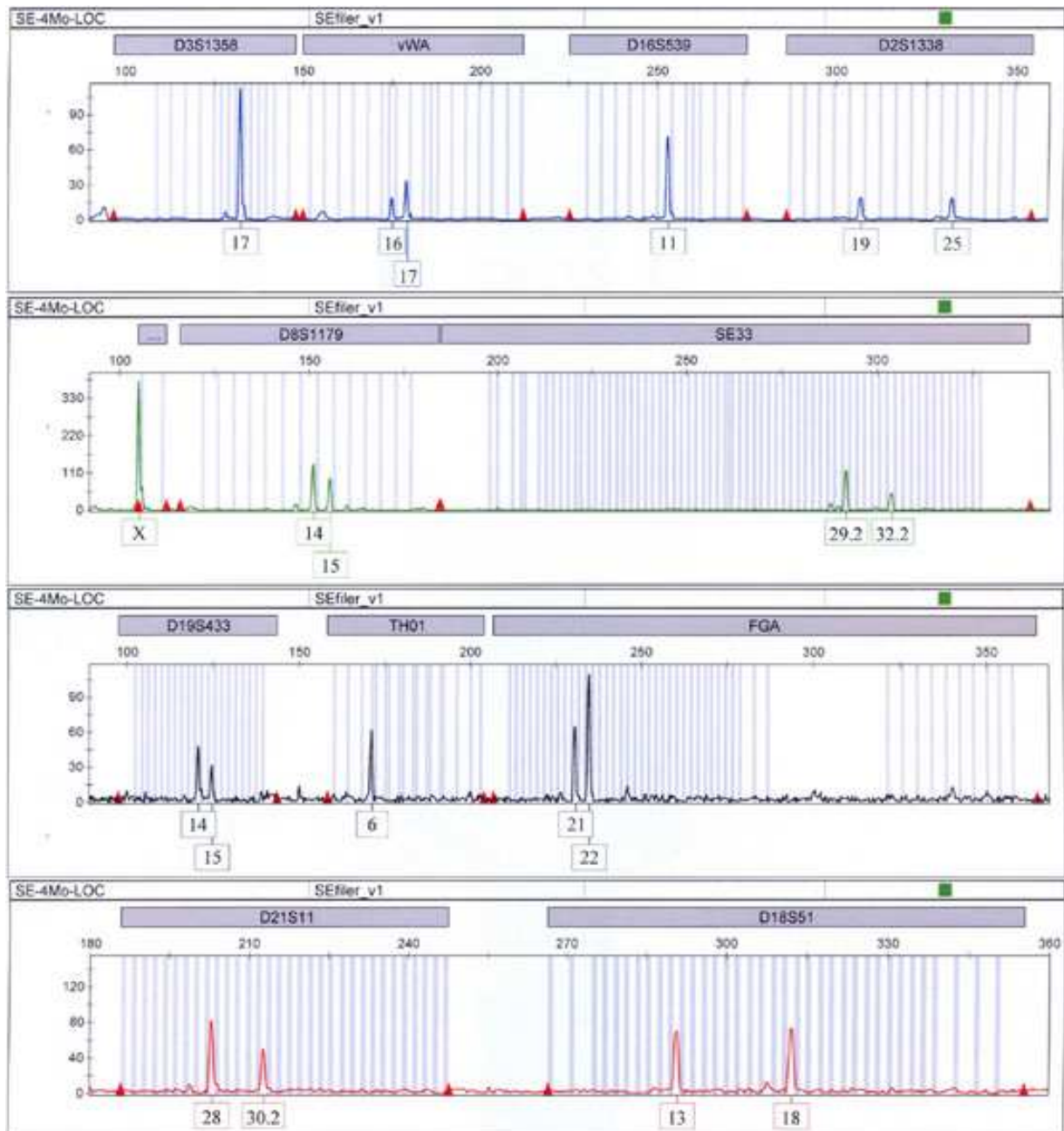


Figure 38. Fragment length analysis of dried blood spots after 3 months of drying analyzed on LOC chips. Peak heights reached not constantly values clearly above the generally accepted threshold of 50 rfu, signaling authentic marker peaks. Values of 20 rfu at minimum and 350 rfu at maximum were obtained for 3 months old dried blood spots, analyzed on LOC chips. However, clear marker peaks without contaminating effects could be detected.

A non-inhibitory PCR performance on whole EDTA K-treated blood as well as age-dependent typing of dried blood spots could successfully be demonstrated. As a KOD DNA

polymerase operated PCR system was used, predestined for amplification of crude sample material, allelic profiles could be obtained in dependence of age and alteration of blood spots during the drying and coagulation process. Blood DNA typing was performed in 1 μ l total reaction volume containing only 1% whole blood (v/v) on a chemically structured surface, using a multi LV-PCR microdevice as well as LOC chips. Due to this one step procedure no additional purification steps were necessary while increasing analysis sensitivity by reduced target material.

As validated in **chapter 4.2**, again the LV-PCR performance concerning PCR product output was more efficient in multi LV-PCR microdevice-based amplifications. STR profiling peaks reached clearly higher signal intensities compared to LOC chip-based operations. This phenomenon could again be due to a less optimal LV-PCR setup concerning the contacting of master mix droplet to surface area, resulting in a less efficient heat transfer. Despite LOC-chip-based amplification peaks were partially below an accepted 50 rfu-threshold of authentic peak signals, clear STR profiles could be obtained due to a highly unsoiled background signal. Authentic peaks could unambiguously be separated from background fluctuations. As contamination effects could successfully be eliminated, peak signals could clearly be detected and typing results were interpretable at all, the applicability of a lab-on-a-chip based approach for a sensitive forensic relevant analysis like this could definitely be demonstrated. Successful LV-PCR DNA amplification on whole unpurified blood represented the applicability of the lab-on-a-chip for forensic relevant applications like e.g. blood DNA profiling. Allelic profiles were obtained reproducibly and concentration dependencies could be detected. A reliable experimental performance could be noted and savings in time and cost could be highlighted due to eliminated purification steps prior to PCR. Preparative steps could be neglected, as only a very small amount of sample material was needed for LV-PCR and a special DNA polymerase was used, which could tolerate inhibitory effects better than *Taq* polymerases.

In conclusion, the use of DNA polymerases resistant to PCR-inhibitory components in combination with the use of appropriate facilitators of analysis efficiency (like LV-PCR), could, to some extent, eliminate the need for extensive processing of blood samples prior to PCR. Furthermore, the relative concentration of PCR inhibitors in this low reaction volume, if present, is probably less critical. As could be reported in the next application (**chapter 5.3**), LV-PCR is a valuable tool for highly sensitive analysis of ancient DNA material (Woide D *et al.*, 2010) as well as single cell analysis (Mayer V *et al.*, 2009), as reported earlier, while providing reliable contamination free performances. Reagent-saving LV-PCR also provides considerable economies. As genetic analysis trends to get smaller-volume, faster, more cost-

efficient and most sensitive, a contamination-free lab-on-a-chip procedure like this might signify a big benefit. It can be used with commercially available PCR amplification kits, allows validation and comparison with existing data sets and is capable of being integrated easily into laboratory routine. Cost-effectiveness is especially important when using these costly commercially available PCR amplification kits and most economic when applying the highly priced and costly multiplex STR DNA profiling kits.

Generally, the applicability of blood on a chip seems to be easier when using a planar open processing surface, like the virtual reaction chamber concept. For most cavity- and channel-based lab-on-a-chip systems it is hard to accept whole blood as crude sample material for analysis, and thus a lot of pre-purification steps were necessary to make blood samples chip-compatible. Another promising approach for blood analysis on a planar chip including purification, cell separation and PCR amplification, was introduced by Pippert *et al.* (2007). Superparamagnetic particles were utilized for sample tracking and DNA amplification was performed using virtual reaction chamber low-volume PCR in a clockwork lab-on-a-chip principle. However, here blood purification was included prior to PCR analysis. As shown in the previous experiments described here, PCR amplification on a planar chip can be performed much easier. When just a small amount of blood is applied to reactions (like e.g. 1% blood (v/v)) and an appropriate DNA polymerase is used, more resistant to inhibiting effects related with whole blood, labor-intensive purification procedures can be circumvented and eliminated, speeding up reaction performances.

5.3 Nanotechnological analysis of ancient bone tissue material

The best opportunity to validate the capability of a PCR system is to test for a highly sensitive analysis on low-copy number sample material (LCN). LCN samples are generally defined as samples having a very low amount of amplifiable DNA material, generally less than 100 pg like e.g. single cells comprising about 7 pg of DNA target material, as well as samples containing degraded DNA. DNA degradation means fragmentation of DNA strands due to environmental influences, preparative sample treatment steps or simply age dependent effects on the DNA material. LV-PCR analysis was performed on ancient bone tissue material originating from Egyptian mummy material. This kind of sample material was definitively expected to be affected by several DNA degradation events, qualifying it perfectly as „difficult-to-analyze“ sample material to determine the potential of LV-PCR for sensitive analysis on pathological relevant material. However, LV-PCR analysis was applied on

purified mummy DNA material after DNA extraction, which was performed off-chip, due to complexity of DNA extraction from hard sample materials like bone tissue.

The study of ancient DNA plays an important role in archaeological and palaeontological research as well as in pathology and forensics. Molecular archaeology, which was first described in the early eighties, is a particularly promising emerging archaeometric discipline for dealing with molecular biological analyses of human remains (Pääbo S, 1985). For instance, sex determination of human findings can easily be defined using small amounts of remains such as bones and teeth via i.e. polymerase chain reaction (PCR) (Hummel S and Herrmann B, 1991; Faerman M *et al.*, 1995; Faerman M *et al.*, 1997). For a significant genetic analysis usually 1 to 2 grams of bone or tooth material are adequate. This material is purified and pulverized, and ancient DNA (aDNA) is then chemically extracted. Here, the co-extraction of humic acids, these are organic compounds originating from the soil, being present in soil buried bones and teeth, and having the same chemical characteristics as DNA can cause a problem inhibiting enzymatic reactions like PCR (Goodyear PD *et al.*, 1994). Various ancient DNA extraction methods are currently in use, which rely on different principles like spin column, alcohol precipitation or silica binding. All of these methods aim to maximize DNA yields, while minimizing the co-extraction of PCR inhibitors. No single method has been shown to outbalance the others therefore no standardized procedure exists so far.

Microdissection techniques, performed on tissue structures from histological preparations, enable the precise manipulation and isolation of genetic material in the range of several micrometers (Greulich KO and Leitz G, 1994; Thalhammer S *et al.*, 2004). These techniques can be combined with subsequent analysis of DNA in these microdissectants. Several dissection techniques such as extraction via glass needle (Weimer J *et al.*, 2001), laser capture (Simone NL *et al.*, 1998), laser pressure catapulting (Thalhammer S *et al.*, 2003), laser impulse (Kirschner J and Plaschke-Schluetter A, 2007) or via gravity effects (Di Martino D *et al.*, 2004 (a+b)) are commonly in use. Recently, we could introduce the novel LOC-related technique based on the combination of laser microdissection and low-pressure technology (Woide D *et al.*, 2009). This technique enabled gently controlled extraction and horizontal transfer of a smallest amount of isolated material.

The reduction in target material requires an additional enhancement of analysis sensitivity, which can be achieved by reducing the reaction volume of PCR reactions (Gaines ML *et al.*, 2002; Kricka LJ and Wilding P, 2003; Leclair B *et al.*, 2003). It is believed that this enhanced sensitivity may result from the better contact between primer or polymerase molecules and

the DNA because the overall amount of DNA is less diluted than in a higher volume (Proff C *et al.*, 2006; Schmidt U *et al.*, 2006). Thus, using low-volume PCR (LV-PCR) technology in combination with the laser-based DNA extraction method, offers the opportunity to further reduce the amount of DNA starting material needed while retaining sensitive genetic analysis.

DNA of four mummy samples was extracted in two independent approaches, where a novel laser microdissection-based method was highlighted compared to a conventionally used extraction technique. Main results concerning target DNA amount as well as PCR amplification were summarized in **table 8**. Laser microdissection, SPATS transfer and LV-PCR were applied on mummy material, presenting a pathological applicability of the modular lab-on-a-chip system. The contamination-free performance comprised extraction of smallest, best preserved amounts of paraffin-embedded bone particles via laser microdissection and subsequent gentle low-pressure mediated transfer of particles into PCR-tubes containing DNA extraction buffer. The amount of microdissected DNA was checked via real-time PCR. This laser-based DNA extraction method was compared to a conventional DNA extraction technique used in pathology, operating with pulverization of whole bone tissue pieces. Extracted DNA amounts of pulverized samples were detected by UV spectrophotometry. After DNA extraction, amelogenin and β -actin fragments were amplified using LV-PCR to check DNA quality and preparation-dependant PCR efficiency of both DNA extraction methods. For validation of results, sequencing was performed on microdissected PCR products as well as DNA typing via STR fragment length analysis. Thus, possible DNA contamination of mummy sample material with recent DNA originating from scientists or else could clearly be excluded.

DNA extraction. In our laboratories, strict precautions were taken during all molecular genetic analysis minimizing the hazard of amplifying contaminating modern DNA in ancient specimens, and controls performed at all steps were consistently negative. Based on the results of DNA typing analysis, we were able to widely exclude contamination and cross-contamination of the ancient bone samples. Ancient DNA could successfully be extracted out of pulverized mummy bone material via DNA precipitation (Zink A *et al.*, 2003). DNA extraction using 1 g of pulverized bone tissue material of each mummy sample revealed DNA amounts of 2.1-10.0 ng/ μ l, as measured via UV spectrophotometry. For the laser microdissection-based approach, nested isolation of bone tissue pieces was performed (**figure 40 A**) to reduce the risks of external contaminating effects. After paraffinization, microtome-

5. Applications of the Lab-on-a-chip System in Forensic Sciences

cuts of paraffin-embedded bone tissue slices were prepared on PEN-membrane coated object slides (**figure 39**).

Several single osteon islets comprising 150 to 350 μm in diameter could successfully be isolated out of mummy bone tissue via laser microdissection (**figure 40 B**).



Figure 39. Preparation of mummy sample material for laser microdissection. Nested bone tissue pieces were paraffin-embedded and paraffin blocks were cut to 3-5 μm thin slices. Microtome-cut slices were mounted onto PEN-carrier membrane coated object slides and were applicable for laser microdissection after deparaffinization. The images show paraffin-embedded tissue blocks and microtome-cut tissue slices of A) mummy1, B) mummy2, C) mummy3 and D) mummy4.

Tissue material was taken exclusively from the inner parts of the bone tissue slices for subsequent conventional DNA extraction. Thus, tissue pieces were pooled from several sections in order to enrich the material. Osteons, about 50 to 500 μm in diameter, are composed of concentric layers of mineralized matrix surrounding a Haversian canal, which is 20 to 150 μm in diameter. Particle transfer was mediated via the low-pressure operated SPATS device, and sample material was released directly into a small amount of DNA extraction buffer (**figure 40 C-F**). Numerous blank extraction controls, containing PEN carrier-membrane but no tissue sample material, were processed in parallel and were consistently negative.



Figure 40. Preparation and collection of smallest amounts of target material from ancient bone tissue. A) For sample extraction, the outer surface was removed from bone material and tiny tissue blocks were prepared out of the inner bone tissue parts (arrow). B-F) Workflow of bone particle isolation as performed in the laser-

5. Applications of the Lab-on-a-chip System in Forensic Sciences

based extraction method. The isolated particle could be tracked along the entire isolation and transfer process. **B)** Laser microdissection-based isolation of an osteon bone particle comprising 300 μm in diameter. The laser cut, isolating the osteon particle from its surrounding, was marked by an arrow. **C)** SPATS mediated sample take-up is shown, where isolated bone material was adsorbed to a collection grid via applied low-pressure technology. **D)** The sample extraction area after successful particle isolation is displayed. **E)** Release of the low-pressure transferred particle into a 0.2 μl droplet of lysis solution. **F)** Magnification of the isolated and released bone particle.

Due to the fact that osteons consist to the greatest extent of concentric layers of mineralized matrix and that the Haversian canal enclosed forms just a minor part, the DNA amount extracted from microdissected mummy osteon material was approximately 60 pg of DNA present in 1 μl of extracted mummy sample material, as revealed via real-time PCR (**figure 41**). Real-time PCR was performed on sample mummy4, exemplarily for all of four mummy samples. Simultaneously, standard concentrations of 5 ng, 1 ng, 500 pg, 100 pg, 50 pg and 20 pg were co-amplified as reference DNA concentrations. For validation of amplification results of mummy4, its amplification plot was related to the plots of standard DNA concentrations (**figure 42**).

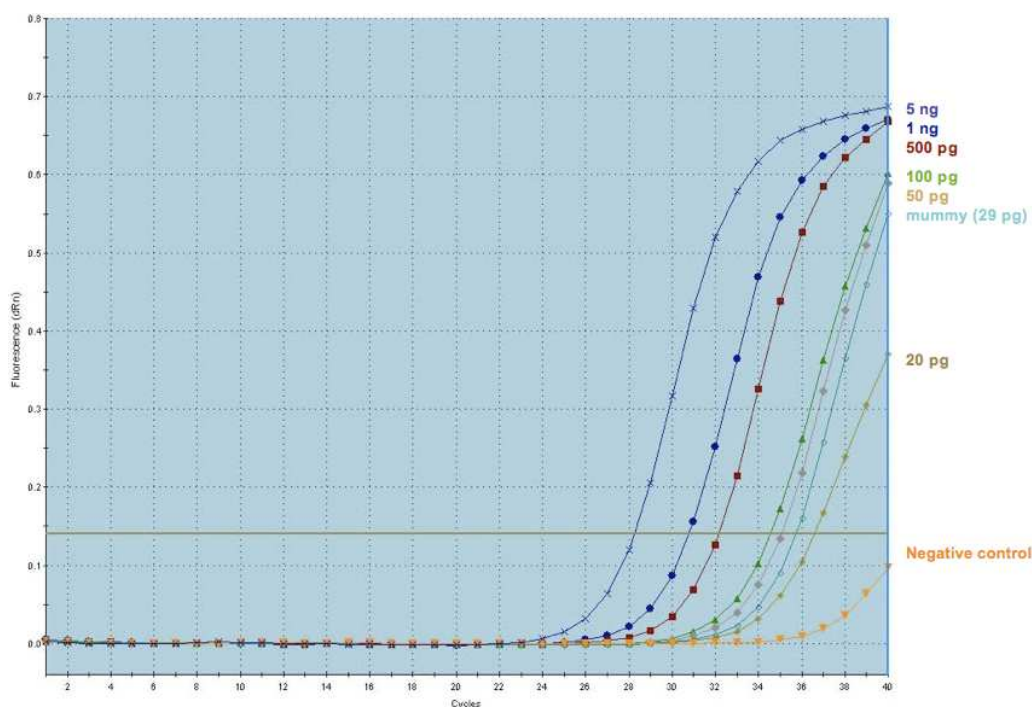


Figure 41. Amplification plots of real-time PCR performed on microdissected mummy DNA. Amplification plots of RT-PCR analysis of sample mummy4 compared to cycled standard concentrations of 5 ng, 1 ng, 500 pg, 100 pg, 50 pg and 20 pg of human genomic reference DNA. The graphs show the cycle number from cycle 1 to 40 plotted against fluorescence intensity from 0 dRn to 0.8 dRn. The plot of mummy4 clearly revealed a DNA starting amount between 50 pg and 20 pg DNA, as located between these two standard curves. Negative control represents a reaction where no input DNA was present during RT-PCR cycling.

The exact DNA concentration of sample mummy4 was detected via standard curve, plotting the initial DNA quantity to the particular Ct-value of each amplification curve (**figure 42**). The Ct-value is described as the value, at which the DNA concentration in the RT-PCR

reaction mix reached an amplification threshold. Higher starting concentrations reach this threshold earlier than lower ones. Thus the Ct-value can be taken as measure for initial DNA concentrations, when reference specimens are present. Data analysis revealed the following Ct-values of 1 μ l of reference DNA concentrations, as plotted in the standard curve: 30.83 dRn for 1 ng, 32.20 dRn for 500 pg, 34.81 dRn for 100 pg, 35.22 dRn for 50 pg and 35.89 dRn for 20 pg. For sample mummy4 a Ct-value of 35.82 dRn was obtained, representing a DNA amount of 29.41 pg. As only 0.5 μ l of mummy4 DNA were applied to the real-time PCR, data analysis revealed a DNA amount of 29.41 pg present in 0.5 μ l of extracted mummy material. When translating these results to 1 μ l of extracted microdissected mummy material, this meant a final DNA concentration of about 60 pg present in 1 μ l of extracted microdissected DNA material of mummy4.

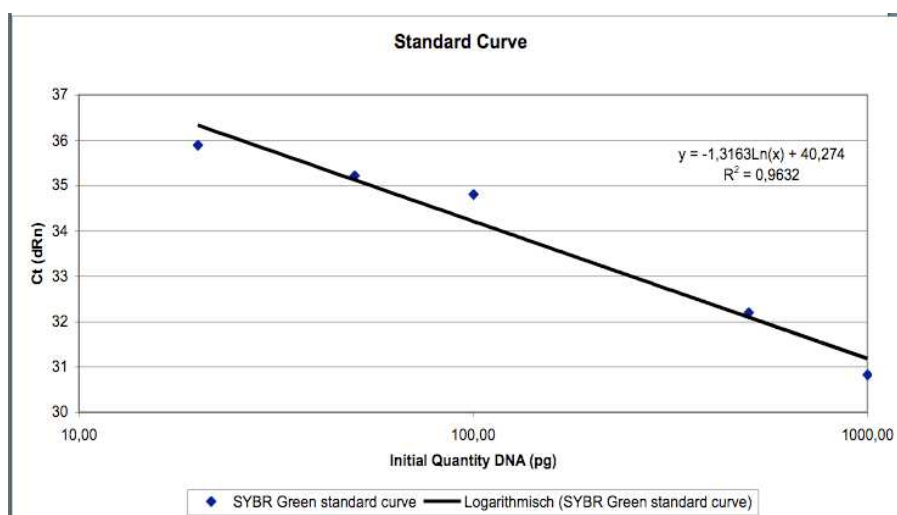


Figure 42. Standard curve of real-time PCR analysis. Initial DNA concentrations of human genomic reference DNA samples were plotted against measured Ct-values [dRn]. The standard curve of RT-PCR analysis revealed an extraction amount of approximately 60 pg DNA present in 1 μ l of extracted microdissected mummy material.

Amplification of β -actin and amelogenin gene fragments using low-volume PCR. DNA amplification experiments were performed using low-volume PCR in 1 μ l total reaction volume covered with 5 μ l of mineral oil. The reliability of this method was 90-95%, apart from 1-2 reaction batches out of about 20. These reactions were accidentally destroyed by bubbling reaction mixes, which might be due to evaporating gas bubbles present in the aqueous master mix. This was either caused by too extensive mixing of reagents or by inferior surface chemistry of the slides. Amplification was performed on 106/112 bp fragments of the amelogenin gene for gender determination, as well as on a larger fragment of the human β -actin gene comprising 297 bp. DNA was extracted from each of the four mummy samples at least twice in separate preparations. Each mummy DNA extract was tested at minimum of

five to eight times via PCR for amplifiable β -actin and amelogenin gene fragments. Amplified gene fragments were rated as reproducible and authentic only after a) five PCR reactions showed consistent fragment determination, b) this result could be reproduced in another extract from the same mummy sample and c) all controls were negative.

a) LV-PCR amplification of pulverized samples. When amplifying small gene fragments of 106/112 bp of the amelogenin gene, two out of the four mummy samples revealed a successful amplification of sex specific fragments (**table 8**). While samples mummy3 and mummy1 showed no positive PCR products (**figure 43 C and D**), sample mummy2 revealed female specific 106 bp fragments (**figure 43 A**) and sample mummy4 revealed male specific fragments of 106 bp respectively 112 bp in size (**figure 43 B**). Amplification of a 297 bp fragment of the β -actin gene was less successful. Despite repeated efforts, samples mummy1 and mummy4 revealed inconstant positive amplification products, while mummy2 and mummy3 revealed no positive amplification product at all (**table 8**). Sample mummy1 showed an amplification rate of about 2:4, revealing a positive β -actin PCR product in two out of six reactions. The amplification rate of sample mummy4 was about 1:5, having just one positive PCR product in six reaction batches. All extraction and PCR negative controls including lysis mix, PEN supporting membrane, H₂O control and the PCR master mix containing no DNA, were consistently negative (**figure 43**).

b) LV-PCR amplification of microdissected samples. Microdissected samples mummy1-4 were tested for the existence of amplifiable nuclear DNA, in respect to isolated osteon islets, comprising a very minute tissue amount of just a few micrometers (corresponding to 1 to 5 μ g) compared to standard amounts of 1 to 2 g of bone tissue material. All of four mummy samples revealed successful amplification products of 106/112 bp male and female amelogenin fragments (**table 8**). While samples mummy2 and mummy1 showed female 106 bp segments (**figure 43 A and D**), samples mummy4 and mummy3 produced male segments of 106 bp and 112 bp (**figure 43 B and C**). Concerning the larger 297 bp segment of the human β -actin gene, in each approach human β -actin fragments could successfully and constantly be amplified and detected in each of the microdissected samples mummy1-4 (**figure 43; table 8**). All extraction and PCR negative controls like lysis mix, PEN supporting membrane, H₂O control and PCR master mix, containing no DNA, were consistently negative in all cases (**figure 43**).

5. Applications of the Lab-on-a-chip System in Forensic Sciences

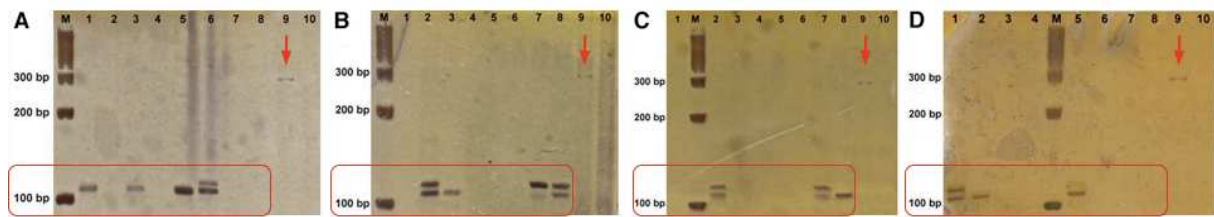


Figure 43. Polyacrylamide gel electrophoresis data of isolated and via LV-PCR amplified mummy DNA. Four different mummy samples were examined. PCR was performed on fragments of the human gene β -actin (297 bp) and the sex specific amelogenin gene (female specific 106 bp fragment, male specific 106/112 bp fragments). M: 100 bp molecular length standard (PeqLab Biotechnologie GmbH, Erlangen, Germany). **A) LV-PCR results of sample mummy2.** Lane 1: ~60 pg female mummy2 DNA (amelogenin PCR, laser microdissection-based DNA extraction method); lane 3: 50 pg female mummy2 DNA (amelogenin PCR, conventional DNA extraction method); lane 5+6: 100 pg female and male human reference DNA (amelogenin PCR, positive control); lanes 2, 7, 4, 8: PEN carrier membrane, lysis buffer, PCR master mix and H₂O control (amelogenin PCR, negative controls); lane 9: ~60 pg mummy DNA (β -actin PCR, laser microdissection-based DNA extraction method); lane 10: PCR master mix (β -actin PCR, negative control). **B) LV-PCR results of sample mummy4.** Lane 8: ~60 pg male mummy4 DNA (amelogenin PCR, laser microdissection-based DNA extraction method); lane 7: 100 pg male mummy4 DNA (amelogenin PCR, conventional DNA extraction method); lane 2+3: 100 pg male and female human reference DNA (amelogenin PCR, positive control); lanes 6, 5, 4, 1: PEN carrier membrane, lysis buffer, PCR master mix and H₂O control (amelogenin PCR, negative controls); lane 9: ~60 pg mummy DNA (β -actin PCR, laser microdissection-based DNA extraction method); lane 10: PCR master mix (β -actin PCR, negative control). **C) LV-PCR results of sample mummy3.** Lane 2: ~60 pg male mummy3 DNA (amelogenin PCR, laser microdissection-based DNA extraction method); lane 1: 100 pg male mummy3 DNA (amelogenin PCR, conventional DNA extraction method); lane 7+8: 100 pg male and female human reference DNA (amelogenin PCR, positive control); lanes 3, 4, 5, 6: PEN carrier membrane, lysis buffer, PCR master mix and H₂O control (amelogenin PCR, negative controls); lane 9: ~60 pg mummy DNA (β -actin PCR, laser microdissection-based DNA extraction method); lane 10: PCR master mix (β -actin PCR, negative control). **D) LV-PCR results of sample mummy1.** Lane 5: ~60 pg female mummy1 DNA (amelogenin PCR, laser microdissection-based DNA extraction method); lane 4: 100 pg female mummy1 DNA (amelogenin PCR, conventional DNA extraction method); lane 1+2: 100 pg male and female human reference DNA (amelogenin PCR, positive control); lanes 6, 8, 7, 3: PEN carrier membrane, lysis buffer, PCR master mix and H₂O control (amelogenin PCR, negative controls); lane 9: ~60 pg mummy DNA (β -actin PCR, laser microdissection-based DNA extraction method); lane 10: PCR master mix (β -actin PCR, negative control).

Table 8. Summary of the compared DNA extraction methods and results of LV-PCR amplification. The preparation part shows a comparison of the standard extraction method and the novel microdissection-based one in relation to the extraction amounts of the ancient material. The analysis part presents a summary of the obtained aDNA LV-PCR results according to the applied extraction method. The nested paraffin-embedding procedure combined with most precise material extraction made the working performance highly sensitive, reducing contaminations compared to the traditional method using pulverized whole bone tissue pieces.

Sample	Preparation				Analysis			
	Starting amount of sample material for DNA extraction		DNA concentration after extraction procedures		Fragment amplification via low-volume PCR on chemically structured object slides			
	Laser-based DNA isolation method	Powder-based DNA isolation method	Laser-based DNA isolation method	Powder-based DNA isolation method	Laser-based DNA extraction method (~60 pg of target DNA present in 1 μ l total reaction volume)		Powder-based DNA extraction method (50-100 pg of target DNA present in 1 μ l total reaction volume)	
					amelogenin 106/112 bp	β -actin 297 bp	amelogenin 106/112 bp	β -actin 297 bp
Mummy1	Several 150-350 μ m osteon islets	1 g of bone powder	~ 60 pg/ μ l	2.1 – 10.0 ng/ μ l	female	+	-	+/- (2:4)
Mummy2					female	+	female	-
Mummy3					male	+	-	-
Mummy4					male	+	male	+/- (1:5)

c) Performance on LOC chips. Comparable to amplification reactions performed on the multi LV-PCR microdevice, LV-PCR has been performed on LOC chips as well. Amelogenin PCR has been performed on extracted microdissected material of sample mummy4. Fragments of amelogenin gene amplification could successfully be detected via PAAGE (**figure 44**), verifying sample mummy4 to originate from a male individual as 106/112 bp fragments were obtained.

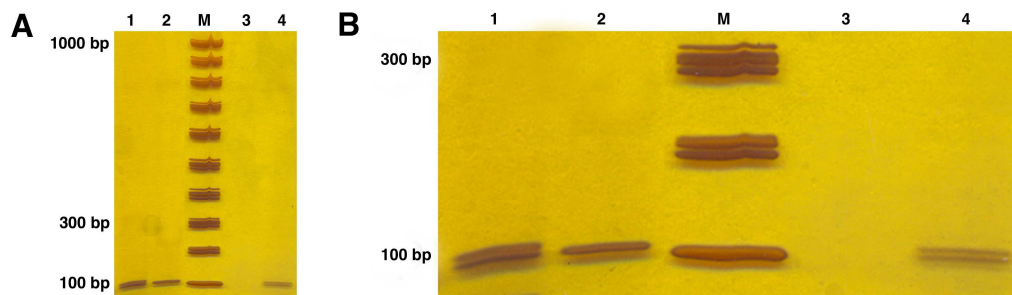


Figure 44. PAAGE image data of LOC chip-performed LV-PCR amelogenin amplification of sample mummy4. M = molecular length standard (ReddyRun Superladder-low 100 bp ladder, Thermo Scientific, ABgene, Epsom, Surrey, UK). **A)** Overview of PAAGE data. No contaminating bands were detected, no side products and no genomic DNA smear, accounting for a highly sensitive analysis. Solely the molecular length standard showed a bad run having thick and split marker bands. **B)** Closeup view of obtained gender determining PCR products. Clear bands were detected. Lane 1: 100 pg human genomic male reference DNA showing male characteristic 106/112 bp fragments (performed on multi LV-PCR microdevice); lane 2: 100 pg human genomic female reference DNA showing female characteristic 106 bp fragments (performed on multi LV-PCR microdevice); lane 3: negative control (performed on multi LV-PCR microdevice); lane 4: 60 pg male DNA of sample mummy4 showing male characteristic 106/112 bp fragments (performed on LOC chips).

Sequencing of PCR products from a microdissected mummy sample. Sequencing analysis was performed on amelogenin and β -actin PCR products, amplified from the microdissected male mummy sample mummy4, exemplarily for all of four mummy samples. Sequencing results were aligned to human nucleotide sequences, recalled from the human genomic database of NCBI (www.ncbi.nlm.nih.gov). Sequencing 106/112 bp amelogenin PCR products showed sequence identities to amelogenin loci of 90% for the Y-fragmental sequence and 97% for the X-fragmental sequence. Sequencing the 297 bp β -actin PCR product showed sequence identities to the β -actin data of 96-98% (**figure 45**). Via the sequencing analysis, successfully the authenticity of PCR products could be verified. False positive PCR products originating from suboptimal PCR conditions as well as external contamination of extracted ancient DNA could clearly be excluded.

5. Applications of the Lab-on-a-chip System in Forensic Sciences

```

Sequence 1      >[ref|NT_007819.16|Hs7_7976] [D] Homo sapiens chromosome 7 genomic contig, reference assembly
                  Length=47690382

Related gene    → Features in this part of subject sequence:
                  beta actin

Sequence matches → Score = 350 bits (189), Expect = 8e-94
                  Identities = 204/211 (96%), Gaps = 1/211 (0%)
                  Strand=Plus/Plus

Sequencing product → Query  41      TGGCCATCTCTTGCTAAAATTCCAGGGGACGATCACAGCTTCTCCTTAATGTCACGCA 100
Database reference → Sbjct  5056988  TGGCCATCTCTTGCTCGAAGTCCAGGGCGACGTAGCACAGCTTCTCCTTAATGTCACGCA 5057047

Query 101      CGATTTCGCGCTCGGCCGTGGTGAAGCTGTAGCCGCGCTCGGTGAGGATCTTCATGA 160
Sbjct 5057048  CGATTTCGCGCTCGGCCGTGGTGAAGCTGTAGCCGCGCTCGGTGAGGATCTTCATGA 5057107

Query 161      GGTAGTCAGTCAGGTCCCGCCAGCCAGTCCAGACGCACGATGGCATGGGGGAGGGCAT 220
Sbjct 5057108  GGTAGTCAGTCAGGTCCCGCCAGCCAGTCCAGACGCAGGATGGCATGGGGGAGGGCAT 5057167

Query 221      ACCCTCGTAGATGGGGCACAGTGTGGGTGA 251
Sbjct 5057168  ACCCTCGTAGATGGG-CACAGTGTGGGTGA 5057197

Sequence 2      >[ref|NT_007819.16|Hs7_7976] [D] Homo sapiens chromosome 7 genomic contig, reference assembly
                  Length=47690382

Related gene    → Features in this part of subject sequence:
                  beta actin

Sequence matches → Score = 342 bits (185), Expect = 1e-91
                  Identities = 191/194 (98%), Gaps = 0/194 (0%)
                  Strand=Plus/Minus

Sequencing product → Query  48      CTCGCCGAGCGCGGCTACAGCTTCACCACCACGGCCGAGCGGGAAATCGTGCCTGACATT 107
Database reference → Sbjct  5057096  CTCACCAGCGCGGCTACAGCTTCACCACCACGGCCGAGCGGGAAATCGTGCCTGACATT 5057037

Query 108      AAGGAGAAGCTGTGCTACGTGCGCCCTGGACTTCGAGCAAGAGATGGCCACGGCTGCTTCC 167
Sbjct 5057036  AAGGAGAAGCTGTGCTACGTGCGCCCTGGACTTCGAGCAAGAGATGGCCACGGCTGCTTCC 5056977

Query 168      AGCTCCTCCTGGAGAAGAGCTACGAGCTGCCCGATGGCCAGGTCATACCATTGGCAAT 227
Sbjct 5056976  AGCTCCTCCTGGAGAAGAGCTACGAGCTGCCCGATGGCCAGGTCATACCATTGGCAAT 5056917

Query 228      GAGCGGTTCCGCTG 241
Sbjct 5056916  GAGCGGTTCCGCTG 5056903

```

Figure 45. Sequencing results of β -actin fragments amplified from sample mummy4. Amplified 297 bp long fragments were sequenced from both sites using both primers, and were named sequence 1 and sequence 2. Sequence alignments were investigated using the particular operation at www.ncbi.nlm.nih.gov, housing references sequences of a huge amount of human genes.

Typing mummies and scientific staff. To further verify absent external contamination of extracted aDNA, which might have been caused by people having been in close contact with any kind of mummy material, DNA typing was performed in two independent approaches. DNA typing reactions were accomplished using heterozygotic marker loci on extracted mummy material as well as genomic DNA of archaeologist/excavator, technical assistance staff, laboratory members and involved scientists, simply all people who have been knowingly in contact with laboratory equipment and consumables and any kind of mummy material used. In the following these typed individuals are referred to as ‘scientific staff’. For DNA profiling analysis, particularly mummy DNA originating from the laser microdissection-based DNA extraction method was used. DNA typing experiments were performed by STR marker analyses using three selected heterozygotic STR markers D7S1824, D9S302, D10S2325 and in addition the AmpF/STR[®] SEfiler[™] PCR amplification kit on all mummy samples, all people who worked in the laboratory and those who have been

5. Applications of the Lab-on-a-chip System in Forensic Sciences

in contact with examined bone samples, paraffin-embedded tissue blocks, tissue slides, laboratory working places and laboratory working tools like optical inverted microscope, DNA extraction equipment and PCR thermocyclers. Hereby, the focus was not on typing mummy material perfectly, but rather on obtaining allelic profiles of involved scientific staff for excluding extraneous contamination of mummy material.

Typing via selected three heterozygotic STR markers D7S1824, D9S302 and D10S2325 provided very usable results on typed scientific staff's DNA material (**figure 46 A**). PCR analyses revealed mostly heterozygotic marker fragments, which could reliably be used for DNA typing as no allelic or loci drop out could be detected. On the contrary, typing mummy DNA material revealed just scattered marker peaks and none whole typing profile (**figure 46 B**). As only 2 or 3 peaks were detectable, allelic and loci drop out effects were clearly visible, making a reliable DNA profiling analysis impossible. However, as these sparsely detected peaks and thus the fragment's lengths did not match any of the scientific staff's genetic profile, cross-contamination could definitely be excluded.

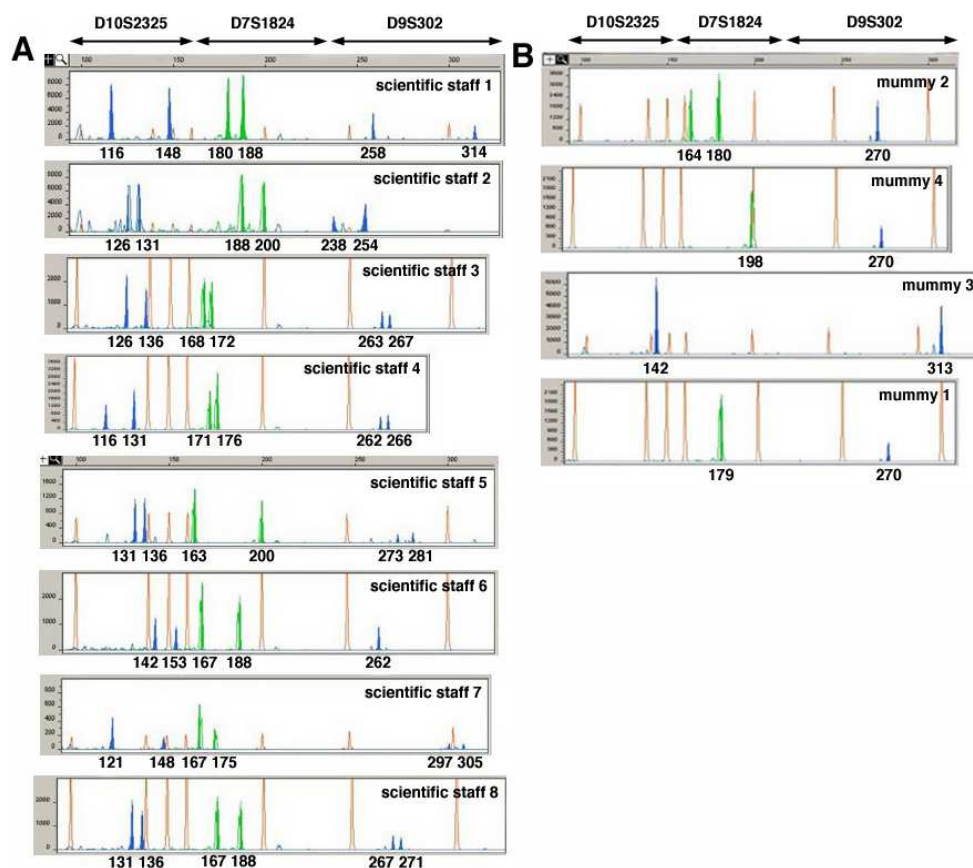


Figure 46. Genotyping performed via heterozygotic STR markers D7S1824, D9S302 and D10S2325. GeneScan™ 3.7 software electropherograms showing the PCR amplification results for the three STR loci selected and analyzed on an ABI PRISM 3130 XL Genetic Analyzer. **A)** Genotyping laboratory members as well as involved scientists, archaeologist/excavator and technical assistance staff, named “scientific staff 1-8”. **B)** Genotyping ancient mummy material, which was obtained through the laser microdissection-based DNA extraction method.

5. Applications of the Lab-on-a-chip System in Forensic Sciences

Typing present DNA material of scientific staff via the AmpF/STR[®] SEfiler[™] PCR amplification kit also produced usable results in all 12 STR loci, whereas mummy DNA material could just severely be typed (**figure 47**). Allelic profiles of scientific staff again showed no allelic drop out or loci drop out effects, but clear and unsoiled STR marker peaks, several hundred rfu in height, indicating reliable individual allelic genetic profiles obtained. Mummy material revealed just partly allelic profiles, accompanied with a lot of allelic and loci drop out events, while peak heights were consistently close to or even below the validation threshold of 50 rfu. Incomplete mummy typing profiles might be due to the very low amounts of mummy target DNA available and used for analyses. However, in amplifying also an amelogenin marker, at least the AmpF/STR[®] SEfiler[™] kit confirmed the determined genders of mummy samples.

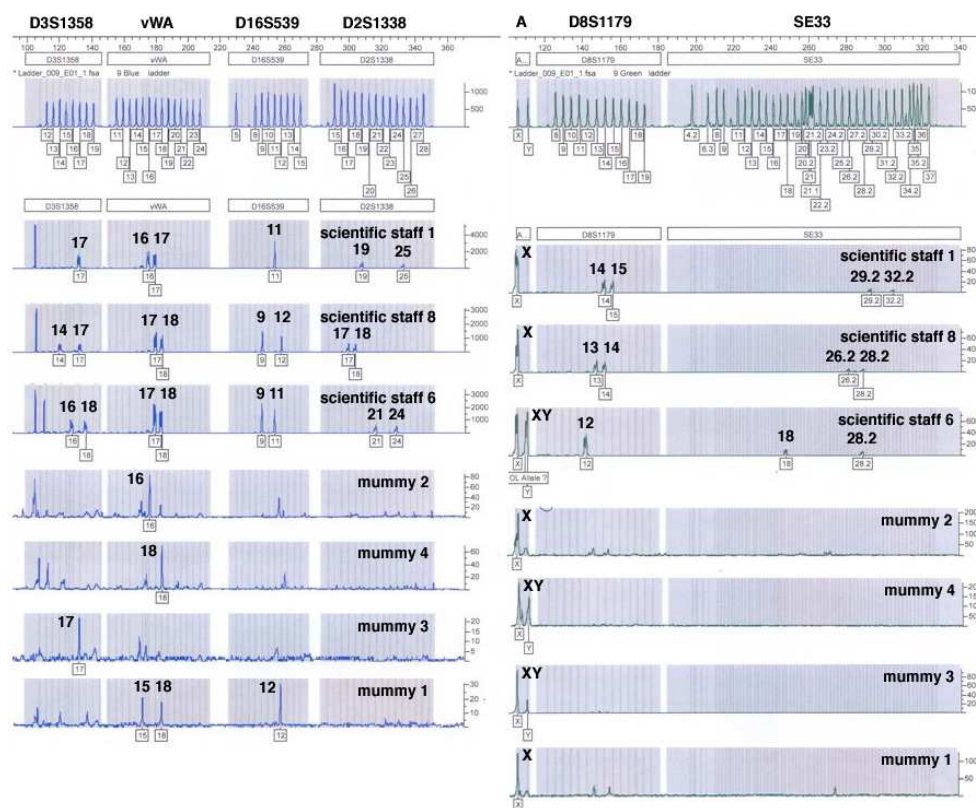


Figure 47. Except of DNA typing analysis using a multiplex STR PCR amplification kit. Peak data of seven out of 12 amplified STR marker loci are shown. Genotyping of ancient mummy material as well as archaeologist/excavator and most relevant involved scientists (named “scientific staff 1, 6, 8”) is shown, performed via the AmpF/STR[®] SEfiler[™] PCR amplification kit. GenTyper[™] 3.7 software electropherograms showing an except of the AmpF/STR[®] SEfiler[™] PCR amplification kit results for six STR loci and the amelogenin locus analyzed on an ABI PRISM 3130 XL Genetic Analyzer.

In these two autonomous DNA profiling approaches, external contamination could explicitly be excluded. As a result, we were able to widely exclude contamination and cross-contamination of the ancient bone samples. Despite we did not obtain full allelic profiles from mummy sample material, the most important information obtained by those typing

5. Applications of the Lab-on-a-chip System in Forensic Sciences

experiments was that no cross-contamination was detectable at all. As shown by these results, typing of all people who have been in contact with mummy material worked quite fine and gave reliable results. Every DNA typing profile was individual and every marker peak combination was unique among all tested scientific staff and mummy samples (**figure 46** and **figure 47**). As no peak combination of present material could clearly be detected in mummy typing profiles (**table 9**), contamination of ancient mummy samples by recent DNA of scientists, archaeologist, technical assistance staff and laboratory members could be eliminated successfully. Typing results received from mummy material clearly showed that cross-contamination from people involved in experiments did not occur and thus could widely be excluded.

Table 9. DNA profiling. Results of typing DNA of mummy material compared to scientific staff's genomic material. Characteristic fragment sizes of amplified STR markers are shown.

	DNA profiling using STR markers			DNA profiling of several STR fragments using the AmpF/STR® SEfiler™ PCR amplification kit:						
	D7S1824	D9S302	D10S2325	D3S1358	vWA	D16S539	D2S1338	A	D8S1179	SE33
Scientific staff 1	116/148	180/188	258/314	17/-	16/17	11/-	19/25	X	14/15	29.2/32.2
Scientific staff 2	126/131	188/200	238/254	-						
Scientific staff 3	126/136	168/172	263/267	-						
Scientific staff 4	116/131	171/176	262/266	-						
Scientific staff 5	131/136	163/200	273/281	-						
Scientific staff 6	142/153	167/188	262/-	16/18	17/18	9/11	21/24	XY	12/-	18/28.2
Scientific staff 7	121/148	167/175	297/305	-						
Scientific staff 8	131/136	167/188	267/271	14/17	17/18	9/12	17/18	X	13/14	26.2/28.2
Mummy1	-/-	-/179	270/-	-/-	15/18	12/-	-/-	X	-/-	-/-
Mummy2	-/164	180/-	270/-	-/-	16/-	-/-	-/-	X	-/-	-/-
Mummy3	142/-	-/-	-/313	17/-	-/-	-/-	-/-	XY	-/-	-/-
Mummy4	-/-	-/198	270/-	-/-	18/-	-/-	-/-	XY	-/-	-/-

To enhance our analysis sensitivity, all aDNA PCR analyses were performed by virtual reaction chamber low-volume PCR, using 1 µl total reaction volume. One can easily imagine that there is a much higher impact probability between reactants and DNA template enclosed in small volume assays (1 µl) than in macroscopic samples like e.g. in 25 µl standard reaction volumes. Using this low-volume PCR method further enabled us to significantly reduce the starting amounts of extracted ancient DNA sample material needed for PCR reactions. This is an important reason for using virtual reaction chamber lab-on-a-chip systems dealing with reaction volumes in the micro- and nanoscopic range. As plastics were identified as potential sources of bioactive environmental contaminants, it will be an advising step to depart from plastic PCR-tubes to analysis devices fabricated of modified glass substrates. Moreover, it was also reported that processing agents from laboratory plastic ware could be leaking into biological media and solvents, particularly during storage (McDonald GR *et al.*, 2008). Due

to these criteria, PCR-tubes, even when declared as “sterile”, were assumed to contain leaching agents and facilitate contamination of PCR reactions when heated. However, as reported several times, working with aDNA originating and extracted from soil buried bones and teeth is by itself associated with problems like low DNA quantity, high DNA degradation, the presence of PCR inhibitors and most importantly DNA contamination (Primorac D *et al.*, 1996; Alonso A *et al.*, 2001).

Extraneous contamination can arise from adjacent treatments such as the handling of the remains by excavators and laboratory staff, airborne contaminants and contaminants present within laboratory reagents or on consumable items (Tuross N, 1994). Soil type and microbial community characteristics can adversely affect DNA recovery (Zhou J *et al.*, 1996). The total DNA extraction from soil entails co-extraction of humic substances, mainly humic acid, as well as DNA originating from external organisms like bacteria and fungi (Tsai YL and Olson BH, 1992; Tebbe CC and Vahjen W, 1993; Kreader CA, 1996; Zhou J *et al.*, 1996). These interferences can provide false-negative results in case of PCR inhibition (Zhou J *et al.*, 1996; Zipper H *et al.*, 2003) or false-positive ones (like non-specific products) in case of contamination, greatly reducing the information, which can be attained.

The expansive variety of DNA extraction techniques being employed (as reported by Anderung C *et al.* (2008) and Rohland N and Hofreiter M (2007)), highlights that all of these procedures are affected by the problems and limitations concerning DNA quality, quantity and co-extracted PCR inhibitors as mentioned above. As an effort to minimize these interfering troubles as efficiently as possible, in the present study the surface of bone tissue sample fragments was carefully decontaminated. First by chemical cleaning with DNA-degrading sodium hypochlorite, which was followed by a mechanical removal of the outer layers of the bone fragments before sample processing procedures. However, post mortem contaminations can hardly be removed completely as reported by Gilbert MTP *et al.* (2005 and 2006). Nevertheless, there seems to be a significant correlation between the sector of extraction, outer versus inner sectors of bones, and the amount of DNA present in resulting samples (Kaiser C *et al.*, 2008). The outer sectors, adjacent to the soil, were shown to have higher DNA concentrations than the inner ones, due to the presence of bacteria and fungi DNA. Furthermore, it was shown that the localization within the bone piece influences its degree of degradation. This is the result of varying degrees of protection against destructive environmental influences like temperature, humidity, pH and the geochemical properties of the soil including presence of microorganisms, UV irradiation and radioisotopes (Burger J *et al.*, 1999). Since the outer surface is significantly more influenced by the direct contact to the

environmental soil, DNA is best preserved in the inner part of bones (Kaiser C *et al.*, 2008). Based on laser microdissection of internal bone areas, the present study thus introduced a promising method for contamination-reduced bone tissue particle isolation and subsequent aDNA extraction. With respect to extracted aDNA quality, the grade of DNA degradation, and interfering destructive factors, the laser microdissection-based approach significantly excelled the traditional method. While the current DNA extraction operating procedure used whole bone tissue particles for pulverization and subsequent DNA extraction, the laser-based method concentrated on internal bone areas including osteon systems. The focus of bone particle isolation was on tissue areas containing these osteon systems in order to isolate fragments with the highest probability of preserved vascular cell material. Thus, several osteon areas were microdissected exclusively from the inner parts of the bones where surface contamination and inhibitor influences were least possible to occur. Despite higher DNA recovery and extraction rates in the classical extraction methods, the DNA quality was supposed to be considerably worse. This was most likely caused by present interfering substances and less authentic DNA provided by the pulverization method. For the higher DNA amount was little informative about the source of DNA and provided probably a mixture of desired mummy DNA and DNA of bacterial and fungal origin. In contrast, the advantages of the laser microdissection-based technique included a) minimization of contamination during handling of specimens, b) sample extraction exclusively from internal bone parts with a minimization of degradation effects and co-extraction of inhibiting substances and c) a reduction in the amount of starting material down to single osteon islets allowing maximum preservation of ancient material.

X- and Y-chromosomal amelogenin fragments of 106/112 bp in length as well as a 297 bp-sized fragment of the human multicopy gene β -actin were amplified by LV-PCR. In amplification reactions, particular attention was paid to the quality of extracted DNA, including possible effects of degradation or PCR inhibitors. In microdissection-based mummy samples, the amplification of amelogenin gene as well as β -actin gene fragments resulted in reproducible, constantly positive PCR products using only about 60 pg of DNA starting material (**figure 43**). When amplified on LOC chips instead of a multi LV-PCR microdevice, mummy DNA could successfully be detected as well in a reliable manner (**figure 44**). This successful amplification clearly qualified the complete lab-on-a-chip system for a reliable applicability on highly sensitive and „difficult-to-analyze“ sample material like e.g. necessary in the pathological research area. In contrast, PCR results of samples based on pulverized bone tissue showed just 50% success in amplifying amelogenin gene fragments (mummy2

and mummy4; **figure 43 A and B**) and no reliable positive amplification products for β -actin fragments using 100 pg of DNA starting material. These lower yields of PCR products may be due to poorer DNA quality, consistency or state because of degradation effects. Taking into account that also primer dimerization occurred during PCR, the failing amplification may more likely be attributed to DNA degradation than to present inhibiting substances. Moreover, here, especially the inconsistent amplification of 297 bp β -actin fragments was in agreement with a general amplification limit discussed for aDNA. Propagating amplification fragments longer than 200 bp are very unlikely due to degradation processes (Pääbo S, 1989). Here, amplification success correlated negatively with the length of the amplicon. This was supposed to be the result of contaminating outer bone layers, where extensive DNA degradation could have occurred. However, this larger β -actin fragment could be amplified reliably in microdissection-based samples, where the analyzed bone segments originated from the more preserved inner part of bone particles.

Furthermore, sequencing of amelogenin and β -actin PCR products was performed on one male microdissection-based mummy sample (mummy4). This enabled us to confirm authentic PCR products and eliminate possible false positives, which may indeed show the right lengths of the wanted amelogenin and β -actin fragments while presenting a different sequence of DNA base pairs. Analysis of the sequencing data for both the 106/112 bp X- and Y-chromosomal amelogenin fragments and the 297 bp β -actin fragment definitively identified them as human amelogenin and β -actin sequences once aligned to gene sequences from the human genomic database of NCBI (**figure 45**). Furthermore, sequencing results were also important to invalidate the possibly occurring phenomenon of jumping PCR, induced by damaged template DNA and resulting in the production of a chimeric sequence, as first reported by Pääbo S *et al.* (1990). Thus, via sequencing, the authenticity of the amplified DNA could be confirmed. Both, the successful amplification of a fragment significantly longer than 200 bp and the successful sequence alignment results of β -actin gene fragments highlighted the advantage of laser microdissection for ancient material extraction.

Overall, we always obtained higher yields of PCR products by using laser microdissected samples than by amplifying samples being extracted via the classical method. This may be attributed to a better DNA quality present in microdissected samples due to less exposure to degradation effects. These results implicated that isolation of tiny target tissue material by laser microdissection combined with standard kit DNA extraction methods was sufficient for aDNA extraction and successful amplification. Combined with low-volume PCR using planar

microdevices, our method enabled the amplification of minute amounts of laser-microdissected material in extremely small reaction volumes.

Results of analyzing ancient bone tissue originating from Egyptian mummy material strongly highlighted the combination of laser microdissection and low-volume PCR as a promising new technique in ancient DNA analysis. The combination of several modules of the lab-on-a-chip like e.g. laser microdissection, SPATS transfer and LV-PCR provided a wealthy platform for highly sensitive genetic analysis with minimum risk of contamination. Ancient mummy DNA could successfully be amplified in a highly sensitive and reliable analysis, while the risk of contamination could dramatically be minimized due to the application of novel techniques and technologies. Macroscopically, contamination effects could be eliminated via intelligent nested sample preparation followed by highly precise laser microdissection-based material isolation. The benefit of the laser microdissection-based extraction method was the chance of exact sample extraction, directly from the more preserved inner parts where authentic ancient DNA was most possible to occur, while circumventing co-extraction of PCR inhibitors or external bacterial or fungal DNA, interfering strongly with PCR analyses. Microscopically, contamination events could be eliminated through the utilization of highly sensitive virtual reaction chamber low-volume PCR on chemically treated PCR microdevices. The presented nanotechnological approach provided an adequate tool for reliable and highly sensitive DNA analysis, ensuring the optimum use of limited evidence material. This approach could adapt the preparative and extraction procedures to the low amount of preserved ancient DNA, thus offering the possibility to increase the amount of extracted, less degraded and less contaminated, authentic genetic material and decreasing the effect of destructive factors. In this approach, for the first time isolation, amplification and detection of ancient DNA in smallest sample amounts circumventing pulverization could be demonstrated. This new tool for aDNA analysis, which overcame contamination problems, DNA degradation and the negative effects of PCR inhibitors while reducing the amount of starting target material in the picogram range, was presented in a paper ("PCR analysis of minimum target amount of ancient DNA", Woide D *et al.*, 2010). The reported clash of new fashion technologies with ancient sample material is a fascinating starting point for revolutionizing and optimizing archaeological research on ancient sample material while employing high fashion lab-on-a-chip technology.

5.4 Critical assessment of the analytical power of the lab-on-a-chip

Diagnostic testing especially for the forensic research area has emerged a lot of analysis methods due to various forensic relevant problems. Of particular importance are diagnostic tests for genetic diseases, microbial and viral infections, forensic analyses like blood typing or blood banking, as well as forensic human DNA identification. Typical target materials in forensic and pathological analyses are soft materials like e.g. pieces of dermal tissue, blood spots or other dried body fluids like saliva or sperm, but also hard materials such as bones and teeth. Preparing these samples for laboratory analysis is labor-intensive, time- and cost-consuming, particularly when handling hundreds of samples per day during routine laboratory work. Additionally, sample material is a valuable property and the amount of target sample material used for analysis needs to be reduced to a minimum to be utilized as economically as possible. The lowest amount, which is aimed to be used for analysis, is surely the DNA content of just one single cell, comprising about 7 pg target DNA material. Due to the scarcity of material available and possible material contamination, the most important thing in DNA analysis is a sensitive, reliable and unflinching performance, while excluding risks of contamination during sample handling.

Based on the needs to be able to reproducibly and reliably handle, process and analyze microscopic amounts of sample material and due to the tendency of standard laboratory analysis to become “smaller”, “faster”, “cheaper” and “more sensitive”, μ TAS are becoming more and more relevant to be the right platform serving these purposes and revolutionizing human genetic analysis. After a longer developmental period, nowadays, micro total analysis systems are on their way to reach a state of applicability. Miniaturization of analysis systems yields an enormous saving in time and cost in regard to parallelization, automatization, waste of test tubes and biochemical reagents. Automation can render analysis more economic and reliable, and a smaller reaction volume favors low material consumption and implies an enhanced analysis sensitivity and homogeneity of detection. Furthermore, designed as disposables, microdevices can circumvent possible sample-to-sample cross-contaminations.

However, the majority of developed lab-on-a-chip microdevices is fixed to just one specific application and can accept only one kind of sample material, thus lacking flexibility. Lab-on-a-chips, combining all sample processing steps on one single device, are technically most challenging. And if realized, up to now they consist of complex 3-dimensionally architected integrated systems, fixed to just one particular biological problem and additionally struggling with too expensive fabrication and sales costs to be used as disposables. However, an integrated system holds the distinct advantage of minimal manual sample handling, thus

decreasing the risk of possible cross-contaminations originating from laboratory sources. Due to complexity, lab-on-a-chip systems with “sample-in-answer-out” capabilities are up to now sparsely reported in literature (Burns MA *et al.*, 1998; Roper MG *et al.*, 2005; Easley CJ *et al.*, 2006 (b); Lien KY *et al.*, 2007). And with a few exceptions (Chen L *et al.*, 2007; Zhang CS *et al.*, 2006; Panaro NJ *et al.*, 2005; Pipper J *et al.*, 2007) most of the reported miniaturized devices for nucleic acid amplification are integrated stand-alone systems replacing only the role of a conventional PCR thermocycler. Additionally, they are based on template DNA, that has already been processed off-chip by using established bench-scale procedures.

As especially the forensic research area is in the need of practical, time, costs, labor and material saving micro total analysis systems, here, a unique modular lab-on-a-chip system with “open” applicability was introduced. Due to its modular character, the lab-on-a-chip provided a broad range of sample processing applications performed on separate devices, including sample material isolation, DNA amplification as well as product detection. The 2-dimensional architecture of the presented lab-on-a-chip system’s operating chip platform gets the user away from fixed applications being performed. Due to its open accessible chip surface, it was flexible in application and capable of accepting a broad range of biological input materials. Those were liquids ones, such as purified DNA material and also whole blood, as well as solid ones like e.g. crude sample material like fixed microdissected tissue particles. However, using hard sample material like bone tissue pieces still needed preprocessing steps performed off-chip, as those procedures for DNA extraction were highly specific and could not be done on the microscale yet. Anyway, this μ TAS provides a promising platform of enabling nanotechnologies for the forensic field of research due to several reasons. 1) Due to the modular character, the whole system or at least parts of it can easily be integrated into laboratory routine. 2) Benefitting from a planar “open accessible” chip design, it can accept a wide variety of sample materials, which was never realized and reported in literature before. Loading the sample onto the chip can either happen via laser-microdissection and SPATS transfer for solid sample materials or via the automatic dispensing device BioSpot[®] for liquid sample materials. 3) As the analysis chip is separate from all modular equipment providing the technical support, it can simply be used as a disposable. The CytoCycler chip-holder itself houses all electronic devices for temperature support and SAW actuation. LOC chips can easily be replaced for analysis, eliminating cross-contamination between reactions in subsequently performed operations. 4) PCR product detection can be performed by a variety of individually selectable detection methods. Open access is provided to sample material and PCR droplets at any time due to the open planar

surface design of the amplification unit. Thus, detection can be conducted either on-chip like e.g. via real-time PCR or array technologies, or even off-chip in electrophoresis-based techniques. 5) It is predestined to work free of contamination due to a) sample loading based on laser microdissection and SPATS transfer and b) performed low-volume PCR. Sample isolation via laser microdissection and contamination-free particle transfer via the low-pressure operated SPATS device is an important tool for validating the presented lab-on-a-chip system for being capable of highly sensitive analysis. Several contamination-free applications have been reported, like e.g. isolation and transfer of single cells (Woide D *et al.*, 2009; Mayer V *et al.*, 2009) as well as soft tissue material and ancient bone material (Woide D *et al.*, 2010). Blank and negative controls, of e.g. co-microdissected and transferred PEN carrier-membrane, also validated a contamination-free transfer process. Due to low-volume PCR, the lab-on-a-chip is operating small-scale reaction volumes, which were profitable as increasing analysis sensitivity while reducing the amount of input sample material needed. In utilizing virtual reaction chamber PCR, for reliable analyses only 25 pg of DNA input material were needed, and reproducible PCR performances were obtained using just smallest microdissected tissue particles or 1% of whole blood. In general, such planar virtual reaction chamber-based microdevices bear the highest chance for being integrated into laboratory routine. As droplet-based virtual reaction chamber PCR needs just an easy scale-down of biochemical protocols applied to benchscale systems (Mukhopadhyay R, 2006), this flexibility cannot be matched by chamber- or flow-through-based architectures (Daw R and Finkelstein J, 2006). And scaling reaction volumes down is especially important for cost savings when pricy PCR amplification kits are used. 6) Each module can be operated independently and integrated into laboratory routine apart from the other units, but most importantly, all modules can be combined together in a whole workflow-process, providing the basis for complete automation. Thus, the presented lab-on-a-chip comes very close to the scientific demands for a micro total analysis system, as being applicable for many kinds of sample materials, utilizing smallest sample amounts, providing highly sensitive PCR analysis and detection, while excluding any risk of external contamination during sample handling.

All in all, the presented lab-on-a-chip presents a step forward towards a universal micro total analysis system. It fulfills key features like cost savings and enhanced analysis sensitivity in applying low reaction volumes and disposable microchips. Major drawbacks are surely the bulky devices needed for operating chip performances as well as no highspeed analysis times. Certainly, due to low-volume PCR reaction times were faster than those of conventional thermocyclers, but not comparable to heating methods other than a Peltier element, like e.g.

via IR heating. Additionally, reaction volumes used were still in the microliter range and not in the nanoliter range as realized in several other devices, reaching from 280 nl (Easley CJ *et al.*, 2006 (a)), down to 200 nl (Lagally ET *et al.*, 2004; Guttenberg Z *et al.*, 2005), 100 nl (Neuzil P *et al.*, 2006 (b)), 40 nl (Matsubara Y *et al.*, 2004; Matsubara Y *et al.*, 2005), 33 nl (Morrison T *et al.*, 2006), 29 nl (Koh CG *et al.*, 2003), 3 nl (Liu J *et al.*, 2003), 0.45 nl (Marcus JS *et al.*, 2006) and astonishing 85 pl (Nagai H *et al.*, 2001). However, up to now, there is no definitive correlation between PCR volume and e.g. PCR cycling time. Only chip architecture and the mode of heating can transform the advantages of small-volume reaction systems into fast temperature transition and thus rapid analysis times and more efficient PCR amplifications. Thus, the detected 5 sec minimal cycling time per PCR cycle step provides a good basis for a fast analysis. However, the presented lab-on-a-chip system was not developed for the purposes, to be the fastest or the smallest one, but rather to provide highest flexibility in performed analyses and applied sample materials instead. Though, the biggest drawback can be attributed to the single reaction center presented on the chip surface. The design of the chip surface must be updated to provide several reaction centers. This would render the analysis chip to be capable of performing several reactions in parallel, as most importantly negative and positive controls are on demand to be included on-chip.

6. Conclusion and Outlook

Due to its universal applicability, a modular lab-on-a-chip like the presented one could definitely provide solutions and gain value in the scientific fields dealing with highly sensitive analysis, like e.g. in cytogenetics, forensics, legal medicine and pathology. Especially the way of contamination-free sample isolation via laser microdissection combined with highly sensitive LV-PCR amplification using smallest amounts of sample material provide tools of high-resolution analysis for scientific relevant questions, like e.g application on the single cell level e.g. in cancer diagnostics. This system is worldwide unique in its modular design, there are no competitive devices on the market combining these techniques. As up to now most developed microdevice chips are dependent on the capability of accepting either prepurified or completely liquid sample materials, the presented convergence of high fashion lab-on-a-chip technology with „difficult-to-handle“-scientific relevant sample material represented an important step towards sophisticated micro total analysis systems' application.

However, as the developmental focus is especially on automation, working speed and high mobility of the devices for providing on-site analysis, some improvements would support an even better performance. Up to now, there are integrated systems reported, providing even faster analysis times, possibilities for parallel processing as well as smallest chip architectures in total being capable of being used as fast on-site portable analytic system. However, no modular system has been reported up to now providing any of these features. In the presented modular system, PCR performance is fixed to the heating rate capacity of the Peltier element and the architecture suffers from bulky devices like the microscope and the BioSpot[®] while all modules require a huge power supply. Even if the miniaturization of bulky devices remains difficult, at least heating rates could be optimized via an even more sophisticated design of the heating device. Additionally, a definite improvement of the presented system would be an upgrade of chip architecture to provide multiple reaction centers for performing several reactions at a time. This would allow parallelization, high-throughput and automation as via automatization the reproducibility would also be enhanced to a big amount. As the system is totally software controlled, the first step towards automation is done building a base for further improvement. However, besides some drawbacks, the scientific progress described in this work presents a big step forward towards the generation of an ultimate micro total analysis device.

7. References

- Adessi C, Matton G, Ayala G, Turcatti G, Mermod JJ, Mayer P and Kawashima E. 2000. Solid phase DNA amplification: characterisation of primer attachment and amplification mechanisms. *Nucleic Acids Res.* 28(20), e87.
- Alonso A, Andelinovic S, Martin P, Sutlovic D, Erceq I, Huffine E, de Simon LF, Albarran C, Definis-Gojanovic M, Fernandez-Rodriguez A, Garcia P, Drmic I, Rezic B, Kuret S, Sancho M and Primorac D. 2001. DNA typing from skeletal remains: evaluation of multiplex and megaplex STR systems on DNA isolated from bone and teeth samples. *Croat. Med. J.* 42(3), 260-266.
- Al-Soud WA, Lantz PG, Bäckman A, Olcen P and Radström P. 1998. A sample preparation method which facilitates detection of bacteria in blood cultures by the polymerase chain reaction. *J. Microbiol. Methods* 32, 217-224.
- Al-Soud WA and Radström P. 1998. Capacity of nine thermostable DNA polymerases to mediate DNA amplification in the presence of PCR-inhibiting samples. *Appl. Environ. Microbiol.* 64, 3748-3753.
- Al-Soud WA and Radström P. 2000. Effects of amplification facilitators on diagnostic PCR in the presence of blood, feces, and meat. *J. Clin. Microbiol.* 38, 4463-4470.
- Anderung C, Persson P, Bouwman A, Elburg R and Götherström A. 2008. Fishing for ancient DNA. *Forensic Sci. Int. Genet.* 2(2), 104-107.
- Ashkin A, Dziedzic JM and Yamane T. 1987. Optical trapping and manipulation of single cells using infrared-laser beams. *Nature* 330, 769-771.
- Ashkin A and Dziedzic JM. 1987. Optical trapping and manipulation of viruses and bacteria. *Science* 235, 1517-1520.
- Auroux PA, Iossifidis D, Reyes DR and Manz A. 2002. Micro total analysis systems. 2. Analytical standard operations and applications. *Anal. Chem.* 74, 2637-2652.
- Auroux PA, Koc Y, deMello A, Manz A and Day PJR. 2004. Miniaturised nucleic acid analysis. *Lab Chip* 4, 534-546.
- Bauer M, Thalheimer A and Patzelt D. 2002. Paternity testing after pregnancy termination using microdissection of chorionic villi. *Int. J. Legal Med.* 116, 39-42.
- Bessis M, Gires F, Mayer G and Nomarski G. 1962. Irradiation des organites cellulaires a l'aide d'un laser a rubis (Irradiation of cellular organisms with a ruby laser). *C. R. Acad. Sci.* 255, 1010-1012.
- Bing DH, Boles C, Rehman FN, Audeh M, Belmarsh M, Kelley B and Adams CP. 1996. Bridge amplification: a solid phase PCR system for the amplification and detection of allelic differences in single copy genes. In *Genetic Identity Conference Proceedings, Seventh International Symposium on Human Identification.*

7. References

- Brody JP, Yager P, Goldstein RE and Austin RH. 1996. Biotechnology at low Reynolds numbers. *Biophys. J.* 71(6), 3430-3441.
- Brzoska JB, Azouz IB and Rondelez F. 1994. Silanization of solid substrates: a step toward reproducibility. *Langmuir* 10, 4367-4373.
- Burckhardt J. 1994. Amplification of DNA from whole blood. *Genome Res.* 3, 239-243.
- Burger J, Hummel S, Herrmann B and Henke W. 1999. DNA preservation: A microsatellite-DNA study on ancient skeletal remains. *Electrophoresis* 20(8), 1722-1728.
- Burns MA, Johnson BN, Brahmasandra SN, Handique K, Webster JR, Krishnan M, Sammarco TS, Man PM, Jones D, Heldsinger D, Mastrangelo CH and Burke DT. 1998. An integrated nanoliter DNA analysis device. *Science* 282(5388): 484-487.
- Chen ZY, Qian SZ, Abrams WR, Malamud D and Bau HH. 2004. Thermosiphon-based PCR reactor: experiment and modeling. *Anal. Chem.* 76, 3707-3715.
- Chen L, Manz A and Day PJR. 2007. Total nucleic acid analysis integrated on microfluidic devices. *Lab Chip* 7, 1413-1423.
- Chiou J, Matsudaira P, Sonin A and Ehrlich D. 2001. A closed-cycle capillary polymerase chain reaction machine. *Anal. Chem.* 73, 2018-2021.
- Chung YC, Jan MS, Lin YC, Lin JH, Cheng WC and Fan CY. 2004. Microfluidic chip for high efficiency DNA extraction. *Lab Chip* 4(2), 141-147.
- Clark JM. 1988. Novel non-templated nucleotide addition reactions catalyzed by procaryotic and eucaryotic DNA polymerases. *Nucl. Acids Res.* 16 (20), 9677-9686.
- Craighead H. 2006. Future lab-on-a-chip technologies for interrogating individual molecules. *Nature* 442, 387-393.
- Dasgupta PK, Eom IY, Morris KJ and Li JZ. 2003. Light emitting diode-based detectors: absorbance, fluorescence and spectroelectro-chemical measurements in a planar flow-through cell. *Anal. Chim. Acta* 500, 337-364.
- Daw R and Finkelstein J. 2006. Lab on a chip (Nature Insight). *Nature* 442, 367-412.
- Di Martino D, Giuffrè G, Staiti N, Simone A, Le Donne M and Saravo L. 2004. Single sperm cell isolation by laser microdissection. *Forensic Sci. Int.* 146, 151-153. (a)
- Di Martino D, Giuffrè G, Staiti N, Simone A, Todaro P and Saravo L. 2004. Laser microdissection and DNA typing of cells from single hair follicles. *Forensic Sci. Int.* 146, 155-157. (b)
- Dittrich PS, Tachikawa K and Manz A. 2006. Micro total analysis systems. Latest advancements and trends. *Anal. Chem.* 78, 3887-3907.

7. References

Easley CJ, Karlinsey JM and Landers JP. 2006. On-chip pressure injection for integration of infrared-mediated DNA amplification with electrophoretic separation. *Lab Chip* 6, 601-610. (a)

Easley CJ, Karlinsey JM, Bienvenue JM, Legendre LA, Roper MG, Feldman SH, Hughes MA, Hewlett EL, Merkel TJ, Ferrance JP and Landers JP. 2006. A fully integrated microfluidic genetic analysis system with sample-in-answer-out capability. *Proc. Natl. Acad. Sci. U. S. A.* 103, 19272-19277. (b)

El-Ali J, Sorger PK and Jensen KF. 2006. Cells on chips. *Nature* 442, 403-411.

Elliott K, Hill DS, Lambert C, Burroughes TR and Gill P. 2003. Use of laser microdissection greatly improves the recovery of DNA from sperm on microscope slides. *Forensic Sci. Int.* 137(1), 28-36.

Faerman M, Filon D, Kahila G, Greenblatt CL, Smith P and Oppenheim A. 1995. Sex identification of archaeological human remains based on amplification of the X and Y amelogenin alleles. *Gene* 167(1-2), 327-332.

Faerman M, Kahila G, Smith P, Greenblatt C, Stager L, Filon D and Oppenheim A. 1997. DNA analysis reveals the sex of infanticide victims. *Nature* 385, 212-213.

Fedurco M, Romieu A, Williams S, Lawrence I and Turcatti G. 2006. BTA, a novel reagent for DNA attachment on glass and efficient generation of solid-phase amplified DNA colonies. *Nucleic Acids Res.* 34(3), e22.

Fixman M and Freire JJ. 1997. Theory of DNA melting curves. *Biopolymers* 16(12), 2693-2704.

Gaines ML, Wojtkiewicz PW, Valentine JA and Brown CL. 2002. Reduced volume PCR amplification reactions using the AmpF/STR[®] Profiler Plus[™] Kit. *J. Forensic Sci.* 47(6), 1224-1237.

Ganong WF. 2003. Review of medical physiology. 21st Edition Publisher, McGraw-Hill Professional, Lange Medical Books, p. 518. ISBN 0071217657.

Gascoyne PRC, Vykoukal JV, Schwartz JA, Anderson TJ, Vykoukal DM, Current KW, McConaghy C, Becker FF and Andrews C. 2004. Dielectrophoresis-based programmable fluidic processors. *Lab Chip* 4(4), 299-309.

Gilbert MTP, Rudbeck L, Willerslev E, Hansen AJ, Smith C, Penkman KEH, Prangenberg K, Nielsen-Marsh CM, Jans ME, Arthur P, Lynnerup N, Turner-Walker G, Biddle M, Kjolbye-Biddle B and Collins MJ. 2005. Biochemical and physical correlates of DNA contamination in archaeological human bones and teeth excavated at Matera, Italy. *J. Archeol. Sci.* 32, 785-793.

Gilbert MTP, Hansen AJ, Willerslev E, Turner-Walker G and Collins M. 2006. Insights into the processes behind the contamination of degraded human teeth and bone samples with exogenous sources of DNA. *Int. J. Osteoarchaeol.* 16(2), 156-164.

7. References

- Giordano BC, Ferrance J, Swedberg S, Hühmer AFR and Landers JP. 2001. Polymerase chain reaction in polymeric microchips: DNA amplification in less than 240 seconds. *Anal. Biochem.* 291, 124-132. (a)
- Giordano BC, Copeland ER and Landers JP. 2001. Towards dynamic coating of glass microchip chambers for amplifying DNA via the polymerase chain reaction. *Electrophoresis* 22, 334-340. (b)
- Goodyear PD, MacLaughlin-Black S and Mason IJ. 1994. A reliable method for the removal of co-purifying PCR inhibitors from ancient DNA. *BioTechniques* 16(2), 232-235.
- Greulich KO and Leitz G. 1994. Light as microsensor and micromanipulator: laser microbeams and optical tweezers. *Exp. Techn. Phys.* 40(1), 1-14.
- Guttenberg Z, Rathgeber A, Keller S, Rädler JO, Wixforth A, Kostur M, Schindler M and Talkner P. 2004. Flow profiling of a surface-acoustic-wave nanopump. *Phys. Rev. E* 70, 056311.
- Guttenberg Z, Müller H, Habermüller H, Geisbauer A, Pipper J, Felbel J, Kielpinski M, Scriba J and Wixforth A. 2005. Planar chip device for PCR and hybridization with surface acoustic wave pump. *Lab Chip* 5(3), 308-317.
- Hashimoto M, Chen PC, Mitchell MW, Nikitopoulos DE, Soper SA and Murphy MC. 2004. Rapid PCR in a continuous flow device. *Lab Chip* 4(6), 638-645.
- Hedman J, Nordgaard A, Rasmusson B, Ansell R and Radström P. 2009. Improved forensic DNA analysis through the use of alternative DNA polymerases and statistical modeling of DNA profiles. *BioTechniques* 47(5), 951-958.
- Horsman KM, Bienvenue JM, Blasier KR and Landers JP. 2007. Forensic DNA analysis on microfluidic devices: a review. *J. Forensic Sci.* 52(4), 784-799.
- Huang Y, Mather EL, Bell JL and Madou M. 2002. MEMS-based sample preparation for molecular diagnostics. *Anal. Bioanal. Chem.* 372(1), 49-65.
- Hühmer AFR and Landers JP. 2000. Noncontact infrared-mediated thermocycling for effective polymerase chain reaction amplification of DNA in nanoliter volumes. *Anal. Chem.* 72(21), 5507-5512.
- Hummel S and Herrmann B. 1991. Y-chromosome-specific DNA amplified in ancient human bone. *Naturwissenschaften* 78(6), 266-267.
- Ibrahim MS, Lofts RS, Jahrling PB, Henchal EA, Weedn VW, Northrup MA and Belgrader P. 1998. Real-time microchip PCR for detecting single base differences in viral and human DNA. *Anal. Chem.* 70(9), 2013-2017.
- Janasek D, Franzke J and Manz A. 2006. Scaling and the design of miniaturized chemical-analysis systems. *Nature* 442, 374-380.
- Jin LJ, Ferrance J and Landers JP. 2001. Miniaturized electrophoresis: an evolving role in laboratory medicine. *BioTechniques* 31(6), 1332-1335, 1338-1340, 1342, passim.

7. References

- Kaiser C, Bachmeier B, Conrad C, Nerlich A, Bratzke H, Eisenmenger W and Peschel O. 2008. Molecular study of time dependent changes in DNA stability in soil buried skeletal residues. *Forensic Sci. Int.* 177(1), 32-36.
- Katcher HL and Schwartz I. 1994. A distinctive property of Tth DNA polymerase: enzymatic amplification in the presence of phenol. *BioTechniques* 16, 84-92.
- Kermekchiev MB, Kirilova LI, Vail EE and Barnes WM. 2009. Mutants of Taq DNA Polymerase resistant to PCR inhibitors allow DNA amplification from whole blood and crude soil samples. *Nucleic Acids Res.* 37(5), e40.
- Kirschner J and Plaschke-Schluetter A. 2007. Advancing forensics with precise target excision: the CellCut Plus laser microdissection instrument. *Nat. Methods* 4.
- Kloosterman AD and Kersbergen P. 2003. Efficacy and limits of genotyping low copy number (LCN) DNA samples by multiplex PCR of STR loci. *J. Soc. Biol.* 197(4), 351-359.
- Köhler JM, Dillner U, Mokansky A, Poser S and Schulz T. 1998. Micro channel reactors for fast thermocycling. In 2nd International Conference on Microreaction Technology, New Orleans, LA, USA, Springer, 241-247.
- Koh CG, Tan W, Zhao MQ, Ricco AJ and Fan ZH. 2003. Integrating polymerase chain reaction, valving, and electrophoresis in a plastic device for bacterial detection. *Anal. Chem.* 75(17), 4591-4598.
- Kopp MU, deMello AJ and Manz A. 1998. Chemical amplification: continuous-flow PCR on a chip. *Science* 280(5366), 1046-1048.
- Kreader CA. 1996. Relief of amplification inhibition in PCR with bovine serum albumin or T4 gene 32 protein. *Appl. Environ. Microbiol.* 62(3), 1102-1106.
- Kricka LJ and Wilding P. 2003. Microchip PCR. *Anal. Bioanal. Chem.* 377(5), 820-825.
- Krishnan M, Burke DT and Burns MA. 2004. Polymerase chain reaction in high surface-to-volume ratio SiO₂ microstructures. *Anal. Chem.* 76(22), 6588-6593.
- Lagally ET, Simpson PC and Mathies RA. 2000. Monolithic integrated microfluidic DNA amplification and capillary electrophoresis analysis system. *Sens. Actuators B* 63, 138-146.
- Lagally ET, Medintz I and Mathies RA. 2001. Single molecule DNA amplification and analysis in an integrated microfluidic device. *Anal. Chem.* 73, 565-570.
- Lagally ET, Emrich CA and Mathies RA. 2001. Fully integrated PCR-capillary electrophoresis microsystem for DNA analysis. *Lab Chip* 1(2), 102-107.
- Lagally ET, Scherer JR, Blazej RG, Toriello NM, Diep BA, Ramchandani M, Sensabaugh GF, Riley LW and Mathies RA. 2004. Integrated portable genetic analysis microsystem for pathogen/infectious disease detection. *Anal. Chem.* 76(11), 3162-3170.

7. References

- Lau EC, Mohandas TK, Shapiro LJ, Slavkin HC and Snead ML. 1989. Human and mouse amelogenin gene loci are on the sex chromosome. *Genomics* 4, 162-168.
- Leclair B, Sgueglia JB, Wojtowicz PC, Juston AC, Frégeau CJ and Fourney RM. 2003. STR DNA typing: increased sensitivity and efficient sample consumption using reduced PCR reaction volumes. *J. Forensic Sci.* 48(5), 1001-1013.
- Lee DS, Park SH, Yang HS, Chung KH, Yoon TH, Kim SJ, Kim K and Kim YT. 2004. Bulk-micromachined submicroliter-volume PCR chip with very rapid thermal response and low power consumption. *Lab Chip* 4(4), 401-407.
- Lehmann U, Vandevyver C, Parashar VK and Gijs MA. 2006. Droplet-based DNA purification in a magnetic lab-on-a-chip. *Angew. Chem. Int. Ed. Engl.* 45, 3062-3067.
- Lien KY, Lee WC, Lei HY and Lee GB. 2007. Integrated reverse transcription polymerase chain reaction systems for virus detection. *Biosens. Bioelectron.* 22, 1739-1748.
- Lindemann T, Streule W, Birkle G, Zengerle R and Koltay P. 2004. PipeJet™ – A simple disposable dispenser for the nanoliter range. *Proc. ACTUATOR 2004*, 224-227.
- Liu J, Enzelberger M and Quake SR. 2002. A nanoliter rotary device for polymerase chain reaction. *Electrophoresis* 23, 1531-1536.
- Liu J, Hansen C and Quake SR. 2003. Solving the "world-to-chip" interface problem with a microfluidic matrix. *Anal. Chem.* 75, 4718-4723.
- Liu RH and Grodzinski P. 2003. Development of integrated microfluidic system for genetic analysis. *J. Microlithogr. Microfabr., Microsyst.* 2(4), 340-355.
- Liu RH, Yang JN, Lenigk R, Bonanno J and Grodzinski P. 2004. Self-contained, fully integrated biochip for sample preparation, polymerase chain reaction amplification, and DNA microarray detection. *Anal. Chem.* 76(7), 1824-1831.
- Liu Y, Garcia CD and Henry CS. 2003. Recent progress in the development of μ TAS for clinical analysis. *Analyst* 128(8), 1002-1008.
- Lutz-Bonengel S, Sanger T, Heinrich M, Schon U and Schmidt U. 2007. Low volume amplification and sequencing of mitochondrial DNA on a chemically structured chip. *Int. J. Legal Med.* 121, 68-73.
- Magnuson VL, Ally DS, Nylund SJ, Karanjawala ZE, Rayman JB, Knapp JI, Lowe AL, Ghosh S and Collins FC. 1996. Substrate nucleotide-determined non-templated addition of adenine by Taq DNA polymerase: implications for PCR-based genotyping and cloning. *BioTechniques* 21, 700-709.
- Mange EJ and Mange AP. 1999. *Basic Human Genetics*. 2nd ed., Sinauer Associates, Inc., Sunderland, MA, 31.
- Manz A, Graber N and Widmer HM. 1990. Miniaturized total chemical analysis systems: a novel concept for chemical sensing. *Sens. Actuators B Chem.* 1, 244-248.

7. References

- Marcus JS, Anderson WF and Quake SR. 2006. Parallel picoliter RT-PCR assays using microfluidics. *Anal. Chem.* 78, 956-958.
- Matsubara Y, Kerman K, Kobayashi M, Yamamura S, Morita Y, Takamura Y and Tamiya E. 2004. On-chip nanoliter-volume multiplex TaqMan polymerase chain reaction from a single copy based on counting fluorescence released microchambers. *Anal. Chem.* 76(21), 6434-6439.
- Matsubara Y, Kerman K, Kobayashi M, Yamamura S, Morita Y and Tamiya E. 2005. Microchamber array based DNA quantification and specific sequence detection from a single copy via PCR in nanoliter volumes. *Biosens. Bioelectron.* 20, 1482-1490.
- Mayer V, Schoen U, Holinski-Feder E, Koehler U and Thalhammer S. 2009. Single cell analysis of mutations in the APC gene. *Fetal Diagn. Ther.* 26(3), 148-156.
- McCusker J, Dawson MT, Noone D, Gannon F and Smith T. 1992. Improved method for direct PCR amplification from whole blood. *Nucleic Acids Res.* 20(24), 6747.
- McDonald GR, Hudson AL, Dunn SM, You H, Baker GB, Whittall RM, Martin JW, Jha A, Edmondson DE and Holt A. 2008. Bioactive contaminants leach from disposable laboratory plasticware. *Science* 322(5903), 917.
- Mercier B, Gaucher C, Feugeas O and Mazurier C. 1990. Direct PCR from whole blood, without DNA extraction. *Nucleic Acids Res.* 18(19), 5908.
- Mohr S, Zhang YH, Macaskill A, Day PJR, Barber RW, Goddard NJ, Emerson DR and Fielden PR. 2007. Numerical and experimental study of a droplet-based PCR chip. *Microfluid. Nanofluid.* 3, 611-621.
- Moroney RM, White RM and Howe RT. 1991. Microtransport induced by ultrasonic Lamb waves. *Appl. Phys. Lett.* 59, 774-776.
- Morrison T, Hurley J, Garcia J, Yoder K, Katz A, Roberts D, Cho J, Kanigan T, Ilyin SE, Horowitz D, Dixon JM and Brenan CJH. 2006. Nanoliter high throughput quantitative PCR. *Nucleic Acids Res.* 34(18), e123.
- Mukhopadhyay R. 2006. Diving into droplets. *Anal. Chem.* 78, 1401-1404.
- Mullis KB, Ferre F and Gibbs RA. 1994. *The polymerase chain reaction*. Birkhauser, Boston, 395-405.
- Nagai H, Murakami Y, Morita Y, Yokoyama K and Tamiya E. 2001. Development of a microchamber array for picoliter PCR. *Anal. Chem.* 73(5), 1043-1047.
- Nakano H, Matsuda K, Yohda M, Nagamune T, Endo I and Yamane T. 1994. High-speed polymerase chain reaction in constant flow. *Biosci. Biotechnol. Biochem.* 58, 349-352.
- Neuzil P, Pipper J and Hsieh TM. 2006. Disposable real-time microPCR device: lab-on-a-chip at a low cost. *Mol. BioSyst.* 2, 292-298. (a)

7. References

- Neuzil P, Zhang C, Pipper J, Oh S and Zhou L. 2006. Ultra fast miniaturized real-time PCR: 40 cycles in less than six minutes. *Nucleic Acids Res.* 34(11), e77. (b)
- Ng SY, Gunning P, Eddy R, Ponte P, Leavitt J, Shows T and Kedes L. 1985. Evolution of the functional human beta-actin gene and its multi-pseudogene family: conservation of noncoding regions and chromosomal dispersion of pseudogenes. *Mol. Cell. Biol.* 5(10), 2720-2732.
- Nickisch-Rosenegk M, Marschan X, Andresen D, Abraham A, Heise C and Bier FF. 2005. On-chip PCR amplification of very long templates using immobilized primers on glassy surfaces. *Biosens. Bioelectron.* 20, 1491-1498.
- Northrup MA, Ching MT, White RM and Watson RT. 1993. DNA amplification in a microfabricated reaction chamber. *Proceedings of the 7th International Conference on Solid-State Sensors and Actuators, Transducers '93*, 924-926.
- Northrup MA, Bennett B, Hadley D, Landre P, Lehew S, Richards J and Stratton P. 1998. A miniature analytical instrument for nucleic acids based on micromachined silicon reaction chambers. *Anal. Chem.* 70(5), 918-922.
- Novak L, Neuzil P, Pipper J, Zhang Y and Lee S. 2007. An integrated fluorescence detection system for lab-on-a-chip applications. *Lab Chip* 7, 27-29.
- Nyborg WL. 1998. Acoustic streaming. In *Nonlinear Acoustics*, edited by Hamilton MF and Blackstock DT (Academic Press, San Diego, CA, USA).
- Obeid PJ, Christopoulos TK, Crabtree HJ and Backhouse CJ. 2003. Microfabricated device for DNA and RNA amplification by continuous-flow polymerase chain reaction and reverse transcription-polymerase chain reaction with cycle number selection. *Anal. Chem.* 75, 288-295.
- Oda RP, Strausbauch MA, Hühmer AFR, Borson N, Jurrens SR, Craighead J, Wettstein PJ, Eckloff B, Kline B and Landers JP. 1998. Infrared-mediated thermocycling for ultrafast polymerase chain reaction amplification of DNA. *Anal. Chem.* 70(20), 4361-4368.
- Pääbo S. 1985. Molecular cloning of ancient Egyptian mummy DNA. *Nature* 314(6012), 644-645.
- Pääbo S. 1989. Ancient DNA: extraction, characterization, molecular cloning, and enzymatic amplification. *Proc. Natl. Acad. Sci. U.S.A.*, 86, 1939-1943.
- Pääbo S, Irwin DM and Wilson AC. 1990. DNA damage promotes jumping between templates during enzymatic amplification. *J. Biol. Chem.* 265(8), 4718-4721.
- Pääbo S, Poinar H, Serre D, Jaenicke-Despres V, Hebler J, Rohland N, Kuch M, Krause J, Vigilant L and Hofreiter M. 2004. Genetic analyses from ancient DNA. *Annu. Rev. Genet.* 38, 645-679.
- Panaccio M and Lew A. 1991. PCR based diagnosis in the presence of 8% (v/v) blood. *Nucleic Acids Res.* 19(5), 1151.

7. References

- Panaro NJ, Lou XJ, Fortina P, Kricka LJ and Wilding P. 2005. Micropillar array chip for integrated white blood cell isolation and PCR. *Biomol. Eng.* 21(6), 157-162.
- Park SJ, Kim JY, Yang YG and Lee SH. 2008. Direct STR amplification from whole blood and blood- or saliva-spotted FTA[®] without DNA purification. *J. Forensic Sci.* 53(2), 335-341.
- Parsche F and Nerlich A. 1997. Suitability of immunohistochemistry for the determination of collagen stability in historic bone tissue. *J. Archaeol. Sci.* 24(3), 275-281.
- Pipper J, Inoue M, Ng LFP, Neuzil P, Zhang Y and Novak L. 2007. Catching bird flu in a droplet. *Nat. Med.* 13(10), 1259-1263.
- Pipper J, Zhang Y, Neuzil P and Hsieh TM. 2008. Clockwork PCR including sample preparation. *Angew. Chem. Int. Ed. Engl.* 47(21), 3900-3904.
- Primorac D, Andelinovic S, Definis-Gojanovic M, Drmic I, Rezic B, Baden MM, Kennedy MA, Schanfield MS, Skakel SB and Lee HC. 1996. Identification of war victims from mass graves in Croatia, Bosnia, and Herzegovina by use of standard forensic methods and DNA typing. *J. Forensic Sci.* 41(5), 891-894.
- Proff C, Rothschild MA and Schneider PM. 2006. Low volume PCR (LV-PCR) for STR typing of forensic casework samples. *International Congress Series* 1288, 645-647.
- Reyes DR, Iossifidis D, Auroux PA and Manz A. 2002. Micro total analysis systems. 1. Introduction, theory, and technology. *Anal. Chem.* 74, 2623-2636.
- Rohland N and Hofreiter M. 2007. Comparison and optimization of ancient DNA extraction. *BioTechniques* 42(3), 343-352.
- Roper MG, Easley CJ and Landers JP. 2005. Advances in polymerase chain reaction on microfluidic chips. *Anal. Chem.* 77, 3887-3894.
- Rutledge RG. 2004. Sigmoidal curve-fitting redefines quantitative real-time PCR with the prospective of developing automated high-throughput applications. *Nucleic Acids Res.* 32(22), e178.
- Saiki RK, Scharf S, Faloona F, Mullis KB, Horn GT, Ehrlich HA and Arnheim N. 1985. Enzymatic amplification of beta-globin genomic sequences and restriction site analysis for diagnosis of sickle cell anemia. *Science* 230, 1350-1354.
- Saiki RK, Gelfand DH, Stoffel S, Scharf SJ, Higuchi R, Horn GT, Mullis KB and Ehrlich HA. 1988. Primer-directed enzymatic amplification of DNA with a thermostable DNA polymerase. *Science* 239, 487-491.
- Sanders CT, Sanchez N, Ballantyne J and Peterson DA. 2006. Laser microdissection separation of pure spermatozoa from epithelial cells for short tandem repeat analysis. *J. Forensic Sci.* 51(4), 748-757.
- Schena M. 1999. *DNA microarrays: a practical approach.* Oxford University Press, Oxford, Hong Kong.

7. References

- Schmidt U, Lutz-Bonengel S, Weisser HJ, Sanger T, Pollak S, Schon U, Zacher T and Mann W. 2006. Low-volume amplification on chemically structured chips using the PowerPlex16 DNA amplification kit. *Int. J. Legal Med.* 120(1), 42-48.
- Schmidt U, Proff C, Schneider PM, Matt K, Sanger T, Zacher T and Lutz-Bonengel S. 2008. [DNA amplification on chemically structured chips in forensic STR analysis]. Amplifikation von DNA auf chemisch-strukturierten Chips in der forensischen STR-Analyse. *Arch. Kriminol.* 222(3-4), 117-127.
- Schutze K and Lahr G. 1998. Identification of expressed genes by laser-mediated manipulation of single cells. *Nature Biotechnol.* 16, 737-742.
- Schwartz EI, Khalchitsky SE, Eisensmith RC and Woo SLC. 1990. Polymerase chain reaction amplification from dried blood spots on Guthrie cards. *Lancet* 336(8715), 639-640.
- Sethu P and Mastrangelo CH. 2004. Cast epoxy-based microfluidic systems and their application in biotechnology. *Sens. Actuators B: Chem.* 98(2-3), 337-346.
- Shadrach B, Commane M, Hren C and Warshawsky I. 2004. A rare mutation in the primer binding region of the amelogenin gene can interfere with gender identification. *J. Mol. Diagn.* 6(4), 401-405.
- Shiokawa S, Matsui Y and Ueda T. 1989. Liquid streaming and droplet formation caused by leaky Rayleigh waves. *Proc. IEEE Ultrason. Symp.*, 643-646.
- Simone NL, Bonner RF, Gillespie JW, Emmert-Buck MR and Liotta LA. 1998. Laser-capture microdissection: opening the microscopic frontier to molecular analysis. *Trends Genet.* 14(7), 272-276.
- Srinivasan R. 1986. Ablation of polymers and biological tissue by ultraviolet lasers. *Science* 234, 559-565.
- Srinivasan V, Pamula VK and Fair RB. 2004. Droplet-based microfluidic lab-on-a-chip for glucose detection. *Anal. Chim. Acta* 507, 145-150.
- Strobl CJ, Guttenberg Z and Wixforth A. 2004. Nano- and pico-dispensing of fluids on planar substrates using SAW. *IEEE Transactions on Ultrasonics, Ferroelectrics and Frequency Control*, 51(11), 1432-1436.
- Taylor TB, Winn-Deen ES, Picozza E, Woudenberg TM and Albin M. 1997. Optimization of the performance of the polymerase chain reaction in silicon-based microstructures. *Nucleic Acids Res.* 25(15), 3164-3168.
- Tebbe CC and Vahjen W. 1993. Interference of humic acids and DNA extracted directly from soil in detection and transformation of recombinant DNA from bacteria and a yeast. *Appl. Environ. Microbiol.* 59(8), 2657-2665.
- Thalhammer S, Stark RW, Schutze K, Wienberg J and Heckl WM. 1997. Laser microdissection of metaphase chromosomes and characterization by atomic force microscopy. *J. Biomed. Optics* 2(1), 115-119.

7. References

- Thalhammer S, Lahr G, Clement-Sengewald A, Heckl WM, Burgemeister R and Schütze K. 2003. Laser microtools in cell biology and molecular medicine. *Laser Phys.* 13(5), 681-691.
- Thalhammer S, Langer S, Speicher MR, Heckl WM and Geigl JB. 2004. Generation of chromosome painting probes from single chromosomes by laser microdissection and linker-adaptor PCR. *Chromosome Res.* 12(4), 337-343.
- Thalhammer S, Guttenberg Z, Koehler U, Zink A, Heckl WM, Franke T, Paretzke HG and Wixforth A. 2007. Programmierbares, zytogenetisches Submikroliter-Chiplabor für molekular-diagnostische Anwendungen. *GenomXPress* ISBN: 1617-562X, 1.07: 29-31.
- Thalhammer S, Höhn N, Zink A and Heckl WM. 2008. Verfahren und Vorrichtung zum Übertragen einer mikroskopischen, isolierten Probe, Mikrodissektionssystem mit einer derartigen Vorrichtung sowie Verfahren zur Herstellung eines Nanosaugers für eine derartige Vorrichtung. *Europäisches Patentamt* 08150662.8.
- Thalhammer S. 2009. Free programmable planar lab-on-a-chip. Habilitation Thesis, Experimental Physics, University Augsburg.
- Thalhammer S. 2009. Programmable lab-on-a-chip system for single cell analysis. *SPIE Europe "Microtechnologies for the new millenium"*. Proceedings, Proc. SPIE 7364, 7364B; DOI: 10.1117/12.820942.
- Thalhammer S, Schneider MF and Wixforth A. 2009. Integrated lab-on-a-chip systems in life sciences. In *Nanoscale Phenomena – Fundamentals and Applications*. Edt.: Hahn H, Siderenko A, Tiginyanu I, ISBN 978-3-642-00707-1. Springer: 161-190.
- Tsai YL and Olson BH. 1992. Rapid method for separation of bacterial DNA from humic substances in sediments for polymerase chain reaction. *Appl. Environ. Microbiol.* 58(7), 2292-2295.
- Tschachotin S. 1912. Die mikroskopische Strahlenstichmethode, eine Zelloperationsmethode. *Biol. Zentralbl.* 32, 623-630.
- Tuross N. 1994. The biochemistry of ancient DNA in bone. *Cell. Mol. Life Sci. (Experientia)* 50(6), 530-535.
- Uchida T, Suzuki T and Shiokawa S. 1995. Investigation of acoustic streaming excited by surface acoustic waves. *IEEE Ultrason. Symp.*, 1081-1084.
- Venter JC, *et al.* 2001. The sequence of the human genome. *Science* 291(5507), 1304-1351.
- Vilkner T, Janasek D and Manz A. 2004. Micro total analysis systems. Recent developments. *Anal. Chem.* 76, 3373-3385.
- Wang H, Chen J, Zhu L, Shadpour H, Hupert ML and Soper SA. 2006. Continuous flow thermal cyclers microchip for DNA cycle sequencing. *Anal. Chem.* 78, 6223-6231.
- Waters LC, Jacobson SC, Kroutchinina N, Khandurina J, Foote RS and Ramsey JM. 1998. Microchip device for cell lysis, multiplex PCR amplification, and electrophoretic sizing. *Anal. Chem.* 70, 158-162.

7. References

Weimer J, Koehler MR, Wiedemann U, Attermeyer P, Jacobsen A, Karow D, Kiechl M, Jonat W and Arnold N. 2001. Highly comprehensive karyotype analysis by a combination of spectral karyotyping (SKY), microdissection, and reverse painting (SKY-MD). *Chromosome Res.* 9(5), 395-402.

Whitesides GM. 2006. The origins and the future of microfluidics. *Nature* 442, 368-373.

Wiedbrauk DL, Werner JC and Drevon AM. 1995. Inhibition of PCR by aqueous and vitreous fluids. *J. Clin. Microbiol.* 33, 2643-2646.

Wilding PJ, Shoffner MA and Kricka LJ. 1994. PCR in a silicon microstructure. *Clin. Chem.* 40(9), 1815-1818.

Wilhelm J and Pingoud A. 2003. Real-time polymerase chain reaction. *ChemBioChem.* 4, 1120-1128.

Wixforth A. 2003. Acoustically driven planar microfluidics. *Superlattices and Microstructures* 33, 389-396.

Woide D, Mayer V, Neumaier T, Wachtmeister T, Paretzke HG, Guttenberg Z, Wixforth A and Thalhammer S. 2008. Programmable cytogenetic submicrolitre lab-on-a-chip for molecular diagnostic applications. *Biodevices 2008 Proceedings of the first international conference on biomedical electronics and devices Vol 2*, ISBN: 978-989-8111-17-3: 265-271.

Woide D, Mayer V, Wachtmeister T, Hoehn N, Zink A, Koehler U and Thalhammer S. 2009. Single particle adsorbing transfer system. *Biomed. Microdevices* 11(3), 609-614.

Woide D, Zink A and Thalhammer S. 2010. PCR analysis of minimum target amount of ancient DNA. *Am. J. Phys. Anthropol.*, doi 10.1002/ajpa.21268.

Woolley AT, Hadley D, Landre P, deMello AJ, Mathies RA and Northrup MA. 1996. Functional integration of PCR amplification and capillary electrophoresis in a microfabricated DNA analysis device. *Anal. Chem.* 68, 4081-4086.

Xia Y and Whitesides GM. 1998. Soft lithography. *Angew. Chem. Int. Ed. Engl.* 37, 550-575.

Yager P, Edwards T, Fu E, Helton K, Nelson K, Tam MR and Weigl BH. 2006. Microfluidic diagnostic technologies for global public health. *Nature* 442(7101), 412-418.

Yang J, Liu Y, Rauch CB, Stevens RL, Liu RH, Lenigk R and Grodzinski P. 2002. High sensitivity PCR assay in plastic micro reactors. *Lab Chip* 2(4), 179-187.

Zhang CS, Xu JL, Ma WL and Zheng WL. 2006. PCR microfluidic devices for DNA amplification. *Biotechnol. Adv.* 24, 243-284.

Zhang C and Xing D. 2007. Survey and summary. Miniaturized PCR chips for nucleic acid amplification and analysis: latest advances and future trends. *Nucleic Acids Res.* 35(13), 4223-4237.

7. References

Zhang Y, Bailey V, Puleo CM, Easwaran H, Griffiths E, Herman JG, Baylin SB and Wang TH. 2009. DNA methylation analysis on a droplet-in-oil PCR array. *Lab Chip* 9, 1059-1064.

Zhang Y and Ozdemir P. 2009. Microfluidic DNA amplification – a review. *Anal. Chim. Acta* 638, 115-125.

Zhou J, Bruns MA and Tiedje JM. 1996. DNA recovery from soils of diverse composition. *Appl. Environ. Microbiol.* 62(2), 316-322.

Zink A, Sola C, Reischl U, Grabner W, Rastogi N, Wolf H and Nerlich AG. 2003. Characterization of *Mycobacterium tuberculosis* complex DNAs from Egyptian mummies by spoligotyping. *J. Clin. Microbiol.* 41(1), 359-367.

Zipper H, Buta C, Lämmle K, Brunner H, Bernhagen J and Vitzthum F. 2003. Mechanisms underlying the impact of humic acids on DNA quantification by SYBR Green I and consequences for the analysis of soils and aquatic sediments. *Nucleic Acids Res.* 31(7), e39.

8. Curriculum Vitae

Personal data

Name: Daniela Rita Woide
Date & place of birth: 28.03.1980 in Munich, Germany
Profession: Biologist (Dipl.-Biol. Univ.)
Nationality: German
Address: Weißpfennigweg 13, 81825 Munich, Germany
Email: DanielaWoide@web.de

Education

2007-2010 Ludwig-Maximilians-University (LMU), Munich; Faculty of Geosciences,
Prof. Dr. Wolfgang Heckl; graduation, Ph. D.
→ the work was performed at the Helmholtz Zentrum Munich – German
Research Center for Environmental Health, Institute of Radiation Protection,
AG Nanoanalytics, PD Dr. Stefan Thalhammer

2001-2006 Technical University Munich (TUM)
Course of studies: Biology (focus in genetics, biochemistry, virology)
Certificate: university diploma, final grade 1.3
Academic degree: Dipl.-Biol. Univ.

2000-2001 Ludwig-Maximilians-University (LMU), Munich
Course of studies: Pharmaceutics

1991-2000 High school, Munich
Certificate: high school diploma, final grade 1.8

1990-1991 Secondary modern school, Munich

1986-1990 Primary school, Munich

9. Appendix

9.1 Laboratory-internal operating procedures

Laboratory-internal operating procedures (LOP) were written for general laboratory applications concerning the lab-on-a-chip system.

LOPs were written for handling laser microdissection as well as the SPATS transfer system (**chapter 9.1.1** and **chapter 9.1.2**), for the CytoCycler split into LOC chips (**chapter 9.1.3**) and LV-PCR (**chapter 9.1.4**), as well as for the BioSpot[®] automatic dispensing device (**chapter 9.1.5**) and the Fluorescence Reader (**chapter 9.1.6**).

LOP protocols are provided on a separate data medium (CD) enclosed to this work.

9.1.1 LOP of building adsorbing heads for the SPATS

“Protocol for the fabrication of adsorbing head devices for the SPATS”

A. Material

- Universal compressed gas can (210g/400ml) + pistol adaptor for compressed gas can (Propan/Butan gas can with thread, Art. Nr. 52109, CFH Löt- und Gasgeräte GmbH, Offenau, Germany)
- Glass capillary tube (Kapillaren zur Schmelzpunktbestimmung, open at both sides, AD 1,75 LG 100mm, 1000 pieces, Hirschmann Laborgeräte GmbH & Co.KG, Eberstadt, Germany)
- Metal block device with fixed conventional micrometer step motor for high-precision XY-adjustment; metal block for bending of glass capillary tubes
- Sharp/spiky item (e.g. needle or other) used for applying the adhesive
- Glass Petri dish used as platform for applying the adhesive
- Scalpel/tiny slotted screwdriver for adjusting screws of devices (screw threads)
- Copper hole-rings (AGAR scientific Ltd., Stansted, Essex, U.K.; ordered from PLANO GmbH, Wetzlar, Germany)
 - G2605C 1500 μ m hole copper 3.05mm
 - G2600C 1000 μ m hole copper 3.05mm
 - G2680C 800 μ m hole copper 3.05mm
 - G2660C 600 μ m hole copper 3.05mm
 - G2630C 300 μ m hole copper 3.05mm
- Copper meshes (G2786C 2000 square mesh copper 3.05mm, AGAR scientific Ltd., Stansted, Essex, U.K.; ordered from PLANO GmbH, Wetzlar, Germany)
- UV lamp 220V 50Hz, 230V 60Hz (System Papst-Motor Typ 8550, Papst-Motoren GmbH & Co.KG, St. Georgen, Germany)
- Adhesive = Norland optical adhesive (ultraviolet curing) 88, LOT 164 (Norland products Inc., Cranbury, NJ, USA)

(This adhesive, which is a single-package system, contains no solvent and cures by exposure to long wave ultraviolet light (320-400nm). It is suitable for fast precision bonding to glass, metal, and many plastics. Use it in any application that requires critical alignment or exact positioning.)

B. Operating procedure

I. Bending of glass capillary tubes

- Glass capillary tube is inserted into borehole of metal block (a centered, straight positioning should be achieved; use screw thread!) (**figure 1 A**, red arrow).
- Start melting/bending of glass capillary tube by heating the desired kink using a compressed gas can; most precise and straight bending is achieved when heating from above (vertical heating is ideal for eliminating unwanted sloped kinks).
- In an optimum way, bended glass capillary tube comprises a bending angle of exact 90° (**figure 1 B**), a straight bending without narrowing or squeezing diameter of glass capillary tube or angling the course of the glass capillary tube.
- Glass capillary tube needs to cool down before further processing!

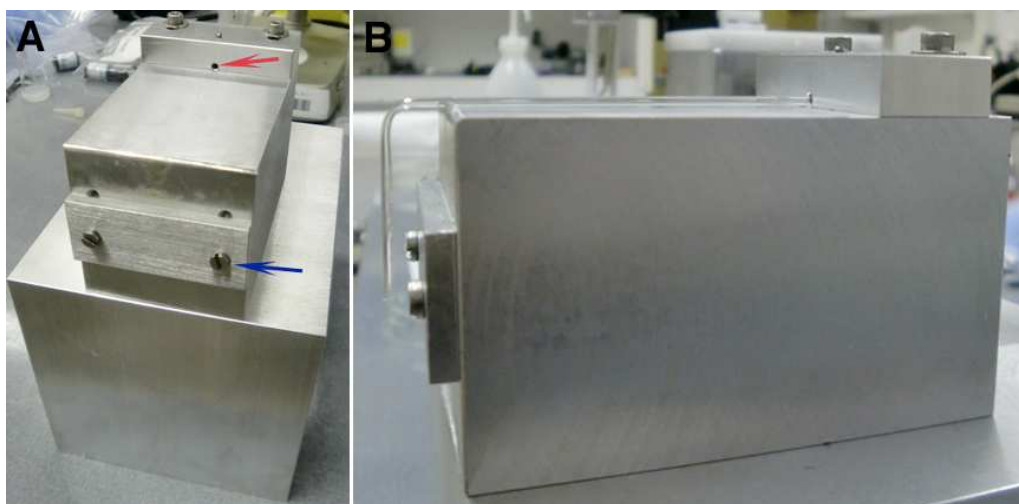


Figure 1. Bending of glass capillary tubes. A) Metal block for bending of glass capillary tubes to an angle of 90° . Borehole in the upper part, centered (red arrow), provides fixation of glass capillary tube (screw thread); centered metal plate in front (anchored via 2 screws, blue arrow) supports achieving an exact bending of the glass capillary tube to an optimum angle of 90° (B).

II. Attachment of hole-rings and meshes

- Long end of glass capillary tube is fixed into a borehole of the small metal block, which is connected to micrometer step motor (use screw thread) (**figure 2 B**); bended short end of glass capillary tube is pointing bottom-up first, to apply the adhesive.
- A tiny amount of adhesive is squeezed onto the surface of the glass Petri dish.
- Apply a tiny amount of adhesive to bended short end of glass capillary tube, exactly at the cutting site/cut surface; use any spiky metal item for applying the adhesive.

- Hole-ring needs to be exactly attached to the cut surface of the glass capillary tube; hole of hole-ring and hole of cut surface should match perfectly. (Caution: diameter of glass capillary tube may not be narrowed by inclined/leaned hole-ring AND adhesive may not seal hole!). For attachment either the micrometer step motor plus supporting tip hole surface as ring-holder can be used, or attaching the hole-ring can be performed manually (**figure 2 A**, red arrow, and **figure 2 C**).
- For curing of adhesive capillary glass tube needs to be exposed to an UV light source for 1-2 min.
- Glass capillary tube needs to be readjusted into small metal block, connected to the micrometer step motor (using screw thread); bended short end of glass capillary tube points bottom-up for applying the adhesive.
- A tiny amount of adhesive is applied to the outmost edge of hole-ring (use any spiky metal item for applying adhesive). (Caution: adhesive may not contact hole of hole-ring, as in this case adhesive would seal mesh and interfere with low-pressure efficiency!).
- Mesh needs to be exactly attached to hole-ring; shapes of both rings should match perfectly! (Do not move mesh extensively; avoid spreading adhesive!).
- For curing of adhesive capillary glass tube needs to be exposed to an UV light source for 1-2 min.

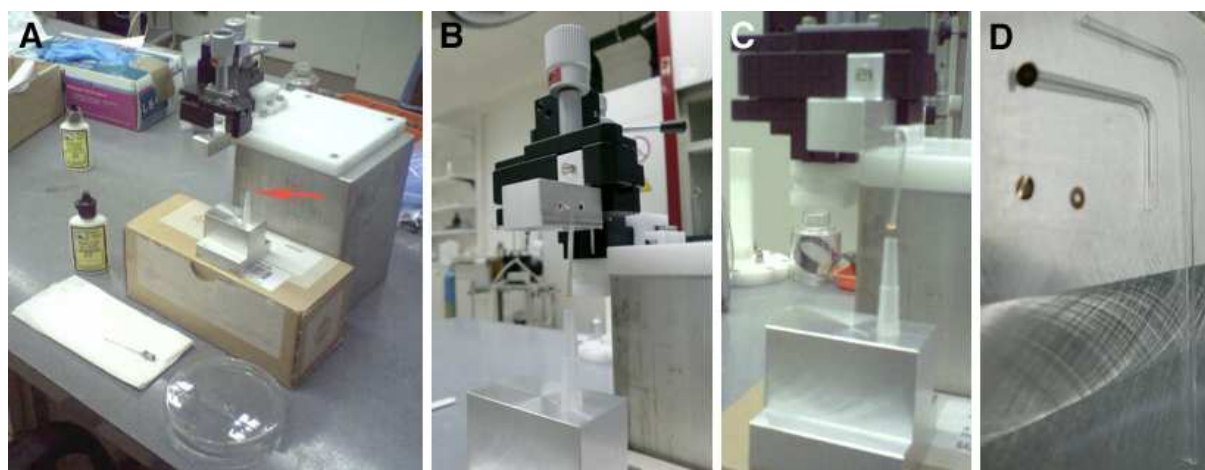


Figure 2. Working platform for applying hole-rings and meshes. A) Micrometer step motor fixed at a big metal block for XY-fine-positioning; small metal block with fitted supporting surface for attaching hole-rings and meshes (tip hole, arrow); UV curing adhesive; glass Petri dish as application platform for a tiny amount of adhesive; sharp/spiky item (metal tip) used for dosage and application of adhesive. B) Small metal block (fixed at the micrometer step motor) encompassing 2 boreholes for fixing the long end of bended glass capillary tube (screw thread); the short bended end of the glass capillary tube is facing the supporting surface (tip hole). C) Glass capillary tube after attaching hole-ring or mesh, respectively. D) Constituent parts of an adsorbing head device: glass capillary tube, hole-ring and mesh forming the sample take-up device.

9.1.2 LOP of LMD (laser microdissection) & SPATS transfer

“Transfer of microdissected material via low-pressure SPATS device”

A. Material

- New adsorbing head (glass tube, hole ring, lattice/grid according to **chapter 9.1.1**)
- Sample material fixed on PEN carrier membrane coated object slides (2 µm PEN-slides; MicroDissect GmbH, Herborn Germany)
- UVC light source (PCR Workstation, PeqLab Biotechnologie GmbH, Erlangen, Germany)
- Laser control box (CryLaS FTSS 355-50, CryLaS GmbH, Berlin, Germany)
- Softwares “Nanosauger 2.5/2.6/2.7” (XYZ High Precision, Darmstadt, Germany)
- Color firewire camera (PixeLINK, Megapixel Firewire Camera, BFI Optilas, Munich, Germany)
- Black & white CCD camera (Rolera-XR, QImaging, Surrey, BC, Canada)
- Softwares “QCapture” or “QCapture Pro 6.0” (QImaging, Surrey BC, Canada)
- Pressure-supplying pneumatic picopump (PLI-100 pressure control unit, Harvard Apparatus, Holliston, US)

B. Operating procedure

I. Preparations

- Switch on computer, microscope power supply box 231 and microscope button.
- Switch on laser control box → switch key to from “0” to “1”, a green light appears (left side) → now the laser lamp is getting pre-warmed → wait until the second green light turns on (right side) → now the laser can be started by pressing the red button located between both green lights (“Laser On/Off”) → when right green light turns to red, laser is ready to use.

II. Laser microdissection (LMD)

- Decontaminate adsorbing head by using a UVC light source.
- Make sure, that the arm of the transfer device is positioned out of the working area, on the right side of the XY-stage as a) this position favors an easy installation/fixation of the adsorbing head into the low-pressure supporting arm and b) the arm has enough space above to move up, as the software “Nanosauger” performs a calibration run of the XY-stage and the SPATS carrier arm when getting started.
- Either use the color firewire camera for colored images, or switch on the black & white CCD camera for black and white images.
- Run software “Nanosauger 2.5” (desktop) for fast working procedures (**figure 1**) and “Nanosauger 2.6” (desktop) for slow working procedures, both without using autofocus unit, or “Nanosauger 2.7” for working with implemented autofocus function (desktop). Softwares “Nanosauger” serve the color firewire camera, while for utilizing the black & white CCD camera additionally the software “QCapture” or “QCapture Pro 6.0” needs to be started.
- Optionally the stage movement direction can be adjusted via clicking “Control Via Buttons” and then clicking “Inverted X-Direction” as well as “Inverted Y-Direction”; re-activate the box “Control Via Joystick”.
- Speed of stage movement and up/down-direction of SPATS arm can be set by clicking “Control Via Buttons”, then the speed can be adjusted by moving the mode controller in the box “Speed” (settings 1-7); re-activate the box “Control Via Joystick”.
- The SPATS arm can be move up/down by turning the joystick knob to the left and right; it can be moved left/right by pressing the arrow buttons in the box “Rotation”, the speed of sideways movement can be adjusted by clicking “Low Speed”, “Medium Speed” or “High Speed”; the length of the SPATS arm can be adjusted by turning the rotary knob located at the micrometer step motor.
- Test, if lattice is centered to the view field of the microscope by approaching the adsorbing head to the 10x objective; if not, center grid for easier sample take-up.
- For microdissection of single particles use the 40x objective; set microscope to “DL auf” (*Durchlicht* function is activated); laser can be switched on by operating the footswitch, or by activating the silver switch at the laser control box (“TRIGGER INT/EXT”) to “INT” position; set microscope to “AL auf” (*Auflicht* function is

activated) calibrate the laser beam by focusing it onto the level of the PEN-carrier membrane, adjust laser focus and cut energy → a thin focused cut line is desired.

- Isolate single areas by keeping laser running and moving the microscope's XY-stage.
- To switch off laser, either loosen footswitch or turn silver switch (“TRIGGER INT/EXT”) to “EXT” position.

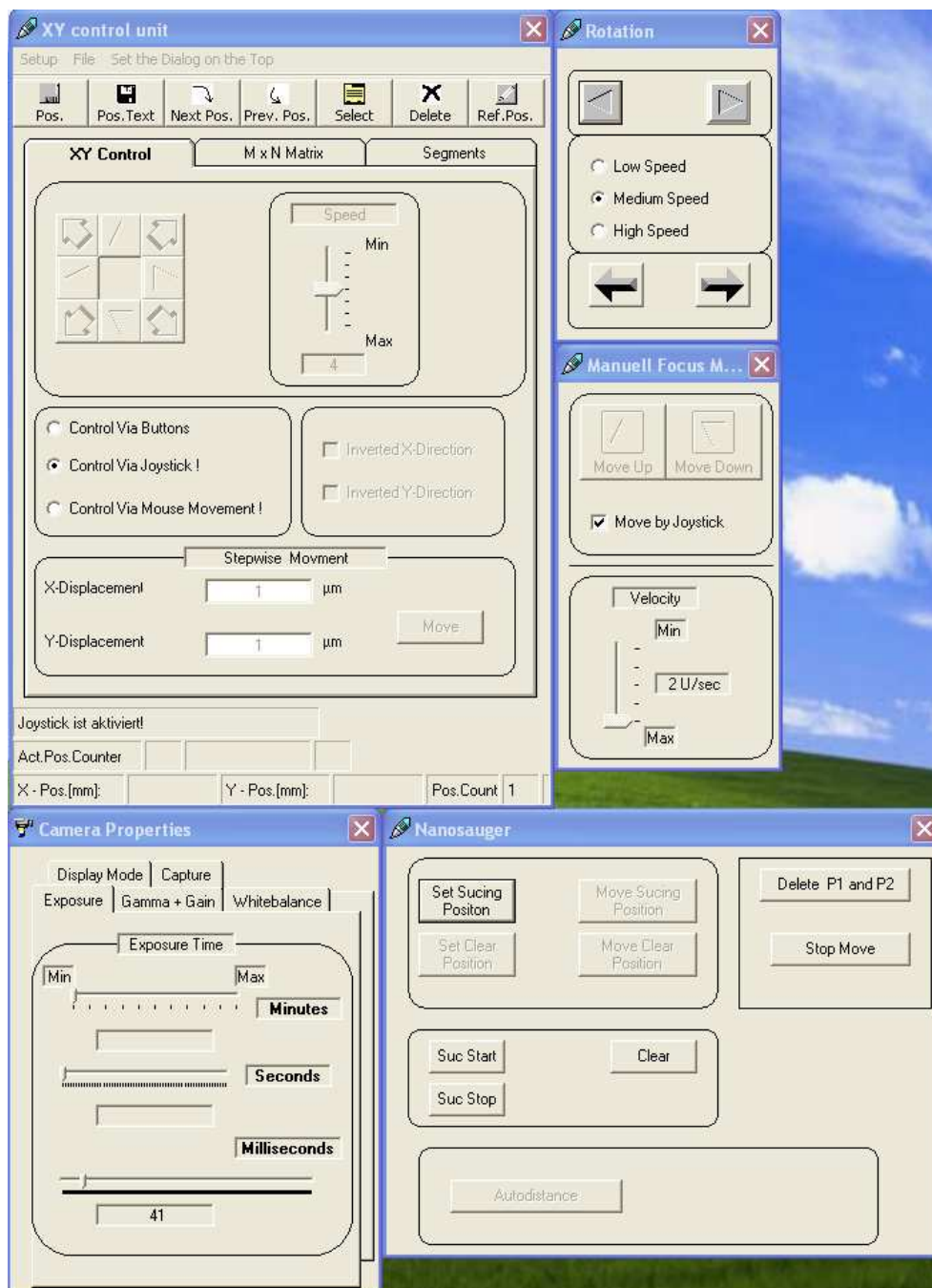


Figure 1. Screenshot of software “Nanosauger 2.5”. Via the panel “XY Control unit” settings of the XY-stage can be changed. Activating the panel “Rotation” can move the SPATS device horizontally and various speed settings can be adjusted. The “Camera Properties” window allows taking pictures and provides several settings for optimized image taking. Via operating the “Nanosauger” panel, the low-pressure operation can be started (Suc Start/Suc Stop), stopped and a short impulse of high pressure can be applied by pressing “Clear”.

III. Single particle adsorbing transfer system (SPATS)

- Use the 10x objective for controlled extraction/transfer via the SPATS device.
- Switch on pressure-supplying pneumatic picopump and turn on compressed air.
- Approach the grid/lattice of the adsorbing head to the surface of the isolated particle, start low-pressure process by clicking “Suck Start” (**figure 1**); check if particle is fixed to the grid and that the area of PEN-membrane is empty where isolation happened.
- Move SPATS up and transfer particle to a tube, planar device or else; release particle by pressing “Suck Stop” and “Clear” for providing a short impulse of high-pressure.
- Check particle release by having a look at the grid; for doing so, move adsorbing head back to the 10x objective and approach grid to objective lens.
- To quit operations, move SPATS arm out of the working area, to the right side of the XY-stage; remove adsorbing head and store it accurately; switch off microscope, switch off microscope power supply box, turn off laser by pressing the red button at laser control box (“Laser On/Off”), switch off laser control box via moving the key from “1” to “0” position, quit software, turn off camera, shut down computer.

9.1.3 LOP of LOC chips

“Application of LOC chips and of the LOC system”

A. Material

- LOC chips Cyto1, Cyto2, Cyto3 (Advalytix AG/Beckman Coulter Biomedical GmbH, Munich, Germany)
- Ultrasonic cleaner (VWR International, Leuven, Belgium)
- UVC light source (PCR Workstation, PeqLab Biotechnologie GmbH, Erlangen, Germany)
- CytoCycler (PCR device incl. chip-holder, temperature control device, SAW control high frequency (HF) generator, particular software “CytoCycler” (Advalytix AG/Beckman Coulter Biomedical GmbH, Munich, Germany))
- HF generator (FC 1201 HF, Advalytix AG/Beckman Coulter Biomedical GmbH, Munich, Germany)
- Software “CytoCycler” (Advalytix AG/Beckman Coulter Biomedical GmbH, Munich, Germany)
- Tickopur (DR. H. STAMM GmbH, Berlin, Germany)
- Acetone (Merck KGaA, Darmstadt, Germany)
- EtOH 100% (Merck KGaA, Darmstadt, Germany)
- PCR master mix (free of choice) and mineral oil cover (Sealing Solution, Advalytix AG/Beckman Coulter Biomedical GmbH, Munich, Germany)
- Sterile 0.2 ml PCR tubes (Eppendorf AG, Hamburg, Germany)

B. Cleaning of LOC chips (1-2x) in ultrasonic cleaner

- Clean chips with 70% EtOH, remove EtOH with paper towel (carefully tap the chip).
- Wash chips for about 5 min in 2% Tickopur solution using ultrasonic cleaner.
- Rinse chips thoroughly with H₂O^{dd}.
- Clean chips for 2-3 min in H₂O^{dd} (ultrasonic cleaner); blow dry with N₂.
- Clean chips for 2-3 min in acetone (ultrasonic cleaner); blow dry with N₂.
- Clean chips for 2-3 min in 100% EtOH (p.A. grade) (ultrasonic cleaner); blow dry with N₂.

- Incubate chips for 20 min using a UVC light source for decontamination.
- Successful cleaning can be tested by performing a negative control reaction on cleaned chips followed by detection via PAAGE \Rightarrow PCR should reveal no PCR product!

Important: as counting scale (graduation) at ultrasonic cleaner begins at “1” and not at “0” as written, add +1 min of time when starting the run (for 5 min put 6 min instead).

C. General information concerning LOC chips

- Currently, there are 4 different designs of LOC chips: Cyto1, Cyto2, Cyto2 plus microarray, Cyto3 plus microarray (**figure 1 C-E**).
- Cyto1 = original design, July 2007; hydrophilic reaction points A and B comprising a diameter of 40 μm and a hydrophilic track width of 15 μm (**figure 1 C**).
- Cyto2 = design for cell culture applications, January 2008; hydrophilic reaction point A comprises a larger diameter of 500 μm , instead of 40 μm as so far, for to let cells grow on the surface (the rest of the chip remained unchanged). Additionally, this chip charge was designed with a hydrophilic array field of 1x1 mm^2 next to reaction center B, for supporting microarray applications (**figure 1 D**).
- Cyto3 = totally new design, January 2009; hydrophilic track width was broadened to 200 μm instead of 15 μm as so far, especially concerning main track between reaction centers A and B (between transducer 10 and 5), and all tracks leading to reaction center B (between transducer 3 und 7); diameters of almost all reaction points (A, B and centers in front of IDT 3 and 7) are comprising 500 μm instead of 40 μm (red circles in **figure 1 E**); additionally, an intermittent hydrophilic circle is surrounding reaction point B to keep the oil cover more fixed to the surface (same design as used for the AmpliGrid™ AG480F, but with 4 gaps of 500 μm width). This chip charge was also designed with a hydrophilic array field of 1x1 mm^2 next to reaction center B, for supporting microarray applications.
- Spotting of oligonucleotide probes for microarray applications was performed using a “Nadelspotter” which can spot 100 μm spots, while the minimal distance between spots should be 50 μm . The 1x1 mm^2 array field (reaction point C) comprises dimensions of 1x1 mm^2 , thus 36 spots can be arranged in a 6x6 array. Spotting can also be performed in reaction spot B, while there only a 3x3 array is possible due to smaller diameter.

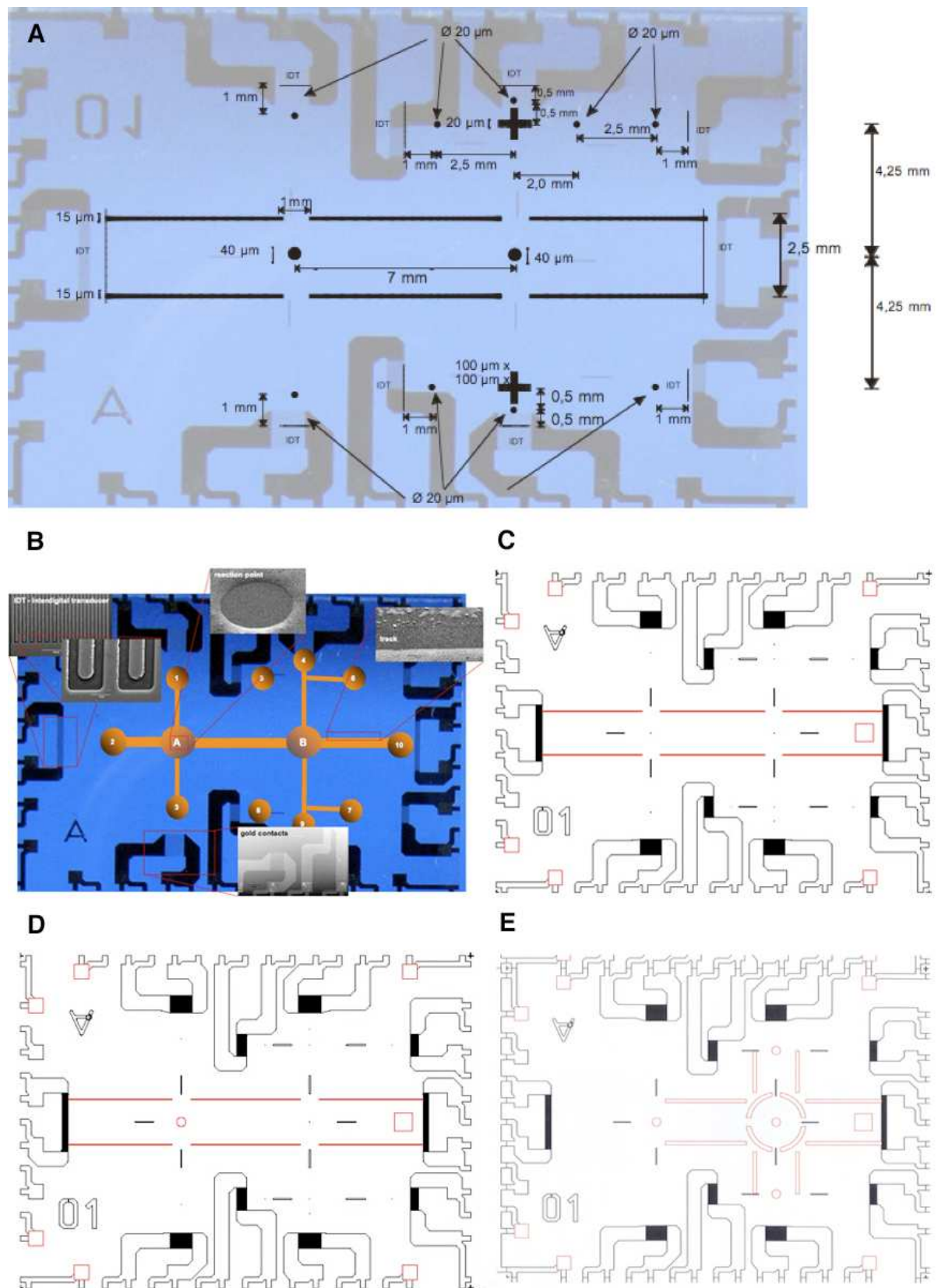


Figure 1. Design of LOC chips. A) Design and dimensions of chip charge Cyto1. B) Electromicroscopy images of hydrophobic/hydrophilic track system and reaction points. C) Layout of Cyto1: \varnothing point A 40 μm , \varnothing point B 40 μm , track width 15 μm . D) Layout of Cyto2, with microarray: \varnothing point A 500 μm , \varnothing point B 40 μm , 1x1 mm array field (point C), track width 15 μm . E) Layout of Cyto3 with microarray: \varnothing point A 500 μm , \varnothing point B 500 μm , 1x1 mm array field (point C), track width of red lined tracks 200 μm .

- Chips were manufacturer and provided by Advantix AG/Beckman Coulter Biomedical GmbH, Munich, Germany; spotting operations were done there as well.
- The basic material of each chip is LiNbO₃. Each chip comprises 10 interdigital transducers (IDTs) with service connections and gold contact pads. Big IDTs for serving the main track should provide an aperture of 3 mm to be capable of moving 5 µl of oil, the smaller ones for moving droplets an aperture of 1 mm. There must be at least 4 different SAW frequencies to operate 4 IDTs at a time. A homogeneous passivation using SiO₂ enables chemical modification. The surface chemistry features hydrophobic and hydrophilic areas. Hydrophilic areas provide tracks for controlled droplet movement by surface acoustic wave operation (SAW) and distanced reaction centers, which enable independent temperature control.

D. Installation of LOC chips into the CytoCycler device and setting frequencies/channels at the FC 1201 HF generator for the particular chip charge

- The FC 1201 HF generator distributes according to the joystick settings high frequency signals in the range from 120-170 MHz to one of four channels. The maximal power/capacity comprises 35 dBm and is controlled continuously from 7 dBm to maximum via the deflection of the joystick. The HF generator has 3 different switching-status options, marked via grouping into A, B and C (**figure 2 A**). The particular switching status is displayed in the upper middle of the front panel (**figure 2 A**, blue arrow). States can be switched by tripping the left joystick button. By tripping the right joystick button, the generator switches to maximum power in the direction the joystick is moved along the main track. By pressing the “fire” button on top of the joystick, maximum power in the appropriated direction is provided, while the maximum corresponds to the set value. Each switching status operates 4 different HF channels and connected SAW transducers by moving the joystick (**figure 2 A**, red arrow). The relation of each transducer to the single groups is shown in **figure 2 C**.
- When installing chips into the chip-holder of the CytoCycler, the temperature control device must be switched off – otherwise the temperature sensor and the whole device will get damaged! Additionally, the HF generator (SAW control box) may not be run without a chip installed! (HF channels may not be run with “open end” respectively without connected SAW LOC chip).

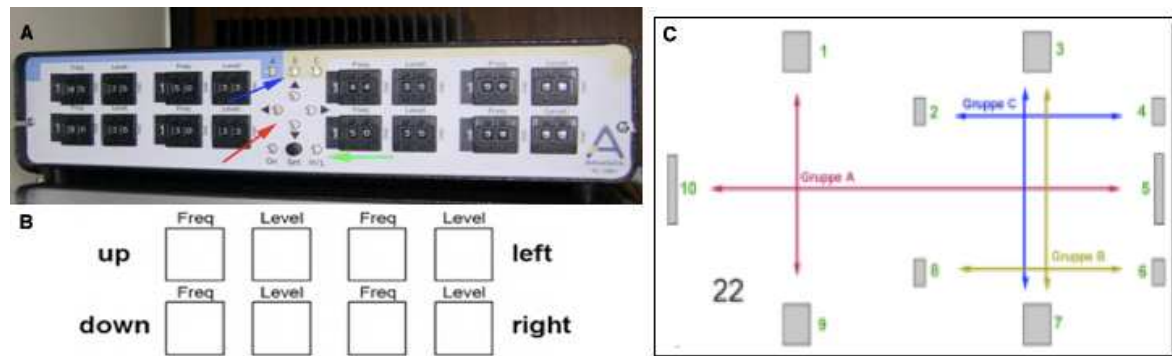


Figure 2. Operations on a LOC chip. A) Switching-status options A, B and C displayed at the panel (blue arrow). Joystick deflection shows operating HF channels (A, red arrow and B). C) The image shows the relation of transducers and switching status grouping. The arrows display the movement capacities/facilities of a droplet under the influence of the transducers of this group.

- For installing a chip, the contacting lid for the high frequency support of the chip-holder is opened by turning both screws and release the click-fastening mechanism (**figure 3**, red arrows); carefully remove SAW control lid and put in a chip preferably fixed to the left corner of the cavity for being optimally connected to IDTs by gold contacts and gold contact pins.

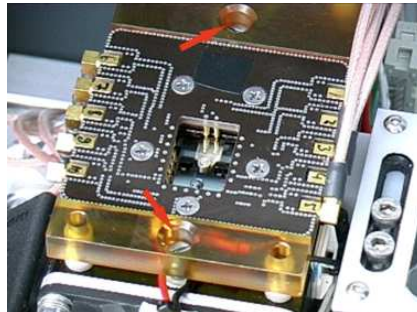


Figure 3. Installation of LOC chips. Chips are inserted into the chip-holder via screw-operated “click-fastening mechanism”.

- Re-attach SAW control lid and fasten screws.
- For each chip-charge, a report is provided telling the numbers of the chips, the number of single defect transducers as well as dedicated frequencies/channels for being tuned at the HF generator.
- Those frequencies/channels and the power level then need to be set at the front panel of the HF generator due to the following scheme (**figure 2 A**): the four control elements on the left side are valid for area A on the chip, while the four control elements on the right side are valid for area B as well as area C. Always 4 transducers must be operable by joystick at a time. So an 8-channel HF generator is used, whereby

2 channels at a time should provide the same frequency. The joystick provides a switch to shift between the first 4 and the second 4 channels. The HF generator provides a PC-interface to enable software-controlled droplet movement. Thereby the upper left control element represents values for “up”, the lower left one for “down”, upper right one for “left” and the lower right one for “right” (**figure 2 B**); given directions are related to the tracks in the respective area in which the droplets are moved according to the acting IDTs. Thus, directions display the agitation facilities of a droplet being under the influence of these interdigital transducers. Currently droplet movement can only be carried out manually via joystick, but not yet via software. Important: changed values need to be saved, validated and transferred to the SAW control unit by activating the “Set” button. For details about the connection of IDTs and 1201 HF generator please refer to the “FC 1201 HF-Generator Manual” provided by Zeno Guttenberg (Advalytix AG/Beckman Coulter Biomedical GmbH, Munich, Germany) in 2006. Important: in case of a non-working joystick (shown by blinking lights at the front panel), the joystick needs to be re-adjusted. This can be done by opening the joystick covering at the rear side and measuring the co-current flow of the contacts for joystick deflections. The measured value should be set around 2.5 V.

- The chip-holder is sometimes also named “CytoCycler”. It has a cavity for installing a single chip. The contacting lid for the high frequency support, which must be removed and reassembled for installing a chip, provides power connections for 10 transducers including 20 gold contact pins.

E. Operating the CytoCycler for performing PCR

- Install a new chip in the LOC chip-holder; important: the temperature control device may only be switched on when a chip is inserted – otherwise it might be damaged!
- Start computer, switch on temperature control device (black heating device), run software “CytoCycler” (desktop). For a detailed description of the software and the different program cards please refer to the “CytoCycler Software Manual” provided by Zeno Guttenberg in 2006 (Advalytix AG/Beckman Coulter Biomedical GmbH, Munich, Germany).
- The software provides different register cards, where programs for the load resistor heating (serving reaction point A) as well as the Peltier element (serving reaction point B and the array field C) can be saved; required register cards can be activated/marked

in the box “Status” (working procedure then happens from A1 to B3); for performing a normal PCR, simply register card B2 is required, where a complete PCR program can be typed in, saved and changed via “Save” or “Save as”. Saved programs can be changed and activated by “Load” → “All Files“ → choose program. Single boxes in the cards, where the duration was set as “0” s, are going to be ignored.

- Load resistor heating accepts temperatures from 20°(room temperature)-90°C, with a heating rate of 0.01-10 K/s; duration of temperature steps can be set to up to 16 h (60000 sec). The Peltier element accepts temperatures from 4°-105°C, with a heating/cooling rate of 0.01-5 K/s (cards A1, A2, B1) and a fixed heating rate of 3 K/s and cooling rate of 4 K/s. Cycling times can be chosen up to 200 s per temperature step, and times for pre-annealing or post-elongation up to 3000 s. Temperature increments can be set from 0.1-5 K, and time increments from 0.1-5 sec. The number of cycles can be adjusted from 0-60.
- Load a saved program file: “Load” → “All Files” → choose program; parameters can be changed individually; run program by clicking “Start Process”; after chosen parameters have been checked by the software, a message box appears (“B2 Kommentar”) to definitely start the reaction by clicking “Ok”; each program can be stopped by clicking “Abort Process”.
- Before starting a PCR, each new chip which is installed into the chip device, needs to be pre-heated to 95°C for about 15 min C (during this procedure, the material of the chip expands due to the high temperature – this prevents the droplet afterwards, when starting the initial denaturation step of the PCR at 95°C, to be moved/deformed due to material stress); afterwards, let the chip cool down completely.
- For performing PCR, first, add 1 µl of master mix onto reaction point B, then cover the reaction by adding 5 µl of mineral oil (Sealing Solution) to prevent evaporation and cross-contamination. Evaporation might inhibit the amplification reaction, as via evaporation the salt concentration of the reaction solution gets enhanced.
- Start PCR by “Start Process”.
- Let chip CytoCycler cool down after PCR is finished (wait until ventilation stops).
- Transfer 1 µl PCR into a sterile 0.2 ml PCR tube for storage (e.g. add 1 µl of 6x gel-loading-dye as well as 4 µl of water, then extract 6 µl volume from PCR tube for PAAGE application).

9. Appendix

- Clean used LOC chips immediately with 70% EtOH and H₂O^{dd}, then store in water for a distinct period of time to remove dried PCR remains; continue with cleaning procedure (paragraph A of this LOP).
- Insert a “dummy chip” into the cavity of the chip-holder serving as a placeholder, as CytoCycler device may never be assembled without a chip inside!!

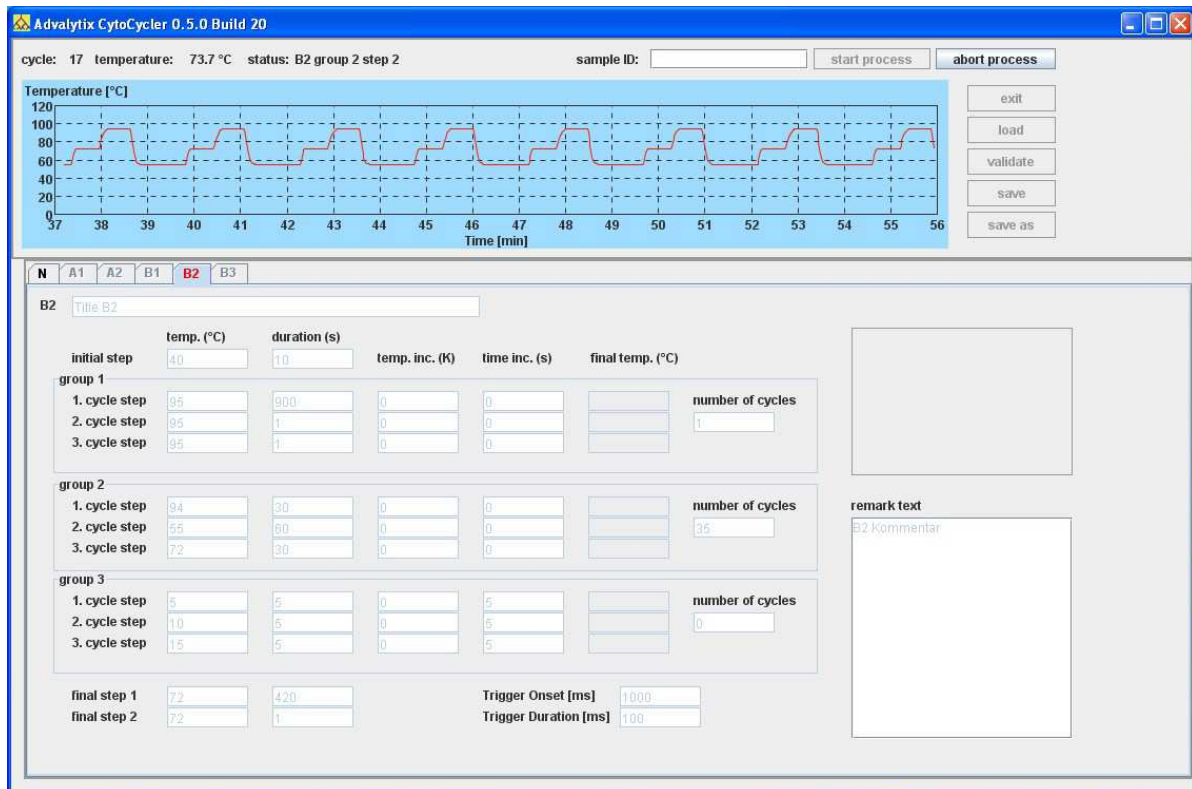


Figure 4. Screenshot of software “CytoCycler” (Advalytix AG/Beckman Coulter Biomedical GmbH, Munich, Germany). Several working sheets N-B3 comprising various PCR programs and protocols are independently addressable and operable. In the upper left corner a steady overview is provided concerning cycle number, temperature and activated working sheet. The temperature profile of the passed 20 minutes is shown graphically as well.

9.1.4 LOP of LV-PCR (low-volume PCR)

“Low-volume (LV-PCR) for application on AmpliGrid™ AG480F and the LOC system”

A. Material

- AmpliGrid™ AG480F or LOC chips Cyto1, Cyto2, Cyto3 (Advalytix AG/Beckman Coulter Biomedical GmbH, Munich, Germany)
- AmpliSpeed slide cyclers (Advalytix AG/Beckman Coulter Biomedical GmbH, Munich, Germany)
- UVC light source (PCR Workstation, PeqLab Biotechnologie GmbH, Erlangen, Germany)
- CytoCycler (PCR device incl. chip-holder, temperature control device, SAW control high frequency (HF) generator, particular software “CytoCycler” (Advalytix AG/Beckman Coulter Biomedical GmbH, Munich, Germany))
- HF generator (FC 1201 HF, Advalytix AG/Beckman Coulter Biomedical GmbH, Munich, Germany)
- Software “CytoCycler” (Advalytix AG/Beckman Coulter Biomedical GmbH, Munich, Germany)
- Sealing Solution (Advalytix AG/Beckman Coulter Biomedical GmbH, Munich, Germany)
- Sterile 0.2 ml PCR tubes (Eppendorf AG, Hamburg, Germany)
- Purified DNA material or crude sample material for direct cell lysis, but not more than 1 ng target DNA material – this might overload the reaction volume!
- Master mix (MM) for performing PCR including buffer for DNA polymerase, dNTPs, MgCl₂, oligonucleotids (primers), DNA polymerase: it is important to use an appropriate MM, which DOES NOT mix/fuse with the cover oil (Sealing Solution)!! Most suitable turned out to be PCR kits provided by QIAGEN GmbH (Hilden, Germany) like e.g. QIAGEN® Fast Cycling PCR kit; QIAGEN® Multiplex PCR kit; QuantiFast™ SYBR® Green I PCR kit; QuantiTect™ SYBR® Green I PCR kit).
- Master mixes need to be calculated down to exactly 1 µl of total reaction volume per reaction; there are two possibilities: a) calculate master mixes (w/o DNA) to 1 µl per reaction point excluding volume of target DNA, as target DNA or the tissue

9. Appendix

sample/cell respectively has already been placed at the reaction point and dried at room temperature; b) master mixes are calculated to 1 μl per reaction including volume of target DNA (standard procedure). Caution: drying sample material at room temperature on LOC chips worked always suboptimal and caused a lot of bubbling master mixes when applied to the sample; thus, just procedure b) should be used for LOC chips. On the AmpliGrid™ AG480F, both procedures worked comparable well!

- AmpliGrid™ AG480F PCR: all cycling times for PCR need to be extended a bit, as slide cycler needs some time to reach the desired temperature (each temperature step about 20 sec longer); use higher concentration of polymerase (1U/ μl); some kits perform better when scaled down, others worse (best: PCR kits by QIAGEN GmbH can be scaled down 1:1); primer concentration about 0.2 μM in PCR; use a DNA starting amount of about 100-200 pg, 1 ng at maximum; concentration of Mg^{2+} about 1-5 mM; initial denaturation step as well as final elongation step each about 5-10 min.
- 1 μl of PCR reaction master mix is generally covered with 5.0 μl of Sealing Solution. When using microdissected material, the PEN-carrier membrane might interfere amplification; thus, time of initial denaturation could be extended to 15 min. When droplets next to each other merge, less oil needs to be used (4.8-5.0 μl) (**figure 1**).

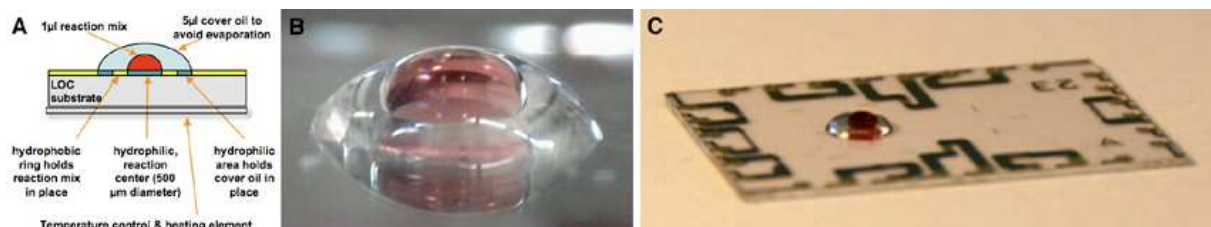


Figure 1. Principle of low-volume PCR (LV-PCR). A) Schematic overview: 1 μl of hydrophilic master mix is placed on a hydrophilic reaction spot and kept in place by a surrounding hydrophobic ring; hydrophobic oil coverage prevents evaporation and is kept in place by a surrounding hydrophilic ring. B) Close-up of the droplet-in-oil principle of LV-PCR on chip. C) LOC chip presenting a placed PCR reaction, comprising 1 μl droplet of master mix (red colored as containing blood) covered by 5 μl of mineral oil.

B. Operating procedure

I. Preparing the master mix

- Clean room (use overshoes, gloves, lab coat): all PCR reagents are stored at -20°C in the freezer, EXCEPTING DNA!!!
- 1 μl LV-PCR master mix for β -actin or amelogenin PCR respectively (QIAGEN® Fast Cycling PCR kit): 0.5 μl 2x QIAGEN Fast Cycling PCR Master Mix (final 1x), 0.1 μl

9. Appendix

10 μM forward primer (final 1 μM), 0.1 μl 10 μM reverse primer (final 1 μM), 0.0-0.3 μl sterile water (Ampuwa[®], Fresenius GmbH, Bad Homburg, Germany) (depends on DNA amount/volume used or if DNA was dried on chip). Amelogenin primers (stock solution 100 pmol/ μl) = 'Amel1' (5'-CCC-TGG-GCT-CTG-TAA-AGA-ATA-GTG-3') and 'Amel2' (5'-ATC-AGA-GCT-TAA-ACT-GGG-AAG-CTG-3'); β -actin primers (stock solution 100 pmol/ μl) = ' β -Actin up' (5'-TCA-CCC-ACA-CTG-TGC-CCC-ATC-TAC-GA-3') and ' β -Actin down' (5'-CAG-CGG-AAC-CGC-TCA-TTG-CCA-ATG-G-3').

- Calculate at least 1 negative control (just MM w/o DNA) and 1 extra reaction per reaction batch (as reserve, that there will be enough master mix for all reactions – note, that there are pipetting inaccuracies due to natural measurement error of pipets and MM sticking to filter tips and tubes!).
- Important: mix reactants of master mix just by 'agitating/stirring the pipet', DON'T mix up and down!!! Extensive mixing might create smallest air bubbles in the master mix, which could lead to the generation of big bubbles in the reaction mix while heated to 95°C (Loss of reactants! Loss of volume! Change of concentrations!).

II. Setting up a LV-PCR

- Decontaminate AmpliGrid[™] AG480F and LOC chips for 15-20 min using a UVC light source.
- Position negative control first and then add DNA to the mix (in case that DNA has not been air dried at reaction points).
- Add 1 μl MM per reaction point (volume can even be scaled down to 200 nl [1]), then cover droplets by using 4.8-5.1 μl of Sealing Solution to prevent evaporation and cross-contamination (**figure 1**). Evaporation might inhibit the amplification reaction, as via evaporation the salt concentration of the reaction solution gets enhanced.
- Important item when pipetting: empty pipet just until the first pressure point is reached!!! Emptying pipet down to the second pressure point can cause bubble formation in master mix and Sealing Solution due to the additionally blown off dead volume (enhanced pressure)!!

III. Standard PCR programs

- β -actin and amelogenin PCR: 5-15 min at 95°C initial denaturation (depends on MM and required activation time of HotStart DNA polymerase), 35-40 cycles of 94°C for 30 sec, 60°C for 30 sec, 72°C for 30 sec and final extension at 72°C for 1 min (cycling times and temperatures can be adjusted individually).
- “Touch down PCR” for DNA typing using primers D7S1824, D9S302, D10S2325: 10-15 min at 95°C initial denaturation (depends on MM and required activation time of HotStart DNA polymerase), 14 cycles of 94°C for 30 sec, 64°-50°C for 60 sec (temperature increment -1°C per cycle), 72°C for 30 sec, followed by 25 cycles of 94°C for 30 sec, 50°C for 30 sec, 72°C for 30 sec, final extension at 72°C for 7 min.
- AmpF/STR[®] SEfiler[™] PCR amplification system (Applied Biosystems, Darmstadt, Germany): 11 min at 95°C initial denaturation for HotStart AmpliTaq Gold[®] DNA polymerase (5-15 min, depends on MM and required activation time of HotStart DNA polymerase), 28 cycles of 94°C for 1 min, 59°C for 1 min, 72°C for 1 min, followed by 60°C for 45 min final extension (for AmpliTaq Gold[®] DNA Polymerase mediated non-template adenylation) or respectively 15 min (for KOD Xtreme[™] DNA Polymerase = blunt ends, normal extension).

C. Operating the AmpliSpeed (LV-PCR on AmpliGrid[™] AG480F)

- Switch on AmpliSpeed slide cycler; log in as ‘Administrator’; wait until self-test and calibration is done (display changes from “Self test” to “Idle”).
- Load a saved program file: “File” → “Load” → “PROTOKOLLE” → choose program → click “Ch. Dir”, which stands for “ok”.
- For changing some parameters of the selected program: address/click on the parameter (e.g. time, temperature or cycle number) using the touch screen, change settings using the arrow buttons; when starting the changed program, automatically the software calls for saving the changed program – this can be confirmed, otherwise the changed program can be save using a new file name.
- Position the AmpliGrid[™] AG480F onto the heating area of the AmpliSpeed slide cycler and close the lid.
- Run program by activating the “Start” button (arrow button).
- After PCR has finished, stop program by clicking the “Stop” button (square button).

D. Operating the chip system (LV-PCR on CytoCycler)

- Install a new chip in the LOC chip-holder (important: the temperature control device may only be switched on when a chip is inserted – otherwise it might be damaged) (see detailed description in the “LOP of LOC chips”, **chapter 9.1.3**).
- Start computer, switch on black temperature control box, run software “CytoCycler” (desktop).
- Load a saved program file: “Load” → “All Files” → choose program; parameters can be changed individually; run program by clicking “Start Process”; after chosen parameters have been checked by the software, a message box appears (“B2 Kommentar”) to definitely start the reaction by clicking “Ok”; each program can be stopped by clicking “Abort Process”.
- Before starting a PCR, each new chip which is installed into the chip-holder, needs to be pre-heated to 95°C for about 15 min C (during this procedure, the material of the chip expands due to the high temperature – this prevents the droplet afterwards, when starting the initial denaturation step of the PCR, to be moved/deformed due to material stress); afterwards, let the chip cool down completely.
- First, add 1 µl of master mix onto reaction point B, then cover the reaction by adding 5 µl of mineral oil (Sealing Solution) to prevent evaporation and cross-contamination (**figure 1**). Start PCR.
- Let chip CytoCycler cool down after PCR is finished (wait until ventilation stops).
- Transfer 1 µl PCR into a 0.2 ml sterile PCR tube for storage (e.g. add 1 µl of 6x gel-loading-dye as well as 4 µl of water, then extract 6 µl volume for PAAGE applications).
- Clean used LOC chips immediately with 70% EtOH and H₂O^{dd}, then store in water for a distinct period of time to remove dried PCR remains; continue with cleaning procedure (see “LOP of LOC-chips”, **chapter 9.1.3**).
- Insert a “dummy chip” into the cavity of the chip-holder serving as a placeholder, as CytoCycler device may never be assembled without a chip inside.

9.1.5 LOP of BioSpot® (PipeJet™)

“Application of BioSpot® for automatic spotting of solutions onto the LOC”

A. Material

- BioSpot® dispenser and software “BioSpot®” (BioFluidix GmbH, Freiburg, Germany)
- 0.2 ml sterile PCR tubes (Eppendorf AG, Hamburg, Germany) used as reservoirs/flasks for fluids (e.g. master mix, Sealing Solution, SSC washing solutions after hybridization/array amplification, etc...)
- e.g. master mix solution (without DNA, to not contaminate tips/PipeJets™ of BioSpot®), filled into 0.2 ml Eppendorf reaction tubes, for reaction center A or B
- Sealing Solution (Advalytix AG/Beckman Coulter Biomedical GmbH, Munich, Germany), filled into 0.2 ml Eppendorf reaction tubes, for reaction point C
- e.g. washing solutions (various concentrations of SSC), filled into 0.2 ml Eppendorf reaction tubes, for reaction center A or B

B. Protocols

I. Starting the Biospot® (Nanodispenser)

- Start computer, switch on hardware (piezo control unit & movement control), start software “BioSpot®” (drive C:\\Program Files/BioSpot/software/BioSpot.exe or via shortcut “BioSpot®” on desktop) → at first, automatically LOC-slide and PipeJets™ move to parking position (reference position) at x=0 or z=0 respectively (initial position).
- Adjust speed/velocity of x- and z-axis in control window “Axis Control“: Xvel = 500, Zvel = 500, press “Set Axis Speed“ to validate changed settings; adjust the trackbar below for “Step width (mm)“ to smallest values as well (= 0.01 mm) ⇒ by adjusting these settings the motor gets prohibited of slippage/wheelspin when movement settings for x-position are changed from 0 to increasing values. In case of wheelspin, recalibrate the system by “Search Reference”.

II. Description of single active control windows (**figure 1**)

- Window “**(1) Axis Control and Axis Movement**”’: for movement of LOC-slide on x-axis and of PipeJets™ on z-axis. For manual handling just the following settings are needed: “Move to Pos“ for moving the LOC-slide and PipeJets™ in desired positions on the x- or z-axis respectively. Simply set desired numbers and start application with “Move“ (black arrow buttons can only be used for movement when window “Enable Keyboard Control“ is activated, but are not needed necessarily. Buttons “Search Reference“, “Stop Search“ and “Move to Parking Position“ (x = 0, z = 0) are not needed for normal application as well). All of the following values given in **table 1** are valid for 0.2 ml Eppendorf reaction tubes, set into the various flasks. Initially 1.5 ml flasks are set into the desired position A, B, C or D of the flask holder, into there 0.5 ml reaction tubes are set, and into there, finally 0.2 ml reaction tubes. That “tube-in-tube”-application is used to keep applied pipetting volumes as small as possible, to get PipeJets™ deeper into tubes and to not waste much fluid just for filling up the big 1.5 ml tubes. Standard values for x- and z-movement are give in **table 1**.

Table 1. Functions and values for using the BioSpot®.

LOC application	Position x-axis [mm]	Position z-axis [mm]
Aspiration PJ1 (flask A)	280	33-37
Aspiration PJ1 (flask B)	266.5	33-37
Aspiration PJ1 (flask C) (best centered)	253.5	33-37
Aspiration PJ1 (flask D)	240.05	33-37
Aspiration PJ2 (flask A)	280	33-37
Aspiration PJ2 (flask B)	266.5	33-37
Aspiration PJ2 (flask C) (best centered)	253.5	33-37
Aspiration PJ2 (flask D)	240.05	33-37
Aspiration PJ3 (flask A) (best centered)	280	33-37
Aspiration PJ3 (flask B)	266.5	33-37
Aspiration with PJ3 using flask C and D is not applicable due to steric interference with cable/wire below the flask holder		
Dispensing PJ1 to reaction center A (H ₂ O)	62 - 62.5	30
Dispensing PJ2 to reaction center B (H ₂ O)	114.2 (115)	30 (28)
Dispensing PJ3 to reaction center C (oil)	164-166	25-28
To check, if tip of PipeJet™ PJ1, PJ2 or PJ3 is centered to flasks A, B, C or D	Flask position	28
SPATS Position (for sample release)	700	-
Fluorescence Reader	459 - 460	-

- Window “**(3) Valve Control and Pump Control**”: to open and close valves of single PipeJets™ and to connect pump with valves, or with air or valves with air (bypass). The valve, which is going to be used to “Aspirate”, must be open and connected to the pump (button “Valves (2)”), the other valves must be closed. The speed „PSpeed“ for „Aspirate“ or „Dispense“ respectively can remain unchanged at 20 ms. The volume „PVol“ can be adjusted: e.g. to 30 µl for H₂O, master mix and washing solution (PJ1 + PJ2), to 40 µl for oil (PJ3). After „Aspirate“ valves can remain connected to the pump, avoiding a low-pressure to occur. The “Dispense” function is needed only to totally empty the valves and to dispense remaining liquids back into the flasks.
- Window “**(2) PipeJet™ Control**”: various settings for automatic shooting of a definite volume using single PipeJets™. There are just slight changes to be validated as most parameters are set as standard values and remain unchanged. Standard settings: Istroke = 36 µm, vdown = 200 µm/ms, thold = 10 µs, vup = 2 µm/ms, n = 5, delay = 100 ms. Just the “Istroke“ is recommended to be changed to 20 µm instead of 36 µm, and the number “n“ from 5 to 20 repetitions, when 1 µl is going to be shot. Any changes in the settings need to be validated by “Set PJ“. A volume of about 1 µl is shot, when having aspirated a volume of about 30 µl with PJ1 or PJ2 and when starting the shoot-function by “Shoot PJ“. Buttons “Detect mode“ as well as „Dispense mode“ do not have a specific function defined by the software and can be neglected.
- Window “**(4) Batch Mode**”: for programming and saving complex operations (in an excel-sheet). Thereby, a numerical code is applied. In the control window „(1) Axis Control and Movement“ x-position values indicate a movement of the LOC-slide, z-position values indicate a movement of the PipeJets™. In the control window „(3) Valve and Pump Control“ for valves V1, V2, V3 a “0“ indicates open valves and a “1“ means closed ones. For using the pump, at “PPos” a “0“ stands for “Bypass”, that is the connection of „Valve with Air“, “1“ indicates a connection “Pump with Air“ and “2“ means the connection “Pump with Valves“. Volumes for “Aspirate“ are indicated at “PVol“ using a “-“ for negative values, volumes for “Dispense“ using a “+“ for positive values. Errors during the operation can be checked and detected by “Check Batch“. The operating process can be started with “Batch execute“ and can be paused with “Pause” or aborted with “Stop execution”. When the “Stop execution” function is activated, the total batch process stops immediately and the execution is cancelled. When pressing “Batch execute” again, the system will try to get back to the initial

9. Appendix

starting positions of the actual batch file (the first line), and x-axis as well as z-axis will move simultaneously. Thus, to avoid PipeJets™ hitting the LOC-slide, use the “(1) Axis Control and Axis Movement” box to get the PipeJets™ (firstly) as well as the LOC-slide (secondly) manually back to the initial positions at z=0 and x=0, before starting “Batch execute” again. When “Pause” is pressed, a window “Batch Processing Paused” will appear. Now it is possible to change settings manually in window (1), (2) and (3), and to perform extra performances. However, the system will be back to the actual position in the batch mode and continue, after pressing “Ok”. So click “Ok” to continue.

The screenshot displays the BioFluidiX software interface with the following sections:

- Axis Control:** Includes 'Axis Setup' with 'Xvel: 500' and 'Zvel: 500', 'Set Axis Speed', 'Search Reference', 'Stop Search', and 'Move to Parking Position' buttons. It features directional arrows for +z, -z, -x, and +x, a 'Step width (mm)' of 1.00, and 'Move to Pos' and 'Actual Pos' fields for X and Z axes (both at 0 mm). There are 'Move' and 'Stop' buttons and an 'Enable Keyboard Control' checkbox.
- PipeJet Control:** A table with columns for PJ, Istroke, vdown, thold, vup, n, and delay. It includes 'Set PJ1-3' and 'Shoot PJ1-3' buttons, and 'Detect mode' and 'Dispense mode' buttons. Below the table are definitions for Istroke, vdown, thold, vup, n, and delay.
- Valve Control:** Shows three valves (V1, V2, V3) with 'Open (0)' and 'Closed (1)' radio buttons. It includes a 'Change PPos:' section with 'Bypass (0)', 'Air (1)', and 'Valves (2)' options, and 'PSpeed (20-600)' and 'PVol (1..1000 µl)' settings with 'Aspirate' and 'Dispense' buttons.
- Batch Mode:** Features 'Open file', 'Save file', 'Check Batch', 'Batch execute', 'Stop execution', and 'Pause' buttons. Below is a detailed data table.

#	X	Z	Xvel	Zvel	V1	V2	V3	PPos	PSpeed	PVol	PJ	Istroke	vdown	thold	vup	n	delay	Pause [s]
1	0	0	500	500	1	1	1	1	20	0	1	30	200	10	1	0	100	0
2	280	0	500	500	1	1	0	2	20	0	1	30	200	10	1	0	100	0
3	280	33	500	500	1	1	0	2	20	0	1	30	200	10	1	0	100	0
4	280	33	500	500	1	1	0	2	20	-40	1	30	200	10	1	0	100	15
5	280	0	500	500	1	1	0	2	20	0	1	30	200	10	1	0	100	0
6	164	0	500	500	1	1	0	2	20	0	1	30	200	10	1	0	100	0
7	164	28	500	500	1	1	0	2	20	0	1	30	200	10	1	0	100	0
8	164	28	500	500	1	1	0	0	20	0	1	30	200	10	1	0	100	4
9	164	28	500	500	1	1	0	2	20	0	1	30	200	10	1	0	100	0
10	164	0	500	500	1	1	0	2	20	0	1	30	200	10	1	0	100	0
11	253.5	0	500	500	1	0	1	2	20	0	1	30	200	10	1	0	100	0
12	253.5	33	500	500	1	0	1	2	20	0	1	30	200	10	1	0	100	0
13	253.5	33	500	500	1	0	1	2	20	-30	1	30	200	10	1	0	100	7

Figure 1. Screenshot of software “BioSpot®” (BioFluidix GmbH, Freiburg, Germany). The software is used for operating the automatic dispensing device BioSpot®. There are four single active control windows namely “(1) Axis Control and Axis Movement”, “(2) PipeJet™ Control”, “(3) Valve Control and Pump Control” for manually operated applications, as well as “(4) Batch Mode” for automatically operating protocols. (1) allows a regulation of speed and x-position of the slide rail and z-position of PipeJets™. (2) allows an adaption of depth of penetration, displacement speed, release speed and holding time of the piezostack driven piston, as well as number of repetitions and delay time. (3) allows opening and closing of PipeJet™ valves, connections to the syringe pump as well as setting speed and volumes for aspiration and dispensation and to start these operations. (4) allows programming complete sequences, which can be run automatically.

III. Manually performed spotting of 1µl of master mix onto reaction point A (PipeJet™1,PJ1)

- (1) “Move” LOC-slide to x-position 253.5 = flask C; “Move” PJ1 to z-position 33-37.
- (3) “Connect” pump to valves, “Open” valve1, “Close” valves 2 and 3; PSpeed = 20, PVol = 30 µl; press button „Aspirate“ (watch, if fluid is aspirated into the tube); pump stays connected to valve1.
- (1) “Move” PJ1 to z-position 0; “Move” LOC-slide to x-position 62 = reaction center A; “Move” PJ1 to z-position 30.
- (2) Adjust the following settings at PJ1: Istroke = 20 µm, vdown = 200 µm/ms, thold = 10 µs, vup = 2 µm/ms, n = 20, delay = 100 ms; validate settings with „Set PJ1“; start spotting with “Shoot PJ1“; about 1 µl will be spotted onto the chip surface.
- (3) After shooting, “Close” valve1 and “Connect” pump to air.
- (1) “Move” PJ1 to z-position 0.
- SAW-Control: 1 µl of fluid can now be move via SAW on the chip surface.
- (1) “Move” LOC-slide to x-position 253.5; “Move” PJ1 to z-position 28-30.
- (3) Release of fluid remains or of the over-aspirated volume from PJ1 back into the reservoir flask C: “Connect” pump to valves, “Open” valve1, activate button “Dispense“ as long as no liquid will be released any more or until the pump is out of range (“Plunger out of range“). In the case that there is still remaining liquid inside the tube, again aspirate some air using pump, and then dispense this volume via valve1: “Move” PJ1 to z-position 0, “Connect” pump to air, “Aspirate” (1-2x 30 µl), “Connect” pump to valves, “Move” PJ1 to z-position 28-30, “Dispense” (as long as all liquid is removed from the tube and pump reaches the initial position), “Close” valve1.
- (1) “Move” PJ1 to z-position 0.
- Trouble shooting: (3) when “aspirating“ about 30 µl, and then want to “Dispense“ just 5 µl, unfortunately not 5 µl reached the chip surface, but only 1.5 µl. When 3x “dispensing” 5 µl, 11.5 µl reached the chip surface... thus, dispensing an exact volume did not work well.....

IV. Manually performed spotting of 1 μ l of master mix onto reaction point B (PipeJetTM2,PJ2)

- (1) “Move” LOC-slide to x-position 253.5 = flask C; “Move” PJ2 to z-position 33-37.
- (3) “Connect” pump to valves, “Open” valve2, “Close” valves 1 and 3; PSpeed = 20, PVol = 30 μ l; press button “Aspirate“ (watch, if fluid is aspirated into the tube); pump stays connected to valve2.
- (1) “Move” PJ2 to z-position 0; “Move” LOC-slide to x-position 115 = reaction center B; “Move” PJ2 to z-position 30.
- (2) Adjust the following settings at PJ2: Istroke = 20 μ m, vdown = 200 μ m/ms, thold = 10 μ s, vup = 2 μ m/ms, n = 20, delay = 150 ms; validate settings with “Set PJ2“; start spotting with “Shoot PJ2“; about 1 μ l will be spotted onto the chip surface.
- (3) After shooting, “Close” valve2 and “Connect” pump to air.
- (1) “Move” PJ2 to z-position 0.
- SAW-Control: 1 μ l of fluid can now be move via SAW on the chip surface.
- (1) “Move” LOC-slide to x-position 253.5; “Move” PJ2 to z-position 28-30.
- (3) Release of fluid remains or of the over-aspirated volume from PJ2 back into the reservoir flask C: “Connect” pump to valves, “Open” valve2, activate button “Dispense“ as long as no liquid will be released any more or until the pump is out of range (“Plunger out of range“). In the case that there is still remaining liquid inside the tube, again aspirate some air using pump, and then dispense this volume via valve2: “Move” PJ2 to z-position 0, “Connect” pump to air, “Aspirate” (1-2x 30 μ l), “Connect” pump to valves, “Move” PJ2 to z-position 28-30, “Dispense” (as long as all liquid is removed from the tube and pump reaches the initial position), “Close” valve2.
- (1) “Move” PJ2 to z-position 0.

V. Manually performed spotting of 5 μ l Sealing Solution onto reaction point C (PipeJetTM3,PJ3)

- (1) “Move” LOC-slide to x-position 280 = flask A; “Move” PJ3 to z-position 33-37.
- (3) “Connect” pump to valves, “Open” valve3, “Close” valves 1 and 2; PSpeed = 20, PVol = 25 μ l; press button “Aspirate“ (watch, if fluid is aspirated into the tube); pump stays connected to valve3.

- (1) “Move” PJ3 to z-position 0; “Move” LOC-slide to x-position 164 = reaction center C; “Move” PJ3 to z-position 28.
- (3) “Connect” valves to air = “Bypass“, thus, automatically a droplet is generated at PJ3 due to declined low-pressure, which drops automatically onto the chip surface due to gravity; as soon as the droplet reaches the surface, immediately “Connect” the pump to valves, to generate the low-pressure again and to stop the dispensing directly. OR: “Close” valve3, “Connect” valves to air (“Bypass“), “Open” valve3, wait for droplet touching the chip surface, “Close” valve3.
- (1) “Move” PJ3 to z-position 0.
- SAW-Control: 5 μ l of Sealing Solution can now be moved via SAW on the chip.
- (1) “Move” LOC-slide to x-position 280; “Move” PJ3 to z-position 28-30.
- (3) Release of fluid remains or of the over-aspirated volume from PJ3 back into the reservoir flask A: “Connect” pump to valves, “Open” valve3, activate button “Dispense“ as long as no liquid will be released any more or until the pump is out of range (“Plunger out of range“). In the case that there is still remaining liquid inside the tube, again aspirate some air using pump, and then dispense this volume via valve3: “Move” PJ3 to z-position 0, “Connect” pump to air, “Aspirate” (1-2x 25 μ l), “Connect” pump to valves, “Move” PJ3 to z-position 28-30, “Dispense” (as long as all liquid is removed from the tube and pump reaches the initial position), “Close” valve3.
- (1) “Move” PJ3 to z-position 0.
- Trouble shooting: (3) when “aspirating” about 25 μ l, and then want to dispense 4x 5 μ l, only 2.5 μ l were dispensed... thus, dispensing did not work well with oil as well.
- Trouble shooting: (2) the “Shoot PJ3“-function did not work very well with oil... during “Shoot PJ3” single oil droplets were spread over the chip surface and did not combine to an increasing droplet volume. Furthermore, it was not possible to “shoot” more than about 2 μ l – it seems that in that case the PJ-valve ran empty/out of liquid, as the stored fluid in the tube could not flow fast enough into the emptied PJ tip... especially when valve was still connected to pump; but when connecting the valve to air, too much liquid was released and no shooting was possible.....
- (2) Additionally, parameter changes were tested, but did not succeed. Changes in “n“ = 20, 30, 40, 100 produced just a volume of maximum 2 μ l when using “Shoot PJ3“. Changes in “delay“ of 100, 200, 500, 1000 and 2000 did not produce a larger dispensed volume than just 2 μ l when using “Shoot PJ3“.

VI. To program automatic pipetting operations using the “(4) Batch mode”

- Write a working procedure first: step-by-step, what to do (example in **table 2**).
- Final instructions can then be typed into an Excel-sheet in the software according to the “Batch mode”-code (**figure 2**), or respectively, an already existing program can be loaded via “Open file” and then be changed (save changes via “Save file”).
- Via “Batch execute” the list of orders will be run line-by-line.
- The generated working sheet of the „Batch mode“ is saved with a .csv ending – this ending can simply be opened by Excel.
- Working sheets generated in Excel can easily be saved as .xls as well as .csv ending files, and thus can easily be opened in the “Batch mode”.

Table 2. Step-by-step operating procedure of moving PJ1 to reaction center A and PJ3 to reaction center C, which can be transferred to an Excel file and translated according to the “Batch mode”-code.

	PJ1 = e.g. for master mix: use flask C (best centered) PJ3 = e.g. for Sealing Solution: use flask A (best centered)
	Axis Control settings:
(1)	“Xvel“ / “Zvel“ = 500 steps/s; press “Set Axis Speed“ to validate new settings (Axis Control)
(1)	“Step width“ = 0.01 mm (Axis Control)
	To “Aspirate” and “Dispense” the Sealing Solution/mineral oil (PipeJet™3):
(1)	1. “Move” LOC-slide to x = 280 mm to aspirate oil (Axis Movement)
(1)	2. “Move” PJ position to z = 33 mm (Axis Movement)
(3)	3. “Open” valve3 (V3) and keep the others closed (Valve Control)
(3)	4. “Connect” pump to valves by pressing “Valves“ (Pump Control)
(3)	5. Set “PVol“ to 25 µl (Pump Control)
(3)	6. Press “Aspirate“ (Pump Control)
(1)	7. “Move” PJ to the initial position, z = 0 mm (Axis Movement)
(1)	8. “Move” LOC to x = 164 mm to dispense the oil in the reaction center C (Axis Movement)
(1)	9. “Move” PJ to z = 28 mm (Axis Movement)
(3)	10. To dispense the oil, “Connect” the valves to air by pressing “Bypass“ (Pump Control)
(3)	11. Immediately after that the oil droplet reaches the chip surface, “Connect” the pump to valves by pressing “Valves“ (Pump Control)
(1)	12. “Move” PJ to z = 0 mm (Axis Movement)
	To “Aspirate” and “Dispense” the master mix, H₂O, or else (PipeJet™1):
(1)	13. “Move” LOC-slide to x = 253.5 mm to pipette the master mix (Axis Movement)
(3)	14. “Open” valve1 (V1) and “close” valve3 (V3) (Valve Control)
(1)	15. “Move” PJ to z = 33 mm (Axis Movement)
(3)	16. Set “PVol“ to 30 µl (Pump Control)
(3)	17. Press “Aspirate“ (Pump Control)
(1)	18. “Move” PJ to z = 0 mm (Axis Movement)
(1)	19. “Move” LOC-slide to x = 62 mm to dispense the master mix in the reaction center A (Axis Movement)
(1)	20. “Move” PJ to z = 30 mm (Axis Movement)
(2)	21. Change PJ1 settings (PipeJet™ Control): Istroke(20µm); vdown(200µm/ms); thold(10µs); vup(2µm/ms); n(20); delay(100ms)
(2)	22. Press “Set PJ1“ to validate the modifications (PipeJet™ Control)
(2)	23. Press “Shoot PJ1“ (PipeJet™ Control)
(1)	24. “Move” PJ to z = 0 mm (Axis Movement)
(1)	25. “Move” LOC-slide to x = 300 for SAW control and PCR performance (Axis Movement)

Operating procedure written into the Excel working-sheet: “Batch mode”-code (**figure 2**)

To open a “Batch mode” file, press “Open file”. To save setting changes in a file or to save a new created one, press “Save file”. Saved files are stored in the folder “Methods” (drive C:\\Program Files/Biospot/Methods).

For typing any instructions into an Excel-sheet, the following settings have to be considered, providing the “Batch mode”-code:

A-D = (1) Axis Control and Axis Movement (target position of axis system)

- X (A) and Z (B) = position of LOC-slide on x- and of PipeJets™ on z-axis
- Xvel (C) and Zvel (D) = speed of x-axis and z-axis (500 steps/s = standard)

E-J = (3) Valve Control and Pump Control (pumping behavior, valve position, valve velocity, volume)

- V1-3 (E,F,G) = valve 1-3 (1 = closed, 0 = open); keep all the valves closed until the aspiration or dispensing process is desired
- PPos (H) = connection of pump/air/valves (0 = bypass (valves/air), 1 = pump/air, 2 = pump/valves)
- PSpeed (I) = speed of aspiration/dispensing process (20 ms = standard)
- PVol (J) = volume of aspiration/dispensing in [μl]: (-) = aspiration, (+) = dispensing, 0 = standard (no pipetting activity)

K-R = (2) PipeJet™ Control (stroke, downstroke velocity, holdtime, upstroke velocity)

- PJ (K) = number of PJ, which is used to „shoot“ (1, 2 or 3)
- Istroke (L) = penetration depth of piezo (5-36 μm, standard = 30 μm)
- Vdown (M) / vup (O) = down-/upstroke speed of piezo during dispensing process (downstroke 100-250 μm/ms (standard = 200), upstroke 1-10 μm/ms (standard = 1; in use = 2))
- thold (N) = adjustment of piezo holding time (10-1000 μs; standard = 10 μs)
- n (P) = number of repetitions of dispensing process (1-1000); 0 = standard = no “shooting” activity!!!
- delay (Q) = delay time between each repetition (1-2000 ms; standard = 100)
- Changes must be verified by pressing “Set PJ“ button

A

	A	B	Z	Xvel	C	D	E	F	G	H	I	J	K	L	M	N	O	P	Q	R	S	T	U	V	W
	X			Zvel	V1	V2	V3	PPos	PSpeed	PVol	PJ	Istroke	vdown	thold	vup	n	delay	pause							
1	0	0	0	500	500	1	1	1	20	0	0	1	30	200	10	1	0	100							
2	280	0	0	500	500	1	1	0	2	20	0	1	30	200	10	1	0	100							
3	280	33	0	500	500	1	1	0	2	20	0	1	30	200	10	1	0	100							
4	280	33	500	500	500	1	1	0	2	20	-40	1	30	200	10	1	0	100							
5	280	0	0	500	500	1	1	0	2	20	0	1	30	200	10	1	0	100							
6	280	0	0	500	500	1	1	0	2	20	0	1	30	200	10	1	0	100							
7	164	0	0	500	500	1	1	0	2	20	0	1	30	200	10	1	0	100							
8	164	28	0	500	500	1	1	0	2	20	0	1	30	200	10	1	0	100							
9	164	28	500	500	500	1	1	0	2	20	0	1	30	200	10	1	0	100							
10	164	28	500	500	500	1	1	0	2	20	0	1	30	200	10	1	0	100							
11	164	0	0	500	500	1	1	0	2	20	0	1	30	200	10	1	0	100							
12	253.5	0	0	500	500	0	1	1	2	20	0	1	30	200	10	1	0	100							
13	253.5	33	0	500	500	0	1	1	2	20	-30	1	30	200	10	1	0	100							
14	253.5	33	500	500	500	0	1	1	2	20	0	1	30	200	10	1	0	100							
15	253.5	0	0	500	500	0	1	1	0	20	0	1	30	200	10	1	0	100							
16	62.5	0	0	500	500	0	1	1	0	20	0	1	30	200	10	1	0	100							
17	62.5	30	0	500	500	0	1	1	0	20	0	1	30	200	10	1	0	100							
18	62.5	30	500	500	500	0	1	1	0	20	0	1	20	200	10	2	15	100							
19	62.5	0	0	500	500	0	1	1	0	20	0	1	30	200	10	1	0	100							
20	250	0	0	500	500	1	1	0	0	20	0	1	30	200	10	1	0	100							
21	250	0	0	500	500	1	1	1	1	20	0	1	30	200	10	1	0	100							

B

	A	B	Z	Xvel	C	D	E	F	G	H	I	J	K	L	M	N	O	P	Q	R	S	T	U	V	W
	X			Zvel	V1	V2	V3	PPos	PSpeed	PVol	PJ	Istroke	vdown	thold	vup	n	delay	pause							
1	0	0	0	500	500	1	1	1	20	0	0	1	30	200	10	1	0	100							
2	280	0	0	500	500	1	1	0	2	20	0	1	30	200	10	1	0	100							
3	280	33	0	500	500	1	1	0	2	20	0	1	30	200	10	1	0	100							
4	280	33	500	500	500	1	1	0	2	20	-40	1	30	200	10	1	0	100							
5	280	0	0	500	500	1	1	0	2	20	0	1	30	200	10	1	0	100							
6	280	0	0	500	500	1	1	0	2	20	0	1	30	200	10	1	0	100							
7	164	0	0	500	500	1	1	0	2	20	0	1	30	200	10	1	0	100							
8	164	28	0	500	500	1	1	0	2	20	0	1	30	200	10	1	0	100							
9	164	28	500	500	500	1	1	0	2	20	0	1	30	200	10	1	0	100							
10	164	28	500	500	500	1	1	0	2	20	0	1	30	200	10	1	0	100							
11	164	0	0	500	500	1	1	0	2	20	0	1	30	200	10	1	0	100							
12	253.5	0	0	500	500	1	1	0	2	20	0	1	30	200	10	1	0	100							
13	253.5	33	0	500	500	1	1	0	2	20	-30	1	30	200	10	1	0	100							
14	253.5	33	500	500	500	1	1	0	2	20	0	1	30	200	10	1	0	100							
15	253.5	0	0	500	500	1	1	0	2	20	0	1	30	200	10	1	0	100							
16	115	0	0	500	500	1	1	0	2	20	0	1	30	200	10	1	0	100							
17	115	28	0	500	500	1	1	0	2	20	0	1	30	200	10	1	0	100							
18	115	28	500	500	500	1	1	0	2	20	0	2	20	200	10	2	17	100							
19	115	0	0	500	500	1	1	0	2	20	0	1	30	200	10	1	0	100							
20	250	0	0	500	500	1	1	0	0	20	0	1	30	200	10	1	0	100							
21	250	0	0	500	500	1	1	1	1	20	0	1	30	200	10	1	0	100							

Figure 2. Programming operating procedures in “Batch Mode”. Operating procedures can be written into an Excel working-sheet. Parameters can be typed into the columns according to the desired operation to be performed. A+B) Operating procedures for pipetting 1 µl of fluid to reaction point A (A) or B (B) and dispensing 5 µl of Sealing Solution to reaction center C, expressed according to the “Batch mode”-code.

9.1.6 LOP of Fluorescence Reader

“Fluorescence detection for applications like RT-PCR or microarray on the LOC system”

A. Material

- BioSpot[®] device and software “BioSpot[®]” (BioFluidix GmbH, Freiburg, Germany)
- CytoCycler (PCR device incl. chip-holder, temperature control device, SAW control high frequency (HF) generator, particular software “CytoCycler” (Advalytix AG/Beckman Coulter Biomedical GmbH, Munich, Germany))
- Electronics (electronic control): LED power control box (self made), trigger signal break-out box (NI SCB-68 with the PCI ADC/DAC capture the trigger signal, activates the image capture and image processing process; Quick Reference Label, S-Series Devices, National Instruments Germany GmbH, Munich, Germany)
- Optics: - black & white CCD camera (Rolera-XR, QImaging, Surrey BC, Canada)
 - Filter sets (Interferenzfilter of BrightLine series, AHF Analysentechnik AG, Tübingen, Germany): excitation filter $\lambda_{\max} = 498$ nm (spread 35 nm = 464-500 nm); emission filter $\lambda_{\max} = 536$ nm (spread 40 nm = 516-556 nm); both)
 - light source: blue LED ($\lambda_{\max} = 470 \pm 2$ nm LUXEON Rebel LXML-PB01 0023, 3.4 V forward bias, 0.7 A operating current)
- Software: “QCapture” or “QCapture PRO 6.0” (QImaging, Surrey BC, Canada), “LED_Switch.VI”, “Norbert.VI”, “Grand_NIVision_Intensity_Consec_Subtract_Loopback_NewCamera.VI” (LabVIEW 8.6, National Instruments Germany GmbH, Munich, Germany)

B. Operating procedure

I. Start BioSpot[®] (for moving LOC chip-holder to CCD camera (Fluorescence Reader))

- Prepare a test chip into the LOC chip-holder with a droplet in place (1 μ l of water covered with 5 μ l of mineral oil (Sealing Solution) at reaction center B) (see detailed description of chip installation in the “LOP of LOC chips”, **chapter 9.1.3**).

9. Appendix

- Switch on BioSpot[®] control device, start software “BioSpot[®]” (desktop; see “LOP of BioSpot[®]”, **chapter 9.1.5**).
- Move CytoCycler (LOC chip-holder slide) to CCD camera (x-axis position = 460).
- Leave “BioSpot[®]” software open, stored in the background.

II. Run “QCapture” (optimize chip position and camera settings)

- Transfer CCD camera from the microscope and fix it to the holder (big golden screw).
- Switch on CCD camera and connect to computer via firewire connection.
- Start software “QCapture” (desktop; **figure 1**).
- Click “Acquire” for activating window “Live Preview” (the software provides a live image of the chip surface).
- Center camera image to the test droplet, optimize settings like magnification as well as focus (the image from the camera has to be focused sharply).
- OR start software “QCapture Pro 6.0” (desktop; **figure 2**); click on the camera symbol for activating a settings box, where by clicking the “Preview” button a live preview is provided.

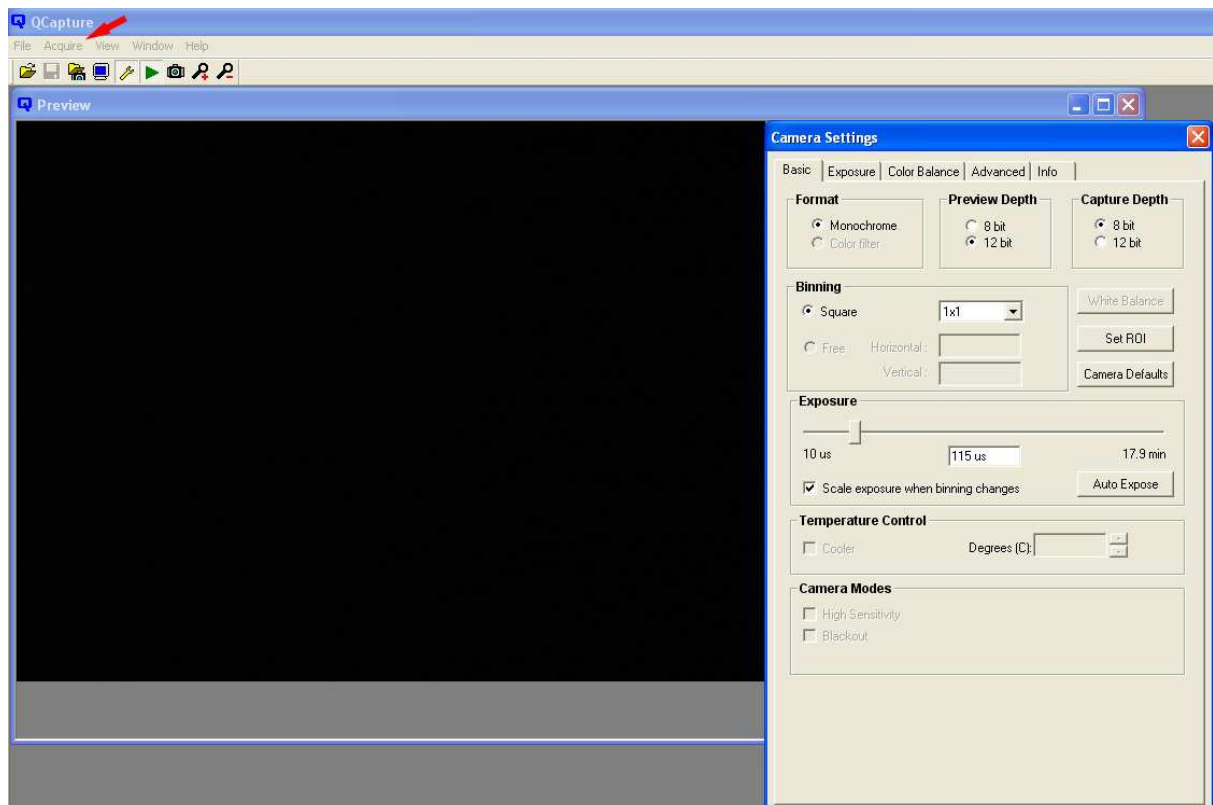


Figure 1. Screenshot of software “QCapture”. Via activating the button “Acquire” (red arrow) a window opens providing a live preview image.

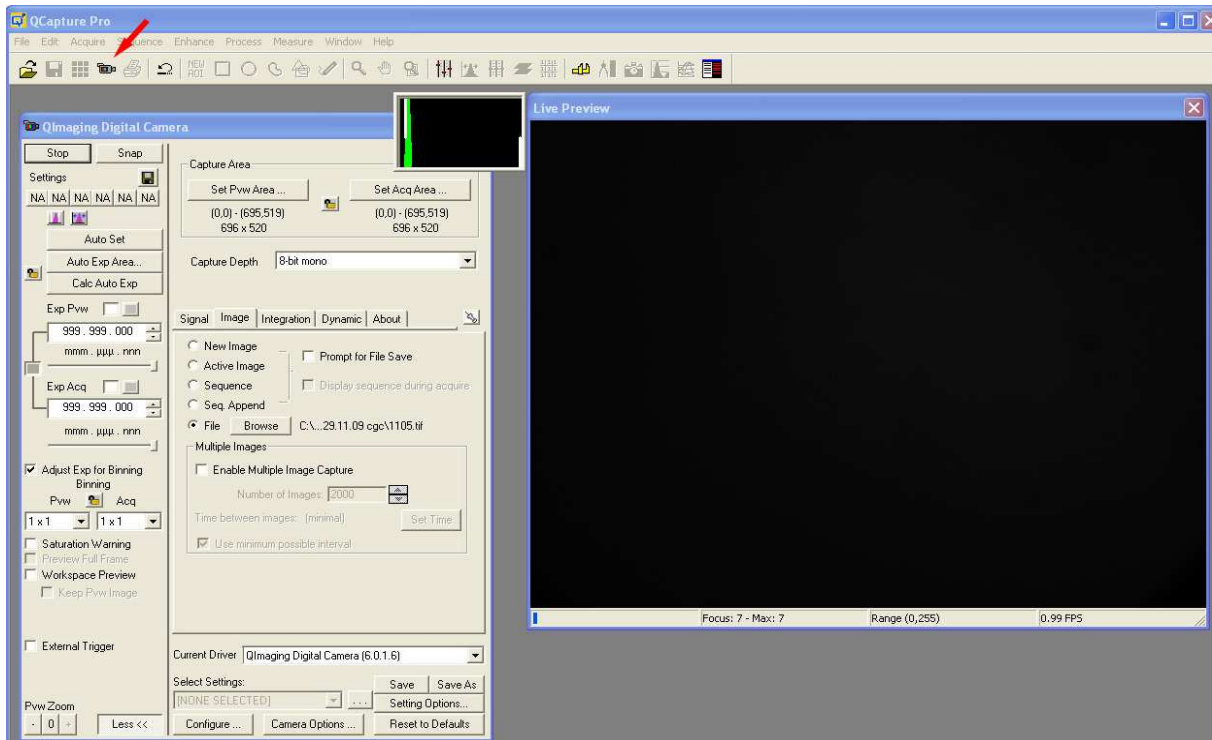


Figure 2. Screenshot of software “QCapture Pro 6.0”. Via activating the “Camera” symbol (red arrow), a window opens providing settings for the live preview. Operating the button “Preview” in these settings window provides then the live image of the camera.

III. Run “LED Switch” (check LED state)

- Switch on LED power control box (red button at the grey self-made box).
- Start software “LED_Switch” (desktop; **figure 3**).
- Run program by clicking the white arrow symbol; activate the center switch for turning blue LED light on and off; adjust LED illumination (the focused light must be centered onto the middle of the test droplet); turn LED off.

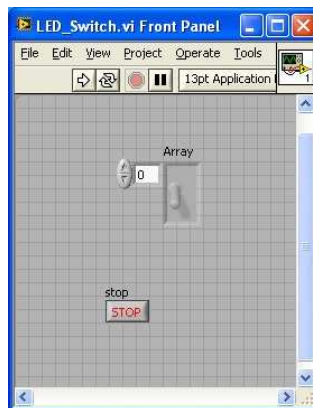


Figure 3. Screenshot of software “LED_Switch.VI”. The white arrow button, the red-circle button and the centered switch are needed to operate the LED light illumination.

9. Appendix

- Stop program by clicking the red-circle button; quit software “LED_Switch” as well as the “QCapture” software.

Important: after these preliminary steps the “QCapture” software as well as the “LED_Switch” software need to be stopped, as only one procedure at a time can have access to the camera as well as to the LED light source (so either “QCapture+LED_Switch” OR “Norbert.VI/Grand_NIVision...” can be run).

Thereafter, the test chip can be removed out of the cavity of the CytoCycler device and a new chip has to be fixed in place, whereon the PCR shall take place.

IV. Run LabVIEW program

- Switch on CCD camera and connect to computer via firewire connection.
- Switch on LED power control box (red button at the grey self-made box).

During PCR, images taken via the LabVIEW programs are stored in folder D://pic (file name = OriginalXX.tiff / OriginalXX.jpeg) → after the PCR these images need to be stored in a separate folder, otherwise images will be overwritten by new saved images when image taking programs are re-opened and run again. The software “Grand_NIVision...” also generates images named ProcessedXX.tiff / ProcessedXX.jpeg – these pictures represent subtracted images showing the calculated difference in fluorescence intensity when subtracting the previous image from the actual image. During PCR, values of fluorescence intensity are stored continuously in the domain named “Array”; additionally, at the “Grand_NIVision...” software, an excel file is generated storing these values when the program is stopped.

Assure that the trigger signal from the PCR CytoCycler is fed into the trigger signal break-out box which itself must be connected to the interface board placed in a computer slot. From the break-out box another two lines have to be connected to the LED power control box. They provide the trigger signal for the LED to be switched on and off. The LED power control box must be switched on as well (red button).

Run “Norbert.VI” (for manual image taking)

- Start software “Norbert.VI” (desktop; **figure 4**).
- Set exposure time (in milliseconds) to desired values like e.g. 100, 200, 400, 1000, and so on in the box “Exposure” (**figure 4**, red arrow 1).
- Run program by clicking the white arrow symbol (**figure 4**, red arrow 2); now images can be taken manually at any time point by clicking the button “Take picture” (**figure 4**, red arrow 3).
- Run PCR (see issue V “Start CytoCycler”).
- Stop program by clicking the red-circle button (**figure 4**, red arrow 4); quit software “Norbert.VI”.
- Save images stored in folder D://pic to a separate folder, as otherwise they will be overwritten.

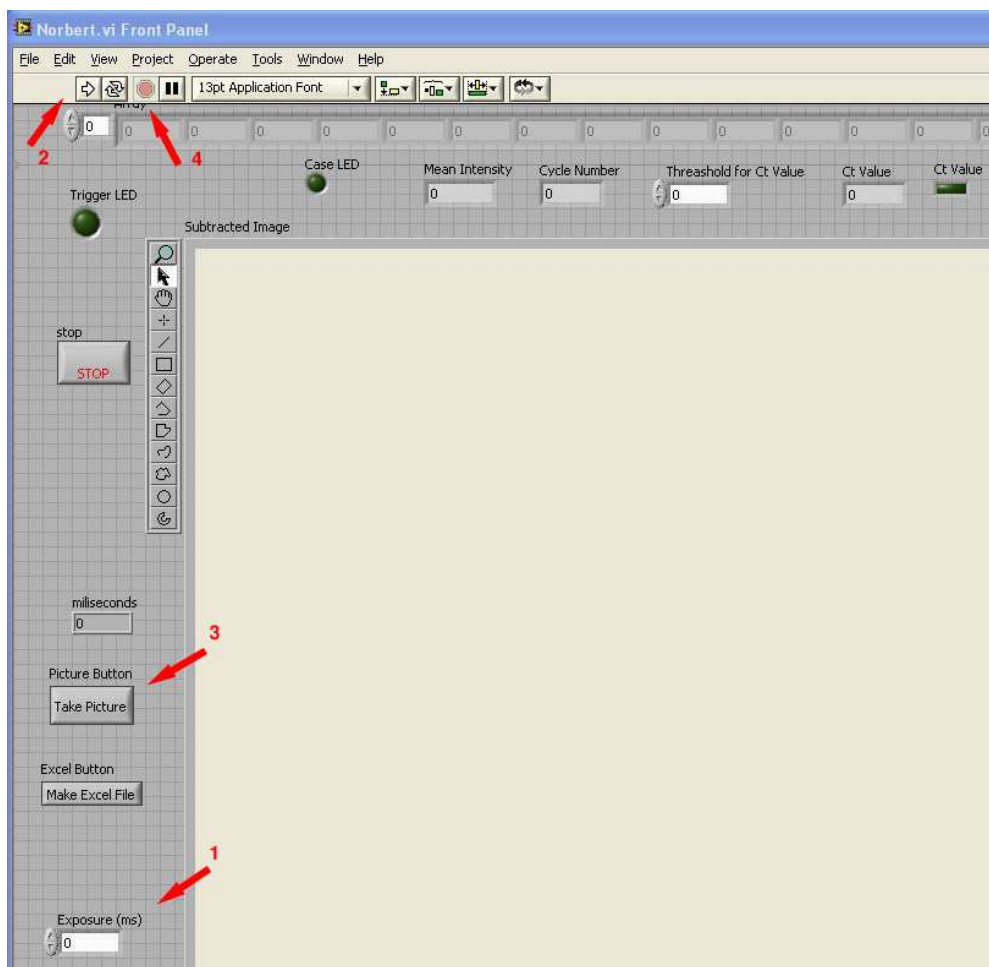


Figure 4. Screenshot of software “Norbert.VI” for taking pictures manually. The white arrow button, the red-circle button and the “Take Picture” button are needed to operate the software, while exposure time needs to be set as well. Measured fluorescence intensities of taken images are shown in the box “Mean Intensity” and are stored consecutively in domains arranged in an array-like manner below the starting button.

or “Grand_NIVision_Intensity_Consec_Subtract_Loopback_NewCamera.VI” (for automatic image taking)

- Start “Grand_NIVision_Intensity_Consec_Subtract_Loopback_NewCamera.VI” (desktop; **figure 5**).
- Set exposure time (in milliseconds) to desired values like e.g. 100, 200, 400, 1000, and so on in the box “Exposure” (**figure 5**, red arrow 1).
- Run program by clicking the white arrow symbol (**figure 5**, red arrow 2); now images are taken automatically at distinct time points; time points depend on the position (front view: left = 1.step of PCR cycle, middle = 2.step, right = 3.step), where the trigger signal break-out box is connected to the backside of the temperature control box for performing 2-step or 3-step PCR: plug 2/middle = images taken at the end of the second temperature step during PCR (around 60°C), plug 3/right = images taken at the end of the third temperature step during PCR (around 72°C)).
- Run PCR (see issue V “Start CytoCycler”); the program now waits for the trigger signals from the PCR CytoCycler.

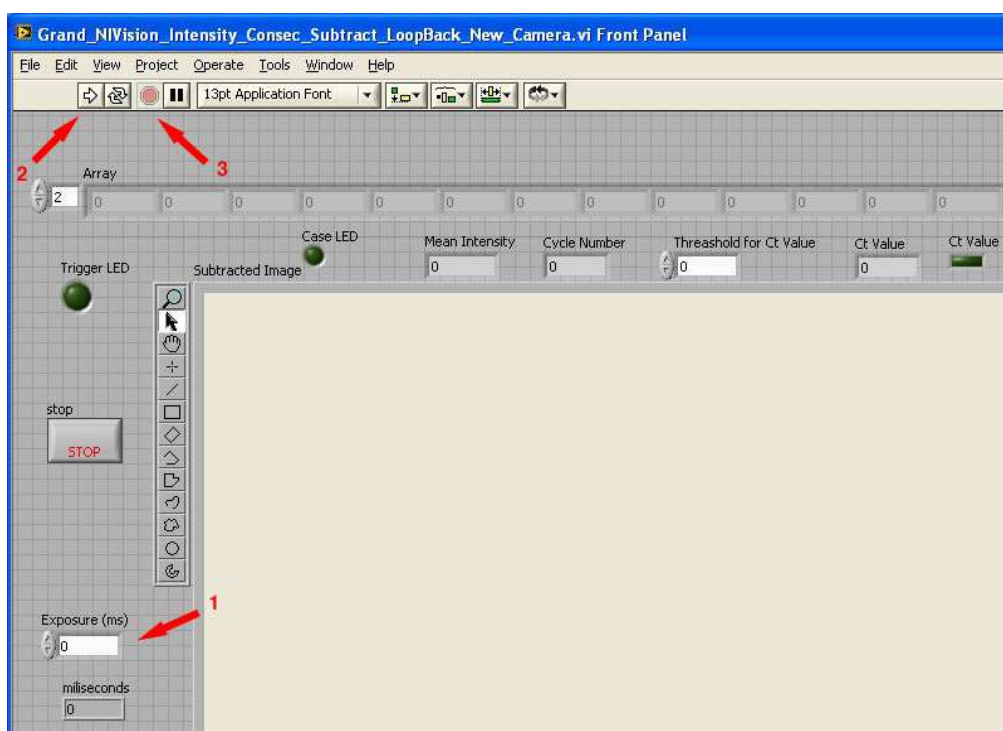


Figure 5. Screenshot of “Grand_NIVision_Intensity_Consec_Subtract_Loopback_NewCamera.VI” software for taking pictures automatically. The white arrow button and the red-circle button are needed to operate the software, while exposure time needs to be set as well. Measured fluorescence intensities of taken images are shown in the box “Mean Intensity” and are stored consecutively in domains arranged in an array-like manner below the starting button.

- Stop program by clicking the red-circle button (**figure 5**, red arrow 3); quit software “Grand_NIVision...”.
- After the PCR, automatically an Excel file is generated showing a summary of measured values of fluorescence intensity.
- Save images stored in folder D://pic to a separate folder, as otherwise they will be overwritten.

V. Start “CytoCycler” (performing PCR)

- Install new chip in LOC chip-holder device; switch on temperature control box, start software “CytoCycler” (desktop) and choose PCR program/settings (see “LOP of LOC chips”, **chapter 9.1.3** and “LOP of LV-PCR”, **chapter 9.1.4**).
- Pre-heat each chip for about 15 min to 95°C (during this procedure, the material of the chip expands due to the high temperature – this prevents the droplet afterwards, when starting the initial denaturation step of the PCR, to be moved/deformed due to material stress).
- Run PCR using 1 µl of master mix, covered by 5 µl of Sealing Solution (see “LOP of LV-PCR”, **chapter 9.1.4**).

9.2 Table of oligonucleotides

Table 10. Sequences and expected fragment sizes of oligonucleotides for PCR and array hybridization assays. Forward primers are marked with “F” or “fw”, while reverse primers are marked with “R” or “rv”. All oligonucleotides, primers as well as probes for hybridization arrays were ordered and purchased from Metabion GmbH, Martinsried, Germany.

PCR primer	Fragment size	*Tm [°C]	Oligonucleotide sequence
Amel1 ⁽¹⁾	106 bp / 112 bp	65.0	5'-CCC-TGG-GCT-CTG-TAA-AGA-ATA-GTG-3' forward
Amel2 ⁽¹⁾	106 bp / 112 bp	64.0	5'-ATC-AGA-GCT-TAA-ACT-GGG-AAG-CTG-3' reverse
Amel1-f-Cy3 ⁽¹⁾	106 bp / 112 bp	65.0	5'-Cy3-CCC-TGG-GCT-CTG-TAA-AGA-ATA-GTG-3' forward
β-Actin up ⁽²⁾	297 bp	71.0	5'-TCA-CCC-ACA-CTG-TGC-CCC-ATC-TAC-GA-3' forward
β-Actin down ⁽²⁾	297 bp	71.0	5'-CAG-CGG-AAC-CGC-TCA-TTG-CCA-ATG-G-3' reverse
DYS392-fw	290-323 bp	60.0	5'-TAG-AGG-CAG-TCA-TCG-CAG-TG-3'
DYS392-rv	290-323 bp	59.0	5'-GAC-CTA-CCA-ATC-CCA-TTC-CTT-3'
DXS10134-fw	240-291 bp	60.0	5'-CCT-GGG-TGA-CAT-AGA-GAG-AC-3'
DXS10134-rv	240-291 bp	59.0	5'-CTT-TCG-TCC-CCG-AGT-TGG-T-3'
STR marker	Fragment size	*Tm [°C]	Oligonucleotide sequence
D7S1824-F ⁽³⁾	163-199 bp	56.0	5'-Hex-GCA-CCT-GTT-TGA-TTC-AGT-CA-3'
D7S1824-R ⁽³⁾	163-199 bp	60.0	5'-CCA-GCC-TGT-GTG-ACT-ATG-TG-3'
D9S302-F ⁽³⁾	258-316 bp	63.0	5'-Fam-GGG-GAC-AGA-CTC-CAG-ATA-CC-3'
D9S302-R ⁽³⁾	258-316 bp	58.0	5'-GCG-ACA-GAG-TGA-AAC-CTT-GT-3'
D10S2325-F ⁽³⁾	119-154 bp	58.0	5'-Fam-CTC-ACG-AAA-GAA-GCC-TTC-TG-3'
D10S2325-R ⁽³⁾	119-154 bp	60.0	5'-GAG-CTG-AGA-GAT-CAC-GCA-CT-3'
Array probes	Fragment size	*Tm [°C]	Oligonucleotide sequence
Amelo1(Y)	112 bp	64.0	5'-C6-Aminolink-(T) ₁₃ -GA-GAA-ACC-ACT-TTA-TTT-GGG-3'
Amelo2(X)	106 bp	64.0	5'-C6-Aminolink-(T) ₁₃ -CT-TGA-GAA-ACA-TTT-GGG-ATG-3'
Amelo3(Y)	112 bp	64.0	5'-C6-Aminolink-(T) ₁₃ -AC-CAC-TTG-AGA-AAC-CAC-TTT-3'
DYfw	290-323 bp	68.0	5'-C6-Aminolink-(T) ₁₃ -TA-GAG-GCA-GTC-ATC-GCA-GTG-3'
DYrv	290-323 bp	67.0	5'-C6-Aminolink-(T) ₁₃ -GA-CCT-ACC-AAT-CCC-ATT-CCT-T-3'
DXfw	240-291 bp	68.0	5'-C6-Aminolink-(T) ₁₃ -CC-TGG-GTG-ACA-TAG-AGA-GAC-3'
DXrv	240-291 bp	67.0	5'-C6-Aminolink-(T) ₁₃ -CT-TTC-GTC-CCC-GAG-TTG-GT-3'
AMfw	106 bp / 112 bp	70.0	5'-C6-Aminolink-(T) ₁₃ -CC-CTG-GGC-TCT-GTA-AAG-AAT-AGT-G-3'
AMrv	106 bp / 112 bp	69.0	5'-C6-Aminolink-(T) ₁₃ -AT-CAG-AGC-TTA-AAC-TGG-GAA-GCT-G-3'

9. Appendix

⁽¹⁾ Primers Amel1 and Amel2 for amplifying 106/112 bp fragments of the human sex determining gene amelogenin were reported by Shadrach B *et al.* (2004). Amelogenin is a protein of dental enamel whose DNA sequence is present on human X- and Y-chromosomes (Lau EC *et al.*, 1989), generating different lengths products in males and females. Most commonly used amelogenin primer sets span a 6 bp deletion on the X-chromosome, resulting in a 112 bp fragment from the Y-chromosome and a 106 bp fragment of the X-chromosome. Therefore male individuals show X/Y PCR products of 106/112 bp while females give X/X single amplification products of 106 bp.

⁽²⁾ Primers β -Actin up and β -Actin down for amplifying a 297 bp fragment of the human multicopy gene β -actin were reported by Taylor TB *et al.* (1997).

⁽³⁾ Primer-pair sequences of D7S1824, D9S302 and D10S2325 were taken from www.ncbi.nlm.nih.gov using the link to UniSTS primer database.

9.3 Material list including source of supplier

Hardware

- 3130xL Genetic Analyzer (Applied Biosystems GmbH, Darmstadt, Germany)
- AdvaWash (Advalytix AG/Beckman Coulter Biomedical GmbH, Munich, Germany)
- AmpliSpeed slide cycler (Advalytix AG/Beckman Coulter Biomedical GmbH, Munich, Germany)
- BioSpot® dispenser device (BioFluidix GmbH, Freiburg, Germany)
- Black & white CCD camera (Rolera-XR, QImaging, Surrey BC, Canada)
- Color firewire camera (PixeLINK, BFI Optilas, Munich, Germany)
- CytoCycler PCR device incl. chip-holder, temperature control device, SAW control high frequency (HF) generator, particular software “CytoCycler” (Advalytix AG/Beckman Coulter Biomedical GmbH, Munich, Germany)
- Electrophoresis Power Supply EPS 601 (Amersham Biosciences Europe GmbH, Freiburg, Germany)
- Filter set ET482/35 and ET536/40 (Interferenzfilter of BrightLine series, AHF Analysentechnik AG, Tübingen, Germany)
- GenePhor electrophoresis unit (Amersham Biosciences Europe GmbH, Freiburg, Germany)
- HBO 100 high-pressure mercury lamp (HBO 100, Leistungselektronik JENA GmbH, Jena, Germany)
- HF generator (FC 1201 HF, Advalytix AG/Beckman Coulter Biomedical GmbH, Munich, Germany)
- Inverted optical microscope (Axio Obsever.Z1, Carl Zeiss GmbH, Jena, Germany)
- Laser control box (CryLaS FTSS 355-50, CryLaS GmbH, Berlin, Germany)
- LED (blue, $\lambda_{\max} = 470\pm 2$ nm) (LUXEON Rebel LXML-PB01-0023, 3.4 V forward bias, 0.7 A operating current)
- LED power control box (self-made)
- Microarray scanner system (ProScanArray Microarray Analysis System, PerkinElmer Life and Analytical Sciences, Shelton, CT, USA)
- PCR thermocycler (advanced Primus 96, PeqLab Biotechnologie GmbH, Erlangen, Germany)
- PCR thermocycler (Cyclone25, PeqLab Biotechnologie GmbH, Erlangen, Germany)
- Pressure-supplying pneumatic picopump (PLI-100 pressure control unit, Harvard Apparatus, Holliston, US)
- Stratagene Real-time PCR cycler (Stratagene Mx 3000P, Stratagene, La Jolla, CA, USA)
- Temperature control device (Advalytix AG/Beckman Coulter Biomedical GmbH, Munich, Germany)
- Temperature measurement device (Präzisionsthermometer GMH 3710, Greisinger electronic GmbH, Regenstauf, Germany)
- Trigger signal break-out box (NI SCB-68 with the PCI ADC/DAC, Quick Reference Label, S-Series Devices, National Instruments Germany GmbH, Munich, Germany)
- Ultrasonic cleaner (VWR International, Leuven, Belgium)
- UV lamp 220V 50Hz, 230V 60Hz (System Papst-Motor Typ 8550, Papst-Motoren GmbH & Co.KG, St. Georgen, Germany)
- UV spectrophotometry (NanoDrop® ND-1000, PeqLab Biotechnologie GmbH, Erlangen, Germany)
- UVA-laser system (Laser control box, CryLaS FTSS 355-50, CryLaS GmbH, Berlin, Germany)
- UVC light source (PCR Workstation, PeqLab Biotechnologie GmbH, Erlangen, Germany)

Software

- “BioSpot®” (BioFluidix GmbH, Freiburg, Germany)
- “CytoCycler” (Advalytix AG/Beckman Coulter Biomedical GmbH, Munich, Germany)
- “GeneMapper® ID v.3.2” (Applied Biosystems GmbH, Darmstadt, Germany)
- “GeneScan™ 3.7” (Applied Biosystems GmbH, Darmstadt, Germany)
- “Genotyper™ 3.7” (Applied Biosystems GmbH, Darmstadt, Germany)
- “Grand_NIVision_Intensity_Consec_Subtract_Loopback_NewCamera.VI” (LabVIEW 8.6, National Instruments Germany GmbH, Munich, Germany)
- “LED_Switch.VI” (LabVIEW 8.6, National Instruments Germany GmbH, Munich, Germany)
- Microarray scanner software (ProScanArray Scanner Software, PerkinElmer Life and Analytical Sciences, Shelton, CT, USA)

9. Appendix

- “MxPro™ – Mx3000P v3.00” (Stratagene, La Jolla, CA, USA)
- “Nanosauger 2.5” (XYZ High Precision, Darmstadt, Germany)
- “Nanosauger 2.6” (XYZ High Precision, Darmstadt, Germany)
- “Nanosauger 2.7” (XYZ High Precision, Darmstadt, Germany)
- “Norbert.VI” (LabVIEW 8.6, National Instruments Germany GmbH, Munich, Germany)
- “OriginPro 7.5 SR0” (OriginLab Corporation, Northampton, MA, USA)
- “QCapture Pro” (QImaging, Surrey BC, Canada)
- “QCapture Pro 6.0” (QImaging, Surrey BC, Canada)

Chemicals

- Acetone (Merck KGaA, Darmstadt, Germany) (Cat. No. 1.00014.2500)
- EtOH 100% (Merck KGaA, Darmstadt, Germany) (Cat. No. 1.00983.2500)
- Tickopur TR 14 (DR. H. STAMM GmbH, Berlin, Germany) (Cat. No. 090328)
- Xylene (Merck KGaA, Darmstadt, Germany) (Cat. No. 1.08685.2500)

Consumables

- 100 bp DNA ladder (New England BioLabs, Beverly, MA, USA) (Cat. No. N3231S)
- 96-well plate (ABgene® PCR Plates, Thermo Scientific, Epsom, Surrey, UK) (Cat. No. AB-0600)
- Adhesive = Norland optical adhesive 88 (ultraviolet curing), (Norland products Inc., Cranbury, NJ, USA) (Cat. No. 100613-1)
- AmpliGrid™ AG480F (multi LV-PCR microdevice) (Advalytix AG/Beckman Coulter Biomedical GmbH, Munich, Germany) (Cat. No. OAX04503)
- Anode and kathode buffers: (-) Delect Cathode Buffer and (+) Delect Anode Buffer for 10% CleanGels and (+/-) DNA HyRes Buffer for HyRes CleanGels) (ETC GmbH, Kirchentellinsfurt, Germany) (Cat. No. 1002-11, 1002-11, 1002-21)
- Copper collection grids (Copper meshes, 2000 square mesh copper 3.05mm, AGAR scientific Ltd., Stansted, Essex, U.K.; ordered from PLANO GmbH, Wetzlar, Germany) (Cat. No. G2786C)
- Copper hole-rings, 3.05 mm (AGAR scientific Ltd., Stansted, Essex, U.K.; ordered from PLANO GmbH, Wetzlar, Germany) (Cat. No. G2600C/G2660C)
- Cotton buds, sterile (Nuova Aptaca, Canelli (AT), Italy) (Cat. No. H087)
- Delect Gel Buffer for 10% CleanGels and DNA HyRes Buffer for HyRes CleanGels (ETC GmbH, Kirchentellinsfurt, Germany) (Cat. No. 1002-11 and 1002-21 and xxx)
- EDTA K treated blood collection tubes 1.3 ml (Monovettes, SARSTEDT AG & Co., Nümbrecht, Germany) (Cat. No. 41.1504.008)
- GeneScan™-500LIZ™ size standard (Applied Biosystems GmbH, Darmstadt, Germany) (Cat. No. 4322682)
- Glass capillary tube, transparent (Kapillaren zur Schmelzpunktbestimmung, open at both sides, outer diameter 1.75 mm, length 100 mm, 1000 pieces, Hirschmann Laborgeräte GmbH & Co.KG, Eberstadt, Germany) (Cat. No. 9201710)
- Heparin-Natrium (B. Braun Melsungen AG, Melsungen, Germany) (Cat. No. 2047217)
- Hi-Di™ Formamide (Applied Biosystems GmbH, Darmstadt, Germany) (Cat. No. 4311320)
- LOC chips Cyto1, Cyto2, Cyto3 (Advalytix AG/Beckman Coulter Biomedical GmbH, Munich, Germany)
- Microscope object slides (Carl Roth GmbH, Karlsruhe, Germany) (Cat. No. H871)
- PCR tubes, sterile, 0.2 and 0.5 ml (Eppendorf AG, Hamburg, Germany) (Cat. No. 0030124.332 and 0030121.023)
- PEN mounted slides (ultra thin 2 µm polyethylene-naphthalate laser supporting carrier membrane (PEN), mounted on 0.17 mm thin microscope cover glass slides or on 1.00 mm thick standard microscope object slides; MicroDissect GmbH, Herborn, Germany) (Cat. No. MDG3P4A)
- Plastic syringes 10 ml (Becton Dickinson GmbH, Heidelberg, Germany) (Cat. No. 110025158)
- Primers, oligonucleotides, probes (Metabion GmbH, Martinsried, Germany; see list in appendix, **chapter 9.2**)
- Polyacrylamide DNA gels (CleanGel 10% or CleanGel HyRes, ETC GmbH, Kirchentellinsfurt, Germany) (Cat. No. 1001-03 or 1001-27)

9. Appendix

- Sealing Solution (Advalytix AG/Beckman Coulter Biomedical GmbH, Munich, Germany) (Cat. No. OAX04207)
- Sterile water (Ampuwa[®], Fresenius, Bad Homburg, Germany) (Cat. No. 40676.00.00)
- ReddyRun Superladder-low 100 bp ladder (Thermo Scientific, ABgene, Epsom, Surrey, UK) (Cat. No. SLL-100S/LD)

DNA analysis kits

- AmpF/STR[®] SEfiler[™] Allelic Ladder (Applied Biosystems GmbH, Darmstadt, Germany) (Cat. No. 4373674)
- AmpF/STR[®] SEfiler[™] PCR amplification kit (Applied Biosystems GmbH, Darmstadt, Germany) incl. AmpF/STR[®] PCR Reaction Mix, AmpF/STR[®] SEfiler[™] Primer Set, AmpliTaq Gold[®] DNA Polymerase 5U/μl, AmpF/STR[®] SEfiler[™] Control DNA 9947A (Cat. No. 4335129)
- First-DNA All-tissue DNA kit (Gen-ial, Troisdorf, Germany) incl. buffers Lyse 1, Lyse 2, Lyse 3, and enzyme Proteinase K 20 mg/ml (Cat. No. D0502000)
- KOD Xtreme[™] Hot Start DNA Polymerase PCR system (Novagen[®], Merck, Darmstadt, Germany) incl. 2x Xtreme[™] Buffer, Xtreme[™] dNTPs (2 mM each), KOD Xtreme[™] Hot Start DNA Polymerase 1U/μl (Cat. No. 71975)
- peqGOLD Tissue DNA Mini Kit (PeqLab Biotechnologie GmbH, Erlangen, Germany) incl. DNA Lysis Buffer T, DNA Binding Buffer, DNA Wash Buffer, Elution Buffer (10 mM Tris-HCl, pH 9.0), Proteinase K, RNase A (20 mg/ml), 10 mM TE Buffer, PerfectBind DNAColumns, 2 ml Collection Tubes (Cat. No. 12-3396-01)
- QuantiFast[™] SYBR[®] Green I PCR kit (QIAGEN GmbH, Hilden, Germany) incl. 2x QuantiFast[™] SYBR[®] Green I PCR Master Mix (HotStarTaq[®] Plus DNA Polymerase, QuantiFast SYBR Green PCR Buffer, dNTP mix, SYBR Green I, ROX passive reference dye), RNase-Free water (Cat. No. 204052)
- QuantiTect[™] SYBR[®] Green I PCR kit (QIAGEN GmbH, Hilden, Germany) incl. 2x QuantiTect[™] SYBR[®] Green I PCR Master Mix (HotStarTaq[®] DNA Polymerase, QuantiTect SYBR Green PCR Buffer, dNTP mix incl. dUTP, SYBR Green I, ROX passive reference dye, 5 mM MgCl₂), RNase-Free water (Cat. No. 204143)
- QIAGEN[®] Fast Cycling PCR kit (QIAGEN GmbH, Hilden, GmbH) incl. 2x QIAGEN Fast Cycling PCR Master Mix (HotStarTaq[®] Plus DNA Polymerase, QIAGEN Fast Cycling PCR Buffer, dNTP mix), 10x CoralLoad Fast Cycling Dye, 5x QIAGEN Q-Solution, RNase-Free water (Cat. No. 203743)
- QIAGEN[®] Multiplex PCR kit (QIAGEN GmbH, Hilden, Germany) incl. 2x QIAGEN Multiplex PCR Master Mix (HotStarTaq[®] DNA Polymerase, Multiplex PCR buffer (6mM MgCl₂), dNTP mix), 5x QIAGEN Q-Solution, RNase-Free water (Cat. No. 206143)
- Silver staining system (DNA silver staining kit, GE Healthcare, Uppsala, Sweden) including 5x Fixing Solution (Benzene sulphonic acid (3.0% w/v in 24% v/v ethanol)), 5x Staining Solution (Silver nitrate (1.0% w/v), Benzene sulphonic acid (0.35% w/v)), 5x Sodium carbonate solution (Sodium carbonate (12.5% w/v)), 5x Stopping & Preserving Solution (Acetic acid (5% v/v), Sodium acetate (25% w/v), Glycerol (50% v/v)), Formaldehyde (37% w/v in water), Sodium thiosulphate (2% w/v in water) (Cat. No. 17-6000-30)